NATIONAL COOPERATIVE HIGHWAY RESEARCH PROGRAM
REPORT **164**

FATIGUE STRENGTH OF HIGH-YIELD REINFORCING BARS

TRANSPORTATION RESEARCH BOARD
NATIONAL RESEARCH COUNCIL

NATIONAL COOPERATIVE HIGHWAY RESEARCH PROGRAM
REPORT 164

FATIGUE STRENGTH OF HIGH-YIELD REINFORCING BARS

THORSTEINN HELGASON, JOHN M. HANSON.
NORMAN F. SOMES, W. GENE CORLEY, AND
EIVIND HOGNESTAD
PORTLAND CEMENT ASSOCIATION
SKOKIE, ILLINOIS

RESEARCH SPONSORED BY THE AMERICAN ASSOCIATION OF STATE HIGHWAY AND TRANSPORTATION OFFICIALS IN COOPERATION WITH THE FEDERAL HIGHWAY ADMINISTRATION

AREAS OF INTEREST:
BRIDGE DESIGN
CEMENT AND CONCRETE

TRANSPORTATION RESEARCH BOARD
NATIONAL RESEARCH COUNCIL
WASHINGTON, D.C. 1976

NATIONAL COOPERATIVE HIGHWAY RESEARCH PROGRAM

Systematic, well-designed research provides the most effective approach to the solution of many problems facing highway administrators and engineers. Often, highway problems are of local interest and can best be studied by highway departments individually or in cooperation with their state universities and others. However, the accelerating growth of highway transportation develops increasingly complex problems of wide interest to highway authorities. These problems are best studied through a coordinated program of cooperative research.

In recognition of these needs, the highway administrators of the American Association of State Highway and Transportation Officials initiated in 1962 an objective national highway research program employing modern scientific techniques. This program is supported on a continuing basis by funds from participating member states of the Association and it receives the full cooperation and support of the Federal Highway Administration, United States Department of Transportation.

The Transportation Research Board of the National Research Council was requested by the Association to administer the research program because of the Board's recognized objectivity and understanding of modern research practices. The Board is uniquely suited for this purpose as: it maintains an extensive committee structure from which authorities on any highway transportation subject may be drawn; it possesses avenues of communications and cooperation with federal, state, and local governmental agencies, universities, and industry; its relationship to its parent organization, the National Academy of Sciences, a private, nonprofit institution, is an insurance of objectivity; it maintains a full-time research correlation staff of specialists in highway transportation matters to bring the findings of research directly to those who are in a position to use them.

The program is developed on the basis of research needs identified by chief administrators of the highway and transportation departments and by committees of AASHTO. Each year, specific areas of research needs to be included in the program are proposed to the Academy and the Board by the American Association of State Highway and Transportation Officials. Research projects to fulfill these needs are defined by the Board, and qualified research agencies are selected from those that have submitted proposals. Administration and surveillance of research contracts are responsibilities of the Academy and its Transportation Research Board.

The needs for highway research are many, and the National Cooperative Highway Research Program can make significant contributions to the solution of highway transportation problems of mutual concern to many responsible groups. The program, however, is intended to complement rather than to substitute for or duplicate other highway research programs.

NCHRP Report 164

Project 4-7 FY '68 and '69
ISBN 0-309-02430-7
L. C. Catalog Card No. 76-4641

Price: $5.60

Notice

The project that is the subject of this report was a part of the National Cooperative Highway Research Program conducted by the Transportation Research Board with the approval of the Governing Board of the National Research Council, acting in behalf of the National Academy of Sciences. Such approval reflects the Governing Board's judgment that the program concerned is of national importance and appropriate with respect to both the purposes and resources of the National Research Council.

The members of the advisory committee selected to monitor this project and to review this report were chosen for recognized scholarly competence and with due consideration for the balance of disciplines appropriate to the project. The opinions and conclusions expressed or implied are those of the research agency that performed the research, and, while they have been accepted as appropriate by the advisory committee, they are not necessarily those of the Transportation Research Board, the National Research Council, the National Academy of Sciences, or the program sponsors.

Each report is reviewed and processed according to procedures established and monitored by the Report Review Committee of the National Academy of Sciences. Distribution of the report is approved by the President of the Academy upon satisfactory completion of the review process.

The National Research Council is the principal operating agency of the National Academy of Sciences and the National Academy of Engineering, serving government and other organizations. The Transportation Research Board evolved from the 54-year-old Highway Research Board. The TRB incorporates all former HRB activities but also performs additional functions under a broader scope involving all modes of transportation and the interactions of transportation with society.

Published reports of the

NATIONAL COOPERATIVE HIGHWAY RESEARCH PROGRAM

are available from:

Transportation Research Board
National Academy of Sciences
2101 Constitution Avenue, N.W.
Washington, D.C. 20418

(See last pages for list of published titles and prices)

Printed in the United States of America.

FOREWORD

By Staff

Transportation Research Board

This report is recommended to engineers, researchers, and members of specification-writing bodies concerned with the use of high-yield reinforcement in concrete. The research that is described consisted of a comprehensive series of laboratory fatigue tests of reinforced concrete beams, each beam containing a single straight deformed bar as the main reinforcing element. The major effects studied were stress range, minimum stress, bar diameter, type of specimen, grade of bar, and bar geometry. On the basis of the observed behavior, a fatigue design provision for deformed reinforcing bars was developed, suggesting that the service load stress range be limited.

Because of an economic advantage gained in many circumstances, the use of high-yield reinforcing bars in concrete construction has increased greatly in recent years. Acceptance of high-yield reinforcement (generally Grades 60 and 75) in American highway bridge design practice has been slow, although highway bridge design specifications now allow use of high-yield reinforcement in all bridge members. Concern over a number of possible countereffects, including fatigue effects, has been responsible for the slow acceptance. The results of research have now overcome most of the earlier apprehensions. The study reported herein has made an important contribution with respect to the avoidance of a fatigue problem.

No fatigue fracture of the reinforcement in a reinforced concrete structure in service has ever been reported. However, fatigue fractures in the reinforcement of the overloaded test bridges in the AASHO Road Test directed attention to the importance of fatigue considerations in bridge design.

In this study, a statistically valid experiment was performed consisting of 353 fatigue tests on concrete beams, each containing one reinforcing bar. Test results were entered in an over-all multiple linear regression analysis. The fatigue design provision that has been recommended based on the results of the study is founded on a firm background of testing.

CONTENTS

ACKNOWLEDGMENTS

The research reported herein was conducted in the Structural Laboratory of the Portland Cement Association by the staff of the Structural Development Section and with the assistance of the staff of the Transportation Development Section. Dr. John M. Hanson, Director of Structural Research, Wiss, Janney, Elstner and Associates (formerly Assistant Manager, Structural Research Section, Portland Cement Association), and Dr. Thorsteinn Helgason, Structural Engineer, Structural Development Section, Engineering Development Department, served as principal investigators. Other principals were: Dr. W. Gene Corley, Director, Engineering Development Department; Dr. Eivind Hognestad, Director, Technical and Scientific Development; and Dr. Norman F. Somes, Scientific Assistant to the Director, Institute for Applied Technology, National Bureau of Standards (formerly Research Engineer, Structural Research Section, Portland Cement Association).

Aside from the principals, several professional staff members of the Association participated in the research project. Dr. Paul Seligman (deceased), Principal Research Physicist, Cement Research Section, was the statistical consultant during planning of Phase I of the test program. Harold W. Conner, Director, Computer Services Department, aided in the organization of the data analysis. Claire G. Ball, Transportation Engineer, Transportation Development Section, supervised construction and testing of the Phase II test beams. George J. Vanisko, Assistant Research Petrographer, Basic Research Department, prepared and tested sectioned bar samples and obtained photographs for the study of bar geometry.

R. K. Richter was the principal technician during Phase I of the investigation. Other present and former members of the technician and clerical staffs of the Association who worked on various stages of the project include: B. W. Fullhart, W. H. Graves, O. A. Kurvits, W. Hummerich, Jr., S. Zintel, E. J. Rymut, R. D. Ward, J. J. DiJohn, R. G. Sander, D. W. Walker, B. G. Firstenberger, Jr., R. McCarley, Jr., S. Rubinoff, A. M. Parisi, R. Kohn, A. A. Nelson, and B. Legan.

FATIGUE STRENGTH OF HIGH-YIELD REINFORCING BARS

SUMMARY

Stress range, minimum stress, bar diameter, grade of bar, and bar geometry were found to affect the fatigue properties of reinforcing bars. The effective depth of a reinforced concrete beam was found to have no direct influence on the fatigue strength of the main reinforcement.

The stress range to which a reinforcing bar is subjected is the primary factor determining its fatigue life. For design purposes, there is a limiting stress range, the fatigue limit, above which a reinforcing bar will have a finite fatigue life and is certain to fracture. At stress ranges below the fatigue limit, a reinforcing bar will have a long fatigue life and may be able to sustain a virtually unlimited number of stress cycles.

The magnitude of the fatigue limit depends on the minimum stress during each stress cycle and on the shape of the deformations rolled onto the bar surface. It may also depend on the diameter and the grade of the bar. For a fatigue life of 5 million cycles, the mean fatigue limit for No. 8 Grade 60 bars from five U.S. manufacturers was found to range from 23.0 to 28.5 ksi when the minimum stress was 6-ksi tension. The lowest stress range at which a fatigue fracture was obtained was 21.3 ksi. This occurred in a No. 11 Grade 60 reinforcing bar subjected to a minimum stress of 17.5 ksi.

Increasing a tensile minimum stress was found to result in a decrease in fatigue strength. On the other hand the fatigue strength was found to increase with an increasing compressive minimum stress. Changing the minimum stress of a stress cycle by 3 ksi was found to be equivalent to changing the stress range by about 1 ksi.

Bar diameter and grade of bar were found to influence the finite-life fatigue cycle by 3 ksi was found to be equivalent to changing the stress range by about 1 ksi.

Bar diameter and grade of bar were found to influence the finite-life fatigue strength of reinforcing bars. The existence of a long-life fatigue effect due to these variables could not be established. Larger size bars have a lowered fatigue strength while higher grade bars have an increased fatigue strength. Other things being equal, replacing No. 5 bars with No. 11 bars results in a decrease in fatigue strength of 3.6 ksi. Replacing a Grade 60 bar with a Grade 75 bar results in an increase in fatigue strength of 1.7 ksi.

Transverse lugs and manufacturer's bar identification marks cause stress concentrations at their juncture with the barrel of a bar. The magnitude of the stress concentration is primarily related to the ratio of the radius at the base of the deformation to its height. In this investigation, all fatigue fractures were initiated at the base of a transverse lug or a bar mark.

The effect of lug geometry on fatigue strength was found to be coupled with that of bar diameter. The larger the bar diameter, the greater was the effect of lug geometry. For a No. 8 bar, a change in the ratio of lug base radius to lug height, r/h, from 0.1 to 1.0 results in an increase in fatigue strength of 7.2 ksi. The effect is potentially larger.

A design recommendation, limiting the allowable service load stress range in reinforcing bars, was developed. This limiting stress range, f_r, varies with the minimum stress, f_{min}, and r/h as follows:

$$f_r = 21 - 0.33 f_{min} + 8(r/h)$$

In this expression, the stresses are measured in kips per square inch and the minimum stress is positive when tensile.

CHAPTER ONE

INTRODUCTION AND RESEARCH APPROACH

BACKGROUND

Deformed steel bars produced in North America for use as concrete reinforcement can conform to any of three ASTM specifications (*1, 2, 3*). Within these specifications are classifications of four different grades of bars—Grades 40, 50, 60, and 75—which indicate respective specified minimum yield levels of 40, 50, 60, and 75 ksi. Generally, bars of Grades 60 and 75 are considered to be high-yield reinforcing bars.

In recent years the use in concrete construction of high-yield reinforcing bars, rather than Grades 40 and 50 bars, has increased greatly. This is due to an economic advantage gained in many circumstances in a structure designed by the load factor (*4, 5*) method. This design method allows full use of the increased strength available in the higher grades of bars. Hognestad (*6*) has discussed the economies attainable by means of high-yield reinforcement and the future requirements to be made of such steels.

North America initiated high-yield reinforcement in highway bridges early in the last decade. By that time, however, its use in European highway bridges was widespread (*7*). Although the European experience was not accepted directly in American bridge design practice, instrumented test bridges (*8, 9*) having high-yield reinforcement were constructed. The performance of these bridges in service indicated that high-yield reinforcement was adaptable to American requirements. Use of such reinforcement was further encouraged by the Bureau of Public Roads publication (*10*) in 1966 of strength and serviceability criteria for reinforced concrete bridge members.

Although present highway bridge design specifications (*5, 11*) allow the use of high-yield reinforcement in all bridge members, some restrictions are placed on the use of Grade 75 bars. In these, and the more recent report of ACI Committee 443 on Concrete Bridge Design (*12*), strength or load factor design methods have been accepted as appropriate for highway bridge design.

In a survey conducted in 1971 in connection with the research work reported herein, 21 of 36 responding state highway departments indicated that they made regular use of high-yield reinforcement. Two state highway departments indicated some use of such reinforcement. Information received did not indicate whether the reinforcement was being used in bridge superstructures or only in support structures.

High-yield reinforcement suffered slow acceptance in American highway bridge design practice because of concern over fatigue effects, earthquake effects, cracking of bridge members, and weldability of the reinforcement. Tests have shown (*13*) that high-yield reinforcement does possess sufficient ductility for use in structures required to resist earthquake forces. Similarly, it has been shown (*14*) that proper detailing ensures adequate crack control in reinforced concrete members. The problem of weldability of reinforcement can also be alleviated (*15*) by means of good detailing and welding practice.

No fatigue fracture of the reinforcement in a reinforced concrete structure in ordinary service has been reported. However, fatigue fracture of reinforcing bars in test bridges in the AASHO Road Test (*16*) was induced by cyclic loading after the completion of vehicular traffic tests. This directed attention to the importance of fatigue considerations in bridge design.

The AASHO investigation of highway pavements and bridge structures required two full-scale reinforced concrete T-beam bridges to be subjected to repeated passage of heavy

vehicular traffic. Intermediate grade deformed reinforcing bars were used in these bridges. Deck reinforcement consisted of No. 4 bars in the longitudinal direction and No. 5 bars in the transverse direction. The beams were reinforced with No. 9 and No. 11 bars.

The highest levels of reinforcement stress in these bridges were obtained in the No. 11 bars. At midspan in each bridge, dead-load stresses in the reinforcement of the exterior beams reached approximately 22 ksi. Corresponding live-load stresses, caused by a single passage of a test vehicle, reached approximately 23 ksi. Each bridge was initially subjected to about 550,000 passages of the test vehicles. No fatigue distress was evident in these bridges at the conclusion of the vehicular traffic tests.

Each bridge was then subjected to accelerated fatigue loading by means of a mechanical oscillator. This loading simulated the average reinforcement stress condition observed at the critical section during the vehicular traffic tests. After about 170,000 cycles at this loading, fatigue fracture occurred in two No. 11 bars in an exterior beam of each bridge.

The fatigue life of these bridges was much less than that considered desirable in bridge design. However, the loading applied by the 107,000-lb test trucks far exceeded that normally encountered in highway traffic. Thus the maximum stress of approximately 45 ksi in the reinforcing bars that fractured in fatigue was greater than that expected to occur repeatedly in bridges. On the other hand, the live-load stress range of approximately 23 ksi is more significant in fatigue considerations than the maximum stress of 45 ksi. Because bridges designed with high-yield reinforcement could have reinforcement stress ranges greater than 23 ksi, the fatigue strength of the reinforcement could be a limiting design consideration.

Objectives

The principal objective of this investigation was the gathering of fatigue test data for Grade 60 reinforcing bars in an experiment designed and executed to permit a valid statistical appraisal of the fatigue-influencing factors. The investigative work was conducted in two phases. In Phase I, major emphasis was to be placed on the evaluation of the effects of the following variables:

1. Stress range.
2. Minimum stress, including reversal of stress.
3. Bar diameter.

Other factors to be included in the experiment were:

1. Type of specimen.
2. Grade of bar.

In Phase II, the major emphasis was placed on determining the influence of bar geometry on fatigue strength.

RESEARCH PROGRAM

Experimental Investigation

A total of 231 fatigue tests on deformed reinforcing bars of a single deformation pattern were scheduled in the main part of Phase I of the test program. Each test was conducted on a rectangular or T-section concrete beam containing a single straight bar as the main reinforcing element.

The tests were arranged into 31 groups of 7 tests each, except for Group No. 1 which consisted of 21 tests. In Group No. 1, the greater number of tests served to establish the reliability of the individual group results. In essence, the Group No. 1 test series was equivalent to three of the regular group test series.

Stress range * was the only intended variable within a group. Tests were carried out at five nominal stress range levels to obtain, for each group of tests, a curve relating stress range, f_r, and fatigue life, N. Such curves are commonly called S-N curves (*17*). Information about the reproducibility of within-group test results was obtained by conducting three tests in each regular group at a common nominal stress range.

A representative S-N curve for steel is shown in Figure 1. This curve shows the effect of stress range on fatigue life for a constant minimum stress. In the present research program, all tests were scheduled in the finite- and long-life regions. Phase I tests were carried out at three stress ranges in the finite-life region and two stress ranges in the long-life region.

Minimum stress level in the test bar, bar size, grade of bar, and type of specimen, as represented by the effective depth of the test beam, were varied one at a time from one group to another. Thus, an individual S-N curve was obtained for all tests on beams containing test bars of a particular size and grade at a prescribed effective depth and subjected to a given minimum stress.

Nominal minimum stress levels of 6-ksi compression, 6-ksi tension, and 18-ksi tension were used in the Phase I test program. These minimum stress levels represent respectively −0.1, 0.1, and 0.3 of the nominal tensile yield strength of Grade 60 reinforcing bars. They were selected to reflect the range of minimum service moment stresses that might be expected in reinforced concrete bridges.

Reinforcing bars tested were No. 5, 6, 8, 10, and 11 deformed bars of Grades 40, 60, and 75. The smaller size bars are commonly used in bridge deck slabs while the larger sizes are commonly used in girders and other main members. Special emphasis was placed on the testing of No. 8 Grade 60 bars.

Each test beam had an effective depth of 6, 10, or 18 in. Those having an effective depth of 6 in. represented conditions found in a bridge deck slab. Deeper beams simulated conditions found in the main members of a bridge.

Whenever a test bar survived 5 million cycles of stress, that test was terminated as a runout. A new test, called a rerun test, was then initiated, using the runout specimen. In the rerun test, the reinforcing bar was subjected to a stress range known to result in fatigue fracture of the test bar.

---

* Terminology used in this report follows, insofar as possible, the recommendations of ASTM Committee E-9 on Fatigue (*17*). Stress range, f_r, is the algebraic difference between the maximum, f_{max}, and minimum, f_{min}, stresses in one cycle. Fatigue life refers to the number of cycles of stress, N, that a given specimen can sustain before fracture occurs. Fatigue strength refers to the value of stress range at which 50 percent of the specimens of a given sample could survive N stress cycles, when subjected to a given minimum stress.

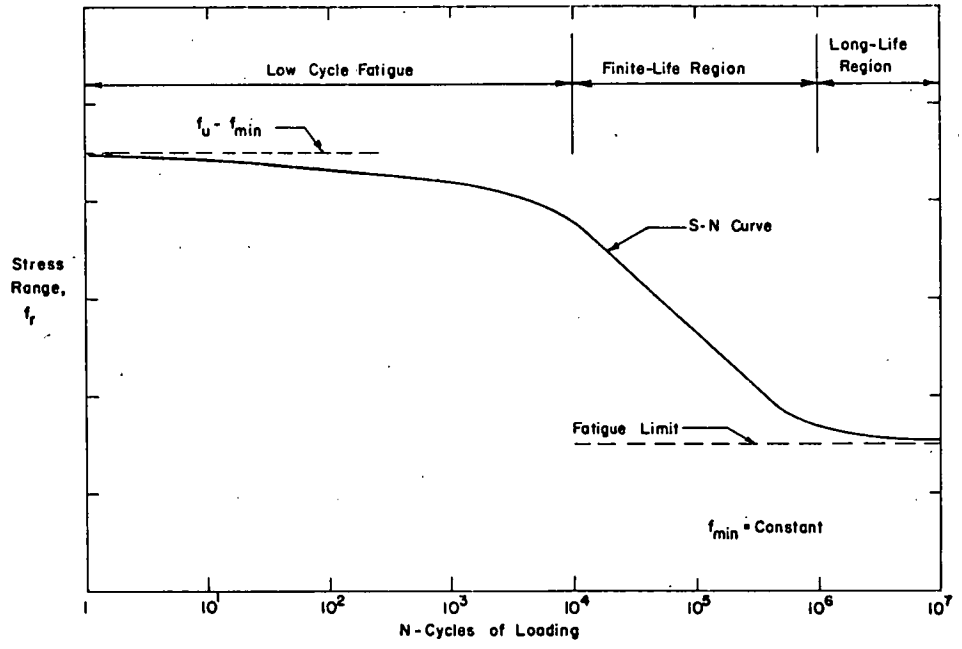

Figure 1. Representative S-N curve for steel.

Properties of the concrete used for each test beam were determined. Concrete strength and modulus were obtained from cylinder tests carried out on the day the fatigue test was started.

Several properties of the test bars were determined. Elongation, and the yield and tensile strengths of each test bar were obtained from tests on bar coupons. The chemical composition and hardness of samples of each size and grade of bar were determined. Longitudinal sections of samples of each size and grade of bar were used to study the microstructure of the steel and to determine the geometry of the rolled-on transverse deformations.

In Phase II of the test program, No. 8 Grade 60 bars from five different manufacturers, designated by the letters A to E, were tested. Four of the manufacturers' bars were selected in a survey of such bars commonly used by state highway departments. Selection criteria centered on obtaining a wide range of transverse lug geometries, as represented by the lug base radius to lug height ratio, r/h. To preserve continuity in the test program, bars used in Phase I of the test program were added as the fifth selection in Phase II. The bars selected for the research program are shown in Figure 2.

A total of 105 tests were originally scheduled to be carried out in Phase II. Each test was conducted on a T-section concrete beam containing a single straight deformed bar as the main reinforcing element. Each test beam had a nominal effective depth of 10 in.

The scheduled Phase II test series was divided into two parts, each composed of five groups of tests, one for each manufacturer's bars. Stress range was the only intended variable within a group. A nominal minimum stress level of 6-ksi tension was used throughout.

Each group in the first part of the Phase II test program was scheduled to consist of 12 tests. These were intended to result in an estimate of the mean fatigue limit at 5 million cycles for each manufacturer's bars. For this purpose, a staircase test procedure (*17*) was used. This procedure allows a statistical evaluation of the mean fatigue limit.

In the second part of the Phase II test program, each group consisted of nine tests. These tests were carried out at three nominal stress range levels and were intended to provide information about that part of the S-N curve where the fatigue life depends strongly on the applied stress range, the finite-life region.

The Phase II program also included a limited study of fatigue crack growth. For this purpose, an eleventh group, consisting of three tests was included in the Phase II test series. These tests were carried out at a common stress range, on bars from a single manufacturer, and were terminated after 100 thousand, 200 thousand, and 300 thousand cycles of applied loading, respectively. Each reinforcing bar was subsequently removed from the test beam and tested in static tension to determine the extent of fatigue damage.

As in Phase I, runout tests at 5 million cycles were terminated. They were then rerun as new tests at the regular finite-life stress range levels. These rerun tests were intended to allow the effect of prior cycling to be determined by comparison with the regular finite-life tests.

Mechanical properties of the test beam concrete were determined from cylinder tests, as was done in Phase I. Similarly, the tensile properties of each test bar were determined in tests on bar coupons. Supplementary tests for chemical composition, hardness, and microstructure properties were carried out on samples of each manufacturer's bars.

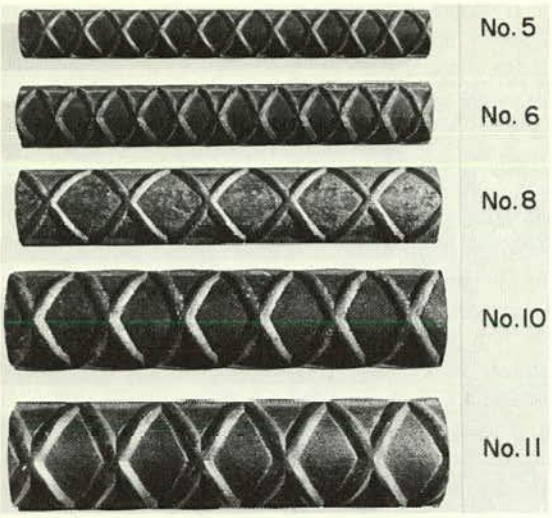

Phase I Test Bars, Grade 60, Manufacturer A

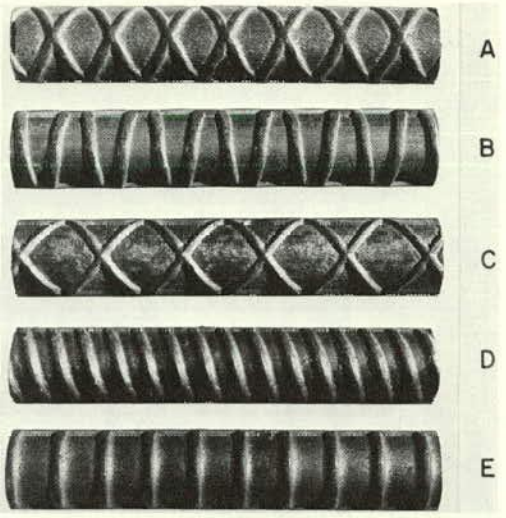

Phase II Test Bars

Figure 2. Reinforcing bars used in test program.

Geometry of the rolled-on transverse deformations of the test bars, as represented by the lug base radius to lug height ratio, was evaluated by three different techniques. Estimates of the critical lug geometry were made by stereomicroscope examination of the bar surface and measurement on photographs of longitudinal sections of bar samples and of sectioned plaster casts of bar samples.

Statistical Analysis

The Phase I test program was designed to allow the gathering of finite-life data from various groups into factorial designs (*18*). Four basic factorial designs, in two and three factors each, allowed the individual effects of the basic test variables and their interactions to be evaluated. Stress range was the third factor in each of these designs.

The Phase II test program was designed to allow an evaluation of the mean fatigue limit at 5 million cycles for each manufacturer's bars by means of a staircase analysis. It was further designed to allow an evaluation of the difference in fatigue strength among the various manufacturers' bars when tested in the finite-life region.

IMPLEMENTATION OF THE RESEARCH PROGRAM

A review of the literature pertinent to the fatigue properties of reinforcing bars was carried out. Previous fatigue studies provided guidance for the implementation of the test program and for the interpretation of the resulting data. Conversely, previously published data were reevaluated in view of the present experimental results.

A full account of the literature review is presented in Appendix A.

Experimental Investigation

In order to obtain a statistically valid experiment free from bias due to personnel, test procedures, and test equipment, the test program was randomized as far as possible. Use of reinforcing bars of a certain size and grade from the stock of bars for a particular manufacturer was fully random. The order of testing was randomized in each phase of the test program.

Each test bar was embedded as the main reinforcing element within a rectangular or T-shaped, single-span concrete beam. Appropriate shear reinforcement and stirrup support bars were placed in each shear span. Concentrated loads were applied to each beam at about the third points of the span. A representative test beam, ready for the application of dynamic loads, is shown in Figure 3.

A nominal effective depth of 6, 10, or 18 in. was used for each test beam. Stem width of the T-shaped beams was 6 in. This was also the width of the rectangular beams. Flange width of the T-beams was varied with the size of the test bar to maintain a uniform depth to the neutral axis for beams having the same effective depth. Flange depth was varied among beams of different effective depths to retain the neutral axis within the flange.

Length of the test beams was varied with the size of the test bar and the effective depth of the beam. A constant moment region of uniform length was maintained for all test beams within a single group. However, the length of each shear span was increased for some tests within a group to preclude any possibility of bond fatigue failure.

Test beams were cast in concrete forms lined with plastic-coated plywood. Concrete was mixed using Type III portland cement, Elgin sand, and ¾-in. maximum size, normal weight, stone aggregate. Design compressive strength of the concrete was 5,000 psi in 14 days. Slump of the concrete was from 2 to 4 in. Three 6 × 12-in. cylinders were cast from the batch placed between the load points of a beam.

After casting, the test specimens were stored under plastic cover for three days. They were then removed from their forms and stored in the laboratory, where temperature and humidity were maintained at 70 F and 55 percent, respectively.

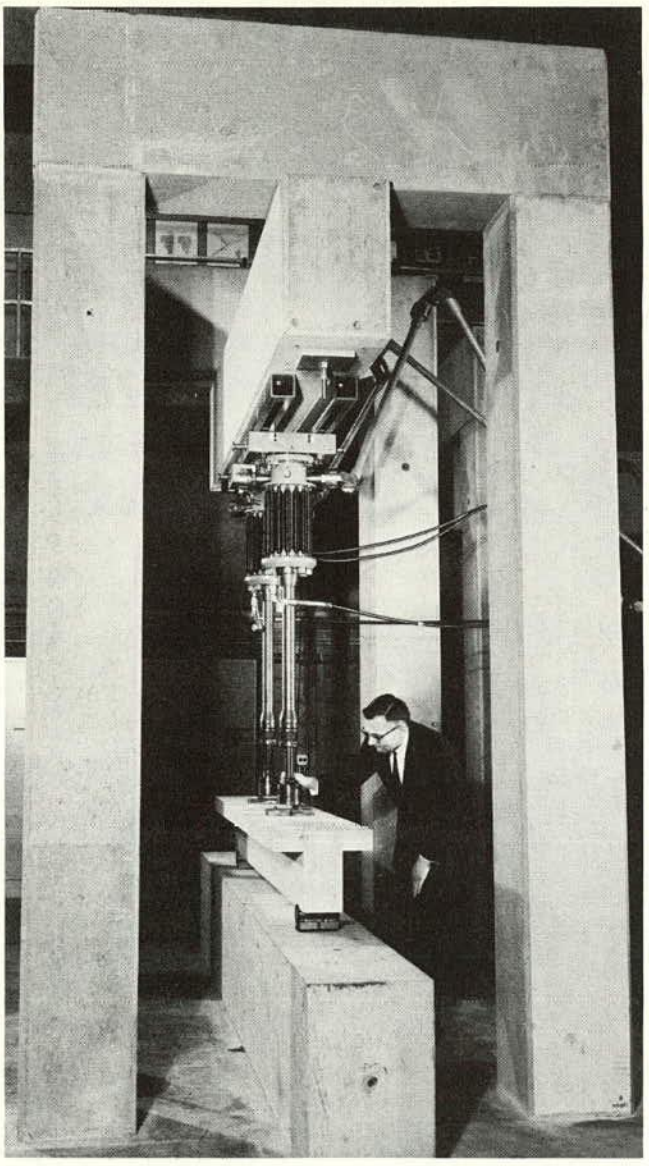

Figure 3. View of a test setup.

Tests were carried out in two reaction frames. Each frame was constructed from precast concrete members that were bolted together and post-tensioned to the laboratory test floor. The test beams were supported on a heavy concrete base. One of the test setups is shown in Figure 3.

Loads were applied to the test beams by means of Amsler hydraulic rams. One or two rams were used to apply load to each beam. When only one ram was used, a spreader beam distributed the load equally to the loading points.

Amsler pulsating-load equipment (*19*) applied a sinusoidally varying load at either 250 or 500 cycles per minute. The loads were set by means of precalibrated oil pressure gages.

Midspan deflection of the test beams was measured with a dial gage and a cantilevered steel rod on which an electric resistance strain gage was mounted. Output from the strain gage was recorded on a Sanborn continuous strip chart recorder (*19*). Deflections were measured to the nearest 0.001 in.

All tests were scheduled to begin when the test beam concrete was 14 to 30 days old. Some tests were initiated a few days earlier or later than scheduled. All tests were carried out in a predetermined random order except the initial and final tests in Group No. 1 and the tests for the study of fatigue crack growth.

Loads to be applied to each test beam were predetermined in the testing order, except for tests carried out in the long-life region. In each case, the loads were assigned in a random manner. In Phase I of the test program, the loading was intended to produce a minimum stress of −6, 6, or 18 ksi and a stress range of 36, 48, or 54 ksi in the bars tested in the finite-life region. In Phase II, a minimum stress of 6 ksi and stress ranges of 34, 44, or 54 ksi were intended.

Two long-life tests were carried out in each group in Phase I of the test program. Stress ranges of about 24 and 25 ksi, respectively, were intended in these tests. However, the stress range for the second of these tests to be carried out was often adjusted to reflect the fatigue life observed in the first test.

Loads on beams tested in the staircase part of Phase II of the test program depended in each case on the result obtained in the immediately preceding test in the appropriate staircase test series. A runout at 5 million cycles in a particular series resulted in a one-step increase in stress range for the succeeding test in that series. Conversely, a fatigue fracture in a test bar resulted in a one-step decrease in stress range for the succeeding test. A nominal step size of 1 ksi was used throughout.

Initially, three cycles of static loading to the desired stress levels were applied to each test beam. A dynamic correction to the applied loads was calculated from the observed deflections during these three cycles. At the conclusion of the static load cycles, each test beam was subjected to dynamic loading at a rate of 250 or 500 cycles per minute. Often the dynamic loading was interrupted after several thousand cycles of loading in order to monitor the dynamic correction. In each case, dynamic loading was continued until fatigue fracture of the test bar occurred or the bar had survived 5 million cycles of stress.

When the minimum stress in a test bar was intended to be 6-ksi compression, external post-tensioning was applied to the test beam during the first static load cycle. The post-tensioning system consisted of a pair of steel rods held at the level of the beam reinforcement and passed through steel springs butting against one end of the test beam. The pre-stress force was measured by load cells.

Runout tests were terminated after 5 million cycles of loading. The test beam was then given a new test number and subjected to additional cycles of loading at one of the finite-life stress range levels until fatigue fracture of the test bar occurred.

After fracture of a test bar had occurred, the location of the flexural tension cracks in the test beam and the dimensions of the beam at the location of the fracture were recorded. These cross-sectional dimensions were subsequently

used in calculating the stress levels to which the test bar had been subjected.

Pieces of the test bar containing the fracture region were removed from the broken test beams. Cross-sectional dimensions of the test bars were subsequently determined from these pieces. An examination of the fractured face of the test bar was also carried out and the location of the primary fatigue crack nucleus determined.

Compressive strength and modulus of the test beam concrete were determined on the day that each fatigue test was started. The static mechanical properties of each test bar were also determined. Furthermore, material properties such as chemical composition and Vickers hardness were obtained from samples of selected test bars.

The critical lug geometry of samples of each size and grade of bar tested in Phase I of the test program was determined from photographs of lug profiles. These lug profiles were obtained by longitudinal sectioning of the bar samples. A similar, but more refined, procedure was used to determine the critical lug geometry of each manufacturer's bars in phase II of the test program. The lug geometry of the Phase II test bars was also evaluated by stereomicroscope observation of the bar surface and by means of photographs of lug profiles obtained from sectioned plaster casts of bar samples.

In Phase I of the test program, fatigue tests were carried out on machined specimens of samples of the No. 8 Grade 60 test bars. In Phase II, static tension tests were carried out on specimens removed from test bars that had fractured in fatigue.

At the conclusion of the scheduled tests in each phase of the test program, a few additional fatigue tests were carried out. Some of these tests were replacements for tests that had been terminated due to fatigue fracture of the test beam concrete. Other tests replaced those where some deviation from the intended test procedure had occurred. A few tests were added to obtain further test data in Phase I groups where the long-life test results were considered incomplete. Finally, several unscheduled tests were required in Phase II of the test program to "zero in" on each staircase test series. Thus, a total of 353 fatigue tests were carried out, 236 in Phase I and 117 in Phase II.

A detailed description of the experimental program and the test procedures used in its execution is presented in Appendix B.

Statistical Analysis

In the statistical analysis of the test data, a distinction was made between finite-life and long-life data. Because Phase I of the test program was not specifically designed for the study of long-life data, a convenient separation point between the two kinds of data was found to be at a stress range of 28 ksi. Tests carried out at a stress range in the test bars greater than 28 ksi were regarded as resulting in finite-life data. No statistical analysis of the Phase I long-life data was possible.

In Phase II of the test program, five groups of tests were intended to result in finite-life data and another five groups in long-life data. However, the long-life groups included some finite-life tests. These were needed to "zero in" on each staircase test series. Such tests were included in the staircase analyses but were excluded from the finite-life data analysis.

No rerun tests were included in the analysis of the finite-life data. Rather, these tests were considered separately. Most tests where the fatigue crack had been initiated at a manufacturer's bar identification mark were included in the statistical analysis. A single rerun test was omitted. All tests where yielding of the test bar had occurred were included in the finite-life data analysis. All but one of the tests where some deviation from the specified test conditions had occurred were included in the finite-life data analysis. However, they were excluded from the analysis of the factorial designs. These tests received special attention throughout the analysis.

Continuity between the two phases of the test program was established prior to the finite-life data analysis. This was done by testing the homogeneity of the Group No. 1 and Group No. 33 finite-life data in an analysis of covariance (*20, 21*). Each of these groups consisted of tests on No. 8 Grade 60 bars from Manufacturer A but belonged to separate phases of the test program.

Validity of the statistical procedures used was established by testing the three fundamental assumptions on which these procedures were based. Randomness of the statistical sample was established by the extensive randomization carried out in the test program. Log-normality of the population of finite-life data was tested by means of the W-test (*22, 23*), probability plotting (*18, 22*) and the chi-square test (*18, 24*). Constancy of variance of the observed finite-life region fatigue lives was tested by probability plotting, Bartlett's test (*20, 25*), and Hartley's test (*26, 27*). Furthermore, the assumption that the finite-life relationship between stress range and the logarithm of the number of cycles to fracture may be expressed by a straight line was tested by partitioning (*20*) of sums of squared deviations about several regression lines.

The effects of the Phase I test variables were studied in four basic factorial designs (*18*). The two factor designs studied were effective depth versus bar diameter, minimum stress level versus bar diameter, grade of bar versus bar diameter, and minimum stress level versus effective depth. In further analysis, stress range was used as the third factor in each of these designs. An analysis of variance (*18, 20*) of each of these factorial designs allowed the individual effects of the variables and their interactions to be studied.

All of the Phase I finite-life data admitted to the statistical analysis were studied as a single whole by means of a stepwise multiple linear regression (*28*). All of the Phase I test variables were entered in the regression, as were those interaction terms that could not be totally rejected in the analysis of the factorial designs.

The effect of bar geometry on the fatigue life of reinforcing bars was studied in separate finite- and long-life analyses of the Phase II test data. Finite-life test data were studied in an analysis of covariance (*20, 21*) while the long-life data were evaluated by a staircase analysis procedure.

None of the available techniques for studying staircase series data were applicable to the observed fatigue data. This was due to the irregular step size obtained in the tests.

For this reason, a procedure capable of estimating the mean value and standard deviation of a staircase series having a variable step size was developed.

Following the study of bar geometry effects, an over-all analysis of the finite-life data obtained in both phases of the test program was performed. The stepwise, multiple linear-regression procedure was used. Variables considered in the regression were those found to be significant in the previous multiple linear regression, along with a bar geometry variable and any other untested variables considered to have had a potential effect on the fatigue life of the test bars.

The effect on the rerun test bars of having previously been subjected to 5 million cycles at a low stress range was considered for the Phase II rerun data. This analysis was performed by testing rerun data regression lines for union (*20*) with regular finite-life data regression lines.

Tolerance limits (*18, 29*), under the Phase II test conditions, were established for each manufacturer's bars. In addition, tolerance limits were established for the finite-life test conditions of the bars tested in Phase I of the test program.

A full account of the statistical procedures used in analyzing the test data is presented in Appendix C.*

* Descriptions of the major computer programs used in the statistical analysis can be obtained from the Program Director, NCHRP.

CHAPTER TWO

FINDINGS

LITERATURE REVIEW

Considerable research to determine the fatigue properties of reinforcing bars has been carried out in recent years in North America, Europe, and Japan. Much of this research has a direct bearing on the fatigue influencing factors investigated in the present work. These research investigations and other investigations into the general fatigue properties of metals, relevant to the present study, are reviewed in detail in Appendix A.

Unfortunately, much of the previously reported research work on reinforcing bars does not easily lend itself to quantitative evaluation of the effects investigated. Thus, the separation of the effects of two or more fatigue-influencing factors, in a small experiment intended for a comparative evaluation of a single effect, often proved to be impossible. For instance, an experiment to determine the effect of bar size on fatigue strength would not take into account the effect of a difference in yield strength or a difference in lug geometry among the various size bars tested.

Most of the fatigue investigations reviewed were not designed for statistical evaluation of the test data. In an experiment where several factors may influence the outcome of the tests, a statistical experimental design and analysis are the only means whereby the effects under study may be separated and quantified.

Many of the fatigue tests reported were concerned with either determining the fatigue limit at 2 million cycles or comparing the effects of various factors influencing the fatigue limit at 2 million cycles. Tests in this region of the S-N curve result in highly scattered data and require sophisticated experimental design and analysis for proper evaluation. For this reason, such test series were generally not given much weight in the conclusions derived from the literature study.

It was observed during the evaluation of the previously published test data that the effect of a fatigue-influencing factor will often show up in both the finite- and long-life fatigue regions. Since the natural scatter in fatigue data with stress range is least in the finite-life region, an effect will usually be much more clearly defined in that region of the S-N curve.

Effect of Stress Range

Stress range was found to be the predominant factor influencing fatigue strength in the finite-life region. The effect of stress range on the fatigue life of selected North American reinforcing bars (*30, 31*) is shown in Figure 4. The S-N diagrams shown represent a visual judgment of the variation in fatigue life with stress range.

Deformed No. 8 and No. 11 reinforcing bars of Grades 40, 60, and 75 and of three different deformation patterns are represented in Figure 4. They were tested as embedded within reinforced concrete beams and were, in each test series, subjected to a constant minimum stress level that ranged from 5 to 24 ksi from one test series to another. The difference in the S-N diagrams is therefore attributable to the effects of minimum stress level, bar diameter, grade of bar, and lug geometry.

In the long-life region, the effect of stress range on fatigue life is greatly diminished. Several investigators (*32-34*) have conducted tests on reinforcing bars for up to 10 million cycles of loading without obtaining fatigue fracture of their specimens. It therefore appears that, for design purposes, reinforcing bars may be considered to possess a fatigue limit.

In Figure 4, the logarithm of fatigue life is seen to vary linearly with stress range in the finite-life region. Although

each S-N diagram represents only an estimate of the actual fatigue properties, it is evident that the effects exhibited in the finite-life region are often carried over into the long-life region.

At high stress range levels, when the maximum stress approaches the tensile strength of the bar, the effect of stress range on fatigue life is again diminished. Only limited testing of reinforcing bars has been carried out at such stress ranges (*35*).

Effect of Minimum Stress Level

Some investigators (*36, 37*) have argued that the minimum stress level has no significant effect on the fatigue strength of reinforcing bars. Others (*30, 38, 41*) indicate that a minimum stress effect is present in their data. Opinions to the contrary seem to have arisen due to the difficulty of separating the effects of other factors masking the effect of the main test variable.

Careful examination of published test data for reinforcing bars indicates that an increased minimum stress results in lowered fatigue strength in both the finite- and long-life regions. Where test data from the finite- and long-life regions are available for the same bar, the effect is seen to be of about equal magnitude for both regions.

Effect of Bar Diameter

Several authorities (*42-45*) agree that specimen size has an effect on fatigue strength. This effect shows up as a gain in fatigue strength with a decrease in the diameter of a test specimen. It is attributed to the additional working of the material to produce smaller size pieces and a statistical size effect related to the probability of finding a critical flaw on the surface of the material.

Previous research (*38, 40, 46*) on the effect of reinforcing bar size on fatigue strength was concerned with determining the fatigue strength at 2 million cycles. A study of the reported test results reveals an increase in fatigue strength as the bar diameter is decreased. However, the relationship is not clearly defined by the test data.

The effect of bar size is influenced by the strain gradient across a bar encased within a concrete beam subjected to bending. For equally stressed bars, in beams of equal effective depth, a steeper strain gradient is obtained within beams having greater depth to the neutral axis. This strain gradient causes the maximum cross-sectional bar stress to be found on the side of the bar farthest from the neutral axis. Thus, the larger the bar diameter, the greater is the difference in stresses across the bar for the same strain gradient.

Due to the strain gradient, the fatigue strength of a reinforcing bar embedded within a concrete beam subjected to bending will be affected by the orientation of the bar within the beam. Orientation of the test bar was a controlled variable in one test series (*31*). A lower fatigue strength was obtained when the longitudinal ribs of the test bars were located in a vertical plane within the test beams than when they were in a horizontal plane. Apparently, the critical fatigue zone on the periphery of the test bars was near the function of the longitudinal ribs with the transverse lugs.

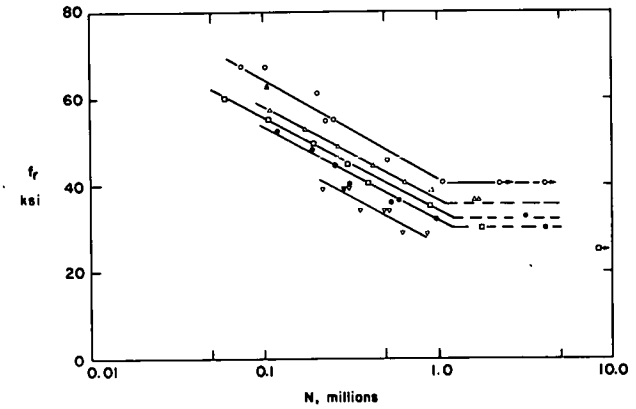

Figure 4. Representative fatigue test results for North American bars.

Effect of Grade of Bar

Previous tests on reinforcing bars of various grades have resulted in divergent opinions as to the effect of steel quality on fatigue strength. Results from three investigations (*30, 47, 48*) show an increase in fatigue strength for the higher grade bars. Other researchers (*38, 40, 46, 49*) have concluded that grade of bar has only slight or no effect on the fatigue strength of reinforcing bars.

On the basis of the reported test results, it was concluded that fatigue strength is increased for the higher grades of bar. However, no regular trend could be observed. This may be due to masking of the effect of the main test variable by other fatigue-influencing factors.

Effect of Type of Specimen

The fatigue test results studied in the review of the literature were obtained using a variety of test methods. Fatigue tests on reinforcing bars have been conducted in flexure on bar coupons in air, axial tension on bar coupons in air, axial tension on concrete-encased bar coupons, and on bars embedded within concrete beams of three types. It is not known to what extent the test results may have been influenced by the test conditions since no comparative test results are available. However, actual service conditions in highway bridges are simulated most closely when the test bar is embedded as the main reinforcing element in a concrete beam subjected to bending.

Effect of Bar Geometry

Stress concentrations are a primary factor in the initiation of fatigue cracks. Rolled-on transverse deformations for improving bond characteristics cause stress concentrations in a reinforcing bar. The severity of the stress concentration effect is not known due to the complex state of stress at a transverse lug. However, a ratio of lug base strain to bar surface strain as high as 1.82 has been measured (*50*) on a reinforcing bar.

Theoretical studies of the stress concentration effects of external notches have been carried out (*50, 51*). Sharpness of the lug base radius was considered to be the most critical factor in causing stress concentrations. Lug width, height, and flank angle were also judged to be important.

Fatigue tests have been carried out (*30, 48*) on bars that were nominally identical except for their deformation patterns. Large differences in fatigue strength were observed in both the finite- and long-life regions. No measurements were made of the lug geometry in one of these investigations (*30*). In the other (*48*), the accuracy of the reported measurements could not be confirmed for lack of detailed information.

The effect of wear of the rolls in producing more smoothly shaped lugs has also been investigated (*48, 52*). An increase in fatigue strength in both the finite- and long-life regions was observed for bars produced after the rolls had become worn. However, the effect was not consistent, being large for one set of bars and relatively small for two others.

Other Effects

Various properties of reinforcing bars, imparted during the manufacturing process, may have an effect on fatigue strength. Among these manufacturer-related fatigue influencing factors are chemical composition, decarburization, mill scale, inclusions, surface deformations, residual stresses, and bar coatings. Some of these are interrelated. Others also relate to the previously discussed effect of grade of bar.

The chemical composition of the steel used in reinforcing bar manufacture affects the fatigue strength of the base metal in proportion to the effect on tensile strength. The benefits due to an increase in carbon content are, however, partially negated by increased decarburization and the formation of mill scale. Decarburization leads to a structural weakening of the bar surface metal and thus to earlier fatigue crack formation than the strength of the base metal would indicate. Stress concentrations will arise at surface pits caused by rolling mill scale into the bar surface during the hot-rolling process. Metallic inclusions in the reinforcing bar steel may also cause stress concentrations.

Residual stresses in the surface of cold-twisted reinforcing bars will affect their fatigue strength. Moderate amounts of cold twisting were found (*53*) to be beneficial but further twisting resulted in decreased fatigue strength. Some indication was found that stressing Grade 40 bars having a long yield plateau beyond yield caused a decrease in fatigue strength (*30*). Galvanization of reinforcing bars may also set up residual stresses at the bar surface. The effect of these stresses on fatigue strength is not known.

Investigations into the effects of some detailing practices on fatigue strength have been carried out. The effects of bending a bar, tack-welding of stirrups to the main reinforcement, and joining bars by welding have been studied.

Tests on specially constructed concrete beams, each containing a single bent bar as the main reinforcement, have been carried out by several investigators (*30, 36, 38*). A greatly reduced fatigue strength in both the finite- and long-life regions was observed (*30*) in bars bent around a 6-in. mandrel. The sharper the bend, the greater was the reduction in fatigue strength (*30*). However, due to the type of specimen used, these tests cannot be considered representative of the conditions to which a bent-up bar in an ordinary reinforced concrete beam is subjected.

Fatigue tests on heavy girders containing bent-up bars as part of the reinforcement have been reported (*54, 55*). Since fatigue fracture of the bars occurred away from the bends, they were not considered to have had a detrimental effect on the fatigue strength of the bars.

The effect of tack welding of stirrups was determined (*31*) in tests on beams having either welded or wire-tied stirrups. Careless field practice in arc welding was simulated in these tests. Tack welding was found to cause a large reduction in both the finite- and long-life fatigue strength of the main reinforcing bars.

Tests on welded joints in reinforcing bars (*15*) and on joints in welded bar mats (*35*) have been carried out. In both cases, the fatigue strength was considerably reduced from that of unwelded bars. However, the type of joint in welded bar splices (*15*) was found to have a large effect. A 60-degree single-V butt joint was found to have the best fatigue characteristics.

EXPERIMENTAL INVESTIGATION

A summary of the test results directly obtainable from the experimental investigation is presented in this section. Results obtainable only through extensive data analysis are presented in the following section. A detailed description of the test procedures used in the experimental investigation and a fuller account of the material covered in this section are presented in Appendix B.

Mechanical Properties of Test Bars

The yield strength, tensile strength, and elongation of each bar tested in fatigue were determined in tests on bar coupons. Average values of these tensile properties are listed in Table 1 for each type of bar tested.

Two different measures of yield strength are listed in Table 1. According to ASTM A615 (*1*), yield strength was determined from the yield plateau, and at 0.5- and 0.6-percent strain, respectively, for the Grades 40, 60, and 75 bars. ACI 318-71 (*4*) allows the yield strength of Grade 60 and stronger bars to be determined at 0.35-percent strain. This procedure was also used for the Grade 40 bars.

The two measures of yield strength are seen to provide nearly identical results for the Grades 40 and 60 bars, except for the No. 6 Grade 60 bars. The difference in results for the No. 6 Grade 60 bars and for the Grade 75 bars is due to a short or nonexistent yield plateau and rapid onset of strain hardening.

The yield strength of test bars of the same grade is seen to vary considerably, as much as 18 percent for the Grade 60 bars. The variation in tensile strength is similar in magnitude to that of yield strength. Elongation of the test bars is seen to decrease with grade of bar and to vary widely for bars of the same grade.

Vickers hardness was measured on transverse sections of samples of No. 8 Grade 40, Grade 60, and Grade 75 bars from Phase I of the test program and on samples of each manufacturer's bars from Phase II. The average hardness obtained is listed in Table 1. It is seen in Table 1 that the hardness of the test bar steel varies with the grade of bar.

TABLE 1

PROPERTIES OF REINFORCING BARS

MANUFACTURER	SIZE OF BAR	GRADE OF BAR	TENSILE PROPERTIES: YIELD STRESS ASTM [a] A615 (KSI)	TENSILE PROPERTIES: YIELD STRESS ACI [b] 318 (KSI)	TENSILE PROPERTIES: ULTIMATE STRESS	TENSILE PROPERTIES: ELONGATION (PERCENT)	CRITICAL DIMENSIONS: r/h	CRITICAL DIMENSIONS: h/w	CRITICAL DIMENSIONS: FLANK ANGLE (DEGREES)	CHEMICAL CONTENT: C (PERCENT)	CHEMICAL CONTENT: MN (PERCENT)	VICKERS HARDNESS
		40	47.8	47.6	82.6	18.4	0.29			0.41	0.72	
	5	60	69.5	67.9	109.7	13.5	0.24			0.40	1.42	
		75	87.2	77.3	118.2	10.4	0.32			0.42	1.82	
	6	60	71.4	69.4	112.1	14.3	0.25			0.40	1.57	
		40	46.1	45.8	79.0	23.1	0.21			0.41	0.89	185
A	8	60	61.6	61.4	102.0	18.0	0.33	0.50	35	0.36	1.32	262
		75	85.2	72.9	120.3	11.4	0.22			0.42	1.77	291
	10	60	59.2	58.7	102.0	17.8	0.17			0.36	1.29	
		40	42.7	42.8	77.4	25.3	0.22			0.38	0.72	
	11	60	67.4	66.1	110.6	15.5	0.26			0.36	1.32	
		75	84.7	79.1	124.5	12.1	0.20			0.43	1.73	
B	8	60	63.7	63.4	104.7	14.8	0.29	0.50	60	0.43	1.04	264
C	8	60	72.7	72.6	114.0	14.0	0.29	0.39	35	0.46	1.81	275
D	8	60	63.2	62.1	107.0	15.9	0.38	0.39	35	0.53	1.52	267
E	8	60	59.8	59.0	111.7	12.1	0.39	0.60	50	0.59	0.59	271

[a] Reference 1. [b] Reference 4.

Geometric Properties of Test Bars

The critical geometric properties of the transverse lugs on the test bars are given in Table 1. The dimensionless ratios listed are, in each case, based on the sharpest lug base radius, r, in the predominant fatigue crack nucleation zone on the periphery of the test bars, and the corresponding lug height, h, and lug width, w. Also given in Table 1 is the less acute of the two flank angles associated with the above-mentioned ratios. The values listed were obtained by measurement from photographs of longitudinal sections of bar samples.

Measurement of lug geometry by means of a stereomicroscope was not successful. Great difficulties were encountered in obtaining sufficient contrast for accurate measurement. Independent measurements by two competent observers were not always consistent.

Lug dimensions determined from photographs of sectioned plaster casts of bar samples were not considered to provide adequate accuracy. Sharp features on the lugs were generally smoothed out on the plaster casts, and difficulties were encountered in obtaining sharply defined photographs of the plaster cast features. Thus, larger lug base radii were obtained by this method than by photography of sectioned bar samples. Furthermore, the plaster had a tendency to entrap air bubbles, particularly near the bar surface. These were often difficult to distinguish from actual features on the bar surface.

The method of determining lug geometry from photographs of sectioned bar samples was found to be satisfactory. However, great care had to be exercised in preparing the sectioned bar surface for photography. All mill scale, along with burrs caused by the sectioning process, had to be removed from the bar surface and the sectioned surface carefully polished prior to photography.

The technique used in preparing sectioned bar samples for photography of the lug geometry was refined during Phase II of the test program. Therefore, of the critical lug dimensions presented in Table 1, those for the No. 8 Grade 60 bars may be considered to be the most accurate.

Material Properties of Test Bars

A spectrographic analysis of samples of the test bars was carried out. The carbon and manganese contents so determined are listed in Table 1. The Grade 40 bars, and the Grade 60 bars except those from Manufacturer C, were found to have been rolled from medium carbon steels. Bars from Manufacturer C and the Grade 75 bars were rolled from alloy steels.

The microstructure of the steel in the No. 8 Grade 60 bars was examined on photographs, magnified 325 times, of longitudinal sections of bar samples. This examination revealed a fairly uniform decarburization of the bar surface material. The depth of the decarburized layer was estimated to vary from 0.003 to 0.006 in.

Properties of Test Beams

Each bar tested in fatigue was subjected to cyclic stresses while encased as the main reinforcement within a concrete beam. In Phase I of the test program, the average strength and modulus of the test beam concrete were found to be 5,64 psi and 3,890 ksi, respectively. In Phase II these were found to be 5,310 psi and 3,490 ksi, respectively.

During cyclic loading of the test beams, the range of deflection for each specimen was found to be essentially constant. However, the minimum deflection of a test beam was found to increase continually with time. This is attributed to time dependent deformations in the beam concrete.

Generally, flexural tension cracks in the test beams were symmetrically spaced about a crack former located at midspan. Average crack spacing in the constant moment region varied with the size of the bar, the effective depth of the test beam, and the bar deformation pattern. On the average, the crack spacing was found to decrease with an increased bar size and to increase with an increased effective depth. The relationship between crack spacing and bar deformation pattern is not clear.

Stresses in Test Bars. Stresses in the reinforcing bar embedded within each test beam were calculated for forces acting at the midspan of the beam. These were considered to be the stresses causing fatigue fracture of the test bar. The fatigue fracture always occurred in the close vicinity of an externally observed flexural tension crack in the test beam concrete. Therefore, calculation of the cyclic bar stresses on the basis of a cracked beam section was justified.

Calculation of stresses in the test bars was based on the straight-line theory of flexural stress and strain given in Section 8.10.1 of the 1971 ACI Building Code (*4*). Measured material properties and dimensions of the test beams were used in calculating the response to the applied test loads.

Experimental and calculated stress levels were compared in special tests carried out on fully instrumented beams representative of the ordinary and prestressed beams used in the test program. The ratio of calculated stress range to that determined from experimentally measured strains ranged from 0.93 to 1.00. The lower value was attributed to the inability of concrete tension cracks to close fully at low minimum stress levels when the beam had only been subjected to a few thousand cycles of dynamic loading. The correlation was found to improve with the number of cycles applied.

Effect of Stress Range

An indication of the relationship between nominal levels of the test variables and the fatigue strength of the test bars is given in Figure 5. In each instance, the logarithm of the number of cycles to fatigue fracture or end of test was plotted versus the calculated stress range. The lines shown represent regression lines for the appropriate sets of data or the fatigue limit as determined by staircase series analysis. The scatter in test results shown in Figure 5 is partly due to the natural scatter observed in fatigue test results and partly to variation in the test parameters about the nominal levels.

As may be seen in Figure 5, stress range was the predominant factor influencing the fatigue strength of the test bars in the finite-life region. The most severe test condition applied occurred inadvertently during testing of a No. 11 Grade 60 bar embedded at a depth of 10 in. within the test beam. This bar was subjected to a minimum stress of 5.9 ksi and a stress range of 68.6 ksi. Fatigue fracture of the bar occurred after 24,100 cycles of loading. This test result is plotted in Figure 5.

The least severe test condition resulted in a fatigue fracture of the test bar in the long-life region or in a runout at 5 million cycles. In Figure 5, runout tests are indicated by an arrow.

The lowest stress range at which a fatigue fracture occurred was 21.3 ksi. This stress range was combined with a minimum stress of 17.5 ksi and was applied to a No. 11 Grade 60 bar embedded at an effective depth of 10 in. within the test beam. Fracture occurred after 1,252,200 cycles.

Most of the tests were carried out at a nominal minimum stress of 6 ksi and at an effective depth of 10 in. In these tests, the lowest stress range resulting in fatigue fracture was 22.4 ksi. This fracture occurred in a No. 10 Grade 60 bar after 1,958,400 cycles. In the staircase test series, a fatigue fracture was recorded after 2,989,900 cycles for a bar from Manufacturer C subjected to a stress range of 23.0 ksi.

The highest stress range at which a runout at 5 million cycles was recorded occurred in the staircase series for bars from Manufacturer E. This bar was subjected to a minimum stress of 6.1 ksi and a stress range of 31.2 ksi.

Effect of Minimum Stress Level

An increase in minimum stress was observed to result in a lowered finite-life fatigue strength. The difference in test results for nominally identical bars subjected to a compressive minimum stress of 6 ksi and a tensile minimum stress of 18 ksi is shown in Figure 5. The high scatter in test results is attributable to variation about the nominal parameter levels. This obscures the potential parallelism of the two S-N diagrams.

Generally, the effect of changing the minimum stress level from 6-ksi compression to 6-ksi tension was found to be greater than that due to a change from 6-ksi tension to 18-ksi tension. However, the possible nonlinearity of the trend cannot be confirmed without further testing at additional minimum stress levels.

The potential existence of a minimum stress effect in the long-life region could not be confirmed. The test program was not designed to provide such confirmation.

Effect of Bar Diameter

It was observed that an increase in bar diameter resulted in a lowered finite-life fatigue strength. The difference in fatigue strength among No. 5 and No. 11 Grade 60 bars subjected to the same nominal minimum stress is shown in Figure 5. The two S-N diagrams are seen to be nearly parallel.

The No. 6 bars tested were found to have the highest finite-life fatigue strength and the No. 10 bars the lowest. This nonlinear trend in the data may be due to the influence of other factors. In this connection, it should be noted that the No. 6 bars had the highest and the No. 10 bars the lowest yield strength of the Grade 60 bars from Manufacturer A. Additionally, the No. 10 bars were found to have the sharpest lug geometry.

As for the other Phase I variables, the potential existence of a bar diameter effect in the long-life region could not be confirmed.

Effect of Grade of Bar

The finite-life fatigue strength of the test bars was observed to increase for the higher grade bars. This may be seen in

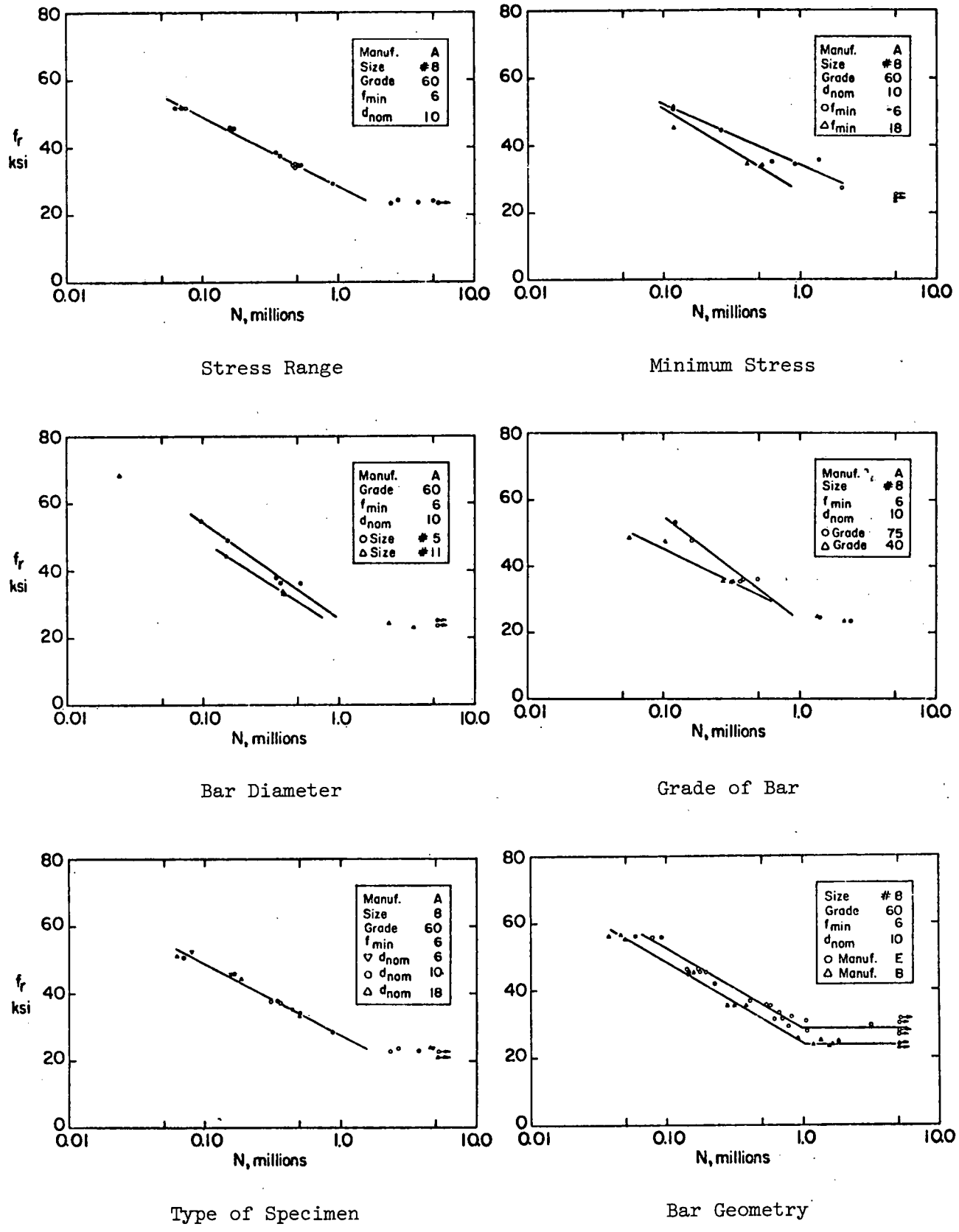

Figure 5. Effect of test variables on fatigue strength.

the comparison of test results for No. 8 Grade 40 and Grade 75 bars in Figure 5.

A large scatter in test results for the Grade 40 bars tested at a nominal stress range of 48 ksi obscures the potential parallelism of the S-N diagrams in Figure 5. In this case, both test bars were subjected to about the same stress levels, with yielding occurring in both bars. However, the yield stress of the bar having the shorter fatigue life was about 5 ksi lower than that of the other test bar. Therefore, the decreased fatigue life may be due to the excessive deformation to which the test bar was subjected.

The potential existence of a grade of bar effect in the long-life region could not be confirmed.

Effect of Type of Specimen

Plots of test results for bars in concrete beams having different effective depths showed little or no variation in finite-life fatigue strength. A representative plot of such data is shown in Figure 5. This plot shows that, in the finite-life region, no fatigue effect can be attributed to variation in effective beam depth. It is considered unlikely that the effective depth of a concrete beam will affect fatigue strength in the long-life region any more than it does in the finite-life region.

Effect of Bar Geometry

Phase II results indicated that there is considerable variation in fatigue strength among bars from different manufacturers. This variation is largely attributable to the effect of transverse lug geometry. Representative test data are shown in Figure 5. The close parallelism of the S-N diagrams in the finite-life region should be noted. It should also be noted that the difference in fatigue strength is about equal in both the finite- and long-life regions.

Bars from Manufacturer C had the lowest fatigue strength. These bars also had the sharpest lug geometry of the Phase II test bars. Conversely, bars from Manufacturer E had the highest fatigue strength and the smoothest lug geometry.

The Phase II tests confirmed the existence of a bar geometry effect in the long-life region of similar magnitude to that observed in the finite-life region. This raises the possibility that the effects of other fatigue influencing factors are similarly transferred from one region to the other.

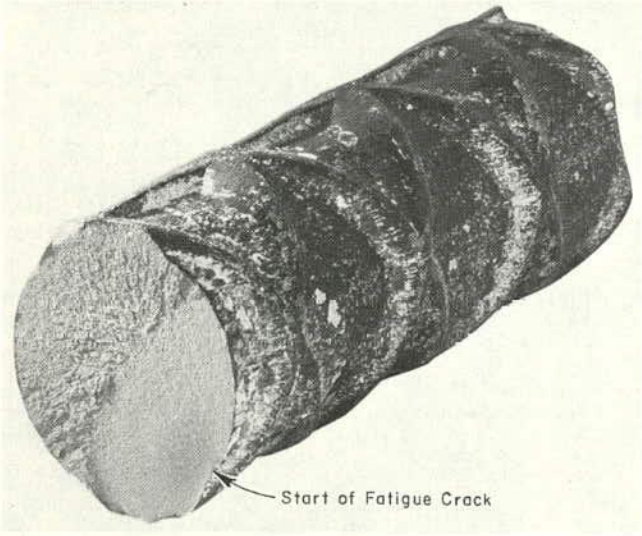

Figure 6. View of a fractured test bar.

Fatigue Fracture of Test Bars

Most of the fatigue fractures in the test bars occurred in the constant moment region between the load points of a test beam. They were distributed about the midspan, where a crack former was located in each test beam. The few fatigue fractures that occurred within a shear span were all located in the vicinity of a load point.

Examination of the fractured face of each test bar revealed a fatigue crack zone having a dull rubbed appearance and surrounded by a crescent-shaped zone generally having a rough crystalline surface. Figure 6 shows a representative fracture face for a bar from Manufacturer A. In some cases the crescent-shaped zone, associated with tension fracture of the bar, exhibited a fine-grained, dull appearance but of darker hue than that of the fatigue crack zone. Such fracture zones were often jagged with shear planes.

Most fatigue crack zones had a single focal point, the fatigue crack nucleus, where the fatigue crack was initiated. Others exhibited several fatigue crack nuclei, generally separated by beach marks. All fatigue cracks were observed to have been initiated at the base of a transverse lug or, in a few cases, the base of a manufacturer's bar identification mark. The role of the bar surface deformations in creating stress concentrations in a reinforcing bar is therefore evident.

Each fatigue crack was observed to have been initiated at a point within that half of the test bar located farthest from the neutral axis of the test beam. This points out the influence on fatigue of the strain gradient across the bar in tests of bars embedded within concrete beams. In some tests, notably those on bars from Manufacturer A, secondary fatigue crack nuclei were observed in that half of the test bar located nearest the neutral axis.

A study of the distribution of fatigue crack nuclei around the periphery of the test bars revealed that the critical fatigue zone on bars from Manufacturer A was located at an angle of approximately 45 degrees from the plane formed by the longitudinal ribs of each bar. All tests were conducted with the longitudinal ribs of the test bars located in a vertical plane, which was also the plane of symmetry for each test beam. Thus, the most highly stressed zone on a test bar was in the close vicinity of a longitudinal rib.

The primary fatigue crack nuclei on bars from Manufacturers B through E were generally located at an angle of 10 to 15 degrees from the plane of the longitudinal ribs. For these bars, few fatigue cracks were found to have been initiated at the junction of a transverse lug with a longitudinal rib. However, the potential effect of this junction on fatigue crack formation cannot be dismissed.

All fatigue crack nuclei in bars from Manufacturer C were observed to be located at the root of the vee formed

by the transverse deformation pattern at the junction with the longitudinal ribs. On the other hand fatigue crack nuclei in bars from Manufacturer A, having reinforcement with a similar deformation pattern to that of bars from Manufacturer C, were widely distributed along the transverse lugs.

An attempt was made during Phase II of the test program to measure the final radius of the fatigue crack zone in each test bar. Such data are of importance in the field of fracture mechanics. Only limited success was achieved in obtaining consistent measurements. This was due to the indistinct transition zone observed to exist, in many cases, between the fatigue and tensile fracture regions.

The average final fatigue crack radii ranged from 0.38 in. at a stress range of 54 ksi for bars from Manufacturer E to 0.76 in. at a stress range of 34 ksi for bars from Manufacturer A. The final crack radius was observed, on the average, to decrease with increased stress range. Furthermore, the average final crack radii varied considerably among the different manufacturers' bars. However, no clear relationship could be established.

Fatigue Strength of Machined Bar Specimens

In Phase I of the test program, a few axial fatigue tests were carried out in air on test specimens machined to a ¼-in. diameter from No. 8 Grade 60 bars. A minimum stress of 6-ksi tension was used in these tests. Load was applied at a rate of 1,000 cycles per minute.

A much higher fatigue strength was obtained for the machined specimens than was obtained in the regular fatigue tests on the parent bars. At 1 million cycles of loading, the increase in fatigue strength was about 35 ksi while at 100,000 cycles the increase was about 22 ksi.

A part of the observed increase in fatigue strength can be attributed to the effect of testing bars of a smaller diameter and possibly also to the difference in test method. However, the lower fatigue strength of the "as-rolled" bars is primarily attributable to the effects of transverse lug geometry, surface roughness, and surface decarburization.

Static Strength of Fatigued Bar Specimens

In Phase II of the test program, a length of bar sufficient for static tension testing was removed from the constant moment region of beams in which a fatigue fracture of the test bar had occurred near one of the load points. Most of these bar coupons exhibited a considerably lower tensile strength and elongation than was obtained in the regular static tension tests of undisturbed coupons from the same bars.

In each case where a lowered tensile strength was observed, an examination of the static tension fracture face revealed the presence of a fatigue crack. These cracks generally had a much smaller radius than that associated with the fatigue fracture obtained in the beam test. Thus, an earlier start or a more rapid fatigue crack growth at a different location on the test bar had precipitated the original fatigue fracture of the test bar. However, the fracture of these bars in the static tension tests occurred in the same abrupt, brittle manner as did the original fatigue fracture. These tests demonstrate that once fatigue crack growth has been initiated in a reinforcing bar subjected to a regular program of dynamic loading, a sudden overload may cause an unexpected, premature fracture of the bar.

Fatigue Crack Growth

A limited study of fatigue crack growth was carried out in Phase II of the test program. Three bars from Manufacturer A were embedded at a depth of 10 in. within concrete beams. Each beam was then subjected to dynamic loading resulting in a minimum stress of 6-ksi tension and a stress range of 34 ksi in the test bar. Loading of these beams was terminated after 100 thousand, 200 thousand, and 300 thousand cycles, respectively.

After the loading on each of the test beams had been terminated, an 8-ft length of the test bar was removed from each beam. These bars were then tested in static tension. Tensile strength and elongation of the bars were found to be essentially identical to those obtained for corresponding undisturbed samples.

No evidence of the formation of a fatigue crack was observed on the fracture face of any of the partially fatigued test bars. Because the mean fatigue life of these bars, for the particular test conditions used, was found to be 482,000 cycles, it must be concluded that the major part of the fatigue crack growth took place during the final 40 percent of their fatigue lives.

STATISTICAL ANALYSIS

The statistical analysis of the test data served to confirm and clarify the gross effects observable in the raw data. Only through such analysis could the various factors influencing the fatigue strength of reinforcing bars be studied simultaneously and their effects separated. Furthermore, it was only by means of statistical procedures that the effects of the various factors could be quantified. Of equal importance, statistical techniques allowed limits to be placed to the effects of the fatigue influencing factors. Such limits provide bounds for use in establishing design specifications. A full description of the statistical analysis carried out is presented in Appendix C.

Continuity in Test Program

Tests in Group No. 1 were carried out in three separate stages. Seven tests were conducted at the initiation of the test program, another seven in the main part of Phase I, and a final seven at the end of Phase I. All 21 had to be shown to represent the same population of test results.

Group No. 33 in Phase II of the test program consisted of tests on bars nominally identical to those in Group No. 1. Except for stress range, these bars were tested under nominally identical conditions. Continuity of the two phases of the experimental investigation was preserved only if these two groups represented the same population of test results.

An analysis of covariance (*20, 21*) was carried out on four sets of finite-life data, three from Group No. 1 and the fourth from Group No. 33. This analysis showed that

the four sets of data were statistically equivalent and could be represented by a single regression line rather than the individual regression lines for the four sets. Thus, test results obtained in one phase of the test program may be compared directly with those obtained in the other.

Validity of Statistical Procedures

The basic assumptions of the statistical procedures used in the analysis of the finite-life data require that the data represent a random sample of all possible test results from a log-normal population having a constant variance at all levels of the test parameters. Furthermore, linear regression analysis in the finite-life region assumes that the data may indeed be represented by a linear relationship.

In the planning and execution of the test program, every effort was made to ensure the elimination of bias through extensive randomization. Consequently, the test results are believed to be virtually free of bias.

Log-normality of the population of test results obtained from Groups No. 1 and 33 was tested by means of the W-test (*22, 23*). The approximate probability of a log-normal population was found to be 72 percent. Other statistical procedures, such as probability plotting (*56, 57*) and the chi-square test (*24, 58, 59*), confirmed this observation.

Test results from Groups No. 1 and 33 were used to test the assumption of constancy of variance with stress range. The finite-life data from these groups were adjusted by means of individual group regression lines to three common stress range levels. Probability plotting and the application of Bartlett's test (*20, 25*) to the adjusted data confirmed the hypothesis of a constant variance. After a similar adjustment of the data, further confirmation was obtained by the application of Hartley's test (*26, 27*) to all of the Phase I finite-life data used in the statistical analysis.

The finite-life test program in Phase II was designed to allow the assumption of a linear relationship between stress range and the logarithm of the number of cycles to fracture to be tested. The statistical procedure consisted of partitioning (*20*) of the squared sums of deviations about individual group regression lines. The hypothesis of a linear relationship could not be rejected, with a probability of 5 percent of being in error, for four out of the five groups of data tested. Consequently, a linear relationship was assumed to hold true for all groups of data.

Analysis of Factorial Designs

The main part of the statistical analysis was initiated by a study of the eight factorial designs contained in the Phase I test program. These classifications of the data into distinct patterns allowed the combined effects of two or three test variables at a time to be separated and studied individually. Furthermore, the effects of these variables could be studied collectively and the existence of an interrelationship determined.

Each factorial design was studied by two- or three-way analysis of variance (*20*), as appropriate. As a refinement of the two-way analysis, a technique of partitioning (*60*) the term representing interaction among the variables was used. This allowed an estimate of the underlying form of the relationship, if any, among the variables to be calculated. These functional forms were then used in further analysis of the data as a whole.

The analysis of the factorial designs showed that stress range, minimum stress level, bar diameter, and grade of bar had statistically significant effects on the fatigue lives of the reinforcing bars tested in Phase I. The existence of any effect of the effective beam depth on fatigue strength was rejected in one factorial design but was confirmed in another. A cubic equation was found to give the best representation of the effect of bar diameter.

The interaction term between bar diameter and effective depth was found to be statistically significant in one two-way design and that between bar diameter and grade of bar in another. In the three-way factorial designs, where stress range was the third factor, no interaction term was found to be statistically significant. Thus, finite-life S-N diagrams, showing the effect of different levels of a variable other than stress range, would be best represented by a series of parallel lines.

Effects of the Specified Test Variables

Following the analysis of the factorial designs, the statistically significant variables in the factorial designs were entered as potential variables in a stepwise multiple linear regression procedure (*28, 61*) applied to the Phase I finite-life data as a whole. This procedure allows each candidate variable to be considered individually on its merit in explaining the variation in the test data. Entrance of the variables to the regression is in the order of their current effectiveness in explaining the data, while full consideration is taken of previously entered variables. Entrance and exit criteria to and from the regression determine which, if any, of the candidate variables possess sufficient statistical significance for retention in the analysis.

A linearly additive mathematical model was used to describe the relationship between the logarithm of fatigue life and the various fatigue influencing factors. Thus, fatigue life would be expressed in terms of a multiple of exponential functions in the different variables. A total of 166 test results were used in this analysis of the Phase I finite-life data.

The multiple linear regression analysis showed that stress range was the most significant variable affecting the finite-life fatigue strength of the reinforcing bars tested in Phase I of the test program. Considering this effect alone, the relationship between the logarithm of fatigue life and stress range was found to be

$$\log N = 6.9690 - 0.0383\, f_r \qquad (1)$$

This relationship explained 76.8 percent of the variation in the test data. The standard deviation for the regression was 0.1657.

When the other variables showing statistically significant effects in the analysis of the factorial designs were considered, a final relationship of the form

$$\begin{aligned}\log N = {} & 4.4190 - 0.0392\, f_r - 0.0130\, f_{min} \\ & + 0.0079\, G + 7.8059\, D_{nom} \\ & - 8.4155\, D^2{}_{nom} + 2.7990\, D^3{}_{nom}\end{aligned} \qquad (2)$$

was obtained. This relationship explained 90.7 percent of the variation in the test data at a standard deviation of 0.1064.

The interaction terms found to be statistically significant in the analysis of the factorial designs were not found to describe the test results effectively when the data were considered as a whole. Other potential influencing variables, such as effective depth and the interaction terms $f_r f_{min}$, $f_r D_{nom}$, $f_r G$, and $f_{min} D_{nom}$, were considered as candidate variables in the regression. None were found to have a statistically significant effect in explaining the test data. Thus, arranged in the order of their effectiveness, only the individual effects of stress range, f_r, minimum stress level, f_{min}, grade of bar, G, and nominal bar diameter, D_{nom}, were found to have influenced the fatigue strength of the Phase I test bars.

The effect of bar geometry, as represented by the ratio of transverse lug base radius to lug height, r/h, was studied in both the long-life and finite-life regions. In the finite-life region, the effect of bar geometry was first considered individually for the Phase II data alone. This effect was then studied in conjunction with that of the other fatigue-influencing factors in a combined analysis of the finite-life data from both phases of the test program.

Analysis of the long-life test data gathered in Phase II centered on determining the mean fatigue limit at 5 million cycles and an estimate of its standard deviation. For this purpose, an analytical procedure, based on the work of Dixon and Mood (*62*), was developed.

The response distribution of each staircase test series was assumed to be the cumulative normal distribution. The probability of occurrence of each series was calculated on the basis of estimates for the values of the mean and standard deviation of the distribution. These estimates were then refined in an iterative process until convergence to the maximum probability of occurrence was obtained.

Results of the staircase analysis showed that the lowest mean fatigue limit at 5 million cycles for the Phase II test bars, under the test conditions applied, was at a stress range of 23.0 ksi. This limit applied to the bars from Manufacturer C, which had an r/h ratio of 0.29. The highest mean fatigue limit was 28.5 ksi for bars from Manufacturer E, having an r/h ratio of 0.39.

A linear regression analysis was performed on the results of the staircase analysis using fatigue limit, f_f, as the dependent variable; it resulted in the relationship

$$f_f = 7.88 + 52.85\ (r/h) \tag{3}$$

However, it is felt that this expression may place an undue emphasis on the effect of bar geometry because the effects of other potential influencing factors such as minimum stress level and yield strength could not be considered.

In the finite-life range, an analysis of covariance (*20, 21*) was used to test for parallelism among the S-N diagrams representing test results for the various manufacturer's bars. This analysis showed four of the five diagrams to be best represented by parallel lines. The exception occurred for the test results for bars from Manufacturer C. However, the different behavior of these test results may not fully reflect the pattern for these bars because the finite-life test results obtained in the staircase test series were not included in the analysis.

A multiple linear regression analysis of the finite-life Phase II test results resulted in the expression

$$\log N = 5.4391 - 0.0399\, f_r + 2.350\ (r/h) + 0.0128\, f_{y2} \tag{4}$$

In this equation, f_{y2} refers to the yield strength determined at 0.35 percent strain for each test bar. The variables are listed in the order of their effectiveness in explaining the variation in the test results. Altogether, Equation 4 explains 96.1 percent of the variation in the data at a standard deviation of 0.0719.

Two different approaches were taken in a combined analysis of the finite-life data from both phases of the test program. First, a multiple linear regression using the calculated stress levels and the nominal values of the other specified test variables was performed. Second, any variable that was considered to have a potential effect on fatigue strength was entered as a candidate in a multiple linear regression. In this latter analysis, the actual rather than nominal parameter values were used. In each analysis, a total of 211 finite-life test results were studied.

Using the first approach, the variation of the test results in terms of the nominal test parameters was most effectively explained by the expression

$$\log N = 4.7663 - 0.0392\, f_r - 0.0130\, f_{min} + 0.0077\, G + 6.4585\, D_{nom} - 7.2143\, D^2_{nom} + 2.4666\, D^3_{nom} + 0.4639\ (r/h) \tag{5}$$

This equation strongly resembles Equation 2 not only in form but also in the values of the regression coefficients. A total of 91.6 percent of the variation in the data was explained at a standard deviation of 0.1036.

The bar geometry variable, r/h, had the lowest statistical significance of the variables presented in Equation 5. Thus, it was the least effective parameter in explaining the variation in the test data. Furthermore, the magnitude of the bar geometry effect is drastically reduced from that given in Equation 4. This may reflect an uncertainty in the r/h values for the Phase I test bars because the technique used for evaluating the r/h values for the Phase II bars was considerably more refined.

In the second approach to the analysis of all of the finite-life data, several different forms of the variables previously found to be significant were tested in order to determine the best representation for the data. In addition, numerous other variables that might have had an effect on the test results were considered. This resulted in the expression

$$\log N = 6.4548 - 0.0407\, f_r - 0.0138\, f_{min} + 0.0071\, f_u - 0.1397\, D^2_{nom} + 0.0026\, Y60 + 0.3233\, D_{nom}\ (r/h) \tag{6}$$

In this equation, f_u represents the tensile strength of the test bars and $Y60$ is a "dummy" variable (*28*) representing the effect of stressing the Grade 60 bars beyond their yield strength. When the maximum stress level in the test bar was less than the yield strength at 0.35 percent strain, this variable was zero. Otherwise, it had the value $(f_{max} - f_{y2})^2$.

In Equation 6, a total of 92.5 percent of the variation in the finite-life data was explained. The standard deviation of the residuals was 0.0975. After admission of the first four variables in Equation 6 to the regression, a better fit to the test data was already achieved than was obtained by the regression on all seven of the variables contained in Equation 5.

The tensile properties of the reinforcing bars were entered as candidate variables in the regression. Tensile strength, f_u, was found to be more effective in explaining variation in the test data than yield strength. Three different measures of yield strength were used in this analysis. These were the ASTM (*1*) yield strength, based on 0.35-percent strain (*4*), and the nominal yield strength. Elongation of the test bars was found not to be significantly related to their fatigue strength.

Various measures of the diameter of the test bars were entered as candidate variables in the regression. The nominal bar diameter was found to be more effective than the diameter based on the unit weight of each bar, the diameter across the ribs, or the diameter across the barrel of each bar. The variable D^2_{nom} was found to be slightly more effective than the nominal bar area in explaining variation in the test data.

The ratio of lug base radius to lug height, r/h, was entered as a candidate variable in the regression along with the interaction effect $D_{nom}\ (r/h)$. The latter was found to result in a better representation of the test data.

No significant effect on fatigue strength could be attributed to the geometry of the manufacturer's bar identification mark in those cases where the fatigue fracture had been initiated at a bar mark. However, a decrease in fatigue strength could be attributed to the bar mark fractures when the Phase I test data were studied alone.

Effect of Experimental Procedures

In the multiple regression analysis described above, several factors concerned with the testing of reinforcing bars as embedded within concrete beams were studied. Also considered were the potential effects of nonscheduled variables in the testing program.

No property of the test beam concrete was found to have significantly affected the fatigue strength of the test bars. Age of the concrete at the time each test was initiated, the concrete modulus, and compressive strength were considered in the analysis.

No dimensional property of the test beams, aside from the diameter of the test bars, was found to have influenced the fatigue strength of the bars. The test beam variables considered were effective beam depth, span length, and spacing of flexural cracks in the concrete.

No effect on fatigue strength could be attributed to the particular test procedure used in each individual test. The rate of loading, use of a test setup, and use of one or two loading rams were found to have had no statistically significant effect on the test results.

Effect of Prior Cycling Below Fatigue Limit

Rerun tests, where the test bar had survived 5 million cycles at a low stress range prior to being fractured in fatigue at a high stress range, were not included in the multiple linear regression analysis. This was because these test bars had been subjected to different treatment from that of the bars in the regular finite-life tests.

The Phase II test program was designed to permit a statistical analysis to determine whether previous cycling at stress ranges near the fatigue limit had a significant effect on the finite-life fatigue strength. Regression lines were determined for both the regular and the corresponding rerun tests. Statistical tests (*20*) were then made to check whether each pair of corresponding regression lines could be considered to be parallel. Four of the five pairs of regression lines were found to share a common slope. Further tests showed that these parallel lines could in each case be considered to be identical. Thus, on the average, no loss or gain in fatigue strength could be attributed to the previous treatment of the rerun test bars.

Limits on Test Results

Because of the inherent scatter in fatigue test results, it is of practical importance to establish bounds for the fatigue test results obtained for any particular treatment of the specimens. The most effective bounds on fatigue test results are expressed by tolerance limits. Such limits can be determined, stating with a 95-percent probability of being correct that 95 percent of all tests results from a certain statistical population will fall within the limits.

Tolerance limits were determined (*18*) for each staircase test series based on the estimates obtained for the mean and standard deviation for the individual series. The fatigue limit at 5 million cycles and the corresponding lower tolerance limit for each staircase series are presented in Table 2.

A No. 8 Grade 60 reinforcing bar from one of these manufacturers that is encased within a concrete beam at an effective depth of 10 in. and subjected to a minimum stress of 6 ksi and a stress range below the tolerance limit has a near 100-percent probability of surviving 5 million cycles of loading.

As a practical matter, the tolerance limit for the bars from Manufacturer E is considered to be unrealistically low. The high scatter in test results for these bars and consequently a high estimate of the standard deviation for the test series resulted in very wide tolerance limits. However, the lowest stress range at which a fatigue fracture occurred in this test series was 27.8 ksi while the highest

TABLE 2

LIMITS ON STAIRCASE TESTS

MANUFACTURER	MEAN FATIGUE LIMIT (KSI)	LOWER TOLERANCE LIMIT (KSI)
A	24.7	21.4
B	23.8	22.2
C	23.0	21.9
D	28.2	26.7
E	28.5	19.7

stress range for a runout at 5 million cycles was 31.2 ksi. Therefore, it is believed that a longer test series would have resulted in considerably narrower tolerance limits for the bars from Manufacturer E.

Tolerance limits were calculated (*63*) for all of the regular finite-life tests from Phase I of the test program. After linearization of the limits, they may be expressed in terms of the following bounds on Equation 1

$$\log N = 6.9690 \pm 0.3586 - 0.0383 f_r \qquad (7)$$

These limits contain virtually all of the Phase I finite-life test results and apply for the wide variety of test bars and test conditions used.

In the interest of developing a proposed specification for the fatigue design of reinforced concrete flexural members, tolerance limits were established for the largest collection in the test program of finite-life test results for a single test condition. This collection consists of the 25 finite-life test results from Groups No. 1 and 33. These test results were found to be bounded by the expression

$$\log N = 7.2714 \pm 0.1285 - 0.0461 f_r \qquad (8)$$

The above limits are linearized for the value determined at a stress range of 54 ksi.

CHAPTER THREE

INTERPRETATION AND APPLICATION

The understanding gained from the survey of previously published test results and from the present investigation of the influence of the major test variables on the fatigue behavior of deformed reinforcing bars is summarized in the following sections.

EFFECT OF STRESS RANGE

The fatigue life of a reinforcing bar is primarily determined by the magnitude of the stress range to which it is subjected. Stress histories consisting exclusively of compressive stresses have no fatigue effect. However, a fatigue fracture may occur when one or both of the extreme stresses of the stress cycle to which a reinforcing bar is subjected are tensile.

Low stress ranges have little or no discernible fatigue effect. There appears to exist a limiting stress range, the fatigue limit, below which a reinforcing bar may be expected to be able to sustain the number of stress cycles likely to be encountered during the practical lifetime of a reinforced concrete structure. For design purposes, this stress range limit may be determined as the lower 95-percent tolerance limit to the mean fatigue limit established at 5 million cycles.

When the applied stress range is nearly equal to the mean fatigue limit but greater than the lower 95-percent tolerance limit, fatigue fracture may occur any time after about 1 million cycles of loading. However, in this long-life region, a great scatter in fatigue life is observed. Thus, for the same stress conditions, one bar might fracture after 1 million cycles while a nominally identical bar might survive 10 million cycles.

In the present test series, 23.0 ksi was the lowest mean fatigue limit at 5 million cycles for five different No. 8 Grade 60 deformed reinforcing bars subjected to a minimum stress of 6-ksi tension. The lowest stress range at which a fatigue fracture occurred was recorded at 21.3 ksi for a No. 11 Grade 60 deformed bar subjected to a minimum stress of 17.5 ksi. This is the lowest stress range at which a fatigue fracture has been obtained in undisturbed North American-produced reinforcing bars.

At stress ranges greater than the mean fatigue limit at 5 million cycles, the fatigue life of a reinforcing bar is dominated by the magnitude of the applied stress range. As the maximum cyclic stress approaches the tensile strength of a reinforcing bar, a great scatter in fatigue life is again observed. Thus, a bar may be expected to fracture after 1 to about 10,000 cycles in this low-cycle fatigue region.

In the finite-life fatigue region, extending from about 10,000 to about 1 million cycles of loading, a linear relationship may be considered to exist between the logarithm of fatigue life and stress range. The scatter in fatigue life at a stress range causing fatigue fracture in the finite-life region is much reduced from that observed in the low-cycle and long-life regions. Thus, at stress ranges greater than the fatigue limit, the fatigue life of a reinforcing bar may be closely predicted, except in the range of low-cycle loadings.

The effect of stress range on the fatigue lives of the reinforcing bars tested in the present investigation may be seen in Figure 7. In this figure, the straight line representing the average relationship between logarithm of fatigue life and stress range was determined from Equation 6. The S-N line represents No. 8 Grade 60 bars having an r/h ratio of 0.3 and subjected to a minimum stress of 6-ksi tension. The apparent high scatter in test results about this line is due to the effects of the other test variables.

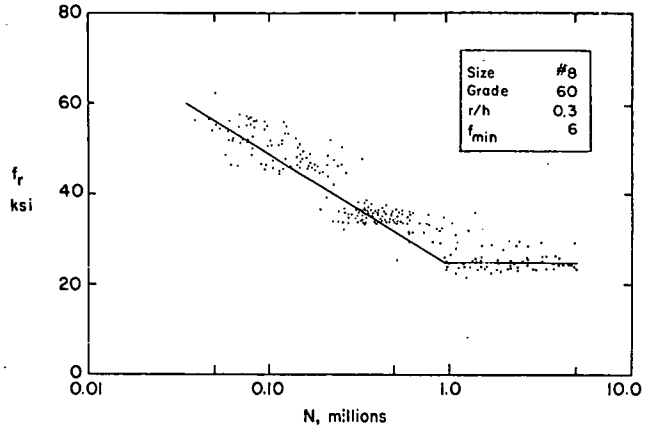

Figure 7. Effect of stress range.

EFFECT OF MINIMUM STRESS LEVEL

Minimum stress level was found to be the second most statistically significant variable in explaining variation in the finite-life test data. This means that, after stress range, the effect was the most sharply defined. Consequently, other than for stress range, the magnitude of the effect was also determined with the greatest precision.

No interaction was found to exist among the effect of minimum stress level and the effects of the other test variables. Thus, in terms of the logarithm of fatigue life, the effect of minimum stress is directly additive to that of stress range. Therefore, a change in the minimum stress level shows up in the finite-life region as a parallel shift of the S-N diagram.

For the reinforcing bars tested in the present investigation, a change in minimum stress from 6-ksi compression to 18-ksi tension was found to have a finite-life region effect equivalent to a reduction in fatigue strength of 8.1 ksi. This is illustrated in Figure 8 for No. 8 Grade 60 bars having an r/h ratio of 0.3. In Figure 8, the straight lines relating the logarithm of fatigue life and stress range were determined from Equation 6.

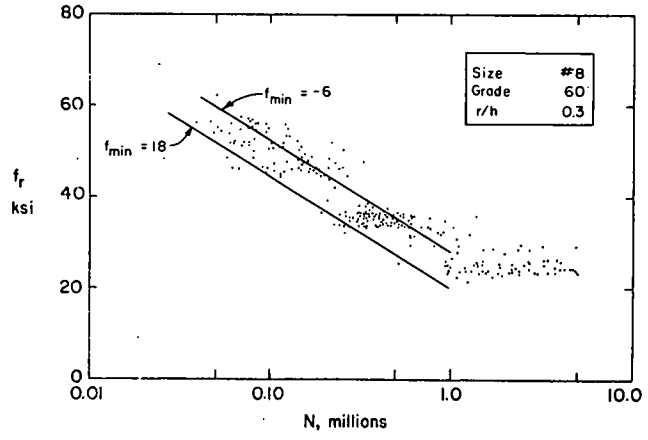

Figure 8. Effect of minimum stress level.

A finite-life effect similar to that shown in Figure 8 may be observed in previously published test results (*30*). However, in these data, the effect is occasionally obscured by the influence of other factors.

An examination of previous test results (*30*) indicates that the minimum stress level also affects the long-life region fatigue properties of reinforcing bars. However, the present test program was not designed to allow the existence of such an effect to be confirmed.

In the absence of long-life region test results allowing a statistical analysis for the effect of minimum stress level, no definitive statements can be made regarding the potential magnitude of such an effect. However, it was observed from previous test results (*30*) that the equivalent stress range effect of the minimum stress level was about equal for the finite- and long-life regions. Thus, it may be assumed that the effect of minimum stress level determined in the present test program is carried over into the long-life region in equal magnitude to that observed in the finite-life region.

EFFECT OF GRADE OF BAR

Grade of bar was found to be a statistically significant variable in explaining the finite-life test results obtained in this investigation. It ranked third among the variables found to be statistically significant. Thus, the magnitude of the grade-of-bar effect is known with less precision than are the magnitudes of the stress range and minimum stress effects but with greater precision than is the magnitude of the bar diameter effect.

Yield strength and tensile strength were among the various measures used for grade of bar in the statistical analysis. Of these, tensile strength was found to be the most effective in explaining variation in the data. In practice, the minimum tensile strengths specified by ASTM (*1*) for the different grade bars tested could be used conservatively to represent the actual tensile strength.

No interaction term relating grade of bar and the other test variables was found to be statistically significant. Thus, as for the effects of minimum stress level and bar diameter, the finite-life region effect of grade of bar is exhibited by a parallel shift of the S-N diagram.

Replacing a Grade 40 bar with an otherwise identical Grade 75 bar corresponds to an increase in the specified minimum tensile strength from 70 to 100 ksi. Using these values in Equation 6, it is found that the finite-life region effect is equivalent to an increase in fatigue strength of 5.2ksi. This effect is shown in Figure 9 for No. 8 bars having an r/h ratio of 0.3 and subjected to a minimum stress of 6-ksi tension.

The beneficial effect on fatigue properties implied by replacing a Grade 40 bar with a Grade 75 bar is somewhat illusory. This is because Grade 40 bars would not, in practical circumstances, be called for in a design requiring a stress range in the finite-life region. The actual benefit from the grade-of-bar effect would therefore arise when replacing a Grade 60 bar with a Grade 75 bar. In this case, the effect is equivalent to an increase in fatigue strength of only 1.7 ksi. In most circumstances such a small change will not be of practical significance.

When the Grade 60 bars were stressed beyond their yield strength, a small increase in fatigue life was detected in the statistical analysis. This beneficial effect may be due to small residual stresses set up in the test bars. On the other hand, a potential decrease in fatigue life was observed when the Grade 40 bars were stressed beyond yield. This agrees with previous observations (*53*) that excessive cold working of a reinforcing bar will decrease its fatigue strength.

Previous investigations (*30, 48*) into the effect of grade of bar in the finite-life region show that an increase in steel quality may result in increased fatigue life. However, some of these tests showed an irregular trend with Grade 40 bars having an equal or greater fatigue strength than Grade 60 bars. This may be due to the effects of other fatigue influencing factors.

No systematic study of the long-life region effect of grade of bar has been carried out. Previously published test results (*30, 48*) indicate, however, the same irregular trend observed in the finite-life region. Thus, confirmation of the existence of a grade-of-bar effect in the long-life region must await further study.

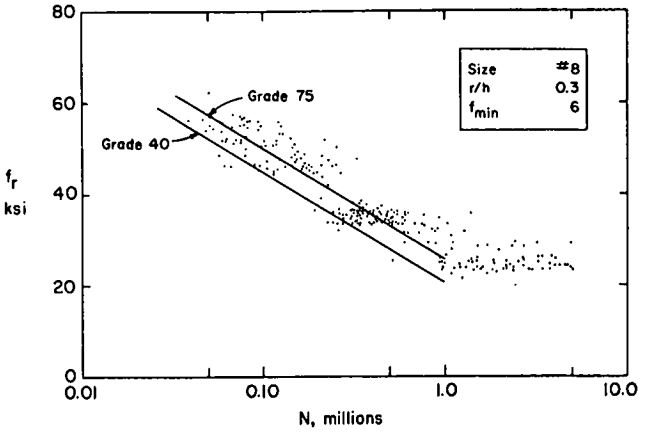

Figure 9. Effect of grade of bar.

EFFECT OF BAR DIAMETER

Analysis of the finite-life data from the present investigation showed that the diameter of the test bars had a statistically significant effect on the test results. However, bar diameter ranked fourth among the variables found to be statistically significant. Thus, the magnitude of the effect is known with less precision than for some of the other variables.

The effect of bar diameter on fatigue life was found to be nonlinear. When no interaction effects were considered in the statistical analysis, the bar-diameter effect for the bars tested was best described by a cubic equation. This equation indicated that fatigue life was decreased for the larger size bars with the No. 6 bars having the longest and the No. 10 bars the shortest fatigue life.

When interaction terms were considered in the statistical analysis, the effect of bar diameter on fatigue life was no longer best represented by a cubic equation. Rather, a combination of the variable D^2_{nom}, representing the bar area, and the variable $D_{nom}(r/h)$, representing the interaction between bar diameter and bar geometry, was found to offer the best description of the variation in the test data. The interaction between bar diameter and bar geometry indicates that the effect of exchanging a large size bar for smaller size bars is greatest when the bar geometry is sharp.

No interaction was found to exist between bar diameter and stress range. Thus, the effect of bar diameter is exhibited in the finite-life region by a parallel shifting of S-N diagrams. This is shown in Figure 10 for No. 5 and No. 11 Grade 60 bars having an r/h ratio of 0.3 and subjected to a minimum stress of 6-ksi tension.

The S-N diagrams shown in Figure 10 were determined from Equation 6. This equation indicates that the effect of replacing No. 5 bars with No. 11 bars is equivalent to a change in fatigue strength of −4.9, −3.6, and +0.8 ksi for bars having r/h ratios of 0.1, 0.3, and 1.0, respectively. It should be noted, however, that the bars tested had a range in r/h ratio from only 0.17 to 0.39. Therefore, the previously mentioned effect for bars having an r/h ratio of 1.0 is based on projection.

The existence of a reinforcing bar diameter effect in the finite-life region has not been systematically investigated by other researchers. However, results similar to those obtained in the present investigation have been observed in the general field of fatigue in metals (*42, 45*). These results also show the effect to be nonlinear. This is attributed (*45*) to a statistical size effect related to the probability of finding a critical notch on the bar surface.

Results obtained by several investigators (*38, 40, 46*) may be interpreted to show the existence of a long-life region effect due to reinforcing bar diameter. However, these findings were not obtained by statistical data analyses and were often based on highly scattered data. Thus, the existence of such an effect is uncertain.

EFFECT OF TYPE OF SPECIMEN

In the present test program, the effect of type of specimen was studied by varying the effective depth of the test beams. This variation was found to have had no statistically significant effect on fatigue life.

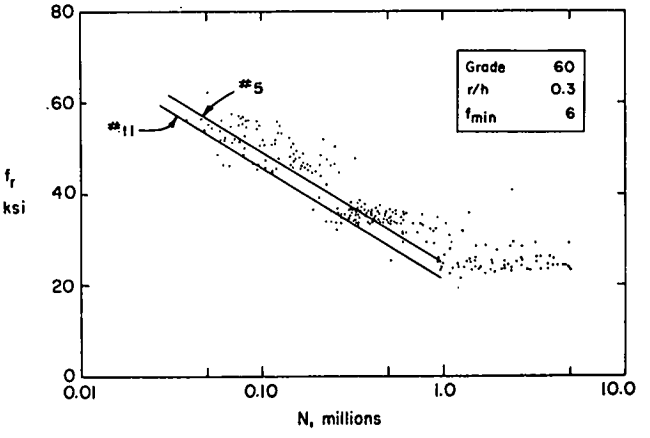

Figure 10. Effect of bar diameter.

Previous fatigue tests on reinforcing bars have been carried out on a variety of test specimens. These have ranged from axial tension tests in air to tests on bent bars encased within concrete beams having a spread-V shape in elevation. Little comparative testing to determine the effect of the test method on fatigue life has been carried out.

A few tests comparing the effect of testing reinforcing bars in air and as encased within concrete beams have been carried out (*54*). These tests indicated that a longer fatigue life was obtained for the concrete-encased test bars. However, the measured concrete modulus of elasticity was not used to calculate the stresses in the encased bars. Thus, the issue remains in doubt.

In tests on bent bars encased within concrete beams having a spread-V shape in elevation, a considerable reduction in fatigue strength relative to that of straight bars encased within straight concrete beams was observed (*30*). However, it is not clear whether this reduction was due to the bending of the test bars or to the type of test specimen used. Tests (*54, 55*) on large girders having bent-up main reinforcing bars, when no longer required for flexure, did not result in fatigue fracture at a bend.

EFFECT OF BAR GEOMETRY

The geometry of the transverse deformations rolled onto the surface of a reinforcing bar to improve its bond characteristics was found to have a statistically significant effect on the fatigue strength of the bar. This effect shows up in both the finite- and long-life regions.

When only the Phase II finite-life test results were considered in the statistical analysis, the effect of bar geometry was found to be sharply defined and of considerable magnitude. However, when the finite-life data from both phases were considered together, the bar geometry effect was less well defined and of lower magnitude. In fact, the bar geometry variable ranked last among those found, in this analysis, to have had a statistically significant effect on finite-life fatigue strength.

The difference in the bar geometry effect with the set of data used in the statistical analysis may be due to the greater accuracy with which the critical geometry of the Phase II bars was determined. In Phase II of the investigation, the techniques for preparing samples for photography of the lug geometry and the subsequent measurement of lug dimensions were considerably improved from those used in Phase I. No reassessment was made of the critical geometry of the Phase I test bars. For the present, the lesser magnitude of the bar geometry effect determined in the over-all analysis must be considered more representative of the general properties of reinforcing bars.

An interaction was found to exist in the finite-life region among the effects of bar geometry and bar diameter. The most efficient bar geometry variable in explaining the variation in the test data was $D_{nom}(r/h)$. Since the ASTM (*1*) specified minimum average lug height for No. 6 to No. 11 bars is a constant ratio of the bar diameter, the above bar geometry effect is essentially due to variation in the lug base radius.

No interaction was found to exist between bar geometry and stress range. Therefore, a change in bar geometry, for otherwise identical bars, will cause a parallel shift of the finite-life S-N diagram.

In the present test series, the r/h ratio was found to vary from 0.17 to 0.39. However, reinforcing bars have been found (*32*) to have a lug base radius to lug height ratio as high as 1.0. Thus, considering a change in the r/h ratio from 0.1 to 1.0, Equation 6 predicts that the finite-life region effect on No. 5, 8, and 11 would be equivalent to an increase in fatigue strength of 4.5, 7.2, and 10.0 ksi, respectively. This is shown in Figure 11 for No. 8 Grade 60 bars subjected to a minimum stress of 6-ksi tension.

Bar geometry was also found to have a pronounced effect on fatigue strength in the long-life region. The lowest mean fatigue limit at 5 million cycles for the five manufacturer's bars tested in Phase II was found for a bar having an r/h ratio of 0.29; the highest limit was for a bar having an r/h ratio of 0.39. These r/h ratios were, respectively, the lowest and highest r/h ratios among the Phase II test bars. The corresponding mean fatigue limits were 23.0 and 28.5 ksi, respectively, and are shown in Figure 12.

The scatter in test results about the mean fatigue limits at 5 million cycles does not allow the direct use of these

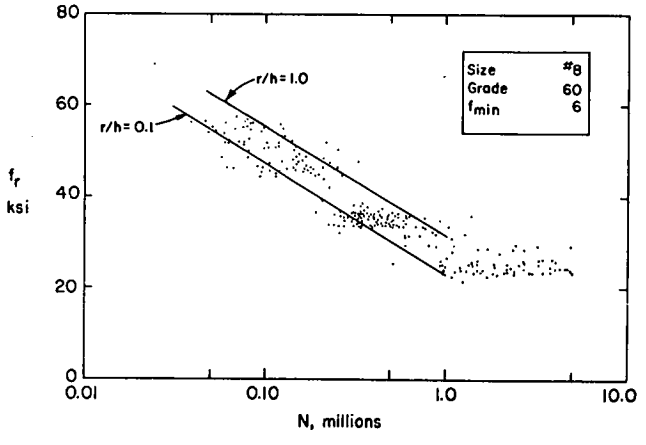

Figure 11. Effect of bar geometry, finite-life region.

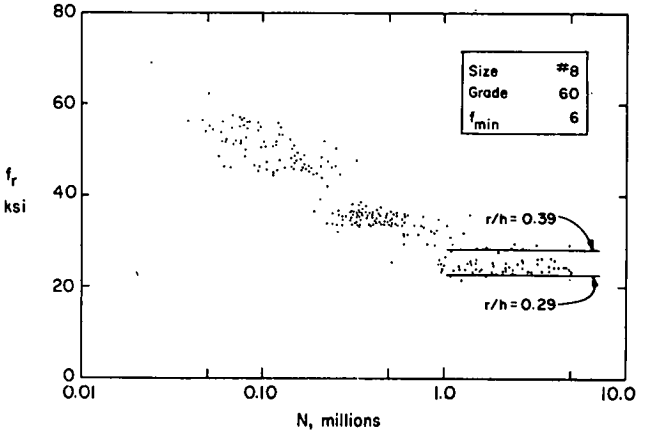

Figure 12. Effect of bar geometry, long-life region.

limits in design. Rather, the effects of the scatter must be removed by the application of tolerance limits to each mean fatigue limit. Such limits can be determined with a 95-percent probability that 95 percent of all test results will lie between the upper and lower limits.

Because the scatter in long-life region tests results was found to be greatest for the bars having the highest mean fatigue limit, consideration of tolerance limits decreases the bar geometry effect shown in Figure 12. Therefore, it is reasonable to approximate the bar geometry effect in the long-life region by assuming its magnitude, in terms of fatigue strength, to be the same as in the finite-life region.

DEVELOPMENT OF A DESIGN PROVISION FOR FATIGUE

The primary concern to a designer of reinforced concrete structures, when considering the fatigue resistance of a structure subjected to cyclic loading, is the establishment of the limiting stress levels below which no fatigue damage is likely to occur during the design lifetime of the structure. Thus, a design provision based on the presently available knowledge of the long-life fatigue behavior of reinforcing bars is highly suitable for such purposes.

On the basis of the previous discussion of the individual effects of the test variables on the fatigue properties of deformed reinforcing bars, the following assumptions can be made regarding long-life region fatigue properties:

1. The effect of minimum stress, in terms of fatigue strength, has the same magnitude in the long-life region as in the finite-life region.
2. Potential bar diameter effects in the long-life region can be neglected.
3. Potential grade of bar effects in the long-life region can be neglected.
4. Effective beam depth does not affect long-life region fatigue properties.
5. The effect of bar geometry, in terms of fatigue strength, has the same magnitude in the long-life region as in the finite-life region.

Assumptions No. 1 and 5 permit the use of Equation 6 as a basis for the formulation of a long-life region relationship for stress range in terms of minimum stress level and bar geometry. Since No. 8 Grade 60 bars were central to the experimental investigation, it is reasonable to use the properties of these bars to eliminate the effects of bar diameter and grade of bar from Equation 6. This results in the expression

$$\log N = 6.9541 - 0.0407\, f_r - 0.0138\, f_{min} + 0.3233\, (r/h) \qquad (9)$$

The above equation describes the finite-life properties of the test bars in terms of the primary variables influencing the long-life properties of the bars. At the fatigue limit, the fatigue life ceases to be affected by these variables. Equation 9 may then be solved for stress range in terms of the minimum stress level and bar geometry variables.

As may be seen in Table 2, bars from Manufacturer E had the smallest value for the lower tolerance limit to the mean fatigue limit at 5 million cycles of the five manufacturer's bars tested. A high scatter in test results about the mean fatigue limit was observed for these bars. For this reason, and because of the relatively low number of tests available to estimate the statistical population distribution, it is believed that the tolerance limits for the bars from Manufacturer E are excessively wide. Therefore, the second smallest value found in this investigation for a lower long-life region tolerance limit will be used in developing the design limit provision.

Bars from Manufacturer A had a lower tolerance limit to the mean fatigue limit of 21.4 ksi. A 95-percent probability exists that 95 percent of all staircase test results for a mean fatigue limit at 5 million cycles on No. 8 Grade 60 bars from Manufacturer A subjected to a minimum stress of 6-ksi tension would fall between this limit and an upper limit of 27.9 ksi.

Using the lower tolerance limit of 21.4 ksi for stress range, a minimum stress of 6-ksi tension, and the r/h value of 0.33 for No. 8 Grade 60 bars from Manufacturer A, a log N value may be calculated from Equation 9. This log N value may in turn be used in Equation 9 to determine f_r in terms of f_{min} and r/h. The result is

$$f_r = 20.81 - 0.3391\, f_{min} + 7.9435\, (r/h) \qquad (10)$$

This equation represents, for reinforcing bars used in concrete structures, the limiting stress range for which no fatigue damage is likely to occur during the practical lifetime of a structure.

For use in design, Equation 10 may be simplified as

$$f_r = 21 - 0.33\, f_{min} + 8\, (r/h) \qquad (11)$$

It should be noted in Equation 11 that the minimum stress is positive for tensile stresses and negative for compressive stresses.

At the present time, insufficient information is available about the actual service load spectra for highway bridges and their effect on the distribution of moments within a span. Furthermore, little information is available regarding the effect of a variable or random load history on the fatigue properties of reinforcing bars. For this reason, it is considered premature to recommend a fatigue design provision that allows the use of reinforcing bar stress ranges in the finite-life fatigue region.

In those cases, where a designer might need to exceed the limiting stress range indicated by Equation 11, the useful life of the reinforcement could be calculated from an equation similar to Equation 6. However, such calculation must take into account the possibility of premature fatigue fracture due to the natural scatter in fatigue test results. Furthermore, once a fatigue crack has been initiated, consideration should be given to the potential for brittle fracture due to a sudden overload.

In Equation 8, tolerance limits were presented for the largest collection of finite-life test results obtained in the present test program for nominally identical bars subjected to nominally identical test conditions other than for stress range. These limits state with 95-percent probability that 95 percent of all such test results would fall between the limits. It may be assumed that limits of a similar magnitude would be obtained for any other test condition. Thus, the limits given in Equation 8 can be applied to Equation 6 to take into account the effect of scatter in test results.

Tests on the bars represented by Equation 8 indicated that no discernible fatigue crack growth took place during the initial 60 percent of their mean fatigue life at a stress range of 34 ksi. Reducing by 40 percent the number of cycles represented by the lower tolerance limit at a stress range of 34 ksi in Equation 8 corresponds to changing the constant in the equation by 0.2219. Applying a similar correction to Equation 6 and assuming the effect to be constant for all stress ranges would tend to ensure against potential brittle fracture.

Neglecting the effect due to yielding of Grade 60 bars, representing the bar diameter squared term by the bar area, and applying the previously discussed corrections, Equation 6 becomes

$$\log N = 6.1044 - 0.0407\, f_r - 0.0138\, f_{min} + 0.0071\, f_u - 0.0566\, A_s + 0.3233\, Dr/h \qquad (12)$$

Equation 12 may be used to calculate a safe fatigue life for all stress ranges above the fatigue limit represented by Equation 11. Again, it should be noted that tensile stresses are considered to be positive.

The limits represented by Equations 11 and 12 are compared in Figure 13 for No. 8 Grade 60 bars having an r/h ratio of 0.3 and subjected to a minimum stress level of 6-ksi tension; the test results were obtained in the present investigation. Also shown in this figure, as dashed lines, are the corresponding limits for No. 5 Grade 75 bars having an r/h ratio of 1.0 and subjected to a minimum stress level of 6-ksi tension. A similar comparison is made in Figure 14 with previously published test results on North American bars.

It is not intended that the limits presented in Equation 12 be used as the basis for a code provision. The equation is only intended as a guide for the designer in those circumstances where higher stresses than those allowed by Equation 11 must be designed for.

Both Equations 11 and 12 should be used with caution in those circumstances where some time-dependent effect may cause change in reinforcing bar properties. Among such factors should be included the possible hazards of severe saltwater corrosion and extreme temperature conditions.

SUGGESTED SPECIFICATION FOR FATIGUE DESIGN

The stress range in a deformed reinforcing bar used as the main reinforcement for a flexural reinforced concrete member subjected to cyclic or repeated loads shall not exceed

$$f_r = 21 - 0.33\, f_{min} + 8\, (r/h)$$

in which

f_r = stress range, in ksi
f_{min} = corresponding minimum tensile stress (positive) or maximum compressive stress (negative), in ksi
r/h = ratio of base radius to height of rolled-on deformation

When r/h is not known, a value of 0.3 can be used.

No welding or bending of main reinforcement shall take place at locations where the stress range is near the above limit.

SERVICE LOADS FOR FATIGUE DESIGN

Present methods for establishing service load conditions for use in load factor (*4, 5*) design are based on methods previously applied for design by working stress theories. For flexural members, this means that the calculated service load moments represent, at each span location, the worst condition to which the member can be subjected. Such conditions may arise only once during the lifetime of a structure, if ever. Therefore, they are not appropriate for fatigue design.

At stress ranges slightly higher than the design fatigue limit, load repetitions of up to 1 million times are required to cause fatigue fracture in reinforcing bars. Therefore, the stress range used in fatigue design should reflect the condition being designed for. Such a design condition might

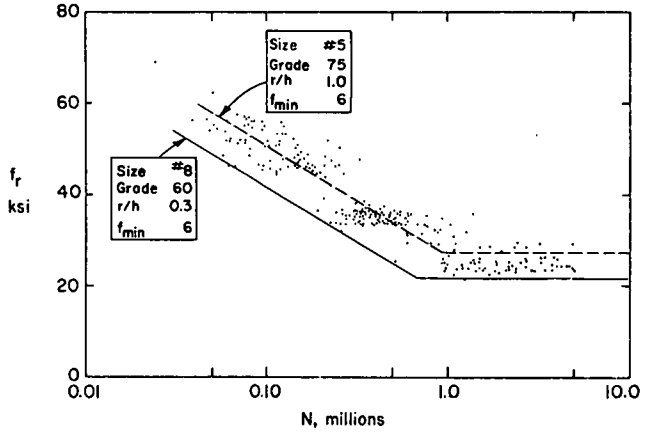

Figure 13. Suggested design provision compared with test results obtained in the present investigation.

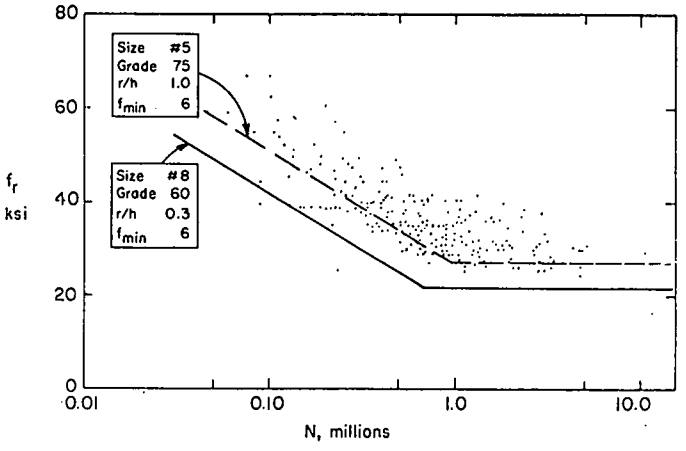

Figure 14. Suggested design provision compared with previously published test results for North American bars.

be based on the use of a specified percentage of the present service load moments. Alternatively, the effect on the structure of a single passage of a given load combination might be considered appropriate for design. However, the actual service load conditions that a reinforced concrete highway bridge might be subjected to in sufficient number to create a danger of fatigue fracture of the reinforcement are not currently known.

DETERMINATION OF CRITICAL BAR SURFACE GEOMETRY

Transverse lugs rolled onto the surface of deformed reinforcing bars cause stress concentrations at the interface with the body of the bar. Similar stress concentrations are caused by the manufacturer's bar identification marks. Any such stress concentrations are potential fatigue crack initiators.

In reinforced concrete beams, all fatigue fractures have been observed to occur in the close vicinity of a flexural tension crack in the concrete. It is not known whether full bond still exists, at the eventual fracture location, between the reinforcing bar and the surrounding concrete during the fatigue crack growth period. Thus, it is not known whether forces are being transmitted through the transverse lugs to the body of the bar at the location of a fatigue crack. In any case, the state of stress at the root of a rolled-on deformation is highly complex.

Determination of the critical surface geometry of a particular reinforcing bar requires initially the identification of the most fatigue-susceptible location on the periphery of the bar. This location must be determined through a series of fatigue tests on bars rolled through fresh rolls. Such tests should simulate as closely as possible the interaction between steel and concrete in the vicinity of a flexural tension crack in the concrete. Simultaneously, such a test should impart as uniform a stress condition as possible to the periphery of the test bar. This would ensure that the critical fatigue location was not subjected to biased loading due to the test method.

If it is assumed that no significant forces are transmitted between concrete and steel in the vicinity of a flexural concrete crack, the bar may effectively be considered to be in air. No statistically valid comparison between fatigue tests of reinforcing bars in air and as encased within concrete beams has been carried out. Therefore, the magnitude of any potential error introduced by testing in air is not known.

Axial tension fatigue tests, where care is taken not to introduce any bending forces to the test specimen, would satisfy the requirement for uniform test conditions on the periphery of a reinforcing bar. Joint recommendations have been issued (*64*) by RILEM, FIP, and CEB for such a test procedure. This procedure should provide a close estimate of the critical fatigue location.

A similar estimate of the critical fatigue location could also be obtained from a rotating bending test. In such a test, the test bar could be loaded at about the third points of its length as a simply supported beam. The bar would be clasped by bearings at the supports and at the load points. Rotation of the bar within the bearings would then cause each point on the periphery of the test bar to be subjected to a uniform strain gradient in the constant moment region. Such a test might simulate actual stress conditions more closely than an axial tension test.

Presently, the geometry of the bar surface at the critical fatigue location is most accurately determined by means of photographs of a longitudinal bar section containing the critical region. For this purpose, a representative 3-in. length of the bar may be used.

Rust and mill scale should be removed from the surface of the sample bar. This may be done by placing the sample for 30 min in a 50-percent solution of hydrochloric acid and water at room temperature. Then, the sample should be immersed in a 5-percent neutralizer solution of sodium carbonate and water, followed by thorough rinsing in cold water. This should be followed by drying for 20 min in an oven at 120 F. After this treatment, the sample should be wire brushed gently and sprayed with a thin coat of silicone spray to prevent rusting.

The prepared sample bar should be milled to a radial plane containing the critical fatigue location. The milled surface should then be lapped until smooth. At this stage, any loose burrs at the edges of the sectioned surface should be removed by brushing and the rolled edges blacked out with thin ink, such as that from a marker pen. A final surface polish is obtained by hand rubbing with 600-grit silicone carbide paper. Hand rubbing is continued until any ink on the sectioned surface has been removed and no burrs remain at the edges of the sectioned surface.

Photographs of the sectioned surface are best obtained with a vertically mounted camera. The sectioned bar surface should be located against a black background. Indirect lighting should be used to minimize reflections from the shiny sectioned bar surface. High-contrast film, such as Kodalith, should be used. After developing, a contact printer should be used to obtain a clear bar image on a black background negative.

Enlarged photographs, using a magnification factor of 2, enable the transverse lug having the sharpest geometry to be identified for further study. Measurements of the critical lug dimensions are then made from photographic prints showing the selected lug magnified about 15 times.

Lug base radii, flank angles, height, and width should be measured. The radii are best determined by comparison with several circles on a circle template. Flank angles may be determined by drawing the lug base line and using a protractor to establish the angle to the most representative slopes on the sides of the lug. The height of the lug is determined as the greatest height from the lug base line. Width of the lug is determined as the distance along the lug base line between the points of intersection of the tangent lines used to determine the flank angles. Dimensionless values are obtained by determination of the ratios of the lug base radius to height and the lug height to width.

At present, the relationship between the lug dimensions and the stress concentration factor is not fully known. However, it is known that its magnitude is related to the lug base radius-to-height ratio, to the lug height-to-width ratio, and to the flank angle. It is expected that future developments will result in a clarification of the relationship.

CHAPTER FOUR

CONCLUSIONS AND RECOMMENDATIONS

This study of the fatigue properties of deformed reinforcing bars included a review of the pertinent literature; tests on 353 concrete beams, each containing a single straight test bar as the main reinforcement; and a statistical analysis of the resulting data. The major test variables studied were stress range, minimum stress level, bar diameter, grade of bar, bar surface geometry, and effective beam depth.

CONCLUSIONS REGARDING THE SPECIFIED TEST VARIABLES

Stress Range

1. For a reinforcing bar subjected to cyclic stresses, the stress range of the cycle is the predominant factor determining the fatigue life of the bar.

2. There is a limiting stress range, the fatigue limit, above which a reinforcing bar is certain to fracture in fatigue. At stress ranges below the fatigue limit, a reinforcing bar may be able to sustain a virtually unlimited number of stress cycles.

3. For design purposes, the fatigue limit for a reinforcing bar may be determined as the lower tolerance limit to the mean fatigue limit at 5 million cycles. In this investigation, the lowest mean fatigue limit at 5 million cycles for No. 8 Grade 60 bars subjected to a minimum stress of 6-ksi tension was 23.0 ksi and the highest was 28.5 ksi. The lowest stress range at which a fatigue fracture was obtained was 21.3 ksi for a No. 11 Grade 60 bar subjected to a minimum stress of 17.5-ksi tension.

4. When a reinforcing bar is subjected to a stress range equal to the mean fatigue limit at 5 million cycles, the minimum fatigue life to be expected is about 1 million cycles.

5. At stress ranges above the mean fatigue limit at 5 million cycles, a linear relationship exists between stress range and the logarithm of the number of cycles to fracture. This relationship is valid in the finite-life region extending from a lower limit of about 10,000 cycles, when the maximum stress is near the tensile strength of the bar, to an upper limit of about 1 million cycles, when the stress range is near the fatigue limit.

Minimum Stress

1. The minimum stress level of a stress cycle has a sharply defined effect on fatigue strength in the finite-life region. When tensile, an increase in minimum stress causes a decrease in fatigue strength. When compressive, an increase in minimum stress causes an increase in fatigue strength.

2. For the present tests, the finite-life region effect of changing the minimum stress by 3 ksi is equivalent to changing the stress range by about 1 ksi.

3. Previously published test results showed that the effect of minimum stress on fatigue strength in the long-life region is about equal in magnitude to that observed in the finite-life region.

Bar Diameter

1. Bar diameter has a statistically significant effect on the fatigue life of reinforcing bars in the finite-life region. In this investigation, the effect was found to be nonlinear and to be coupled with the effect of bar surface geometry.

2. For bars subjected to the same stress conditions, an increase in bar size will generally cause a decrease in fatigue strength. For the bars tested in this investigation, replacing No. 5 bars with No. 11 bars causes a decrease in finite-life fatigue strength of 3.6 ksi when the transverse lug base radius to lug height ratio remains constant at 0.3.

3. Previously published test results indicate that bar diameter has an effect on fatigue strength in the long-life region. However, the nature of the relationship is not clearly defined by existing test data.

Grade of Bar

1. Grade of bar has a statistically significant effect on fatigue strength in the finite-life region. The effect appears to be linear with variation in tensile strength.

2. An increase in steel quality results in increased fatigue strength. In this investigation, replacing a Grade 60 bar with a Grade 75 bar resulted in an increase in finite-life fatigue strength of 1.7 ksi.

3. The existence of a grade of bar effect in the long-life region was indicated by previously published test results. However, the nature of the relationship between grade of bar and fatigue strength in the long-life region is not clearly defined by the existing test data.

Type of Specimen

1. The fatigue properties of the reinforcement in a straight reinforced concrete beam are not affected by the effective depth of the beam except as it affects the reinforcement stresses.

Bar Geometry

1. Rolled-on surface deformations cause stress concentrations at the interface with the barrel of a reinforcing bar. Such deformations include transverse lugs, the manufacturer's bar marks, and surface pits due to rolling mill scale into the bar surface. Fatigue cracks are always initiated at a point of stress concentration.

2. Generally, transverse lugs cause the highest stress concentrations. The magnitude of the stress concentration depends on the sharpness of the lug base radius, the lug height, the lug width, the flank angles of the lug, and the diameter of the barrel of the bar. Low and narrow lugs having a large base radius cause the least stress concentrations.

3. Massive bar marks of sharp geometry may cause higher stress concentrations than the transverse lugs.

4. Test specimens machined from the barrel of a reinforcing bar may have as much as twice the fatigue strength of the undisturbed bar. The lower fatigue strength of the undisturbed bar is attributed primarily to stress concentrations at the rolled-on deformations and to surface decarburization.

5. Geometry of the transverse lugs rolled onto the surface of reinforcing bars affects fatigue strength in both the finite- and long-life regions. In this investigation, the finite-life region effect was found to be coupled with that of bar diameter. The magnitude of the effect of bar geometry alone is about equal in both regions.

6. An increase in the ratio of lug base radius to lug height results in increased fatigue strength. The present tests showed that, for a No. 8 bar, changing the r/h ratio from 0.1 to 1.0 results in an increase in fatigue strength of at least 7.2 ksi. The effect of bar geometry is potentially larger and may be of importance equal to that of stress range.

7. Bar surface geometry is most accurately determined from enlarged photographs of carefully prepared longitudinal bar sections.

Design Provision

1. For the present, a design provision for fatigue in reinforcing bars should be based on limiting the stress conditions within a bar to those presenting no danger of fatigue damage during the expected lifetime of a reinforced concrete structure. This limiting stress should be based on the fatigue limit for each manufacturer's bars with appropriate consideration for possible variation in bar properties.

2. The effects of bar diameter and grade of bar should not be included in a design fatigue limit. This is due to the uncertainty of their effects in the long-life region.

3. The effects of minimum stress and bar surface geometry should be included in a fatigue design provision. Inclusion of the effect of bar geometry in a design specification should encourage reinforcing bar producers to improve the fatigue properties of their products. Equation 11 represents a recommended design provision.

4. Design for a finite reinforcing bar fatigue life requires consideration of the potential for brittle fracture due to a sudden overload after a fatigue crack has been initiated. When such design is necessary, Equation 12 should be used as a guide in determining the probable life of reinforcing bars.

CONCLUSIONS REGARDING GENERAL FATIGUE PROPERTIES OF REINFORCING BARS

1. None of the fatigue-influencing factors studied interacts with the effect of stress range. Therefore, finite-life S-N diagrams showing the effects of variation of factors other than stress range are best represented by a series of parallel lines.

2. The fatigue strength of reinforcing bars having a short or nonexistent yield plateau may be improved slightly by stressing beyond yield. For bars having a long yield plateau, the effect of such stressing may be detrimental.

3. The fatigue strength of reinforcing bars tested in this investigation was not affected by a prior history of cyclic stressing below the mean fatigue limit at 5 million cycles.

4. Fatigue cracks in reinforcing bars are generally initiated at the base of a transverse lug. More than one crack may be initiated along the same lug. Eventually, such multiple cracks join into a single crack with each original crack separated along a beach mark.

5. Fatigue cracks propagate radially from their point of initiation in a direction perpendicular to the axis of a reinforcing bar subjected to tension. At fracture, the relatively smooth, dull-appearing fatigue crack is surrounded by a crescent-shaped, rough and crystalline tension fracture zone.

6. The radius of the fatigue crack zone at fracture depends on the magnitude of the nominal stress to which the bar was subjected. The final depth of the fatigue crack varies for identically stressed bars from different manufacturers and may be related to the surface deformation pattern.

7. Fatigue crack growth is most rapid near the end of the fatigue life. In this investigation, no fatigue damage was observed during the initial 60 percent of the mean fatigue life for No. 8 Grade 60 bars subjected to a stress range of 34 ksi and a minimum stress of 6-ksi tension.

CONCLUSIONS REGARDING STATIC PROPERTIES OF REINFORCING BARS

1. The average yield and tensile strengths for a set of nominally identical reinforcing bars may be as much as 20 percent greater than the minimum specified. Averages lower than the specified minimum may also occur. Considerable scatter occurs about each average value, even for bars from the same heat.

2. Elongation is decreased for the higher grade bars. It may vary considerably for bars of the same grade but from different manufacturers. The amount of elongation obtainable may be related to the bar deformation pattern.

3. Reinforcing bars in which fatigue cracks have been initiated fracture in a brittle manner at stresses below the tensile strength of the undamaged bar. When large fatigue cracks exist, such fracture may take place at nominal stresses below the yield strength.

CONCLUSIONS REGARDING PROPERTIES OF REINFORCED CONCRETE BEAMS

1. The fatigue strength of the main reinforcement in straight reinforced concrete beams of sound normal weight concrete is not affected by the concrete strength and modulus except as they affect the reinforcement stresses.

2. The fatigue strength of the main reinforcement in straight reinforced concrete beams is not affected by the

beam dimensions except as they affect the reinforcement stresses.

3. The average spacing of concrete flexural tension cracks in reinforced concrete beams increases with the effective depth and decreases with increased bar size.

4. The stiffness of reinforced concrete beams, as manifested by the deflection range, is unaffected by a history of uniform cyclic loading. However, the maximum deflection will increase with time due to creep and shrinkage of the concrete.

RECOMMENDATIONS FOR FUTURE RESEARCH

Previous test results have indicated that the minimum stress level in a reinforcing bar subjected to cyclic stresses will affect the fatigue limit for the bar. The magnitude of this effect appears to be about equal to the equivalent stress range effect observed in the finite-life-fatigue region. This observation prompted the recommendation that such an effect be included in a fatigue design provision. However, no statistically valid confirmation of the existence or potential magnitude of the long-life-region effect of minimum stress level is known to be available. Therefore, further research in this area is recommended.

Previous test results have indicated that bar diameter and grade of bar may affect the long-life fatigue region properties of reinforcing bars. However, no clear indication was obtained of how or to what extent the fatigue limit might be affected. For this reason, the potential effects of bar diameter and grade of bar were not included in the recommended fatigue design provision. Further research is needed to clarify the effects of these variables.

In the present investigation, reinforcing bars having a lug base radius to lug height ratio, r/h, ranging from 0.17 to 0.39 were studied. In particular, an intensive study was conducted on the effect of varying the r/h ratio from 0.29 to 0.39. However, the value of the r/h ratio is believed to be as high as 1.0 for some bars. Thus, further study of the effect of high r/h ratios on fatigue strength is needed to confirm the assumed linear variation in fatigue strength with r/h ratio for commercially available reinforcing bars.

Some information is available regarding the stress concentration effects of external lugs and how the various geometric parameters of the lugs affect the stress concentration factor. However, much of the available information concerns lug dimensions other than those found on reinforcing bars. Furthermore, no information is known to be available on the stress concentration effects of lugs inclined to the axis of a reinforcing bar. Therefore a theoretical or photoelastic investigation, designed to extend the presently available information to practical lug geometries, would be in order.

No information is known to be available regarding the potential range of lug dimensions in reinforcing bars. Yet, the effect of lug geometry on fatigue strength is believed to be nearly as important as that of stress range. For this reason, a survey of the lug dimensions obtained by longitudinal sectioning of currently produced United States reinforcing bars would be appropriate. Presently available reinforcing bar samples from a collection of Grade 60 reinforcing bars currently used in highway bridge construction could form the basis for such a survey.

Bent bars, embedded within concrete beams having a spread-V shape in elevation, have been shown to have a considerably decreased fatigue strength from that of straight reinforcing bars. It is not clear whether this reduction in fatigue strength is primarily due to the bending of the test bars or due to the test method. However, the test method used did not realistically represent the stress conditions to which a bent-up bar in a reinforced concrete beam might be subjected. Thus, research is needed to determine the effect of cyclic stressing on bent-up reinforcing bars. Furthermore, such an investigation should determine the relative susceptibility to fatigue fracture of the bent-up and continuing reinforcement, as the latter will ordinarily be subjected to higher stresses.

Current highway bridge specifications (*5, 11*) limit the service load stress range to which a reinforcing bar may be subjected. Often, compliance with these requirements necessitates the extension of bar cutoff locations beyond those selected to satisfy load factor moment capacity. This is due to the high stress range calculated in the remaining bars at the theoretical moment capacity bar cutoff location. However, each bar to be cut off would be continued a sufficient distance beyond the theoretical cutoff point to allow for full development of the bar. Thus, at the theoretical bar cutoff location, the actual stresses in the remaining bars are considerably lower than calculated. Research is needed to determine the fatigue susceptibility of the remaining bars at a theoretical bar cutoff location.

Generally, live loads on highway bridges are due to a random combination of heavy, medium, and light truck traffic mixed with passenger car traffic. The relative proportion of load due to each of these traffic components varies between rural and urban areas and from one state to another. Research is needed to determine the probability of occurrence of the various live load components so the load history of a highway bridge may be predicted. This would allow the actual service load conditions to which a highway bridge is subjected to be established on a more realistic basis than is currently possible. Such knowledge would also permit the design of concrete reinforcement to be based on the expected lifetime of the structure. However, before such finite-life fatigue design is permitted, further information is required about the effect of cumulative damage due to a variable load history on the fatigue life of a reinforcing bar.

No information is known to be available regarding the effects of temperature extremes on the fatigue strength of reinforcing bars. Highway bridges, particularly in Alaska, may be subjected to a wide range in temperature from summer to winter conditions. Low temperatures are known to cause the embrittlement of most construction materials. Thus, such temperatures might have a detrimental effect on the fatigue strength of reinforcing bars. On the other hand, a moderate temperature increase from the usual test temperature of 70 F is known to enhance the fatigue strength of some steels. Finally, it is not known to what extent daily temperature cycles may contribute to the fatigue stressing of reinforcing bars in highway bridges and pavements. A

study of the various effects of temperature on the fatigue life of reinforcing bars is clearly appropriate.

Recently, severe damage to highway bridge decks due to salt corrosion of the reinforcement has been revealed. No information is known to be available to indicate the potential effect of reinforcing bar corrosion on fatigue strength. However, it seems evident that any reduction in bar area due to corrosion would have adverse fatigue effects. Additionally, it is not known how loss of bond due to spalling of bridge deck concrete would affect the fatigue strength of the reinforcement. Further research in this area seems to be called for.

Suggested remedies to the problem of reinforcement bar corrosion in highway bridge decks include the possibility of using protective coatings for the reinforcement. Such coatings might be obtained by galvanizing or dipping the bars in an epoxy compound. No information is known to be available regarding the effects of such coatings on fatigue strength. However, it is known that hot-dip galvanizing can cause residual stresses to be set up on the galvanized surface. Such residual stresses, if tensile, could cause a severe reduction in fatigue strength. It is recommended that the fatigue effects of surface coatings on reinforcing bars be studied before their use is extensively advocated in practice.

Previous fatigue test results have been obtained using a variety of test methods. Particular emphasis has been given to the testing of reinforcing bars in air and as the main reinforcement in straight concrete beams. The latter test method is recommended for its close simulation of actual conditions in reinforced concrete structures. On the other hand, testing in air has the merit of considerably lowered cost. However, no statistically valid comparison of the two test methods has been made. Thus, direct comparison of test results obtained by the two methods is of doubtful value. Furthermore, the cost advantage of testing in air must be considered in conjunction with the potential departure from the actual use conditions until the absence of any adverse effects has been established. Therefore, it is recommended that an effort towards the standardization of reinforcing bar fatigue tests be made through a comparative study of the effects of the two test methods.

REFERENCES

1. "Standard Specification for Deformed Billet-Steel Bars for Concrete Reinforcement." *ASTM A 615-68,* Am. Soc. Testing and Materials, Philadelphia (1968).
2. "Standard Specification for Rail-Steel Deformed Bars for Concrete Reinforcement." *ASTM A 616-68,* Am. Soc. Testing and Materials, Philadelphia (1968).
3. "Standard Specification for Axle-Steel Deformed Bars for Concrete Reinforcement." *ASTM A 617-68,* Am. Soc. Testing and Materials, Philadelphia (1968).
4. *Building Code Requirements for Reinforced Concrete, ACI 318-71,* American Concrete Inst., Detroit (1971) 78 pp.
5. *Standard Specifications for Highway Bridges,* Eleventh Edn. Am. Assoc. State Highway Officials, Washington, D.C. (1973) 469 pp.
6. HOGNESTAD, E., "Trends in Consumer Demands for New Grades of Reinforcing Steel." *Proc.* Concrete Reinforcing Steel Inst. (1967) pp. 22-32; *PCA Devel. Dept. Bull. D130.*
7. HOGNESTAD, E., and WINTER, G., "High-Strength Reinforcing Steels for Concrete Bridges." *Proc. HRB,* Vol. 39 (1960) pp. 103-119.
8. HARDEMAN, E. I., "Use of High-Strength Reinforcing Steel in Bridges." *Jour. ACI, Proc.,* Vol. 62, No. 4 (April 1965) pp. 457-466.
9. ANTONI, C. M., and CORBISIERO, J. A., "Instrumentation and Testing of an Experimental Continuous Concrete Bridge Reinforced with High-Yield-Strength Steel." *Hwy. Res. Record No. 295* (1969) pp. 25-40.
10. *Strength and Serviceability Criteria—Reinforced Concrete Bridge Members—Ultimate Design,* Bridge Div., BPR, U.S. Dept. of Commerce (Aug. 1966) 81 pp.
11. *Strength and Serviceability Criteria—Reinforced Concrete Bridge Members—Ultimate Design,* Second Edn. U.S. Dept. of Transportation, FHWA (Oct. 1969) 97 pp.
12. "Analysis and Design of Reinforced Concrete Bridge Structures." *Jour. ACI, Proc.,* Vol. 71, No. 4 (April 1974) pp. 171-200.
13. HANSON, N. W., "Seismic Resistance of Concrete Frames with Grade 60 Reinforcement." *Jour. Struc. Div., ASCE Proc.,* Vol. 97, No. ST6 (June 1971) pp. 1685-1700.
14. KAAR, P. H., and HOGNESTAD, E., "High-Strength Bars as Concrete Reinforcement, Part 7. Control of Cracking in T-Beam Flanges." *Jour. PCA Research and Development Laboratories,* Vol. 7, No. 1 (Jan. 1965) pp. 42-53; *PCA Devel. Dept. Bull. D84.*
15. SANDERS, JR., W. W., HOADLEY, P. G., and MUNSE, W. H., "Fatigue Behavior of Butt-Welded Reinforcing Bars for Concrete," *Welding Jour.,* Vol. 40, No. 12, Res. Supp. (1961) pp. 529-s to 535-s.
16. "The AASHO Road Test, Report 4, Bridge Research," *HRB Spec. Rep. No. 61D* (1962) 217 pp.
17. "A Guide for Fatigue Testing and the Statistical Analysis of Fatigue Data." *Spec. Tech. Publ. No. 91-A,* Second Edn. Am. Soc. Testing and Materials (1963) 83 pp.

18. DIXON, W. J., and MASSEY, JR., F. J., *Introduction to Statistical Analysis.* Third Edn. McGraw-Hill (1969).
19. HOGNESTAD, E., HANSON, N. W., KRIZ, L. B., and KURVITS, O. A., "Facilities and Test Methods of the PCA Structural Laboratory." *Jour. PCA Research and Development Laboratories,* Vol. 1, No. 1 (Jan. 1959) pp. 12-20 and 40-44; Vol. 1, No. 2 (May 1959) pp. 30-37; Vol. 1, No. 3 (Sept. 1959) pp. 35-41; *PCA Devel. Dept. Bull. D33.*
20. BROWNLEE, K. A., *Statistical Theory and Methodology in Science and Engineering.* Second Edn., Wiley (1965).
21. REEMSNYDER, H. S., "Some Significant Parameters in the Fatigue Properties of Welded Joints." *Welding Jour.,* Vol. 48 (June 1969).
22. HAHN, G. J., and SHAPIRO, S. S., *Statistical Models in Engineering.* Wiley (1967).
23. SHAPIRO, S. S., and WILK, M. B., "An Analysis of Variance Test for Normality (complete samples)." *Biometrika,* Vol. 52 (1965) pp. 591-611.
24. COCHRAN, W. G., "The Chi-Square Test of Goodness of Fit." *Jour. Am. Statistical Assoc.,* Vol. 45 (1950) pp. 77-86.
25. BARTLETT, M. S., "Properties of Sufficiency and Statistical Tests." *Proc. Royal Soc. London,* Series A, Vol. 160 (1937) pp. 268-282.
26. HARTLEY, H. O., "Testing Homogeneity of a Set of Variances." *Biometrika,* Vol. 31 (1940) pp. 249-255.
27. HARTLEY, H. O., "The Maximum F Ratio as a Short-Cut Test for Heterogeneity of Variance." *Biometrika,* Vol. 37 (1950) pp. 308-312.
28. DRAPER, N. R., and SMITH, H., *Applied Regression Analysis.* Wiley (1966).
29. MANDEL, J., *The Statistical Analysis of Experimental Data.* Interscience Publishers (1964).
30. PFISTER, J. F., and HOGNESTAD, E., "High Strength Bars as Concrete Reinforcement, Part 6, Fatigue Tests." *Jour. PCA Research and Development Laboratories,* Vol. 6, No. 1 (Jan. 1964) pp. 65-84; *PCA Devel. Dept. Bull. D74.*
31. BURTON, K. T., and HOGNESTAD, E., "Fatigue Tests of Reinforcing Bars—Tack Welding of Stirrups." *Jour. ACI, Proc.,* Vol. 64, No. 5 (May 1967) pp. 244-252; PCA Devel. Dept. Bull. D116.
32. HANSON, J. M., BURTON, K. T., and HOGNESTAD, E., "Fatigue Tests of Reinforcing Bars—Effect of Deformation Pattern." *Jour. PCA Research and Development Laboratories,* Vol. 10, No. 3 (Sept. 1968) pp. 2-13; *PCA Devel. Dept. Bull. D145.*
33. BANNISTER, J. L., "The Behavior of Reinforcing Bars under Fluctuating Stress." *Concrete,* Vol. 3, No. 10 (Oct. 1969) pp. 405-409.
34. JHAMB, I. C., and MACGREGOR, J. G., "Fatigue of Reinforcing Bars." *Structural Eng. Rept. No. 39,* Univ. of Alberta, Edmonton (1972) 180 pp.
35. PASKO, JR., T. J., "Fatigue of Welded Reinforcing Steel," *Jour. ACI, Proc.,* Vol. 70, No. 11 (Nov. 1973) pp. 757-758.
36. REHM, G., "Contributions to the Problem of the Fatigue Strength of Steel Bars for Concrete Reinforcement." (In German with English and French summaries), *6th Congress Preliminary Publ.,* International Assoc. for Bridge and Structural Engineers, Stockholm (1960) pp. 35-46.
37. FISHER, J. W., and VIEST, I. M., "Fatigue Tests of Bridge Materials of the AASHO Road Test." *HRB Spec. Rep. No. 66* (1961) pp. 132-147.
38. WASCHEIDT, H., "Zur Frage der Dauerschwingfestigkeit von Betonstählen im einbetonierten Zustand (On the Fatigue Strength of Embedded Concrete Reinforcing Steel)." Doctoral thesis, Tech. Univ. of Aachen, Germany (1965); also abbreviated version, *Technische Mitteilungen Krupp—Forschungsberichte,* Vol. 24, No. 4 (1966) pp. 173-196.
39. JHAMB, I. C., and MACGREGOR, J. G., "Fatigue Strength of Deformed Reinforcing Bars." *Structural Eng. Rept. No. 18,* Univ. of Alberta, Edmonton (1969) 155 pp.
40. MACGREGOR, J. G., JHAMB, I. C., and NUTALL, N., "Fatigue Strength of Hot-Rolled Deformed Reinforcing Bars." *Jour. ACI, Proc.,* Vol. 68, No. 3 (March 1971) pp. 169-179.
41. BENNETT, E. W., and BOGA, R. K., "Some Fatigue Tests of Large Diameter Deformed Hard Drawn Wire Used for Prestressed Concrete." *Civil Eng. Public Works Rev.* (London) Vol. 62 (1967) pp. 59-61.
42. WEISMAN, M. H., "Detail Design and Manufacturing Considerations." *Metal Fatigue: Theory and Design,* ed. A. F. Madayag, Wiley (1969).
43. OSGOOD, C., *Fatigue Design.* Wiley-Interscience (1970).
44. KRAVSHENKO, P. YE., *Fatigue Resistance.* Pergamon Press (1964).
45. TETELMAN, A. S., and MCEVILY, JR., A. J., *Fracture of Structural Materials.* Wiley (1967).
46. KOKUBU, M., and OKAMURA, H., "Fatigue Behavior of High Strength Deformed Bars in Reinforced Concrete Bridge Design." *ACI Publ. SP-23,* presented at First Internat. Symposium—Concrete Bridge Design. American Concrete Inst., Detroit (1969) pp. 301-316.
47. LASH, S. D., "Can High-Strength Reinforcement Be Used for Highway Bridges." *ACI Publ. SP-23,* First Internat. Symposium—Concrete Bridge Design. American Concrete Inst., Detroit (1969) pp. 283-299.
48. GRÖNQVIST, N. O., "Fatigue Strength of Reinforcing Bars." *ACI Publ. SP-26,* presented at Second Internat. Symposium—Concrete Bridge Design. American Concrete Inst., Detroit (1971) pp. 1011-1059.
49. JHAMB, I. C., and MACGREGOR, J. G., "Effect of Surface Characteristics on Fatigue Strength of Reinforcing Steel." *ACI Publ. SP-41,* presented at Abeles Symposium on Fatigue of Concrete. American Concrete Inst., Detroit (1974) pp. 139-167.
50. JHAMB, I. C., and MACGREGOR, J. G., "Stress Concentrations Caused by Reinforcing Bar Deformations." *ACI Publ. SP-41,* presented at Abeles Sym-

posium on Fatigue of Concrete. American Concrete Inst., Detroit (1974) pp. 169-182.

51. DERECHO, A. T., and MUNSE, W. H., "Stress Concentration at External Notches in Members Subjected to Axial Loadings." *Eng. Experiment Station Bull. 494,* Univ. of Illinois, Urbana (Jan. 1968) 51 pp.
52. BURTON, K. T., "Fatigue Tests of Reinforcing Bars." *Jour. PCA Research and Development Laboratories,* Vol. 7, No. 3 (Sept. 1965) pp. 13-23; *PCA Devel. Dept. Bull. D93.*
53. GRAF, O., and WEIL, G., "Versuche über die Schwellzugfestigkeit von verdrillten Bewehrungsstählen (Experimental Study I of the Fatigue Limit for Twisted Reinforcing Steels)." *Deutscher Ausschuss für Stahlbeton,* No. 101, Berlin (1948).
54. SORETZ, ST., and WEINER, I., "Influence des sollicitations de fatigue sur le comportement de deux grandes poutres a hourdis armeés d'acier Tor-40 a verrous (Influence of Fatigue Loading on the Behavior of Two Large Simply Supported Girders Reinforced With Deformed TOR-40 Steel)." *Annales de Travaux Publics de Belgique,* No. 5 (1963).
55. SORETZ, ST., "Fatigue Behavior of High-Yield Stress Reinforcement." *Concrete and Constructional Eng.,* Vol. 60, No. 7 (July 1965) pp. 272-280.
56. BLOM, G., *Statistical Estimates and Transformed Beta-Variables.* Wiley (1958).
57. KIMBALL, B. F., "On the Choice of Plotting Positions on Probability Paper." *Jour. Am. Statistical Assoc.,* Vol. 55 (1960) pp. 546-560.
58. MANN, H. B., and WALD, A., "On the Choice of the Number of Class Intervals in the Application of the Chi-Square Test." *Annals of Mathematical Statistics,* Vol. 13, (1942) pp. 306-317.
59. WILLIAMS, JR., C. A., "On the Choice of the Number and Width of Classes for the Chi-Square Test of Goodness of Fit." *Jour. Am. Statistical Assoc.,* Vol. 45 (1950) pp. 77-86.
60. MANDEL, J., and MCCRACKIN, F. L., "Analysis of Families of Curves." *Jour. Res. Natl. Bur. Stds.,* A.V. 67A, (1963) pp. 259-267.
61. RALSTON, A., and WILF, H. S., *Mathematical Methods for Digital Computers.* Wiley (1962).
62. DIXON, W. J., and MOOD, A. M., "A Method for Obtaining and Analyzing Sensitivity Data." *Jour. Am. Statistical Assoc.,* Vol. 43 (1948) pp. 109-126.
63. WALLIS, W. A., "Tolerance Interval for Linear Regression." *Proc. Second (1950) Berkeley Symposium on Mathematical Statistics and Probability,* ed. Jerzy Neyman, Univ. of California Press, Berkeley (1951) pp. 43-52.
64. Reinforcement for Reinforced and Prestressed Concrete, Tentative Recommendations, RILEM-FIP-CEB, *Materials and Structures, Research and Testing* (Paris), Vol. 6, No. 32 (March-April 1973) pp. 79-118.
65. GROVER, H. J., GORDON, S. A., and JACKSON, L. R., *Fatigue of Metals and Structures.* U.S. Department of the Navy, Bureau of Naval Weapons, NAVWEPS 00-25-534, Washington, D.C. (1960) 399 pp.
66. "Properties and Selection of Materials." Vol. 1, Eighth Edn., *Metals Handbook,* Am. Soc. Metals, Novelty, Ohio (1961).
67. FORREST, P. G., *Fatigue of Metals.* Pergamon Press (1962).
68. MAYER, M., "Dauerfestigkeit von Spannbetonbauteilen (Fatigue Strength of Prestressed Concrete Structural Elements)." *Deutscher Ausschuss für Stahlbeton,* Vol. 176, Berlin (1966) 69 pp.
69. *Betonstahl-Prüfung des Stabstahls,* DIN 488, Blatt 3 Beuth-Vertrieb GmbH, Berlin (1968).
70. WÖHLER, A., "Über die Festigkeitversuche mit Eisen und Stahl." *Zeitschrift für Bauwesen,* Vol. 8 (1858).
71. ABELES, P. W., and BROWN, E. I., "Expected Fatigue Life of Prestressed Concrete Highway Bridges as Related to the Expected Load Spectrum." *ACI Publ. SP-26,* presented at Second Internat. Symposium—Concrete Bridge Design. American Concrete Inst., Detroit (1971) pp. 962-1010.
72. CHANG, T. S., and KESLER, C. E., "Fatigue Behavior of Reinforced Concrete Beams." *Jour. ACI, Proc.,* Vol. 55, No. 2 (Aug. 1958) pp. 245-259.
73. HANSON, J. M., and HELGASON, TH., Discussion: "Fatigue Strength of Hot Rolled Deformed Reinforcing Bars." *Jour. ACI, Proc.,* Vol. 68, No. 9 (Sept. 1971) pp. 725-726.
74. *The Making, Shaping, and Treating of Steel.* Eighth edn. Ed. H. E. McGannon, United States Steel Corp.
75. SAMANS, C. H., *Engineering Metals and Their Alloys.* MacMillan (1949).
76. KEYSER, C. A., *Materials of Engineering,* Prentice-Hall (1956).
77. HANKINS, G. A., and BECKER, M. L., "The Fatigue Resistance of Unmachined Forged Steel." *Jour. Iron Steel Inst.,* Vol. 126 (1932) p. 205.
78. HANKINS, G. A., BECKER, M. L., and MILLS, H. R., "The Effect of Surface Conditions on the Fatigue of Steels." *Jour. Iron Steel Inst.,* Vol. 133 (1936) p. 399.
79. SIEBEL, E., and GAIER, M., "The Influence of Surface Roughness on the Fatigue Strength of Steels and Non-Ferrous Alloys." *Zeitschrift des Vereines Deutscher Ingenieure,* Vol. 98 (1956) p. 1715.
80. BATE, S. C. C., "The Strength of Concrete Members Under Dynamic Loading." *Proc., Symposium on the Strength of Concrete Structures.* Cement and Concrete Assoc., London (1958) pp. 487-524.
81. SORETZ, ST., Discussion of Ref. 80, *op. cit.* pp. 537-538.
82. BATE, S. C. C., Reply to Ref. 81, *op. cit.* pp. 553-554.
83. HAIGH, B. P., "The Relative Safety of Mild and High-Tensile Alloy Steels Under Alternating and Pulsating Stresses." *Proc., Inst. Automobile Engrs.,* Vol. 24 (Dec. 1929) pp. 320-347.
84. Roš, M., "Festigkeit under Verformung von auf Biegung beanspruchten Eisenbetonbalken (Stiffness and Deformation of Reinforced Concrete Beams Subjected to Bending)." Eidengenössische Materialsprüfungs und Versuchsanstalt für Industrie, Bauwesen and Gewerbe (EMPA), Rept. No. 141 (1942);

Abstract in *Concrete Constructional Eng.*, Vol. 42, No. 7 (July 1947) pp. 223-228.

85. Roš, M., "Die zukünftige Gestaltung der Stahlbeton-Bauweise (The Future Form of Reinforced Concrete Construction Methods)." *Berichte der Ag. der von Moos'schen Eisenwerke,* Lucerne (March 1952) p. 72.
86. Dallaire, G., "Designing Bridge Decks That Won't Deteriorate." *Civil Eng.*, Vol. 43 (Aug. 1973) pp. 43-48.
87. Love, R. J., "The Influence of Surface Condition on the Fatigue Strength of Steel." *Proc., Symposium on the Properties of Metallic Surfaces,* Inst. of Metals (1952) p. 161.
88. Peterson, R. E., *Stress Concentration Design Factors.* Wiley (1974).
89. Hartman, J. B., and Leven, M. M., "Factors of Stress Concentration for the Bending Case of Fillets in Flat Bars and Shafts with Central Enlarged Section." *Proc., Soc. Experimental Stress Analysis,* Vol. 9 (1951) pp. 53-62.
90. Durelli, A. J., Lake, R. L., and Phillips, E., "Stress Concentrations Produced by Multiple Semi-Circular Notches in Infinite Plates under Uniaxial State of Stress." *Proc. Soc. Experimental Stress Analysis,* Vol. 10 (1952) pp. 53-64.
91. Baud, R. V., "Study of Stresses by Means of Polarized Light and Transparencies." *Proc. Engrs. Soc. Western Pennsylvania,* Vol. 44 (1928) p. 199.
92. Barone, M. R., Cannon, J. P., and Munse, W. H., "Fatigue Behavior of Welded Reinforcement in Reinforced Concrete Beams." Civil Engineering Studies, Structural Research Series No. 407, Illinois Cooperative Highway Research Program Series No. 149, Univ. of Illinois, Urbana (May 1974) 161 pp.
93. Walls, J. C., Sanders, Jr., W. W., and Munse, W. H., "Fatigue Behavior of Butt-Welded Reinforcing Bars in Reinforced Concrete Beams." *Jour. ACI, Proc.*, Vol. 62, No. 2 (Feb. 1965) pp. 169-192.
94. Kobrin, M. M., and Sverchkov, A. G., "Effect of Component Elements of Deformation Patterns on the Fatigue Strength of Bar Reinforcement." (In Russian) *Experimental and Theoretical Investigations of Reinforced Concrete Structures,* ed. A. A. Gvozdev, Academy of Building and Architecture USSR, Scientific Research Institute for Plain and Reinforced Concrete, Gosstroiizdat, Moscow (1963) 225 pp.
95. *Amsler Manual,* Instruction No. 122/10, Alfred J. Amsler & Co., Schaffhausen, Switzerland.
96. Weltman, H. J., Halkias, J. E., Kaarlela, W. T., and Reynolds, J. D., Magnetic Rubber Inspection—A New Dimension in NDT." *Materials Res. Stds.,* Vol. 12, No. 9 (1972) pp. 20-24.
97. *Modern Steels and Their Properties,* Handbook 268-H, Sixth Edn. Bethlehem Steel Corp.
98. *Biometrika Tables for Statisticians,* eds. E. S. Pearson and H. O. Hartley, Vol. 1, Cambridge Univ. Press, London (1954).
99. Acton, F. S., *Analysis of Straight-Line Data,* Wiley (1959) and Dover Publications, Inc. (1966).
100. Reemsnyder, H. S., "Procurement and Analysis of Structural Fatigue Data." *Jour. Struct. Div.*, ASCE, Vol. 95, No. ST7 (1969) pp. 1533-1551.
101. Box, G. E. P., "The Effects of Errors in the Factor Levels and Experimental Design." *Technometrics,* Vol. 5 (1963) pp. 247-262.
102. Wetz, J. M., "Criteria for Judging Adequacy of Estimation by an Approximating Response Function." Unpublished Ph.D. thesis, advisor G. E. P. Box, Univ. of Wisconsin (1964).
103. Dixon, W. J., "The Up-and-Down Method for Small Samples." *Jour. Am. Statistical Assoc.*, Vol. 60 (1965) pp. 967-978.
104. Little, R. E., "Estimating the Median Fatigue Limit for Very Small Up-and-Down Quantal Response Tests and for S-N Data with Runouts." *Probabilistic Aspects of Fatigue, ASTM Spec. Tech. Publ. No. 511,* Am. Soc. Testing and Materials, Philadelphia (1972) pp. 29-42.
105. Anscombe, F. J., and Tukey, J. W., "The Examination and Analysis of Residuals." *Technometrics,* Vol. 5 (1963) pp. 141-160.

APPENDIX A

REVIEW OF LITERATURE

Fatigue Tests on Reinforcing Bars

In the general field of metal fatigue, considerable information[65,66,67] is available that relates to the fatigue strength of common structural steels. Most of this information was obtained from rotating-beam or axial tension fatigue tests on machined specimens. Such data are of greater interest to the aeronautical or mechanical engineer than the highway bridge engineer. However, in many instances, data obtained from such tests serve to indicate or to explain effects that may be of concern to the highway bridge engineer.

Fatigue tests on bridge structural elements have largely been concerned with the effects of joints in built-up or rolled structural steel sections. Base material properties of such steels have often been similar to those used for reinforcing bars. However, research on the fatigue properties of bolted, riveted, or welded joints and cover plates has proven to be of little value in determining the fatigue properties of reinforcing bars. They can only be determined from tests on reinforcing bars, conducted in a manner simulating closely their actual usage in reinforced concrete structures.

Previous investigations into the fatigue properties of reinforcing bars have been conducted with the test bars placed in axial tension in ordinary fatigue testing machines, or embedded in concrete and placed in tension or subjected to bending. Disagreement exists as to whether the fatigue

strength of a reinforcing bar embedded in concrete is lower[36,68] or higher[55] than that of a bar tested in air. The question cannot be resolved on the basis of presently available data since the methods of bar embedment, testing, and stress calculation varied widely. Furthermore, no statistical procedures were applied in the experimental design and analysis of the test results.

No standard test to determine the fatigue properties of reinforcing bars has been developed in the United States. Perhaps this is because the critical method of test is not yet fully known. The Federal Republic of Germany has established a standard, DIN 488[69], that includes a provision for the fatigue testing of reinforcing bars. However, this standard recommends a highly unrealistic method of concrete embedment of the test bar and the test procedure is unduly severe. More recently, a recommended procedure for the fatigue testing of reinforcing bars in axial tension in air has been issued[64] jointly by RILEM, FIP, and CEB.

Strong recommendations[36] have been made for conducting fatigue tests on reinforcing bars with the test bar embedded as the main reinforcement within a concrete beam. Only in this manner is it possible to apply forces to the test bar in the same way that they are applied to a reinforcing bar in a concrete structure. Bond properties of the reinforcing bar affect the manner in which stresses are transferred from concrete to steel. Transverse lugs on deformed reinforcing bars transmit a large part of the force carried by a reinforcing bar to the body of the bar. At the same time, these transverse lugs cause stress concentrations to arise. Simultaneous dowel action of the bar in shear regions, where tension cracks occur in the surrounding concrete, further complicate the stress condition

to which a reinforcing bar is subjected. These considerations have led most researchers to conduct their fatigue tests on embedded bars.

A number of recent test results[30-32,39,47,52] on North American hot-rolled deformed reinforcing bars, embedded within concrete beams, are shown in Fig. A-1. Each of the test beams contained a single, straight reinforcing bar, but the methods of load application varied. Bar sizes tested ranged from No. 5 to No. 11. Grades 40, 60, and 75 bars were included. Calculated minimum stress levels, sustained throughout each test, ranged from 0.1 to 0.4 of the yield strength of the test bar. Not all of the reported test results are shown in Fig. A-1. However, the highest and lowest fatigue strengths obtained are included.

As may be seen in Fig. A-1, the fatigue strength of reinforcing bars varies widely. However, when individual S-N curves are drawn for nominally identical bars tested under nominally identical conditions, the scatter in test results is much reduced. From such graphs it is possible to discern some of the effects of varying bar properties and test conditions other than stress range. The S-N curves reported in the literature for the test results shown in Fig. A-1 were based on a visual evaluation of the run of the data and, thus, on the individual judgment of the observer.

All S-N curves for reinforcing bars show one common characteristic. At low stress ranges, resulting in long fatigue lives, the curves tend to become parallel with the log N axis. This is particularly pronounced for fatigue lives at or in excess of 1 million cycles. At higher stress ranges, resulting in fatigue lives of less than 1 million cycles, a strong relationship between applied stress range and the fatigue life of a reinforcing bar is seen to exist. This relationship is generally taken to

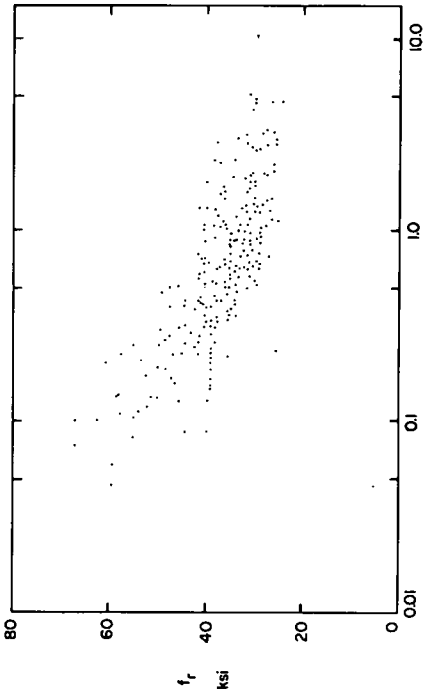

Fig. A-1 Previously Published Fatigue Test Results for Deformed Bars Made in North America

be linear and may show a variety of slopes. For convenience, a test resulting in a fatigue life of less than about 1 million cycles will be considered to be the "finite-life" fatigue region. Similarly, a test resulting in a fatigue life in excess of 1 million cycles will be considered to be in the "long-life" fatigue region.

The variation in the test results shown in Fig. A-1 is partly due to the inherent scatter obtained in fatigue testing but mostly to the diverse factors that affect the fatigue strength of reinforcing bars. Not all of the potential influencing factors are known, but the following are among those that have received some attention in the literature:

1. Stress range
2. Minimum stress level
3. Bar diameter
4. Strain gradient
5. Grade of bar
6. Manufacturing process
7. Shape of transverse deformations
8. Bending of bar
9. Tack welding stirrups to bar
10. Welded joints between bars
11. Type of specimen tested

The first two factors listed -- stress range, f_r, and minimum stress level, f_{min} -- define the fatigue design stress condition in a reinforcing bar. The next three factors -- bar diameter, strain gradient across a bar, and grade of bar -- are also selected by the designer. These are followed by two factors -- manufacturing process and shape of deformations -- that relate to properties imparted to a reinforcing bar during

its manufacture. The next three factors -- bending of a bar, tack welding, and welded joints -- concern construction practice detailing. Finally, the type of specimen tested and the test procedure used have often been selected on the basis of the objectives of a particular investigation. Effects of these factors on the fatigue life of a reinforcing bar will be briefly reviewed in the following sections.

Effects of Design Oriented Fatigue Influencing Factors

Stress Range. It has long been recognized[70] that the magnitude of the stresses applied to a structural member is the primary external factor in determining its fatigue life. However, there is little agreement as to the form in which this factor should be expressed. The various alternatives include expressing S-N diagrams in terms of maximum stress[15,38,41], load or stress ratio[71,72], or stress range[30,32,39,52]. In this report, the effects of stress range and minimum stress are considered separately and they are regarded as individual fatigue influencing factors.

In the long-life region, no specific relationship between stress range and fatigue life is apparent. Experimentally determined S-N diagrams are nearly parallel with the log N axis. Several investigators[32,33,39] have conducted tests on reinforcing bars for up to 10 million cycles of loading without obtaining fatigue fracture of their test specimens. Therefore, it appears that reinforcing bars may possess a fatigue limit. At applied stress ranges below such a limit, a reinforcing bar may be able to sustain a nearly unlimited number of cycles of loading without damage.

A wide variation in the stress range level at which the long-life region is entered is seen to exist in the test results plotted in

Fig. A-1. These previously reported test results on straight deformed North American made reinforcing bars show that fatigue fracture in the long-life region may occur at stress ranges varying from 25 to 40 ksi. Thus, fatigue limits for the various types of bars tested may also be expected to vary within this range. Most of this variation must be attributed to factors other than stress range.

The existence of a finite-life region relationship between stress range and fatigue life is readily apparent from Fig. A-1. Agreement as to to its nature, however, is not universal. Several investigators [30,38,41] indicate a nonlinear relationship between stress range and fatigue life in their S-N diagrams. Others [32,34,52] show a linear relationship. However, it is known[45,67] that, as the maximum applied cyclic stress approaches the tensile strength, the S-N curve again becomes nearly parallel to the log N axis. Thus, a curvilinear transition would connect the stress levels represented by the tensile strength and the fatigue limit. However, this is closely approximated, for reinforcing bars, by a linear relationship in the region bounded by fatigue lives of 10 thousand and 1 million cycles. The entire range of fatigue lives is perhaps best expressed in terms of an exponential function of stress range, but such representation requires more data than are presently available.

Minimum Stress Level. Several researchers[30,36,38,39,41] have discussed the effect of minimum stress on the fatigue strength of reinforcing bars. Some investigators[36,37] claim that minimum stress has no significant effect on fatigue strength. Others[30,38,39,41] state that a minimum stress effect may be distinguished in their data. Only one of these investigations[37] was designed to study the problem on a statistical basis.

However, the results of that investigation may have been influenced by other effects.

Tests on No. 8 and No. 11 bars of Grades 40, 60, and 75 were reported by Pfister and Hognestad[30]. The No. 8 bars had three different deformation patterns designated A, B, and C. Bars of Pattern A were of Grades 40, 60, and 75, while Pattern B bars were of Grades 40 and 75, and bars of Pattern C were of Grade 75. The No. 11 bars had a fourth deformation pattern, designated D, and were of Grade 40. Each test was carried out with a single straight reinforcing bar encased as the main reinforcement within a concrete beam. Minimum stress levels in the reinforcing bars were approximately 0.1 and 0.3 of their yield strength.

The Grade 75 bars were tested at a sufficient variety of stress ranges that an estimate can be made of their finite-life fatigue properties. Results of these tests are shown in Fig. A-2. Also shown are the results of tests on Grade 60 bars of Pattern A. Runout tests are indicated by an arrow.

In each case, the lines shown in Fig. A-2 as representative of finite- and long-life fatigue properties are merely reasonable visual estimates. However, these estimates show a definite decrease in fatigue strength with increased minimum stress level in the finite-life region. Estimates of the fatigue limit show a corresponding decrease.

Trends in the data from tests on bars of Grades 40 and 60 are not as clear as those for the Grade 75 bars. This is partly due to the fact that the test series were not designed for statistical evaluation of the data. Furthermore, many of the tests on the Grade 40 bars resulted in stressing beyond yield. This caused large plastic deformations in the bars and may have had an effect on their fatigue strength.

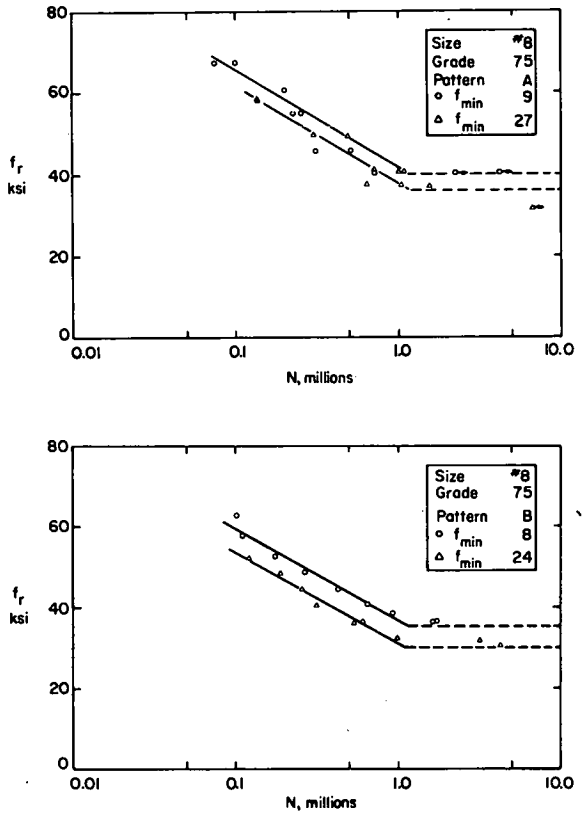

Fig. A-2 Effect of Minimum Stress Level

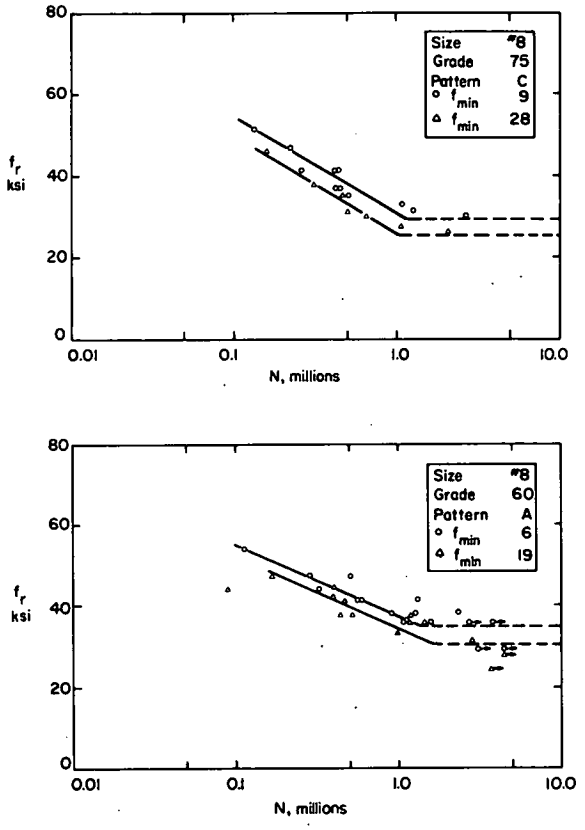

Fig. A-2 Effect of Minimum Stress Level (Continued)

The test results reported by Pfister and Hognestad[30] for bars of Pattern D were analyzed statistically by Fisher and Viest[37]. They reported that changing the minimum stress from 0.1 to 0.3 of the yield stress accounted for a barely significant portion of the variation in the test data. This may be due to the above mentioned effect of yielding of the test bars.

Jhamb and McGregor[39] tested Canadian made No. 8 bars of Grades 40, 60, and 75. The test bars were embedded within concrete beams and subjected to minimum stress levels of 0.1 and 0.4 of their yield strengths. The data do not allow any conclusions to be reached on the effect of minimum stress level in the finite-life region. However, visual estimates of the location of the fatigue limit indicate that it was reduced by about 17% as the minimum stress level was increased.

In a summary paper on his investigations into the fatigue properties of German reinforcing bars, Rehm[36] states that the minimum stress level does not affect fatigue strength. However, he notes that fatigue strength is increased when the stress cycle in the bars includes compressive stresses. Since no individual test results were reported in the paper, no reassessment of his conclusions is possible.

Waschеidt[38] has carried out further tests on German reinforcing bars. These tests indicate that fatigue strength may be influenced by the minimum stress level.

British fatigue tests on plain prestressing wires are reported by Bennett and Boga[41]. Various minimum stress levels were applied. They observed that the fatigue strength was somewhat reduced as the minimum stress level was increased.

Bar Diameter and Strain Gradient Across Bar. In the general field of metal fatigue, it is recognized that the size of a test specimen may affect the fatigue properties attributed to the base metal of machined specimens. Thus, Forrest[67] states that while the fatigue strength of plain unnotched specimens is independent of size in direct tension tests, such an effect does occur in rotating-beam tests. The fatigue strength of plain rotating-beam specimens machined to various diameters from bars of a single diameter was found to increase with decreasing specimen diameter when the diameter was smaller than 1 in. Geometrically similar notched specimens of various diameters also showed an increase in rotating-beam fatigue strength with decreased bar diameter.

The effect of specimen size on the rotating-beam fatigue strength of specimens machined from bars of different diameters is discussed by Weisman[42]. He quotes test results showing a reduced fatigue strength with an increase in diameter from 1 to 6 in. for specimens machined from bars forged to successively smaller diameters. The observed gain in fatigue strength with decreased diameter was attributed by Weisman to the additional working of the material in producing smaller diameter bars. This results in a finer grain structure and the fragmentation and dispersion of inclusions capable of reducing fatigue strength.

Susceptibility of the material to work hardening or strengthening is said by Osgood[43] to strongly affect the amount of variation in fatigue strength observed for geometrically similar specimens of different sizes. Thus he attributes a significant part of the size effect to the total amount of working the material receives, particularly the reduction in thickness from the original ingot to the final form.

Kravshenko[44] points out that an increase in the absolute dimen-

sions of a specimen increases the surface area which is subjected to maximum stress in bending and torsion tests, thus increasing the likelihood of a fatigue crack being initiated. This view is supported by Tetelman and McEvily[45] who state that there is a statistical size effect related to the probability of finding a critical flaw within the most highly stressed region.

In ordinary structural concrete design, only an average tension reinforcement stress is calculated. However, bars in concrete beams and slabs subjected to bending will have a higher stress on that side of the bar farthest from the neutral axis. This is due to the strain gradient across the member and is most pronounced for large diameter bars in shallow beams or thin slabs.

In the fatigue testing of reinforcing bars embedded within concrete beams, the effects of bar size and strain gradient are inevitably linked. As pointed out by Hanson and Helgason[73], all fatigue cracks in such bars have been observed to be initiated within that half of the bar where the tensile stresses are the highest. The larger the diameter of a reinforcing bar, the greater is the effect of the strain gradient, as may be seen in Table C-1.

The effect of the strain gradient on fatigue strength may be seen in test results reported by Burton[52] and by Burton and Hognestad[31]. No. 8 Grades 60 and 75 bars of a single deformation pattern were tested while embedded as the main reinforcement within concrete beams. A minimum stress level of 5.1 ksi was used throughout. Some tests were conducted with the longitudinal ribs of the test bar located in a vertical plane within the test beam, others with the ribs in a horizontal plane.

It was observed that, when the test bars had their longitudinal

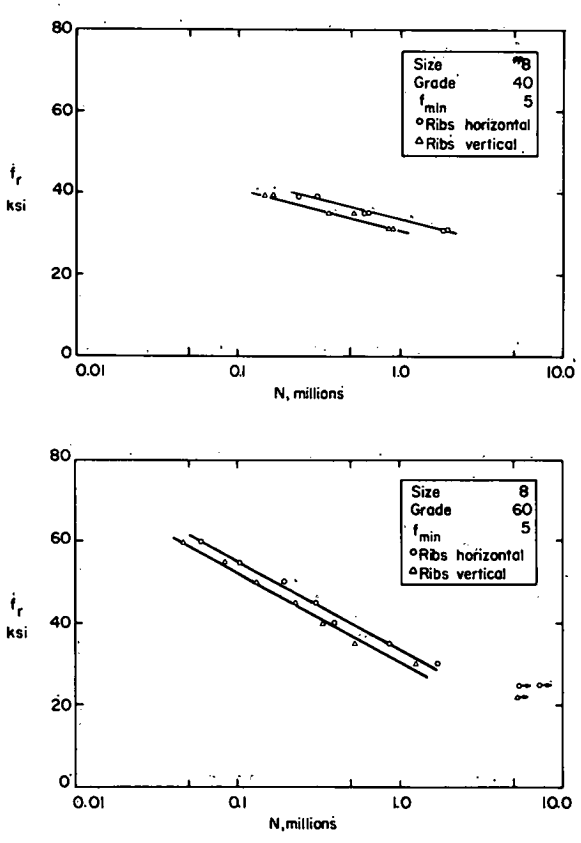

Fig. A-3 Effect of Strain Gradient

ribs located in a vertical plane, the fatigue crack was always initiated in the immediate vicinity of the junction of a transverse lug with the more highly stressed rib. When the ribs were horizontal, the fatigue cracks were generally initiated at the root of a transverse lug, about midway between the ribs, and in the more highly stressed half of the bar. A statistical analysis[52] showed that the bar orientation had a statistically significant effect on the observed fatigue strength.

Results of these tests are shown in Fig. A-3. Bars with the longitudinal ribs located in a vertical plane show a lower fatigue strength than nominally identical bars with ribs located in a horizontal plane. Evidently, the critical fatigue zone for these bars was located at or near the junction between the transverse lugs and the ribs. When the ribs were located in a horizontal plane, the stress range in this critical zone was somewhat less than when the ribs were in a vertical plane. Consequently, the bars with the longitudinal ribs in a horizontal plane were able to survive a greater number of cycles of loading. A random orientation of the critical fatigue zone on the periphery of a reinforcing bar that is embedded in a concrete beam subjected to cyclic loading will thus cause a considerably greater scatter in test results than would be obtained under controlled conditions.

Investigations to determine the effect of bar diameter on the fatigue strength of reinforcing bars have been carried out by Wascheidt[38], Kokubu and Okamura[46], and MacGregor, Jhamb, and Nutall[40]. These test series were intended to result in a determination of the fatigue strength at 2 or 5 million cycles for bars of various diameters. None of the experiments was designed for statistical analysis of the data. Therefore, all evaluations of the fatigue strength at 2 and 5 million cycles were based

on visual inspection of the plotted test data. Such evaluations are of limited accuracy for tests carried out in a fatigue life region where the scatter in test results is widespread. Nevertheless, a certain trend in fatigue strength with variation in bar diameter is discernible from these test results.

Wascheidt tested bars 16 (0.63) and 26 mm. (1.02 in.) in diameter. These bars were of four different grades but had the same deformation pattern and nominally similar transverse lug geometries. All tests were carried out in axial tension in air. A single minimum stress level was used throughout.

Number 6 and No. 8 bars having four different deformation patterns and various guaranteed yield strength levels were tested by Kokubu and Okamura[46]. No information is provided in their paper on the geometric similarity of the transverse lugs rolled onto different size bars having the same deformation pattern. Each test bar was embedded as the main reinforcement within a concrete beam. All bars were subjected to the same minimum stress.

The tests reported by MacGregor, Jhamb, and Nutall[40] were conducted on No. 5, 8, and 10 bars of Grades 40, 60, and 75. Various measurements were made of the transverse lug dimensions. From these, average stress concentration factors, varying from 1.49 to 1.64, were calculated for each size and grade bar tested. Each test was carried out with the test bar encased within a concrete beam. The minimum stress levels used were about 0.1 of the yield strength for each grade of bar.

A comparative summary of the results obtained by these investigators is given in Table A-1. In each case, the reported fatigue strength at 2 or 5 million cycles for a bar equivalent in size to a No. 8 bar is

TABLE A-1 EFFECT OF BAR DIAMETER

Tests by	Grade of Bar	Fatigue Strength at 2 or 5 Million Cycles Relative to Fatigue Strength of No. 8 Bars			
		No. 5	No. 6	No. 8	No. 10
Wascheidt[38]	40	1.11	-	1.00	-
	40	1.05	-	1.00	-
	60	1.05	-	1.00	-
	75	1.10	-	1.00	-
Kokubu and Okamura[46]	40	-	1.12	1.00	-
	60	-	1.04	1.00	-
	60	-	1.10	1.00	-
MacGregor, Jamb, and Nutall[40]	40	1.06	-	1.00	0.99
	60	1.08	-	1.00	0.96
	75	1.20	-	1.00	0.95

taken as a base value. The fatigue strengths obtained for the various bar sizes and grades are then compared in terms of the ratio of each value to its respective base value. The German bars tested by Wascheidt are presented in terms of their equivalent ASTM grades. Two low yield strength German bars are lumped together as Grade 40 bars.

It should be noted, that in comparing the various ratios presented in Table A-1, some allowance must be made for the effect of strain gradient. Tests by Wascheidt were carried out in axial tension and his bars were therefore nominally under uniform stress. The bars tested by Kokubu and Okamura were encased at an effective depth of 6.3 in. in concrete beams. This concrete had a compressive strength of about 5000 psi at the time each test was conducted. The effective depth of beams tested by MacGregor, Jhamb, and Nutall varied with the size of bar tested. These depths were 9, 12-1/2, and 15-5/8 in., respectively, for the No. 5, 8, and 10 bars. Concrete strengths in these tests varied from 3720 to 6050 psi.

10 or 15% of the increase in tensile strength. For tensile strengths greater than 160 ksi, the notch effect becomes predominant and the fatigue limit may be reduced again. A further reduction, throughout the entire range of tensile strengths, was found to occur when the surface of a test specimen was pitted by corrosion. On this basis, it is to be expected that reinforcing bars will exhibit an increasing sensitivity to changes in bar geometry the greater the tensile strength. Therefore, the effect of grade of bar on the fatigue strength of deformed reinforcing bars is best assessed in tests on bars that have been passed through the same rolls.

The effect of grade of bar on the fatigue strength of deformed reinforcing bars has been studied in three North American investigations. In each case, the different grade bars had the same deformation pattern but were not passed through the same rolls. Additionally, the minimum stress level used was increased for the higher grade bars in proportion to the increase in yield strength. Therefore, the effect of grade of bar in these investigations could not be separated clearly from the effects of minimum stress and bar geometry.

Pfister and Hognestad[30] studied the fatigue properties of different grades of No. 8 bars having two deformation patterns, designated A and B, respectively. Each bar was tested while embedded as the main reinforcement within a concrete beam. Minimum stress levels used were 0.1 of the yield strength of the bars.

Results of these tests are shown in Fig. A-4. The test results for the Grade 40 bars of Pattern A are not shown in this figure. Instead, the estimated fatigue limit for these bars is shown.

Grade of Bar. Efforts at assessing the effect of grade of bar on the fatigue strength of reinforcing bars have not always been successful. This is because other fatigue influencing factors have often masked the potential effect due to grade of bar. Thus, when a Grade 40 bar is stressed beyond yield, an additional effect due to the large plastic deformation to which the bar is subjected may show up. Grade 60 and 75 bars have a relatively short or nonexistent yield plateau and are not subjected to large plastic deformations when stressed beyond their yield strengths.

Excessive cold working of reinforcing bars is known[53] to cause a decrease in fatigue strength. This may occur when Grade 40 bars are stressed beyond yield. Therefore, unless this effect is separated from the test results when the grade of bar effect is studied, the finite-life S-N diagram for Grade 40 bars may improperly be considered to have a different slope from the diagrams for Grade 60 and Grade 75 bars.

Fatigue tests on bars of different grades have generally been conducted at a specified minimum stress level that is a fixed multiple of the yield strength of each grade of bar. Thus, bars of Grade 75 have often been tested at twice the minimum stress level of Grade 40 bars, while the test results have been compared on an equal basis by visual inspection of S-N diagrams. Full evaluation of such data is possible only by statistical means.

It has long been accepted[67] that the fatigue limit for machined and polished steel specimens increases with the tensile strength of the steel. For such specimens, the fatigue limit is raised by about one-half of the increase in tensile strength for strengths up to 200 ksi. However, when notches are present, the increase in the fatigue limit may be only

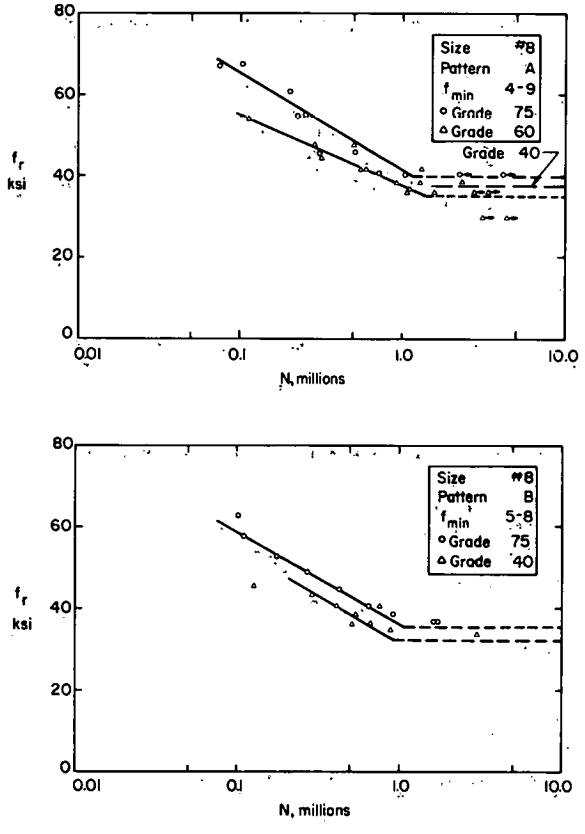

Fig. A-4 Effect of Grade of Bar, American Tests

The lines shown in Fig. A-4, representing the average fatigue properties of the bars tested by Pfister and Hognestad, were determined by visual judgement. It is seen that, regardless of the bar deformation pattern, the Grade 75 bars have a higher fatigue strength than the Grade 40 bars. This is in spite of the Grade 75 bars having been tested at a higher minimum stress level than the Grade 40 bars. Thus, the difference in test results must be attributed to the effect of grade of bar.

It may be seen in Fig. A-4 that the Grade 60 bars of Pattern A have a lower fatigue strength than the Grade 40 bars of the same deformation pattern. This is partly due to the higher minimum stress level at which the Grade 60 bars were tested. However, that does not fully explain the observed behavior and, for lack of information to the contrary, the major part of the effect must be attributed to a difference in bar geometry. This illustrates the difficulty of determining the effect of a single parameter, when the test results are confused by the effects of other factors.

A series of twenty tests on Canadian produced bars of a single deformation pattern and four different grades is reported by Lash[47]. The bars tested were of Grades 40, 50, 60, and 75. Each bar was embedded within a concrete beam for testing. Minimum stress levels used were about 0.25 of the yield strength. One test ended in shear failure, but four each on Grade 40, 60 and 75 bars, and seven on Grade 50 bars ended in fatigue fracture. Two tests were discontinued after the reinforcing bars had survived more than 3 million cycles.

Lash concluded there was no distinct difference in test results among the Grade 40 and 50 bars. However, the Grade 60 and 75 bars tested

showed a definite progressive increase in fatigue strength over the Grade 40 bars.

Further tests on Canadian produced bars are reported by MacGregor, Jhamb, and Nutall[40]. The effect of grade of bar on fatigue strength was studied in tests on No. 5, 8, and 10 Grades 40, 60, and 75 bars of a single deformation pattern. These tests were carried out with each bar embedded as the main reinforcement within a concrete beam. Two minimum stress levels were used, 0.1 and 0.4 of the yield strength of the bars.

It was concluded in this paper that, for design purposes, the fatigue strength at 5 million cycles for hot-rolled deformed reinforcing bars is not affected by changes in the tensile strength of the bars. However, the adequacy of the analysis leading to this conclusion is questionable. Minimum stress effects were eliminated by means of the Goodman diagram, which of itself presupposes a grade-of-bar effect. Measured differences in bar geometry among bars of the same size were, however, not taken into account. Furthermore, a discussion[73] of this paper pointed out that an unusual scatter in test results had been obtained. For these reasons, and since S-N curves for the test results were based on visual estimates, the effect of grade of bar on the fatigue properties of these bars is not clear.

Tests on German reinforcing bars of several grades and having various deformation patterns are reported by Wascheidt[38]. The effect of grade of bar on the fatigue strength at 2 million cycles was studied in axial tension tests that were carried out in air. A single minimum stress level was used for these tests.

Because of differences in bar geometry among the various bars tested, only the results for the bars designated as Type E can be compared

directly. For these bars, the fatigue strength at 2 million cycles, as based on visual estimates, was found to increase slightly with an increase in yield strength.

Grönqvist[48] carried out fatigue tests in axial tension in air on Swedish reinforcing bars. These bars had a diameter of 16 mm. (0.63 in.) and were of Swedish Grades Ks 40, 40s, 60, 60s. Average yield strengths of these bars were about 62, 66, 91, and 96 ksi, respectively. A minimum stress level of 10.7 ksi was used throughout.

The effect of grade of bar on the fatigue properties of these bars may be studied by comparing test results for bars having the same deformation pattern. Bars of Grades Ks 40, 40s, and 60 were rolled to the standard deformation pattern for the Grade Ks 40 bars, while bars of Grades Ks 40, 60, and 60s were rolled to the standard deformation pattern for the Grade Ks 60 bars. However, measurements of the lug dimensions indicate a variation in bar geometry among bars of different grades rolled to the same deformation pattern.

Results of these tests are shown in Fig. A-5. The S-N diagrams shown represent a reasonable visual judgment of the average fatigue properties of the test bars. Of the bars rolled to the standard Ks 40 deformation pattern, the Grade Ks 60 bars had the lowest fatigue strength and the Grade Ks 40 bars the highest. Test results for the Grade Ks 40s bars are not shown in Fig. A-5 but their S-N diagram was intermediate to those for the Grade Ks 40 and Ks 60 bars. For bars having the standard Ks 60 deformation pattern, the Grade Ks 60 bars again had the lowest fatigue strength, while the Grade Ks 60s bars had the highest.

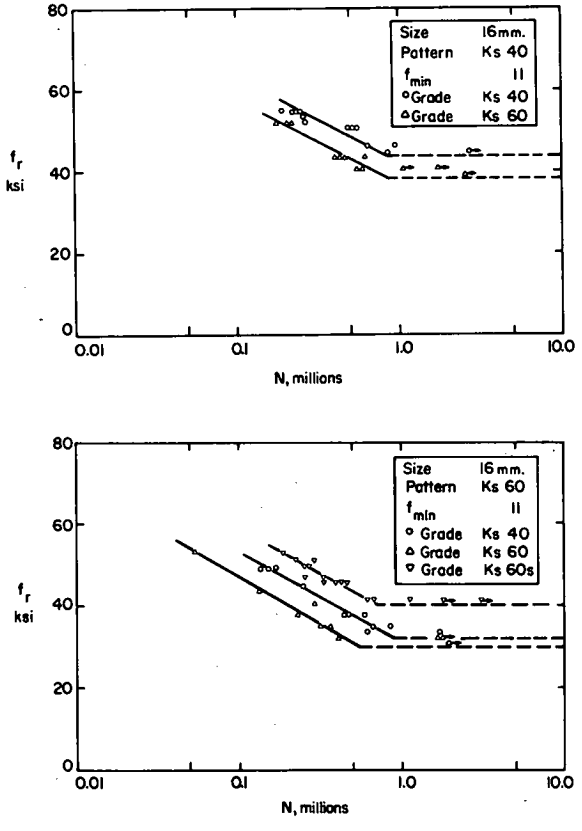

Fig. A-5 Effect of Grade of Bar, Swedish Tests

Grönqvist concluded that grade of bar had an important effect on fatigue strength. He was, however, unable to determine any specific relationship between grade of bar and fatigue strength.

The results of fatigue tests on Japanese reinforcing bars are summarized in a paper by Kokubu and Okamura[46]. A total of 94 tests were carried out on bars embedded as the main reinforcement within concrete beams. These bars were of three different sizes and represented eleven basic varieties of deformation patterns. For two of the deformation patterns, bars having smooth and sharp transverse lug geometries were tested. Guaranteed minimum yield strengths of the test bars varied from 50 to 85 ksi.

A single minimum stress level was used throughout. Two or three stress range levels were used for each set of bars to determine the fatigue strength at 2 million cycles. These stress ranges were selected to result in at least one fatigue fracture between 1 and 2 million cycles.

The fatigue strength at 2 million cycles was found to range between 28 and 51 ksi. Kokubu and Okamura concluded that this variation was largely due to the effect of transverse lug geometry and that the effect of grade of bar was comparatively small. However, there was no direct comparison possible between different grade bars of the same deformation pattern.

Effect of Manufacturer Related Fatigue Influencing Factors

Manufacturing Process. Reinforcing bars are manufactured from low- and medium-carbon steels and from alloy steels. Billets are shaped into reinforcing bars by successive rolling through a series of stands. As many as 15 stands are used to reduce a 4x4 in. billet to a 3/4-in. bar by hot-rolling. Deformations are hot formed in the final roll by passing

the bars between special rolls that have patterns cut into them. The surface of a bar is forced into depressions in the rolls to form characteristic deformations[74].

The chemical composition of reinforcing bars varies considerably, even for bars of the same grade produced by the same mill. Thus, previously reported[30, 32, 40, 52] analyses of the chemical composition of North American produced reinforcing bars of Grades 40, 60, and 75 show a carbon content ranging from 0.32 to 0.58%, manganese from 0.32 to 1.48%, silicon from 0.05 to 0.29%, and molybdenum from less than 0.05 to 0.20%. The only requirement of ASTM specification A615-68[1] concerning the chemical composition of deformed billet steel bars for concrete reinforcement is that the amount of phosphorus shall not exceed 0.05%.

The chemical composition of the European reinforcing bars tested by Wascheidt[38] and Grönqvist[48] also varies widely. Carbon content ranged from 0.04 to 0.53%, manganese from 0.34 to 1.41%, and silicon from less than 0.05% to 1.35%. Molybdenum content was not reported by these investigators.

One of the characteristic fatigue properties of steels is that the S-N curve usually shows a distinct fatigue limit[67]. This behavior is most pronounced for plain carbon steels, but is less evident for alloy steels. It is attributed to the diffusion of carbon and nitrogen atoms within the iron lattice.

In machined specimens, the fatigue strength of steel is strongly related to its tensile strength. Therefore, any factor that tends to increase tensile strength, such as heat treatment or addition of alloying elements, is considered to have a beneficial effect on fatigue strength. The addition of such elements as carbon, manganese, nickel, chromium,

molybdenum, vanadium, copper, boron, and phosphorus to the chemical composition of a steel is considered by Forrest[67] to increase fatigue strength in proportion to their influence on tensile strength. Silicon and manganese, when acting together, are considered by Gamans[75] to tend to improve fatigue strength.

In the production of reinforcing bars, the surface condition of a bar will be influenced by the hot rolling process. Oxidation of the hot-rolled surface results in decarburization of the steel and the formation of loose-clinging scale. These effects combine in creating a surface layer of low tensile strength, extensively covered with small notches. Initiation of fatigue cracks in this surface layer is promoted by its weakness in resisting tensile stresses and by the presence of notches.

Decarburization refers to the loss of carbon from a surface layer of the steel. It occurs in the presence of oxygen, carbon dixoide, or water vapor during high temperature heat treatment. Molybdenum and cobalt, when used as alloying elements, are said by Keyser[76] to tend to promote decarburization.

The effect of decarburization on the fatigue strength of spring steels was studied by Hankins et.al.[77, 78]. They conducted rotating beam fatigue tests both on specimens receiving no treatment after forging and on polished specimens that had been machined to remove the decarburized layer. The relationship between fatigue strength and tensile strength was found to be linear for both types of specimens for tensile strengths up to 130 ksi. Machined specimens had a fatigue strength that averaged about one-half of the tensile strength. The "as forged" specimens, had a considerably reduced fatigue strength. The difference was about 15% for a tensile strength of 60 ksi and 50% for a tensile strength of 130 ksi. Thus, the effect of decarburization becomes ever more important as the

tensile strength of the steel increases.

Mill scale is formed in the presence of oxygen during high temperature heat treatment of steel. Severity of the scaling depends on the composition of the surrounding atmosphere and the duration of the heat treatment. If the scale is not removed during hot working operations, it is pressed into the metal surface, causing surface roughness. Siebel and Gaier[79] used tests on machined specimens to show that surface roughness has an appreciable effect on the fatigue strength of steel.

Inclusions may be formed in steel during the manufacturing process. These may be nonmetallic or intermetallic and consist of complex metallic compounds. Their number and distribution are determined by the chemical composition of the steel, melting and working practices, and the final heat treatment of the material. Inclusions may cause a reduction in fatigue strength by acting as stress raisers.

The size and orientation of an inclusion relative to the direction of stressing is important in determining its effect on fatigue strength. During the rolling process of reinforcing bars, inclusions become elongated and oriented in the longitudinal direction of the bar. Thus they may be expected to have only a small effect on the fatigue strength of reinforcing bars subjected to axial stresses.

Residual stresses may be set up within a reinforcing bar during the manufacturing process. Such stresses usually result either from cold working or from a heat treatment that allows a temperature difference to develop rapidly between the surface and the interior. Compressive residual stresses at the surface of a member subjected to fatigue loading are considered to be beneficial. Tensile residual stresses are detrimental to fatigue strength. A tensile stress field is additive to tensile residual

stresses and thus a lower mean tensile stress is required to cause fatigue fracture.

European reinforcing bars are commonly cold twisted to increase their yield and tensile strengths. This results in residual stresses at the bar surface. The effect of such residual stresses on fatigue strength can only be assessed by comparison of test results for undisturbed bars with those for cold-twisted bars having the same bar geometry. No such test results are known to be available for deformed bars.

Tests on undisturbed and cold-twisted plain reinforcing bars are reported by Graf and Weil[53]. They determined the fatigue limit at 2 million cycles for nominally identical bars that had been subjected to various amount of cold-twisting. All tests were conducted in axial tension in air and at the same minimum stress level. These test bars had a nominal diameter of 27 mm. (1.06 in.).

Graf and Weil expressed the amount of residual twist in terms of the length of pitch in bar diameters. Yield and tensile strengths of the bars were found to increase continuously with decreasing pitch. The undisturbed bars had yield and tensile strengths of 37 and 59 ksi, respectively. These increased to 96 and 100 ksi, respectively, at a pitch of 2.6 diameters. The fatigue strength at 2 million cycles was 34 ksi for the undisturbed bars. This rose to 40 ksi when the pitch was 12.9 diameters and held steady at 40 ksi as the pitch was decreased to 9.4 diameters. A further decrease in pitch caused a decrease in fatigue strength. At a pitch of 2.6 diameters, the fatigue strength was 26 ksi.

These test results have been interpreted in different ways. The investigators did not themselves draw any conclusions regarding the decrease in fatigue strength with excessive twisting. Bate[80] concluded

from these tests that moderate amounts of cold working had a beneficial effect on the fatigue strength of mild steel. Excessive cold working, however would cause a decrease in fatigue strength. This interpretation was disputed by Soretz[81] who attributed the decrease in fatigue strength to notch effects created by rolling streaks in the bars. These streaks were longitudinal in the undisturbed bars but progressively more transversely oriented with increased twisting. Bate[82] acknowledged the stress concentration effect of the rolling streaks, but cited additional work by Haig[83] and Ros[84, 85] on the fatigue properties of mild steel to support his view that the reduction in fatigue strength was caused largely by excessive cold working.

Further fatigue testing of cold twisted reinforcing bars has been carried out by Wascheidt[38]. Both plain and deformed 16 mm. (0.63 in.) diameter bars were tested. The deformed bars had two deformation patterns, designated B and C, respectively. Bars of Pattern B were twisted from bars having longitudinal ribs and no transverse lugs while bars of Pattern C were twisted from bars having both longitudinal ribs and transverse lugs. The plain bars and those of Pattern B were twisted to a pitch of 12 and 8 bar diameters. Bars of Pattern C were twisted to a pitch of 12, 10, and 6.5 bar diameters.

All of the tests were carried out in axial tension, most in air, but some of the bars were also tested as embedded in concrete. A single minimum stress level was used to obtain the test results to be compared.

Yield and tensile strengths of the bars were found to increase with the amount of twisting. For the plain bars and those of Pattern B, the fatigue strength at 2 million cycles was found to decrease by about 6 and 4 ksi, respectively, when the pitch was decreased from 12 to 8 dia-

meters. The bars of Pattern C, when tested in air, had a fatigue strength at 2 million cycles of about 38, 44, and 34 ksi, respectively, when the pitch was 12, 10, and 6.5 bar diameters. Not all of the fatigue fractures in the deformed bars were initiated at the base of a transverse deformation. The concrete embedded bars generally had a lower fatigue strength than the bars tested in air.

Recently, experimental use of galvanized reinforcing bars in bridge decks[86] has been initiated with the aim of eliminating the problem of reinforcing bar corrosion. No fatigue tests are known to have been conducted on such bars. However, hot dipping of a reinforcing bar in the galvanizing solution may create tensile residual stresses at the bar surface, thereby reducing the fatigue strength.

Love[87] reports that a comparison of the fatigue properties of undisturbed and hot-dipped galvanized steel specimens shows a decrease in fatigue strength of 4 to 42% for the galvanized specimens. A steel containing only 0.02% carbon showed a decrease in fatigue strength of 4% while a quenched steel containing 0.45% carbon showed a decrease of 42%. Various other annealed, quenched, or tempered 0.45 and 0.72% carbon steels had a loss of fatigue strength that ranged from 13 to 42%.

Bar Geometry. Rolled on transverse deformations on reinforcing bars provide the means of obtaining good bond with the surrounding concrete in a reinforced concrete structural member. These deformations act as shear keys between the reinforcing bar and the concrete. In the highly stressed regions of a reinforced concrete member, adhesive bond between reinforcing bar and concrete is largely destroyed and forces are transmitted between the bar and the concrete by means of the deformations on the bar.

The state of stress in the near vicinity of a transverse lug on a reinforcing bar embedded in a concrete member is very complex and largely unknown. Transverse deformations, in addition to transmitting forces between the concrete and the reinforcing bar, will also cause stress concentrations in the bar. These stress concentrations occur at the junction of each transverse lug with the body of the bar. Stress concentrations are a primary factor in causing loss of fatigue strength.

External notches, or lugs, are known to cause stress concentrations in bars and shafts subjected to axial tension, bending, or torsion[88]. Photoelastic studies by Hartman and Leven[89], and Durelli, Lake, and Phillips[90] show that the magnitude of the stress concentration factor depends on the base radius, height, width, and spacing of the lugs. The relationship between the stress concentration factor and the lug geometry is complex, but appears to be hyperbolic in nature.

Results of the photoelastic studies by Hartman and Leven[89] show that the lug base radius is the major variable affecting the stress concentration factor. The sharper the radius, the greater is the stress concentration factor. Effects of lug height and lug width are related but, for the same lug height, a wide lug will have a higher stress concentration factor than a narrow lug. Similarly, for the same lug width, a high lug will have a higher stress concentration factor than a low lug.

Baud[91] has shown that high and narrow lugs remain unstressed in the outer part of each lug when an axial force is applied to the parent body. Thus, there appears to be a limiting lug height for each lug width, above which there is no further increase in the stress concentration factor.

Studies by Durelli et.al.[90] showed that the stress concentrations due to several closely spaced notches are smaller than those due to a single

notch of the same geometry. Thus, for a constant lug base radius, the least critical fatigue location on a reinforcing bar with intersecting transverse deformations would be in the immediate vicinity of an intersection, where the crossing lugs are close but still separate. On the other hand, the most critical location would be immediately within the intersection, where the crossing lugs are at their widest.

Strains at the transverse lugs on a reinforcing bar subjected to axial tension in air have been measured by Jhamb and MacGregor[50]. Electric resistance strain gages having a gage length of 0.3 mm were placed on or near the lugs. Strains measured with these gages were compared with those obtained from 1/4-in. gages mounted on the barrel of the bar. The ratio of lug base strain to the reference strain was found to be as high as 1.82. At the top of a lug, strains were found to be 10% of the reference strain.

Theoretical studies of the stress concentration effects of external notches have been carried out by Derecho and Munse[51], and by Jhamb and MacGregor[50]. Derecho and Munse found that the flank angle of a lug is also important in determining the stress concentration effect. The larger the angle, the higher is the stress concentration factor.

Theoretical stress concentration factors determined by Derecho and Munse are shown in Fig. A-6. The curves shown have the typical hyperbolic shape obtained in photoelastic studies. Stress concentration factors calculated by Jhamb and MacGregor[50] by means of a finite element model show a similar trend.

The shape of the transverse deformations has been considered as a test variable in several investigations into the fatigue properties of

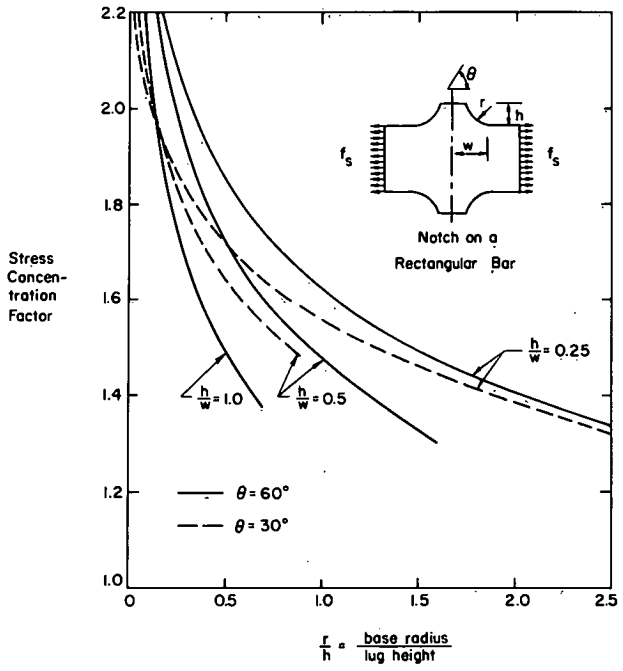

Fig. A-6 Stress Concentration at the Base of a Lug

deformed reinforcing bars. However, none of these investigations resulted in the development of a relationship between measured lug dimensions and fatigue strength.

Pfister and Hognestad[30] tested No. 8 bars of various grades and of three deformation patterns, designated A, B, and C. Material properties of the Grade 75 bars of Patterns A and C, along with the applied minimum stress levels, are sufficiently close that the difference in their fatigue properties must be attributed to lug geometry. Bars of Pattern A had transverse lugs perpendicular to the longitudinal bar axis while the bars of Pattern C had inclined lugs arranged so that the inclination alternated in sawtooth fashion. Each test was carried out with the test bar embedded as the main reinforcement within a concrete beam.

Test results for the bars of Patterns A and C are shown in Fig. A-7. The S-N diagrams shown represent a reasonable visual judgment of the average fatigue properties of the bars. Lug height was the only lug dimension reported by the investigators. Therefore, no assessment of the stress concentration factors is possible.

The effect of change in transverse lug geometry with the wear condition of the rolls used in the manufacturing process was studied by Burton[52]. Number 8 Grade 40 bars processed through new, partially worn, and fully worn rolls of a single deformation pattern were tested. Wear in the rolls resulted in a reduced lug height and flank angle. The lug base radius and the lug width, as measured between the points of tangency of a lug with the barrel of a bar, were increased.

Tests were carried out at three stress range levels. Unfortunately, yielding of the test bar occurred in each test at the highest

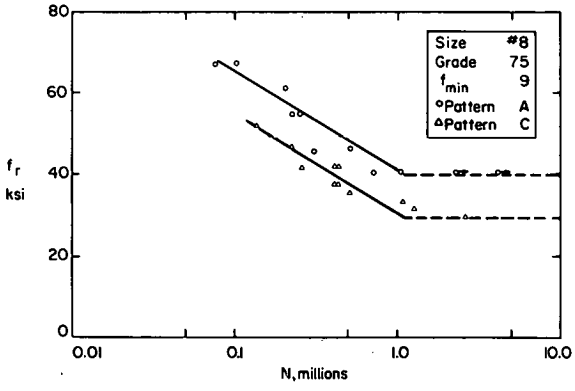

Fig. A-7 Effect of Deformation Pattern, American Tests

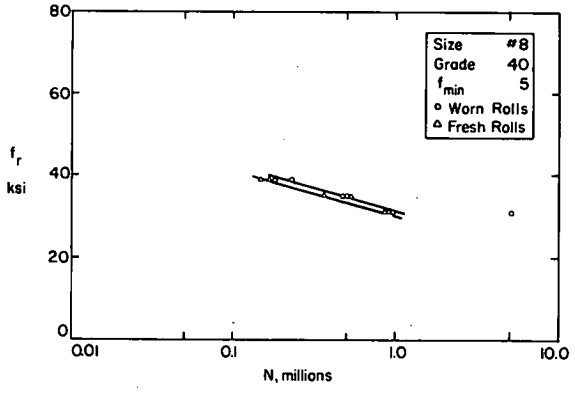

Fig. A-8 Effect of Wear in Rolls, American Tests

stress range level. The large plastic deformation incurred at this stress range constituted substantially different treatment from that at the other stress range levels. Moreover, tests at the lowest stress range level were carried out in the transition zone between the finite- and long-life regions. Therefore, an evaluation of the roll wear effect may only be carried out at the intermediate stress range level. As shown in Fig. A-8, the bars processed through fresh rolls exhibited a lower fatigue strength than the bars passed through worn rolls.

The effect of roll wear on fatigue life was also studied by Grönqvist[48]. Swedish Grades Ks 60 and Ks 60s bars of a single deformation pattern were processed through fresh and worn rolls. Photographs of the lug profiles of these bars show a much flattened and rounded lug being produced by the worn rolls. However, no accurate evaluation of the lug dimensions can be made from these photographs since they were taken of sectioned bar surfaces in their saw cut state. Furthermore, very little contrast was obtained in these photographs between the lug profiles and the photographic background.

Each test was carried out in axial tension in air. A constant minimum stress level was used throughout. Results of these tests are shown in Fig. A-9. The S-N diagrams shown represent a reasonable visual judgment of the average properties of the bars.

The observed difference in fatigue strength for bars of the same grade may be considered to be due to the effect of roll wear on lug geometry. Grönqvist does not explain why the Grade Ks 60 bars were so much more strongly affected by wear of the rolls than the Grade Ks 60s bars. However, a comparison of the lug profiles for the bars rolled through worn

rolls indicates considerably greater wear in the rolls used for the Grade Ks 60 bars. The transverse deformations on the Grade Ks 60 bars rolled through worn rolls appear to be inadequate for providing good bond with concrete.

Grönqvist[48] also studied the effect of deformation pattern on fatigue strength. One group of Swedish Grade Ks 40 bars was rolled to the regular lug pattern. A second group was rolled to the pattern normally used for Grade Ks 60 bars. Similarly, Grade Ks 60 bars were rolled to their regular lug pattern and to that normally used for the Grade Ks 40 bars. As previously stated, lug profile photographs obtained by Grönqvist were of insufficient quality to allow lug dimensions to be assessed.

Results of axial fatigue tests in air on these bars are shown in Fig. A-10. Once again, the S-N diagrams shown represent a reasonable visual judgment of the average properties of the test bars. Since all of the tests were conducted at the same minimum stress level, the observed difference in fatigue strength among bars of the same grade may be attributed to lug geometry alone. It should be noted that the Grade Ks 40 bars with the regular Ks 40 lug pattern were stressed beyond their yield strength when subjected to the three highest stress range levels.

As may be seen in Fig. A-10, the Ks 40 transverse deformations have superior fatigue characteristics to the Ks 60 deformations. The Ks 40 lugs were high and narrow relative to the Ks 60 lugs but had sharper base radii. Apparently, the lesser width of the Ks 40 lugs more than compensates for the increased stress concentration effect due to the decreased lug base radii.

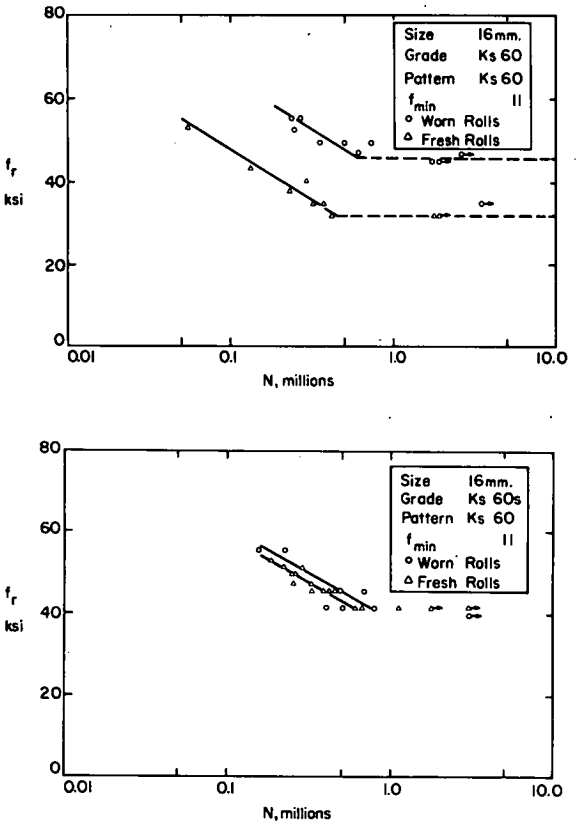

Fig. A-9 Effect of Wear in Rolls, Swedish Tests

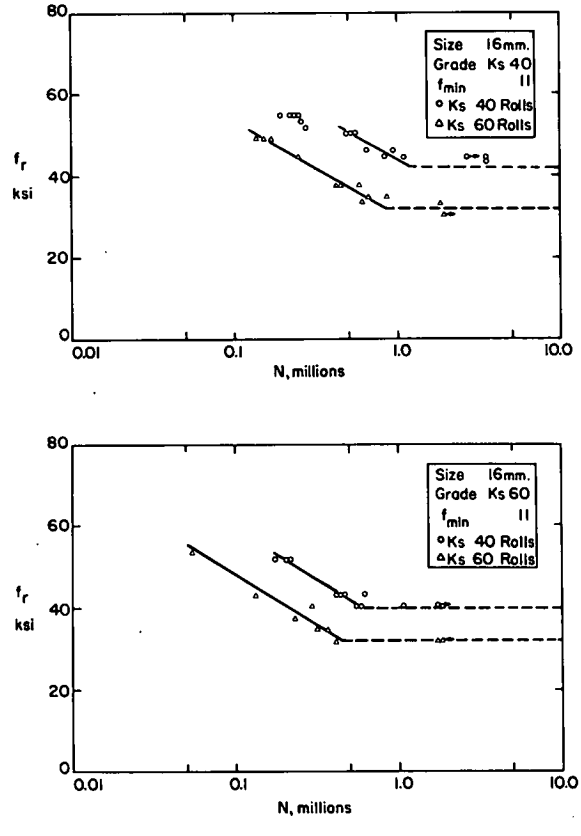

Fig. A-10 Effect of Deformation Pattern, Swedish Tests

Lug base radius and lug height were measured on typical bars used in the fatigue tests reported by Hanson, Burton, and Hognestad[32]. The fatigue properties of an American bar of Grade 40 and a European cold-twisted bar having a yield strength equivalent to that of a Grade 60 bar were determined. A direct comparison of the effect of the lug dimensions on the fatigue strength of these bars is not possible due to the difference in material properties and mechanical treatment.

Lug dimensions were also determined by MacGregor, Jhamb, and Nutall[40] in their tests on Canadian bars. Most of these tests were conducted in the transition zone between the finite-life and long-life regions for the test bars. Therefore, the data show a large amount of scatter and evaluation of either the finite-life or long-life properties of the test bars is difficult.

Research work on the fatigue properties of Japanese reinforcing bars is reported by Kokubu and Okamura[46]. They tested bars of various grades and with several different deformation patterns. Lug base radius to lug height ratios are reported for some of the deformation patterns. For the other deformed bars, it is stated that the transition from the barrel of the bar to the lug was abrupt. No account is given by the researchers of how the lug dimensions were determined.

Kokubu and Okamura attempt to establish a relationship between fatigue strength and the angle the deformation pattern makes with the axis of the bar for bars said to have no lug base radius. However, as pointed out by Hanson and Helgason[73], a considerable difference in lug base radius is observed when measured on a plane perpendicular to the lug and when measured

on a plane parallel to the bar axis. The effect attributed by Kokubu and Okamura to the angle of the lug pattern may have been misinterpreted.

Effect of Detailing Practice on Fatigue Strength

Bending of Bars. Tension reinforcement in reinforced concrete flexural members is commonly bent up into the concrete compression zone when no longer needed to resist tensile forces. In heavily reinforced members, such bends are often located in regions where the remaining tension reinforcement may still be highly stressed. By implication, the bent bars may also be highly stressed in the region of the bend. The fatigue properties of bent bars may therefore be of concern.

Fatigue tests on bent bars have been conducted by Pfister and Hognestad[30] in the United States and by various European investigators. The European research work has been summarized to some extent by Wascheidt[38]. Rehm[36] has published a summary of his test results on bent bars. All of these American and European tests were conducted on test beams so constructed that the bend in the test bar was located in the region of maximum moment. Tests on conventionally designed beams containing bent bars have been reported by Soretz and Weiner[54] and by Soretz[55].

Most fatigue tests on bent bars have been conducted with the test bar embedded as the main reinforcement within a concrete beam having a spread V shape in elevation. The bend in the bar was located at midspan, at the apex of the V. Each test beam was simply supported and subjected to a single concentrated load applied at midspan. The depth of the beams was decreased gradually from midspan with the intention of producing a region of essentially constant internal moment. These test conditions do not realistically represent the conditions to which a bent up bar is subjected.

Pfister and Hognestad[30] conducted their tests on straight and bent No. 8 Grade 60 deformed bars, as embedded within straight and angled concrete beams, respectively. All of the test bars were obtained from the same manufacturer. Two different minimum stress levels were used. Most of the tests were carried out on bars bent around a 6-in. diameter mandrel. Mandrels of 3- and 8-in. diameters were also used.

Test results obtained by Pfister and Hognestad for straight bars and for bars bent around a 6-in. diameter mandrel are shown in Fig. A-11. The S-N diagrams shown represent a reasonable judgment of the average properties of the test bars. Results of tests on bars bent around 3- and 8-in. diameter mandrels showed that the sharper the bend, the greater is the reduction in fatigue strength from that of the straight bars. It is noteworthy that the fatigue strength of the bent bars was greater for a minimum stress level of 19 ksi than for a minimum stress level of 6 ksi.

For the bent bars, the fatigue crack was initiated in the bent region and, in most cases, on the inside of the bend. Wascheidt[38] reports that fatigue crack initiation on the inside of a bend was also observed in similar fatigue tests conducted at the Technical University of Munich. He shows that, due to the elastic spring-back in bending, tensile residual stresses are induced along the inside surface of a bend while the outside surface picks up compressive residual stresses.

Wascheidt theorizes that the curve in a bent bar opens up during loading of a V-shaped test beam. This is caused by the deformation of the concrete when subjected to the compressive resultant force acting in the region of the bend when the test bar is stressed in tension. Such opening of the curve produces additional tensile stresses on the inside of the bend

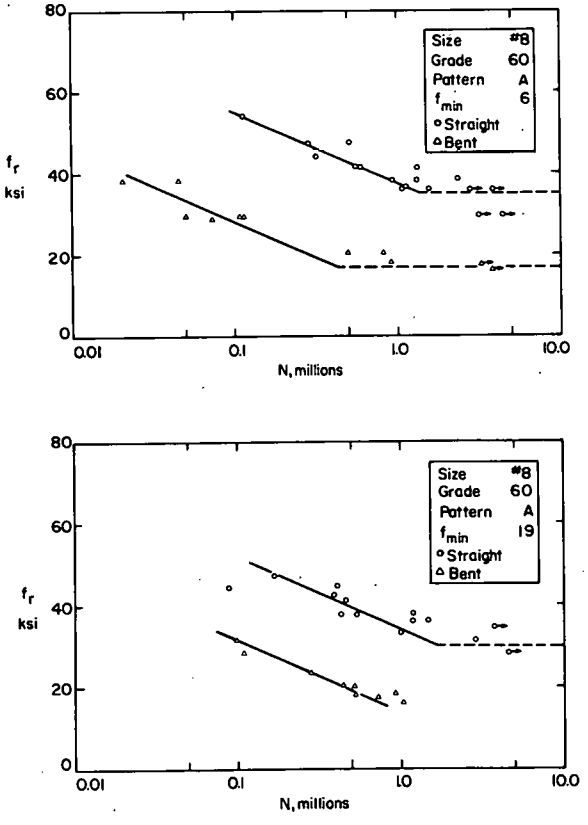

Fig. A-11 Effect of Bend in Bar

and corresponding compressive stresses on the outside of the bend. In their tests, Pfister and Hognestad[30] measured tensile strains on the inside face and compressive strains on the outside face of the bend when load was applied to a test beam.

The effect of sharpness of the bend in reducing fatigue strength is attributed by Wascheidt[38] to the increase in the compressive force acting on the concrete with a decrease in the bend radius. Increased compression of the concrete in the region of the bend would allow the curve to open further during loading of the beam, thereby producing higher tensile stresses on the inside of the bend.

In the tests on bent reinforcing bars embedded in V-shaped test beams, the reduction in fatigue strength relative to straight bars appears to be due to residual tensile stresses and additional tensile stresses set up by the test conditions. Similar residual stresses are set up in any bent bar. On the other hand, it is not known whether the additional tensile stresses due to opening of the curve in the bent bar would also occur in bent up bars in straight beams. However, similar stress conditions might arise in a bent up bar in a straight beam if the inclined part of the bar were crossed by a flexural crack in the concrete.

Fatigue tests on two large railway bridge beams are described by Soretz and Weiner[54] and by Soretz[55]. In these beams, the Grade 60 main reinforcement was bent into the compression zone when no longer needed to resist tensile stresses. The bars were bent to a radius of 10 bar diameters. Calculated stresses in the bottom layer of reinforcement ranged between 5.7 and 47.0 ksi during each load cycle. One or two bars in the bottom layer fractured in fatigue after each beam had been subjected to

1.2 million cycles of loading. The fractures occurred away from the bends. Therefore, the bends were considered to have had no detrimental effect on fatigue strength.

Tack Welding of Reinforcement. Reinforcing bars may be assembled into cages or mats by welding. It is known[67] that a welded steel assembly may have a lower fatigue strength than the individual components. The reduction in fatigue strength becomes more severe the higher the tensile strength of the steel. Therefore, the effect of welding on the fatigue strength of steel has often been associated with its carbon content.

Stress concentrations due to the geometric configuration of the weld metal deposit or to the welding process itself are considered[67] to be the most important factor in causing loss of fatigue strength. Undercutting at the edge of a weld or weld metal buildup above the original surface of a welded component will cause stress concentrations. Internal defects in a weld, such as porosity, slag, or lack of fusion, will also give rise to stress concentrations. Yet another cause of stress concentrations are cracks that may be formed in the weld metal or in the heat affected zone when too rapid cooling of the weld takes place.

High strength steels are less ductile than mild steels. Therefore, it is more likely that cracks will be produced at welds in high strength steels than in mild steels. Additionally, residual tensile stresses in the weld metal and the heat affected zone are likely to be of greater magnitude in high strength steels than in mild steels.

The effect on fatigue strength of tack welding stirrups to the main reinforcement in concrete beams has been investigated by Burton and Hognestad[31]. A single No. 8 Grade 40 or 60 medium-carbon deformed bar

was used as the main reinforcement for each beam. Each bar was placed with the longitudinal ribs oriented in a horizontal or vertical plane. Shear reinforcement consisted of No. 3 deformed bars. One test series for each grade of bar was carried out on beams having tack welded stirrups. Corresponding test series were carried out on beams having wire tied stirrups.

Careless field practice was simulated in arc welding the stirrups to the main reinforcement. For this purpose, high amperage and voltage settings were used on the welding machine. Generally, this led to deeply penetrating welds.

Test results for the bars having the longitudinal ribs oriented in a vertical plane are shown in Fig. A-12. The S-N diagrams shown represent a reasonable visual judgment of the average fatigue properties of the test bars. Some of the results shown for the Grade 40 bars with wire tied stirrups were obtained from a paper by Burton[52]. It should be noted that all of the Grade 40 bars were stressed beyond yield when tested at the highest stress range level.

All fatigue fractures occurred in the main reinforcement. When the stirrups were wire tied, the fatigue fracture was always initiated at the base of a transverse lug. When the stirrups were attached by welding, all fatigue fractures occurred at a weld.

A single minimum stress level was used for all of the tests. Furthermore, the test beams were nominally identical, except for the method of attaching the stirrups. Therefore, the observed reduction in fatigue strength when the stirrups were welded to the main reinforcement must be attributed to conditions created at the welds.

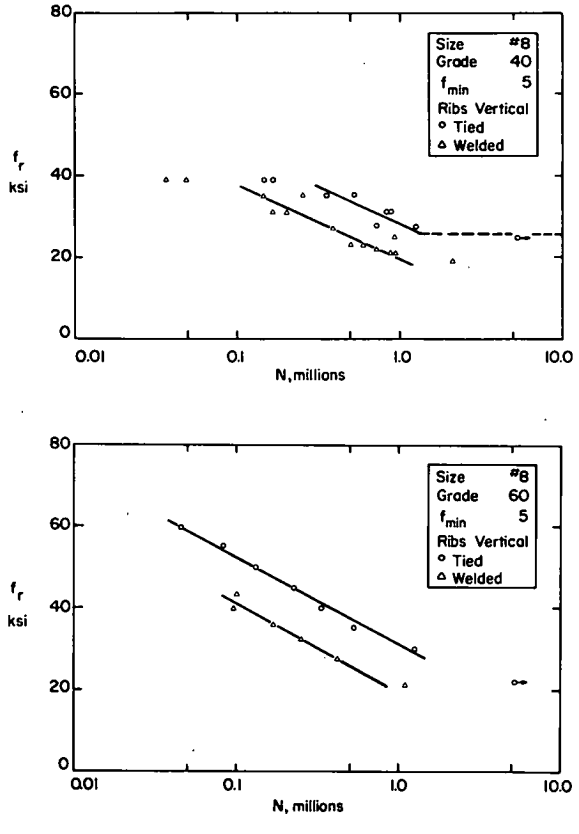

Fig. A-12 Effect of Welding Stirrups to Main Reinforcement

The effect of welding in the fabrication of bar mats on the fatigue strength of the parent material has been studied by Pasko[35]. Axial tension fatigue tests in air were carried out on No. 5 Grade 60 deformed bars used as the longitudinal reinforcement in bar mats having No. 3 deformed bars at 12-in. centers in the transverse direction. Welded bar samples were obtained at a manufacturer's plant from a representative bar mat. Corresponding undisturbed samples were obtained at the same time from bars produced from the same heat.

Test specimens representing unwelded bars were cut from the undisturbed bars and from the region between welds on the welded bars. Welded bars were represented by specimens having a welded intersection at mid-length. Each test specimen was 12 in. long. This specimen length is considered[64] insufficient for determining the axial tension fatigue properties of deformed reinforcing bars. However, this length may have been adequate for the purposes of the test program.

A minimum stress level of 3.2 ksi was used throughout. The stress range was varied to obtain S-N diagrams for the specimens with and without welds. A comparison of the finite-life test results for the undisturbed specimens and the specimens containing a weld showed a uniform reduction in fatigue strength of about 10 ksi for the welded bars.

It should be noted that two of the tests on the undisturbed specimens were carried out at maximum stresses exceeding 90% of the tensile strength. These tests must be considered to have been conducted in the low cycle fatigue region. They are the only fatigue tests on reinforcing bars known to have been carried out in this region.

A-49

Test results for some of the Grade 40 bars tested in air were reported by Sanders, Hoadley, and Munse[15]. A comparison of their evaluation of the average fatigue life at a stress range of 26 ksi for various types of joints is shown in Fig. A-13. This figure shows that the type of welded joint has a large influence on fatigue life.

Further tests[92] on bars of the same deformation pattern showed that a single strap joint had a considerably shorter fatigue life than the angle splice joint. These tests also showed that a double strap joint had about the same average fatigue life as a 60 degree double V joint.

Individual test results for the undisturbed bars and the 60-degree single V butt welded bars are shown in Fig. A-14. The S-N diagrams shown are based on a reasonable visual judgment of the average fatigue properties of the test bars. These diagrams indicate that the fatigue lives shown in Fig. A-13 have been overestimated. However, since most of the fatigue fractures in the undisturbed bars took place in the grips of the testing machine, these bars may well have longer fatigue lives than shown in Fig. A-14. Furthermore, test results for the welded bars show a large scatter at a stress range of 26 ksi. Therefore, these bars may also have longer fatigue lives than shown in Fig. A-14. For these reasons, it is believed that the trend exhibited in Fig. A-13 for the effect of type of joint on fatigue life is valid.

Effect of Type of Specimen Tested

Fatigue tests on reinforcing bars have been conducted in flexure on bar coupons in air, axial tension on bar coupons in air, axial tension on concrete encased bar coupons, and on bars embedded in concrete beams. No statistically valid comparative studies of the influence of the test method on fatigue strength, if any, have been carried out.

A-51

Welded Joints in Reinforcement. The effect on fatigue strength of splicing reinforcing bars by welding has been studied at the University of Illinois[92]. Some of the results obtained from this study have been reported elsewhere[15,93].

Axial tension fatigue tests were conducted on welded and undisturbed bars. Flexural fatigue tests on reinforcing bars embedded as the main reinforcement within concrete beams were also carried out. Most of these tests were on welded bars. Due to the lack of information on corresponding undisturbed bars, the effect of welding on the fatigue strength of concrete embedded bars is not fully known.

Most of the test bars were No. 7 Grade 40 or 60 deformed bars. These bars had four different deformation patterns. However, attempts to evaluate the effects of grade of bar and bar deformation pattern on axial tension fatigue properties were hampered by numerous fractures in the grips of the testing machine.

Emphasis was placed on determining the effect of type of welded joint on fatigue strength. The bars tested in axial tension were spliced by butt welding, lap welding, and welding an angle strap to the bars. The butt joints were 60 degree single V, 60 degree double V, 45 degree single V, and 60 degree single V with a pipe back-up. The lap joints were single strap and double strap. Only the 60 degree single V butt welded joint and a single lap welded joint were used in the beam tests.

Each weld was made up of several puddles resulting from careful passes with an arc welding electrode. This served to maintain low interpass temperatures. Therefore, the welds were representative of the best available welding practice.

A-50

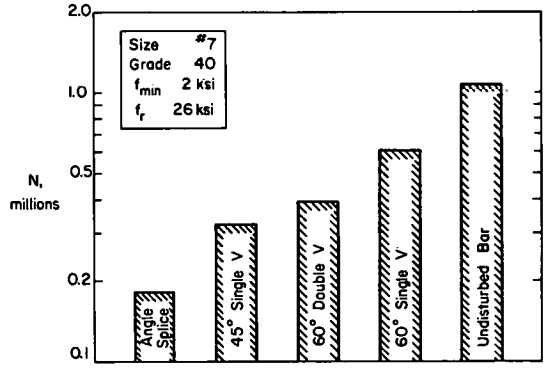

Fig. A-13 Relative Fatigue Resistance of Various Welded Joints

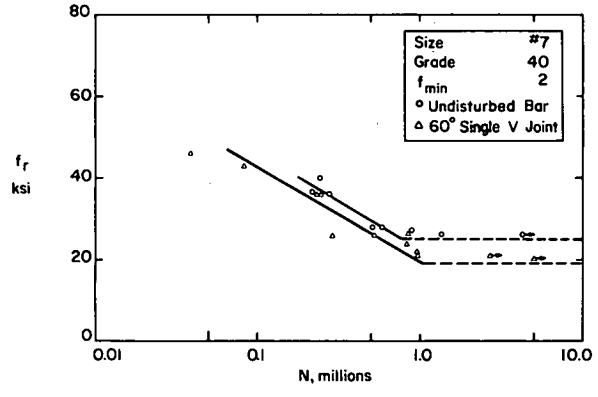

Fig. A-14 Effect of Welded Joint in Reinforcement

Flexural fatigue tests in air were carried out by Kobrin and Sverchkov[94]. First, the critical fatigue location on the periphery of a deformed reinforcing bar was determined in axial fatigue tests. Then, bar coupons were tested as simply supported beams subjected to two point cyclic loading. By controlling the orientation of the bar coupon relative to the plane of flexure, a determination was possible of the effect on fatigue strength of a variation around the periphery of the bar in the geometry of the deformations. A comparison could then be made with the fatigue strength obtained when the fracture was initiated at the critical fatigue location.

This test procedure was designed to allow the relative severity of stress concentrations on the bar surface to be determined. The objective was to obtain information for use in designing bar deformations having improved fatigue characteristics. However, the procedure does not fully simulate the action of the main reinforcement in a concrete beam where the deformations serve to transmit forces between the concrete and the reinforcement. It is not known how the stress concentrations in a deformed reinforcing bar subjected to axial and flexural stresses are affected by forces applied directly to the deformations.

Several investigators[15,35,38,48,49,53] have carried out fatigue tests on reinforcing bars in axial tension in air. However, it is only recently that a standard procedure for such tests has been recommended[64]. Use of this procedure would allow a more direct comparison of axial tension fatigue test results obtained in different laboratories than has been possible.

of the tests, the concrete jacket contained spiral reinforcement. Axial forces were transmitted to the test bar through the concrete. Wascheidt reported that, for deformed reinforcing bars, the fatigue strength of concrete encased bars was equal to or slightly lower than that of corresponding bars tested in axial tension in air.

Barone, Cannon, and Munse[92] describe fatigue tests on welded reinforcing bars cast into 6x12 in. concrete blocks. The test bar was located at a depth of about 2-1/2 in. from one of the narrow faces of the block and protruded sufficiently from the ends of the block to be placed in the grips of a testing machine. A steel collar was placed around the unreinforced end of each block. Thus, compressive stresses were induced in the restrained concrete when the reinforcing bar was pulled in axial tension. A considerably lower fatigue strength was obtained in these tests than in tests on corresponding bars embedded as the main reinforcement in concrete beams.

Fatigue tests on reinforcing bars embedded as the main reinforcement in concrete beams have been carried out by numerous investigators. Single span simply supported beams were used. Most of the beams can be grouped together under the three types shown in Fig. A-15.

Several fatigue investigations[30-32,40,47,52,55] have been carried out with the test bars embedded in beams of Type A. These beams are intended to simulate the conditions encountered at midspan in short single span structures and at interior supports in continuous beams and slabs.

A number of investigators[33,38,46,72,93] have used beams of Type B for concrete encasement of the test bars. Such beams simulate the conditions at midspan in long single span structures and at the location of maximum positive moment in continuous beams and slabs.

A large number of axial tension fatigue tests have resulted in fracture within the grips of the testing machine. This is due to the stress concentrations imparted to the test bar by the grips and, in many cases, to improper positioning of the specimen. Fatigue tests resulting in fracture near or within the grips are not representative of the population of tests resulting in fracture between the grips and should not be included in an analysis of such data.

The frequency of grip fractures varies considerably from one test series to another. Thus, in the tests reported by Jhamb and MacGregor[49], only 3 grip fractures occurred[34] in 88 tests, while Grönqvist[48] reported 12 such fractures in 112 tests. These results may be contrasted with those of Sanders, Hoadley, and Munse[15] who reported most of their fractures in tests on unwelded bars to have occurred at or within the grips.

A major reason for conducting fatigue tests on reinforcing bars in axial tension in air rather than embedded as the main reinforcement within concrete beams has been the relatively low cost of such tests. However, axial tension tests in air are not representative of the complex interaction between concrete and reinforcement in a concrete beam. Comparative tests[54,92] of reinforcing bars in concrete beams and in air have not established whether fatigue strength is enhanced or decreased by testing in air.

Fatigue tests, intended to simulate the stress conditions to which the main reinforcement in a concrete beam is subjected, have been carried out[38,92]. Wascheidt[38] tested reinforcing bars encased in a concrete jacket having a cross-sectional area of about 10 square inches. For some

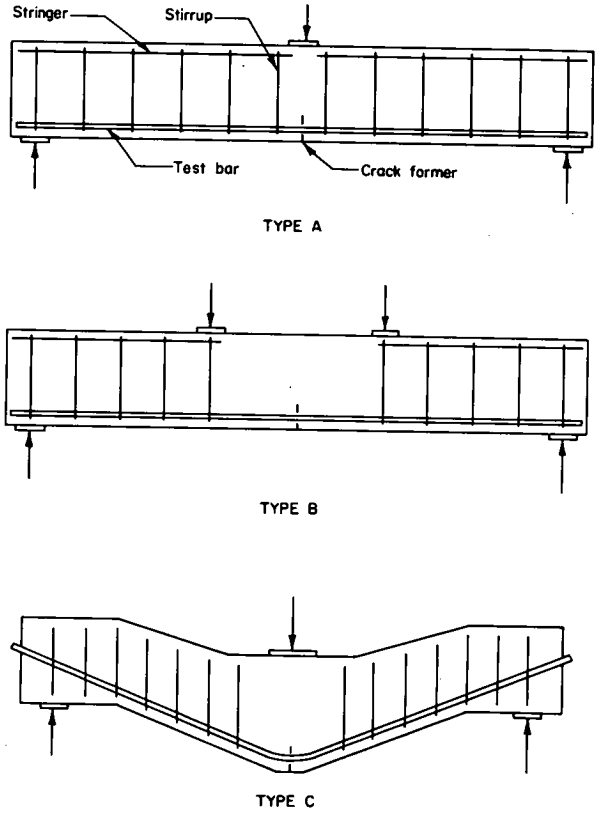

Fig. A-15 Beams for Testing Reinforcing Bars

Tests on reinforcing bars embedded in beams of Type C have been carried out in the United States[30] and in Europe[36,38]. Use of such beams is specified[69] in the Federal Republic of Germany for proof tests of the fatigue strength of reinforcing bars. Simulation of the conditions to which a bent up bar is subjected was intended in the design[36] of the test beam. The decrease in effective depth of the beam, from midspan towards the supports, provides a region of essentially uniform tension in the reinforcement.

The test conditions created in beams of Type C are believed to be unduly severe. A consistently lower fatigue strength was obtained[30] when reinforcing bars were embedded in beams of Type C than in beams of Type A. This is attributable to high residual stresses at the bend, coupled with opening of the bent curve during loading of the beam.

Beams of Type C do not properly simulate the action of bent up reinforcement in a straight concrete beam. No account is taken of the effect of the additional tension reinforcement present when a bar can be bent up. Such reinforcement may be subject to more severe fatigue conditions in the vicinity of a bend than the bent up bar itself. Tests[54,55] on heavy railroad bridge girders containing several bent up bars resulted in fatigue fracture of the tension reinforcement at locations away from the bends.

No comparative tests have been carried out to determine whether any difference in fatigue strength is obtained between bars embedded in beams of Types A and B. However, it is believed that use of beams of Type B results in a more representative evaluation of the fatigue properties of reinforcing bars since a long region of essentially uniform test conditions is provided.

straight deformed reinforcing bar was embedded within a rectangular or T-section concrete beam. Nominal effective depth of the test beams was 6, 10, or 18 in. Width of the compression flange was varied, for the different bar sizes, to maintain a nearly constant depth to the neutral axis for beams having the same effective depth.

Cyclic loading was applied to each test beam to produce a stress range in the test bar. The nominal minimum stress level in a test bar was either 6 ksi compression, 6 ksi tension, or 18 ksi tension. In general, each test was intended to result in fatigue fracture of the test bar after 50,000 to 5 million cycles, depending on the applied stress range, or in a runout after 5 million cycles.

A number of supplementary tests were carried out. These included a chemical analysis, hardness test, and microstructure examination for each manufacturer's bars. Fatigue tests on machined bar specimens were carried out in Phase I of the test program. Static strength tests on fatigued bar specimens were conducted in Phase II.

Selection and Identification of Test Bars

Two objectives of Phase I of the test program were to determine the effects of bar diameter and grade of bar on the fatigue strength of the test bars. To minimize the effects of manufacturer induced properties, these test bars were obtained from a single manufacturer capable of providing the various size and grade bars in a single deformation pattern and from a single mill.

The objective of Phase II of the test program was to determine the effect on fatigue strength of the transverse lug profile rolled onto the bar surface by the manufacturer in producing deformed reinforcing bars.

APPENDIX B

EXPERIMENTAL INVESTIGATION

Scope

The fatigue properties of deformed reinforcing bars were studied in an extensive two phase experimental program. Phase I was concerned with determining the effects of stress range, minimum stress level, bar diameter, grade of bar, and effective depth on fatigue life. In Phase II, the effect of transverse lug geometry was studied. Continuity between the two phases was preserved by further testing in Phase II of the bars obtained for study in Phase I.

Reinforcing bars tested in Phase I of the test program were obtained from a single United States manufacturer. Bars of five different sizes -- No. 5, 6, 8, 10, and 11 -- were tested. Most of the test bars in this phase were Grade 60 bars[1], but Grade 40 and Grade 75 bars were also tested.

All of the bars tested in Phase II of the test program were No. 8 Grade 60 bars. Five different manufacturers were represented in this phase. Each is a major United States producer of reinforcing bars. One manufacturer was represented by the bars remaining on hand from Phase I of the test program. The other four manufacturers' bars were selected in a survey of bars commonly used in highway bridge construction. These bars were believed to span the range in geometry of transverse lugs for United States produced bars.

In the main part of the test program, a total of 353 fatigue tests were carried out—236 in Phase I and 117 in Phase II. In each test, a single

The ratio of lug base radius to lug height was selected as an appropriate measure[51] of the magnitude of the stress concentration induced by the rolled on deformations. To establish the range of this test parameter in United States manufactured reinforcing bars of the size and grade to be tested, a large sample of such bars was obtained from a variety of sources.

Such organizations as the Committee of Reinforcing Bar Producers of the American Iron and Steel Institute, the Concrete Reinforcing Steel Institute, and the Operating Committee on Bridges and Structures of the American Association of State Highway Officials were contacted and their members requested to supply bar samples. A total of 141 samples of Grades 40 and 60 bars were received from 33 state highway departments and five reinforcing bar manufacturers.

Each bar sample was studied under a stereo-microscope after rust and mill scale had been removed from the bar. Lug base radius to lug height ratio was estimated from microscope measurements. On the basis of these estimates, four Grade 60 bars were selected for testing. Bars obtained for use in Phase I of the test program were added as a fifth selection for use in Phase II. This served to preserve continuity in the test program. Further details of the stereo-microscope examination procedure are to be found in a later section entitled "Examination of Shape of Transverse Lugs."

Code letters were used to identify the various manufacturers represented in the test program. The manufacturer of the bars used in Phase I of the test program and whose bars were further tested in Phase II, was designated as Manufacturer A. The manufacturers of the other four bars selected for use in Phase II were identified by the letters B to E.

Bars from Manufacturers B and E were believed to span the range of lug base radius to lug height ratio among commonly used United States manufactured bars. This ratio was believed to vary in a geometric progression from the "sharpest" to the "smoothest" for bars from Manufacturers B to E, respectively. Each manufacturer's bars had a different deformation pattern, as shown in Fig. B-1.

A total of 29 Grade 40, 278 Grade 60, and 31 Grade 75 bars were obtained in 20-ft. lengths from Manufacturer A for use in Phase I of the test program. Upon arrival at the laboratory, a permanent identification number was stamped into the end of each bar. The numbering system used is shown in Table B-1.

Not all of these bars were used in Phase I of the test program. Consequently, the 41 remaining No. 8 Grade 60 bars formed the pool of bars representing Manufacturer A in Phase II.

All of the bars from Manufacturer A were obtained from the same plant. Furthermore, all bars of one size and grade were obtained from a single heat except the No. 10 bars, which were obtained from two separate heats.

A total of 40 No. 8 Grade 60 bars were obtained, in 15-ft. lengths from each of Manufacturers B and D and in 20-ft. lengths from each of Manufacturers C and E, for use in Phase II of the test program. Except for the bars from Manufacturer C, all bars were obtained directly from a single mill of each manufacturer, where they were drawn from a single heat. Bars from Manufacturer C were obtained from a local service center and arrived in two lots. It is not known whether these bars represent a single heat. Upon arrival in the laboratory, a permanent

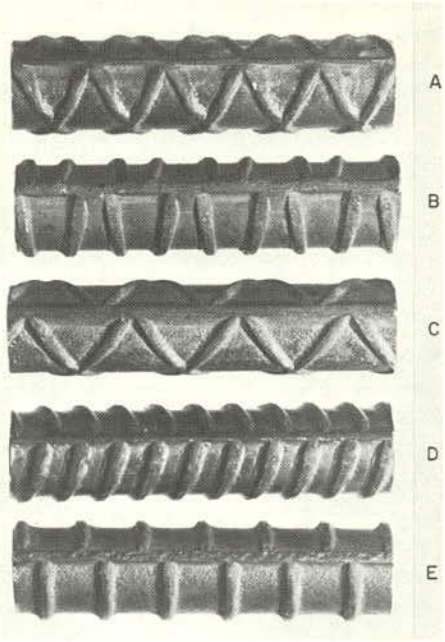

Fig. B-1 Deformation Patterns of Reinforcing Bars Tested

identification number was stamped into the end of each bar according to the listing given in Table B-1.

Arrangement of Test Program

The test program was divided into 42 groups of tests. Stress range was the only nominal within group variable. Phase I was composed of 31 groups of tests while Phase II consisted of 11 groups of tests. Test parameters were varied from one group to another in a manner that permitted statistical evaluation of the effects being tested.

Phase I Tests. The arrangement of the Phase I test program is shown in Table B-2, where each of the 31 numbers refers to a group of tests. The statistical design of the Phase I test program is discussed in the section entitled "Factorial Designs" in Appendix C.

Seven tests were scheduled for each group, except for Group No. 1, which contained 21 tests. Seven of the 21 tests in Group No. 1 were carried out at the start of the test program. This was done to determine the stress ranges to be used in the main part of the Phase I test program. A second set of seven tests comprised the regularly scheduled tests in Group No. 1. The final seven tests in Group No. 1 were carried out to obtain a better estimate of the scatter in test results to be expected within each group. A total of 231 tests were scheduled for Phase I of the test program.

Stress range in the test bar was nominally constant during each test. Within a group of tests, the stress range was varied to obtain fatigue fracture of the test bars after 50,000 to 5 million cycles of loading, as illustrated in Fig. B-2.

TABLE B-1 IDENTIFICATION OF TEST BARS

Manufacturer	Grade of Bar	Size of Bar	Number of Bars	Identification Number
A	40	5	10	1-10
		8	10	11-20
		11	9	21-29
	60	5	55	30-84
		6	30	85-114
		8	105	115-219
		10	12	220-231
		10	21	232-252
		11	55	253-307
	75	5	10	308-317
		8	11	318-328
		11	10	329-338
B	60	8	40	339-378
C	60	8	40	379-418
D	60	8	40	419-458
E	60	8	40	459-498

TABLE B-2 ARRANGEMENT OF PHASE I TEST PROGRAM

Grade of Bar, G	Bar Size No.	Nominal Effective Depth of Test Beams									
		d_{nom} = 18 in.			d_{nom} = 10 in.			d_{nom} = 6 in.		
		Min. Stress Level, f_{min} in ksi			Min. Stress Level, f_{min} in ksi			Min. Stress Level, f_{min} in ksi		
		-6	6	18	-6	6	18	-6	6	18
40	5 8 11	Group Numbers 28 22 30								
60	5 6 8 10 11	5	14 24 2 26 16	8	18	10 12 4 1 13 20 11	19 7 21	6	15 25 3 27 17	9
75	5 8 11					29 23 31				

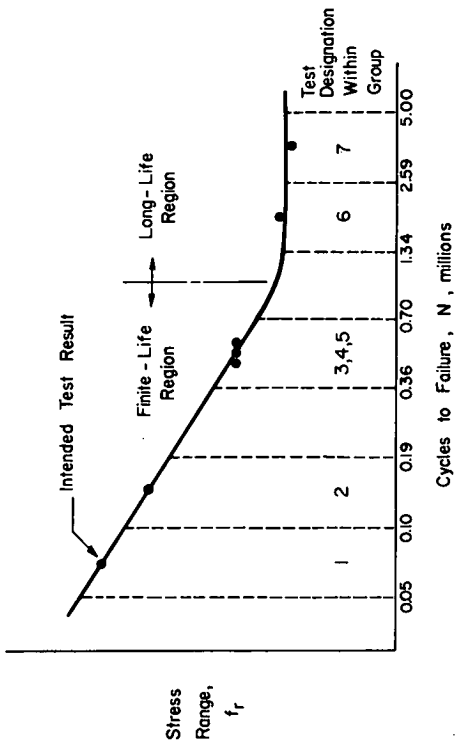

Fig. B-2 Arrangement of Tests Within a Group in Phase I

Five of the seven within group tests were intended to provide information on the fatigue strength of the test bars in the region where it is strongly affected by the applied stress range, the finite-life region. These tests were run at three stress range levels.

Tests numbered 1 and 2 within a group were intended to produce data from the region where a high stress range causes a fatigue failure after a low number of cycles. The remaining finite-life tests within a group, numbered 3, 4, and 5, were conducted at a single nominal stress range, intended to cause fatigue fracture after about 500,000 cycles. These three tests provided information about the reproducibility of test results.

Two of the seven within group tests, numbered 6 and 7, were intended to produce design information on the fatigue strength of the test bars in the region where the S-N curve is nearly flat, the long-life region.

The selection of stress ranges for the first seven tests in Group No. 1 was guided by previously published test results. From the results of these seven tests, nominal stress ranges of 54 and 48 ksi were selected for tests numbered 1 and 2 within a group, respectively. A nominal stress range of 36 ksi was selected for tests numbered 3, 4, and 5 within a group. Stress ranges of about 25 and 24 ksi were selected for tests numbered 6 and 7, respectively.

Tests in the main part of the Phase I test program -- seven tests in each of 31 groups, having assigned test numbers 8 through 224 in the experiment -- were carried out in an order determined using a table of random numbers[18]. The final seven scheduled Phase I tests, having

assigned test numbers 225 through 231 in Group No. 1, were also carried out in a randomized order.

When fatigue fracture did not occur within 5 million cycles, the scheduled Phase I test was terminated, 1000 was added to the test number, and the test continued as a new test at a nominal stress range of 54 ksi.

At the conclusion of the 231 scheduled tests, it was decided that an additional five tests, having assigned test numbers 232 through 236, should be conducted. Three of these were added to replace Tests No. 157, 175, and 224 from Groups No. 30, 22, and 9, respectively. Each of these tests had resulted in fatigue failure of the compression concrete when the test bar was subjected to a nominal stress range of 54 ksi. These replacement tests were carried out at a nominal stress range of 48 ksi. A fourth specimen was added to replace Test No. 43 of Group No. 6. In this test, an improper prestress force had inadvertently been applied to the test beam. The fifth test was added to obtain further information on the long-life properties of Group No. 21. In this group, both of the scheduled long-life region tests had resulted in fatigue fracture of the test bar in less than 1.3 million cycles.

Phase II Tests. This phase of the test program was designed to allow a statistical evaluation of fatigue properties in both the finite- and long-life regions. A separate study of each of these regions was made for each manufacturer's bars. The arrangement of the Phase II test program and its relationship with the Phase I program is shown in Table B-3, where each of the numbers shown refers to a group of tests.

The basic Phase II test program consisted of one group of finite-life tests and one group of long-life tests for the bars from

TABLE B-3 ARRANGEMENT OF PHASE II TEST PROGRAM

Manufacturer	Fatigue Life Region	Bar Size Number				
		5	6	8	10	11
A	Phase I	10	12	1	13	11
	Long	32				
	Finite	33				
	Damage	42				
B	Long	34				
	Finite	35				
C	Long	36				
	Finite	37				
D	Long	38				
	Finite	39				
E	Long	40				
	Finite	41				

each of the five manufacturers, as shown in Table B-3. In addition, a limited study of damage due to fatigue crack growth was carried out in Group No. 42 on bars from Manufacturer A.

Each of the Phase II groups intended for study of the long-life region was scheduled for a series of twelve tests. These tests were arranged in a so-called staircase series[17] where each test resulting in fatigue fracture in less than 5 million cycles was followed by a test at a stress range one step lower than the preceding one. Similarly, a test where the bar had survived 5 million cycles of loading was followed by a test at a stress range one step higher than the preceding one. On the basis of the Phase I test results, a nominal step size of 1 ksi was selected for each staircase test series.

When fatigue fracture did not occur within 5 million cycles, the scheduled Phase II test was terminated. Then 3000 was added to the test number and the test continued as a new test at a stress range intended to cause fatigue fracture in the finite-life region.

A staircase test series was considered to have been initiated when two consecutive tests, at stress ranges two step sizes apart, had resulted in opposite responses, fracture and runout. Since the stress range level at which this would occur was not known for each manufacturer's bars, a total of six additional tests were required to zero in on the staircase series. Some groups of long-life tests therefore consisted of more than twelve tests.

The 60 scheduled staircase tests were arranged in a random order[18] among the five manufacturer's bars. At the conclusion of these tests, the additional six tests needed to complete some of the staircase

series were carried out in a random order.

Stress ranges for the Phase II finite-life tests were selected on the basis of the staircase test results. Selection criteria were to obtain the widest possible range in stress range levels without entering into the long-life region for any of the manufacturer's bars and without causing yielding in a test bar.

Each group of finite-life tests in Phase II of the test program consisted of nine tests. These tests were carried out at three nominal stress range levels—34, 44, and 54 ksi—with three tests intended at each level. However, load levels for one test in each of Groups No. 33 and 41 were inadvertently interchanged. As a result, Group No. 33 had four tests at a nominal stress range of 34 ksi and two tests at 44 ksi, while the reverse was the case in Group No. 41.

The 45 scheduled finite-life tests were arranged in a random order[18] with regard to both manufacturer and applied stress range.

Tests in Group No. 42 were intended for a limited study of fatigue crack growth. Three tests were carried out on bars from Manufacturer A at a nominal stress range in the test bar of 34 ksi. These tests were terminated after 100, 200, and 300 thousand cycles of loading, respectively, at which point the test bar was removed from the test beam and examined for fatigue damage. The order of termination was randomized. Results of the Group No. 42 tests are reported in the section entitled "Static Strength of Fatigued Bar Specimens."

At the conclusion of the scheduled Phase II test program, three tests were added to the staircase part of the program. This was due to an inadvertent exchange of the intended loads in Tests

No. 61 and 62 from Groups No. 38 and 36, respectively. The result of Test No. 62 had caused the wrong decision to be made regarding the loading for Test No. 63. Tests No. 115, 116, and 117 were therefore carried out to obtain the proper staircase series for Groups No. 36 and 38.

Randomization of Tests. The test program was fully randomized with respect to the order of use of the reinforcing bars. In Phase I of the test program, all bars of a single size and grade were arranged in random order[18,20]. The initial seven tests in Group No. 1 were then arranged in random order and matched with the first seven randomized bar numbers from Group No. 1. The 217 regularly scheduled tests were similarly randomized and matched with the corresponding random bar numbers, as were the final seven tests in Group No. 1. The selection from the available stock of bars to be tested, their order of testing, and the test conditions to which the bar would be subjected were thus randomly determined before the initiation of the test program.

Randomization of the Phase II test program was carried out in a similar manner. The entire pool of bars obtained from each manufacturer was arranged in random order. The 60 scheduled staircase tests were randomized with regard to manufacturer and matched with the corresponding random bar numbers. Additional staircase tests were similarly randomized. Finally, the 45 scheduled finite-life tests were randomized with regard to both stress range and manufacturer and matched with the remaining random bar numbers from the pool for each manufacturer's bars.

Description of Test Beams

For each test, a single test bar was cast into a concrete beam. The bar was held within a shear reinforcement cage and was so placed that

the longitudinal ribs of the bar were located in the plane of bending of the beam.

Each test beam was designed for concentrated loads located at about the third points of the span. Thus, a long constant moment region was provided. The test bar was the only reinforcement in this region.

The test beams were either rectangular or T-shaped in cross-section. T-shaped test beams were so designed that the neutral axis was always within the flange. Cross-sections and an elevation of a test beam are shown in Fig. B-3. Nominal test beam dimensions for each group of tests are given in Table B-4.

Effective depth of the test beams was one of the major variables in the test program. A nominal effective depth, d_{nom}, of either 6, 10, or 18 in. was used for all of the test beams. The actual effective depth, d, was the same as d_{nom} in tests where the minimum stress level applied to the test bar was 6-or 18-ksi tension. However, in tests where the minimum stress level was 6-ksi compression, a depth d greater than d_{nom} was used. This difference in the location of the reinforcement served to maintain the distance from the cracked beam neutral axis to the test bar nearly constant for all beams having the same nominal effective depth. A detailed explanation for this is included in Appendix C.

The flange width, b, of the T-shaped test beams was varied according to the size of the test bar. Again, this variation in width was provided to maintain a constant distance from the neutral axis to the centroid of the test bar for beams having the same nominal effective depth. Stem width of the beams was 6 in. This was also the width of the rectangular beams.

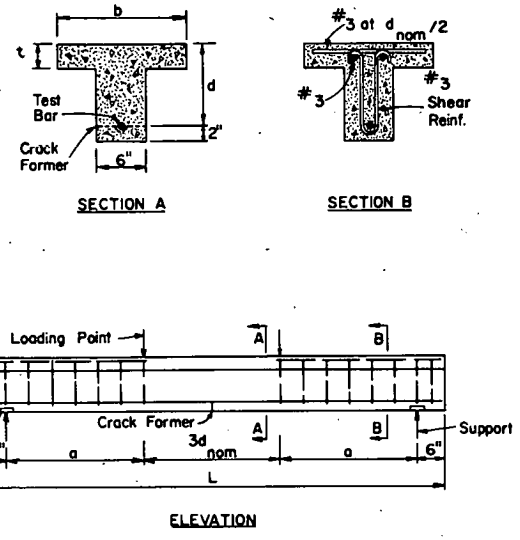

Fig. B-3 Test Beam Details

TABLE B-4 TEST BEAM DIMENSIONS

Group Number	Flange Width, b in.	Flange Thickness, t in.	Effective Depth, d in.	Shear Span, a in.	Length, L in.
1,7,22,23	15.5	3	10	30	102
2,8	15.5	4	18	54	174
3	15.5	2	6	18	66
4	15.5	3	11.5	40	122
5	15.5	4	20	72	210
6	15.5	2	6.75	24	78
9	15.5	2	6	30	90
10,19,28,29	6	-	10	30	102
11¶21¶30,31	30	3	10	45	132
12	8.5	3	10	30	102
13	24.5	3	10	40	122
14	6	-	18	27	120
15	6	-	6	18	66
16*	30	4	18	66	198
17*	30	2	6	42	114
18	6	-	11.5	30	102
20	30	3	11.5	60	162
24	8.5	4	18	36	138
25*	8.5	2	6	18	66
26*	24.5	4	18	57	180
27*	24.5	2	6	36	102
32 to 42	15.5	3	10	30	102

* Exceptions noted in following table

Group Number	Test No.	Shear Span, a in.	Length L in.
11	46	60	162
16	42	72	210
17	17,26,44	48	126
21	29	60	162
25	88	24	78
26	21	63	192
27	39	42	114

Length of the test beams varied. Each test beam was designed to have a constant moment region of a length three times d_{nom}. In general, this was also the length of each shear span, a. However, the distance a was adjusted for some or all of the test beams in certain groups. This was done to preclude any possibility of bond fatigue failure and to keep the applied loads on the test beams within the range of effectiveness of the hydraulic rams used.

Shear reinforcement in the test beams consisted of two-legged stirrups fabricated from No. 3 Grade 60 deformed bars. These were placed in each shear span at a maximum spacing of $d_{nom}/2$. The reinforcement cage was held together at the top by stringer bars placed in the hooked ends of the stirrups. In addition, a small amount of longitudinal and transverse reinforcement was placed in the flanges of the T-shaped test beams. None of this reinforcement was placed in the constant moment region between the load points.

A sheet metal crack former was cast into each test beam. The crack former was located at midspan and served to promote a symmetric tension crack distribution in the concrete. Bearing plates were incorporated into the test beams at the supports.

Fabrication of Test Beams

Each test bar was cut from the straightest part of the length of bar received from the manufacturer. However, the test length was selected so as to avoid the occurrence of a manufacturer's bar mark at the crack former, but still leave a 30-in. coupon for tension testing. The remainder of each bar was stored in the laboratory.

The length of each test bar was measured and its weight recorded. Next, the test bar, shear reinforcement, and stringer bars

were tied together with soft iron wire. When placed in the beam form, the reinforcing unit was supported on wire chairs.

The test beams were cast in concrete forms lined with plastic-coated plywood, as shown schematically in Fig. B-4. Four of these forms were constructed, two for beams with a nominal effective depth of 10 in., and one each for the beams with nominal effective depths of 6 in. and 18 in. Each form was set on steel tubes so the sides could be spread slightly apart to facilitate the removal of a specimen.

A plywood bulkhead was used to form the ends of the test beams. Before each beam was cast, the joints between the form and the side rail or base were covered with masking tape. The faces of the form were sprayed with a light oil before the reinforcement was placed. A 1/2-in. thick, 3-in. wide by 6-in. long steel bearing plate was placed in the form at each beam support point.

Dimensions of the form and placement of the reinforcement were inspected by an engineer before the concrete was cast. The vertical distance to the top of the test bar was measured from a straight edge placed across the form at the center of the beam.

Concrete was mixed using Type III portland cement, Elgin sand, and 3/4-in. maximum size normal weight stone aggregate. Each batch was mixed in a 6-cu.ft. capacity tilting drum mixer. Design compressive strength of the concrete was 5,000 psi in 14 days. Slump of the concrete was from 2 to 4 in.

Test beams were cast in sets of one to four, and according to the predetermined randomized testing order. One to four batches of concrete were required to cast each beam. Three standard 6x12-in.

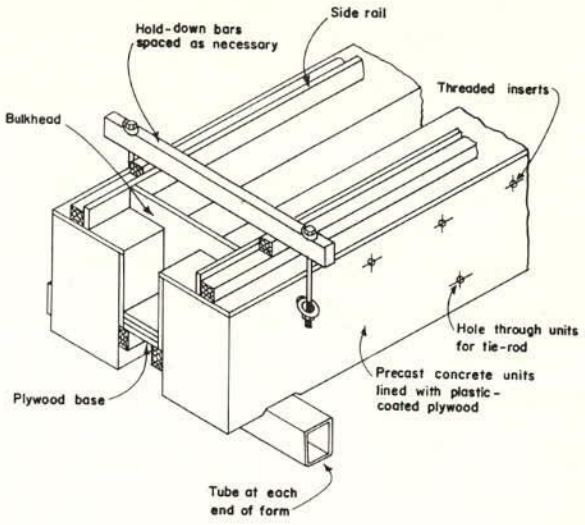

Fig. B-4 Forms for Casting Test Beams

cylinders were cast from the batch placed in the region between the load points of the beam. Consolidation of the test beam and cylinder concrete was by means of an internal spud vibrator.

After casting, the top surfaces of the beams and cylinders were screeded and later finished with a magnesium float. They were then covered with a plastic sheet for three days. Following this curing period, the beams and cylinders were removed from the forms and stored in the laboratory, where temperature and humidity are maintained at 70° F and 55 percent, respectively.

Test Setup and Instrumentation

Tests were carried out in two reaction frames. These frames differed only in that one frame could not accommodate test beams longer than 174 in.

An overall view of a test setup is shown in Fig. B-5. The reaction frame was constructed from heavy precast reinforced concrete beams and columns that were post-tensioned together and to the laboratory floor[19]. The test beams were placed on a heavy reinforced concrete base located between the reaction frame columns. This base and all members of the reaction frame were carefully aligned, levelled, and grouted in place.

In Phase II of the test program, two beams were tested simultaneously in the reaction frame having the longer test base. The test setup was similar to that shown in Fig. B-5, with the exception that the loading rams were located between the reaction frame columns.

Loads were applied to the Phase I test beams using either one or two 22-kip capacity Amsler rams. The method of load application is

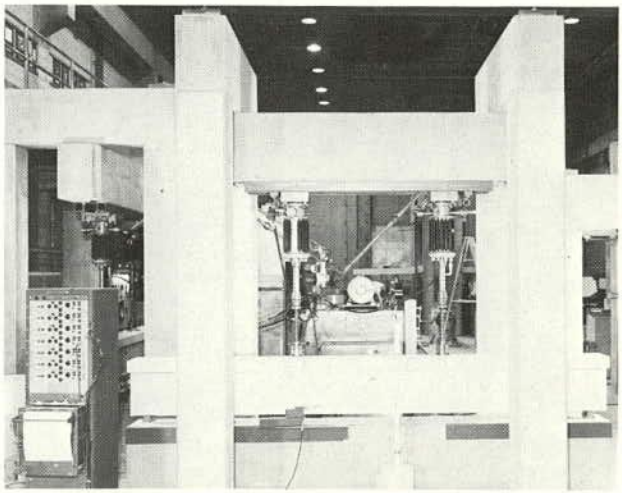

Fig. B-5 Representative Test Setup and Instrumentation

shown in Fig. B-6. When two rams were used, each was aligned over a loading point. When one ram was used, it was placed at the center of the reaction frame and a steel spreader beam was used to distribute the load equally to the two loading points.

Loads on the Phase II test beams were applied by means of 55-kip capacity Amsler rams. One ram was used to apply load to each test beam. The load was distributed to the two loading points through a steel spreader beam in the manner shown in Fig. B-6.

All test beams were supported on 2-in. diameter rods. At one end the rod was free to roll, while at the other end the rod was fixed. Details of the loading points and supports are shown in Fig. B-6.

The Amsler pulsating load equipment used applies a sinusoidally varying load at fixed nominal rates of either 250 or 500 cycles per minute. Actual cycling rates are about 10 percent higher than the nominal rates.

The load was set by means of oil pressure gages that were pre-calibrated to the ram area by the manufacturer. This calibration was checked at intervals by inserting a load cell[19] between the Amsler ram and the spreader beam. Actual loads were found to be within 200 lb of the indicated load throughout the load range used.

For tests having a minimum applied stress level of 6 ksi compression in the test bar, the test beam was externally post-tensioned through a system of springs, as detailed in Fig. B-7. The springs were calibrated in compression in the laboratory and found to have a spring constant of 15.5 kips per inch. Within the region between loading points, guides were used to ensure that the line of action of the pre-

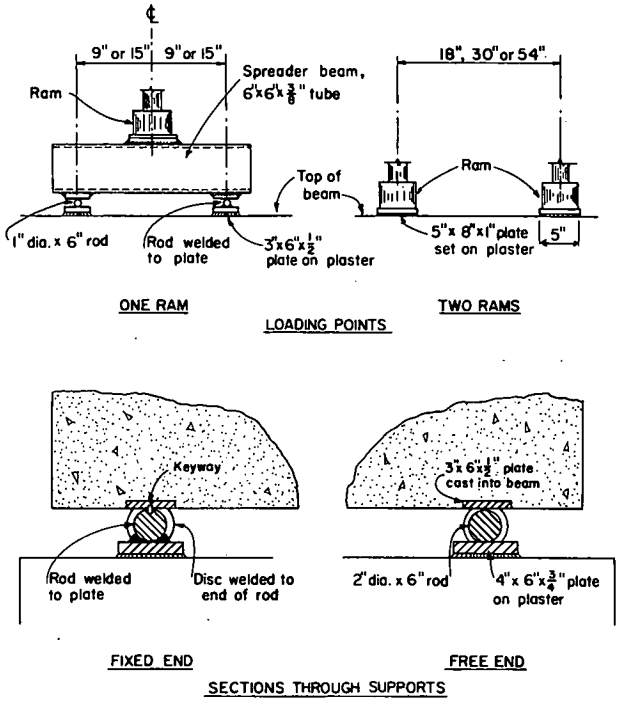

Fig. B-6 Details at Load Points and Supports of Test Beams

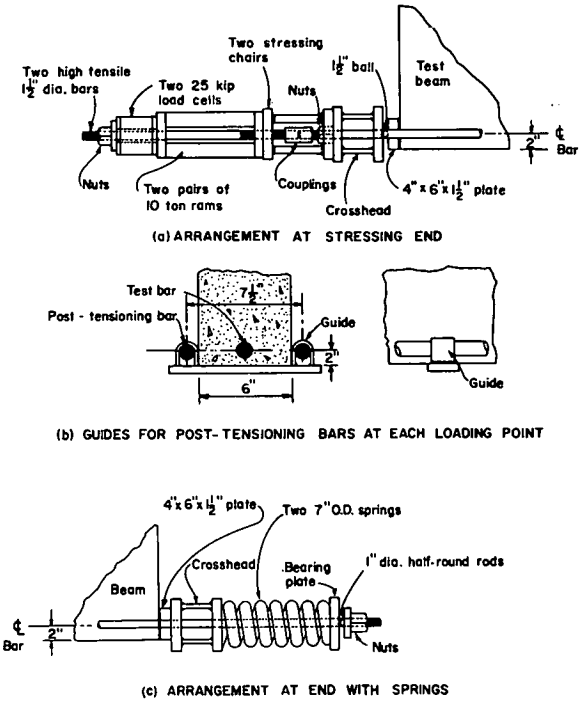

Fig. B-7 Details of Post-Tensioning System

stressing force was at the same level as the test bar.

Midspan deflection of the test beams was measured with a dial gage and a "whip", both of which are shown in Fig. B-5. The smallest division of the dial gage was 0.001 in. The "whip" was a cantilevered steel rod with the free end connected by a wire to a bracket attached to the side of the beam at midspan. An electrical resistance strain gage was mounted near the fixed end of the "whip". Output from this gage was recorded on a Sanborn continuous strip chart recorder.

Deflections of Phase II test beams were measured with a dial gage exclusively.

Test Procedure

All tests were scheduled to begin after the test beam concrete was 14 days old and before it reached an age of 30 days. However, two tests in Phase I were initiated 13 days after the beams were cast and one test in Phase II at a concrete age of 12 days. The early start of the Phase I tests occurred inadvertently, but the Phase II test was deliberately started early to avoid excessive aging of subsequent beams.

Test No. 68 in Group No. 12 was started when the concrete was six days old. A dimensional error had been discovered in the specimen initially cast for Test No. 68. Consequently, a substitute test beam had been cast, using the remainder of the assigned test bar. The early date of test for the substitute beam was assigned to maintain the proper testing order without excessive aging of other test beams.

Several tests in both phases of the test program were started at a concrete age of 31 days because the preceding tests had survived a greater number of load cycles than expected. Test beams No. 59 and 62 of

Phase II reached ages of 34 and 39 days, respectively, before being subjected to load. These delays were caused by malfunction of the test equipment.

The beams were tested in the predetermined random order. Whenever a Phase I test was concluded, the reaction frame in which the test had been conducted was prepared to receive the next beam in the randomized testing order. However, specimens in Groups No. 16 and 21 would only fit in the test setup with the longer base. In this case, the test program was delayed until the appropriate reaction frame became available. Use of the test setups was therefore as random as possible.

The Phase II test program was carried out using a single reaction frame equipped with two dynamic rams. Whenever a Phase II test was concluded, the next beam in the randomized testing order made use of the just vacated test setup. Use of the loading equipment was therefore random.

Loading of Test Beams. Loads applied to each beam were predetermined by the test arrangement, except for the tests designated 6 and 7 within Phase I groups and the staircase tests in Phase II. Tests designated by the number 6 within a group in Phase I of the test program were tentatively assigned a nominal stress range of 25 ksi while tests identified by the number 7 were assigned a stress range of 24 ksi. However, if the result for the first of these two tests to be carried out was close to the result expected for the other, the loading for the subsequent test was modified.

For example, if the test numbered 6 within a group occurred first in the randomized testing order, and resulted in fatigue fracture

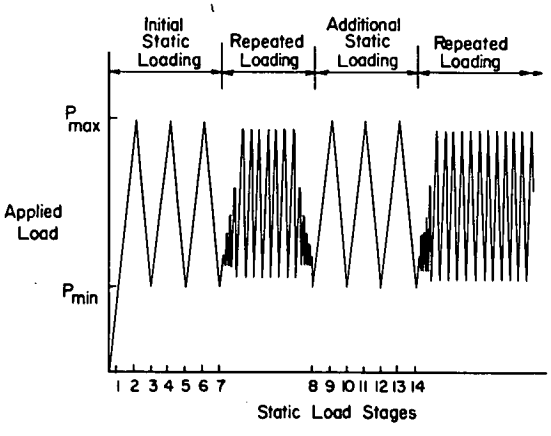

Fig. B-8 Procedure for Loading Test Beams

at more than 2.57 million cycles or a runout at 5 million cycles, the test numbered 7 within that group was subsequently carried out at a higher stress range than 25 ksi. Similarly, if the test numbered 7 within a group was carried out first and ended in fatigue fracture after less than 2.57 million cycles, the test numbered 6 within that group was subsequently carried out at a lower stress range than 24 ksi.

The load on a staircase test beam in Phase II of the test program depended, in each case, on the result of the immediately preceding test in that staircase series. If the preceding test had resulted in fatigue fracture after less than 5 million cycles of loading, the next test in that series was carried out at a stress range nominally 1 ksi lower than the preceding test. Similarly, a runout at 5 million cycles resulted in the next test of that series being conducted at a stress range nominally 1 ksi higher than the preceding test.

The method used to load a test beam is illustrated schematically in Fig. B-8. Initially, three cycles of static loading were applied between P_{min} and P_{max}, the static loads computed to result in the desired minimum stress level and stress range for the nominal test beam. These three cycles correspond to load stages 1 to 7. If the minimum stress in the test bar was to be compressive, prestress was applied at load stage 1. The prestress force was determined by means of load cells placed on each post-tensioning rod, as shown in Fig. B-7.

Midspan deflection of the test beam was measured at each of the static load stages. In general, good agreement was found between the deflections measured in the second and third cycles. When this was not the case, additional cycles of static loading were applied until good reproducibility of deflections was obtained.

Each test beam was subjected to dynamic loading at the conclusion of the static load cycles. Dynamic ram loads differed from the static loads in that their range was decreased while the average load remained the same. This difference in ram loads took into account the dynamic contribution of the weight of the test beam and the loading equipment. The magnitude of this dynamic load correction was computed according to the Amsler Instruction Manual[95] and was based on the measured deflection range in the static load cycles.

Generally, the dynamic load was applied at a rate of 500 cycles per minute. However, if the dynamic load correction exceeded 8 percent of the maximum load, the rate of loading was reduced to 250 cycles per minute.

The transition from static to dynamic load is illustrated in Fig. B-8. The process was manual and normally required a few hundred cycles. However, the cycle counter on the pulsator was not started until the applied dynamic loads were close to their desired values. Therefore, only the number of cycles of full dynamic loading applied to each beam is reported.

Midspan deflection due to dynamic loading on the Phase I test beams was measured intermittently with the "whip" through a Sanborn strip chart recorder. In Phase II of the test program, these deflections were measured by means of a dial gage having graduations of 0.001 in. The measured dynamic deflection range was compared with the measured static deflection range.

Dynamic loading was usually stopped temporarily after the first few thousand cycles of loading had been applied. At this time, additional

cycles of static loading were applied, as illustrated in Fig. B-8. If necessary, a new dynamic load correction was computed, based on the mid-span deflections measured during these static load cycles. Dynamic loading was then resumed and continued until the test bar fractured in fatigue or the bar had survived 5 million cycles of loading.

If the test bar did not fail in fatigue within 5 million cycles of loading, the dynamic loading was terminated. The entire test sequence was then repeated with the test beam subjected to a higher maximum load, computed to cause fatigue fracture of the test bar in the finite-life region.

Post-Fracture Examination. A fatigue fracture was obtained in the test bar in all but three tests. These tests were terminated by fatigue failure of the compression concrete in the test beams.

After fatigue fracture of the test bar had occurred, measurements of the test beam cross-section were obtained at the location of the failure. The location of the bar fracture within the beam was recorded, as were the locations of concrete cracks in the tensile zone of the beam.

The concrete in the region of the bar fracture was subsequently broken apart and a welding torch was used to cut lengths of about 6 in. from the test bar on either side of the fracture. These pieces were then trimmed to 3 in. by removing the torch cut ends with a metal saw. The saw cut ends were stamped with the test number and marks identifying the orientation of each piece within the test beam. The remainder of the test beam was discarded.

After completion of each phase of the test program, the fractured bar specimens were carefully examined. The fracture and the

fractured face were sketched, and the point of fatigue crack nucleation determined. Measurements were made of the distance between diametrically opposite points on the barrel of the bar, the lugs, and the longitudinal ribs.

Tests for Mechanical Properties. The three concrete cylinder specimens cast with each test beam were tested on the day the beam was initially subjected to load. Two of the cylinders were loaded in compression, directly to failure. The third specimen was used to determine the elastic modulus of the concrete before being loaded in failure in compression.

Compressive strength of the concrete was determined as an average of the three tests. Concrete modulus of elasticity was determined by means of an averaging type strainometer, commonly referred to as a compressometer.

The concrete compression tests were carried out in a 300,000 pound capacity universal hydraulic testing machine. Before loading, the test cylinders were capped, using a mixture of sulphur and fire clay. Loads on the cylinders were applied axially through a spherical bearing block.

Tension tests were carried out on coupons cut from the test bars. These tests were carried out in a 300,000 pound capacity universal hydraulic testing machine. The applied load was measured by a built-in pressure cell. Strain in the test coupon was measured with an 8-in. gage length extensometer containing two linear variable differential transducers connected to a Sanborn strip chart recorder. The extensometer signals were averaged and passed to an X-Y recorder used to plot

the measured load-strain relationship for each test bar coupon.

In Phase II of the test program, a test coupon was cut from the fatigued test bar whenever the bar fracture had occurred near a load point on the test beam. Coupons of sufficient length were instrumented and tested in static tension in the manner described above.

Results of Tests

Detailed information was recorded on the results of tests to determine the properties of the test bars and the concrete, the dimensional properties of the test beams and the loads to which the beams were subjected, and the major results of each beam test. Methods used to obtain the test values are described in the following sections. Summaries of the test results are given in the text or in subsequent tables and figures.

Tests on Bars. Unit weight of the test bars was determined by dividing the weight of each bar by its measured length. Tensile properties of the test bars were determined in static tension tests.

Representative force-strain curves for each size and grade of bar tested in Phase I of the test program are shown in Fig. B-9. Curves for the Grade 60 bars are typically shown as having a yield plateau. However, some of the curves obtained for these bars exhibit characteristics of the curves obtained for the Grade 75 bars. This was particularly the case for the No. 6 Grade 60 bars. Representative force-strain curves for

the bars tested in Phase II are shown in Fig. B-10.

Values of yield strength were determined according to both ASTM A615[1] and ACI 318-71[4] for all of the test bars. According to ASTM procedures, the yield strength of the Grade 40 bars was determined from the yield plateau of the force-strain curve. Yield strength of the Grade 60 and Grade 75 bars was determined at 0.5 and 0.6 percent strain, respectively, on the force-strain curve.

ACI 318-71 presents an alternate procedure to that given by ASTM for determining the yield strength of bars of Grade 60 or stronger. According to this procedure, yield strength is determined at 0.35 percent strain.

The yield strength was, in each case, determined by dividing the measured force, at the appropriate strain, by the nominal bar area.

Each tension test bar coupon was stressed until fracture of the bar occurred. The tensile strength recorded for each test bar was, according to ASTM procedures, determined as the applied force at fracture divided by the nominal bar area.

Elongation at fracture was measured by fitting the ends of the fractured specimens together and determining the distance between gage marks punched at an 8-in. interval on a longitudinal rib of the unstressed bar. Three sets of gage marks were located with a 16-in. length on each test coupon. In some instances, the bar fractured outside the gaged length. In such cases, no accurate determination of the elongation was possible. The value of bar elongation recorded was the measured increase in length over the 8-in. gage length.

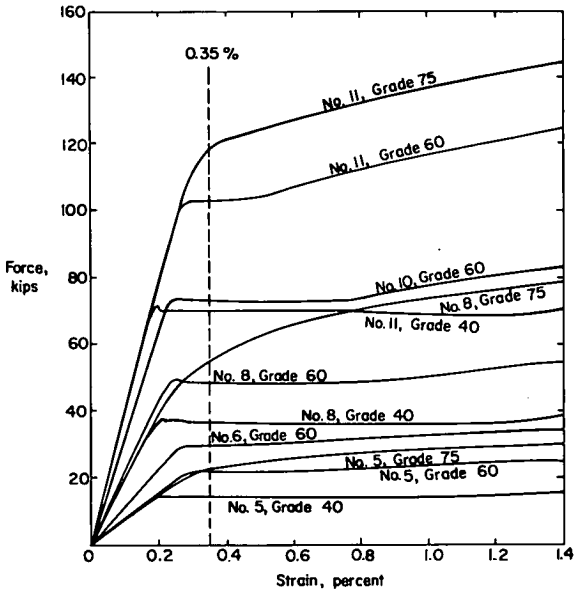

Fig. B-9 Representative Force-Strain Curves for Phase I Test Bars

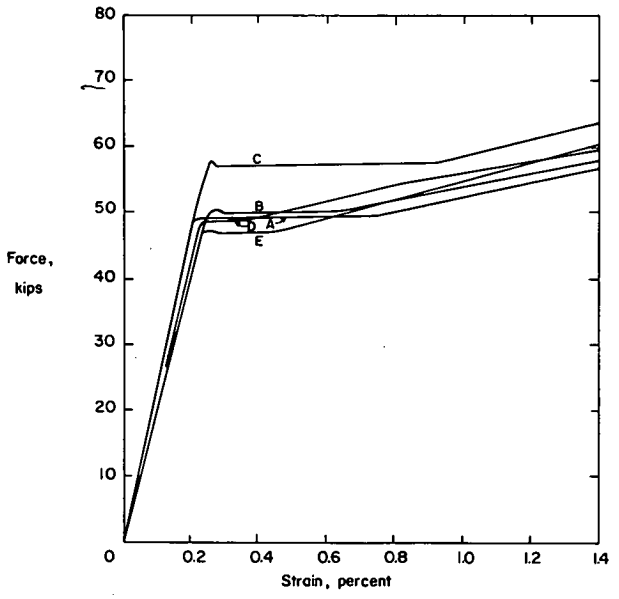

Fig. B-10 Representative Force-Strain Curves for Phase II Test Bars

Average mechanical properties of the test bars are summarized in Table B-5. Since measurement of bar elongation was not always possible, the number of tests determining the elongation statistics was less than the number indicated for the other statistics in Table B-5.

Tests on Concrete. The amount of mixing water to be used for each batch of concrete was determined by means of a slump test. Concrete mix design requirements called for the use of a 2 to 4-in. slump, but occasionally a batch with a higher or lower slump would be used. Slump of the batch placed in the midspan region of each test beam was recorded.

Compressive strength and modulus of 6x12-in. cylinders taken from the concrete placed in the midspan region of each test beam were recorded. The compressive strength was determined as the average of tests on three cylinders. Two of these cylinders were loaded directly to failure in compression. The third cylinder was preloaded three times to a stress of 3000 psi. Strain measurements were then made as the cylinder was loaded to failure. Modulus of elasticity was determined on the basis of the change in strain between 500 and 3000 psi. These cylinder tests were generally carried out on the same day that a test beam was initially subjected to load. The age of each test beam at initial application of load was recorded.

Average concrete strength for Phase I of the test program was found to be 5635 psi with a standard deviation of 498 psi. The corresponding modulus of elasticity was 3889 ksi with a standard deviation of 240 ksi. In Phase II the average concrete strength was 5312 psi with a standard deviation of 473 psi. The average modulus was 3485 ksi with

TABLE B-5. AVERAGE PROPERTIES OF TEST BARS

Manufacturer	Size of Bar	Grade of Bar	No. of Tests	Weight, pounds per ft.		Yield Strength, ksi				Tensile Strength, ksi		Elongation, inches per 8 in.	
						ASTM A615		0.035 Strain					
				Ave.	Std. Dev.	Ave.	Std. Dev.	Ave.	Std. Dev.	Ave.	Std. Dev.	Ave.	Std. Dev.
A	5	40	7	1.043	0.007	47.8	1.29	47.6	1.35	82.6	2.31	1.47	0.17
		60	35	1.043	0.017	69.5	2.53	67.9	2.27	109.7	2.89	1.08	0.13
		75	7	1.021	0.011	87.2	0.97	77.3	0.40	118.2	1.42	0.83	0.12
	6	60	21	1.508	0.028	71.4	6.84	69.4	5.58	112.1	6.62	1.14	0.12
	8	40	8	2.641	0.009	46.1	1.08	45.8	1.75	79.0	3.62	1.85	0.16
		60	103	2.743	0.013	61.6	1.09	61.4	1.15	102.0	0.96	1.44	0.13
		75	7	2.647	0.011	85.2	0.42	72.9	0.57	120.3	1.02	0.91	0.09
	10	60	21	4.304	0.015	59.2	1.26	58.7	1.01	102.0	2.63	1.42	0.12
	11	40	8	5.250	0.032	42.7	1.12	42.8	1.20	77.4	0.58	2.02	0.21
		60	36	5.270	0.019	67.4	1.85	66.1	1.52	110.6	2.31	1.24	0.12
		75	7	5.218	0.008	84.7	1.50	79.1	1.15	124.5	1.26	0.97	0.06
B	8	60	21	2.650	0.015	63.7	1.33	63.4	1.30	104.7	1.48	1.18	0.09
C	8	60	25	2.617	0.013	72.7	0.58	72.6	0.54	114.0	0.90	1.12	0.07
D	8	60	24	2.616	0.020	65.2	1.02	62.1	0.85	107.0	1.59	1.27	0.06
E	8	60	23	2.639	0.019	59.8	1.78	59.0	1.52	111.7	3.42	0.97	0.10

a standard deviation of 269 ksi.

Test Beam Dimensions. Cross-sectional dimensions of each test beam were recorded. Flange width, stem width, flange depth, and total depth of each beam were measured at the location of fracture of the test bar. Depth to the top of the reinforcing bas was also measured on the fractured beam. The effective beam depth was determined as the sum of the depth to the top of the test bar and one-half of the measured bar diameter across the ribs.

Loads on Test Beams. The external loading applied to each test beam was recorded. The prestress force was measured when the beam was subjected to the minimum static ram load. External dead loads were those due to the weight of the spreader beam and the weight of the hydraulic ram and platen. The spreader beam was considered to represent both a static and a dynamic load while the mass of the ram caused dynamic loads only. Dynamic ram loads were the nominal values to which the pulsator was set by means of oil pressure gages.

Response of Test Beams to Load. Test beam deflections were measured at various times during each test. The minimum deflection was the deflection due to application of P_{min}, the minimum static ram load, relative to the initial unloaded position of the test beam. The recorded value was that measured at the static load stage immediately prior to initial application of the dynamic loading. Prestressed beams have a negative minimum deflection due to the camber acquired in the prestressing operation. No minimum deflection was reported for the rerun tests.

It was observed that the minimum deflection, as defined above, increased continually with time. This additional deflection was largely due to time dependent deformations in the beam concrete.

The range of deflection due to an increase in load from P_{min} to P_{max} during the initial static load cycles was found to be about 10% less than the subsequent dynamic deflection range. However, after the application of a few thousand cycles of dynamic loading, the static and dynamic deflection ranges were found to be identical within the accuracy of the measurement. The dynamic deflection range was observed to be essentially constant for the duration of each test.

Tension cracks were marked on each test beam while the beam was subjected to P_{max}, the maximum static load applied, during the last of the initial static load cycles. At the end of each test, the crack pattern was sketched on the appropriate data sheet. Average crack spacing (that was observed in the constant moment region only) was subsequently determined from these data. Crack spacing in each shear span was observed to be similar to that obtained in the constant moment region.

Additional cracking under dynamic load was rarely observed. When such cracks appeared, they were either additional shear cracks or they were observed immediately adjacent to existing cracks. In the latter case, the new crack usually joined the previously observed crack. Generally, no new cracks appeared when beams that had survived 5 million cycles at load loads were subsequently tested at higher loads. No measurements were taken of crack widths.

Average crack spacing in the constant moment region varied with the size of the bar, the effective depth of the test beam, and the bar deformation pattern. The relationship between average crack spacing and effective beam depth for the various bar sizes is shown in Fig. B-11. Average crack spacing results are summarized in Tables B-6 and B-7.

The difference in average crack spacing between those Phase II test beams containing bars from Manufacturer A and those reinforced with bars from Manufacturer E is statistically significant at the 5 percent confidence level. No explanation is available for the difference in average crack spacing observed among bars from Manufacturer A in Phases I and II of the test program.

An account of the methods used in calculating the stresses occurring in a test bar embedded in a concrete beam subjected to dynamic loads is presented in Appendix C. Values of the computed minimum stress level and the stress range to which each test bar was subjected were recorded. In each case, these values are based on cross-sectional areas determined from the individual bar weights. For this purpose, it was assumed that the reinforcing steel had a unit weight of 490 pounds per cubic foot.

Fatigue Strength of Test Bars. The number of cycles of loading required to cause failure of a test beam was recorded. Most beam failures were due to a fatigue fracture of the reinforcing bar. In a few instances the beam failure was caused by fatigue of the compression concrete.

Not all tests were continued until failure of the test beam occurred. When a test beam had survived 5 million cycles of loading, the

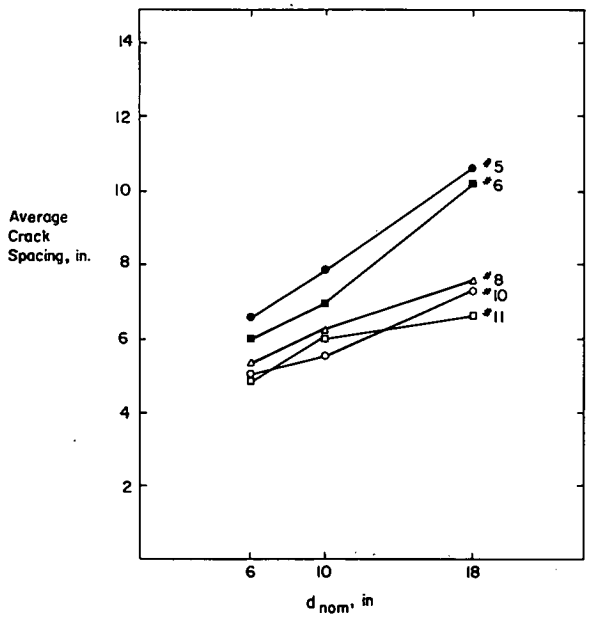

Fig. B-11 Average Flexural Crack Spacing in Test Beams

TABLE B-6 AVERAGE CRACK SPACING IN PHASE I TEST BEAMS

Bar Size	Nominal Effective Beam Depth, in.								
	6			10			18		
	No. of Tests	Ave. Spac-ing, in.	Std. Dev.	No. of Tests	Ave. Spac-ing, in.	Std. Dev.	No. of Tests	Ave. Spac-ing, in.	Std. Dev.
5	7	6.62	1.13	35	7.87	1.09	7	10.64	1.97
6	7	6.00	1.15	7	6.96	0.57	7	10.19	2.52
8	23	5.31	0.97	50	6.24	1.13	21	7.53	0.95
10	7	5.04	0.94	7	5.57	0.26	7	7.32	1.39
11	7	4.98	0.56	37	6.02	1.11	7	6.63	0.76

TABLE B-7 AVERAGE CRACK SPACING IN PHASE II TEST BEAMS

Manu-fac-turer	No. of Tests	Ave. Spac-ing, in.	Std. Dev.
A	24	7.12	1.06
B	21	6.84	0.91
C	25	6.84	0.69
D	24	6.82	1.03
E	23	6.53	0.93

test was terminated and a new test started by subjecting the test beam to a more severe loading. In each instance, the number of cycles to termination of loading was recorded.

Within group plots of calculated stress range versus the logarithm of the number of cycles to failure or termination of loading for tests in Groups No. 1 to 41 are shown in Fig. B-12. In each case, the individual group regression line, obtained in the manner described in Appendix C, is also shown. For Groups No. 1 to 31 this is the regression line to the finite-life data obtained for each group, excluding all rerun tests. For Groups No. 32 to 41 the regression line shown is that obtained from the finite-life group data for the particular manufacturer's bars, rerun tests again being excluded from the regression.

To facilitate a visual comparison of the data, the regression line for the Group No. 1 finite-life data is shown as a dashed line in each plot. The result of a regularly scheduled test is shown in Fig. B-12 by a dot, an arrow being added if the test bar survived 5 million cycles of loading. The result of a rerun test is indicated by a cross.

Also shown in Fig. B-12 are the mean fatigue limits determined from the staircase tests in Phase II of the test program for each manufacturer's bars. These are shown in the graphs for Groups No. 32, 34, 36, 38, and 40. A comparison of the results obtained from the rerun tests in these groups with the corresponding finite-life regression line is also presented.

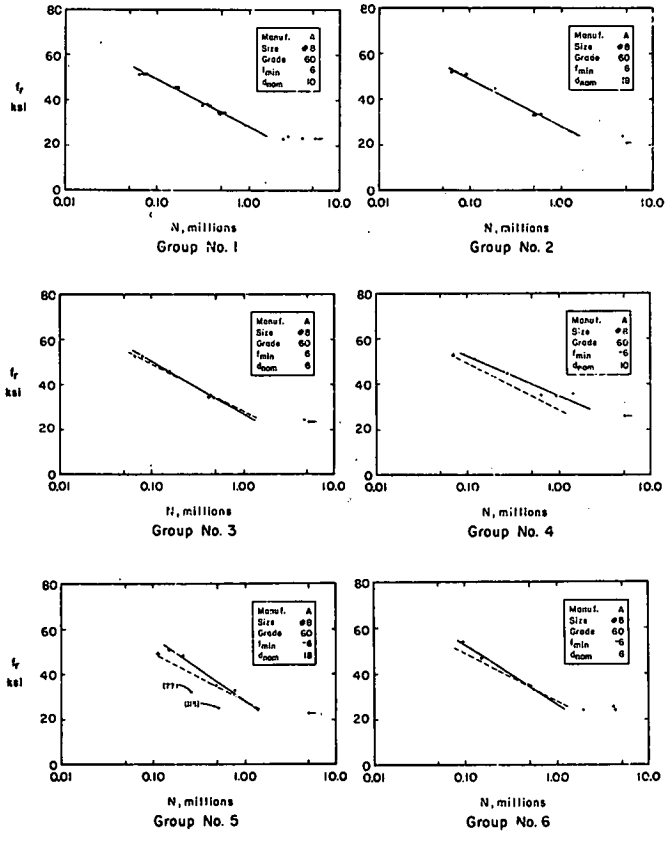

Fig. B-12 Within Group Fatigue Test Results

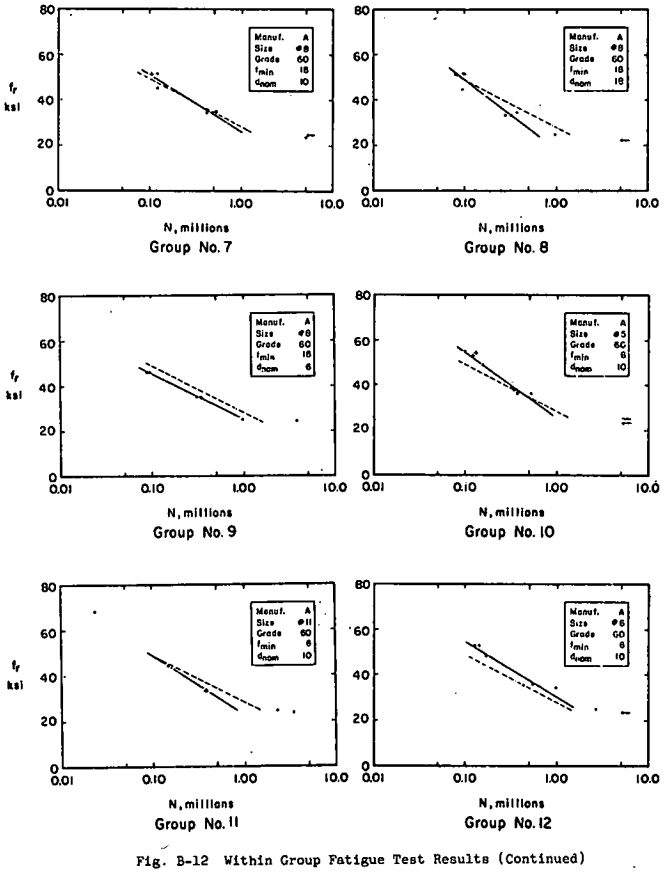

Fig. B-12 Within Group Fatigue Test Results (Continued)

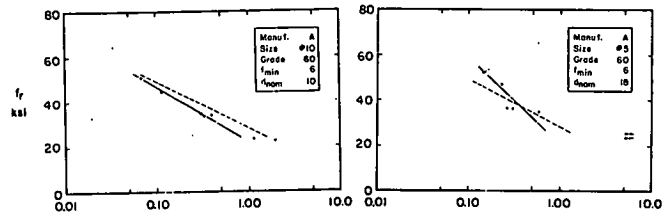

Group No. 13

Group No. 14

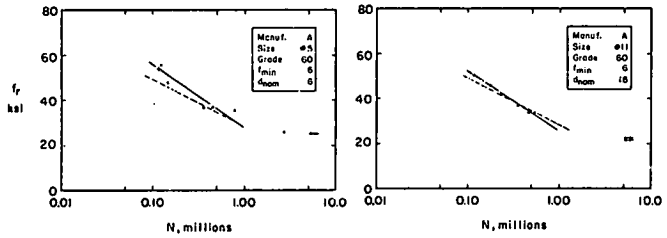

Group No. 15 Group No. 16

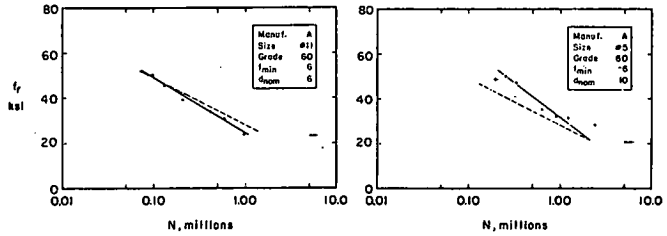

Group No. 17 Group No. 18

Fig. B-12 Within Group Fatigue Test Results (Continued)

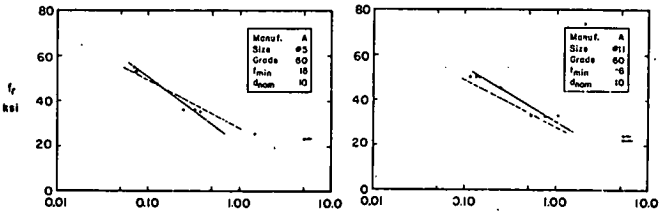

Group No. 19 Group No. 20

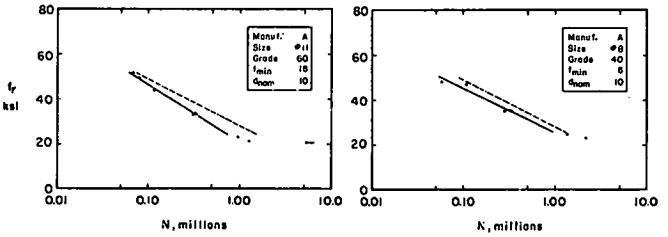

Group No. 21 Group No. 22

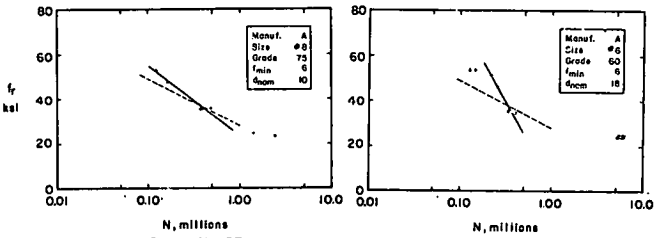

Group No. 23 Group No. 24

Fig. B-12 Within Group Fatigue Test Results (Continued)

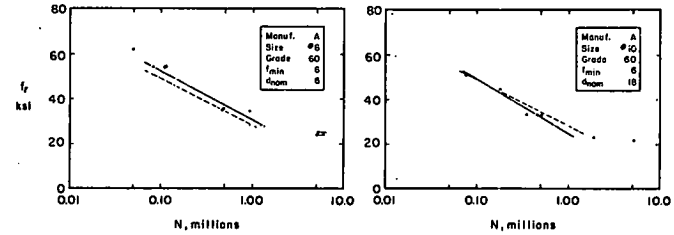

Group No. 25 Group No. 26

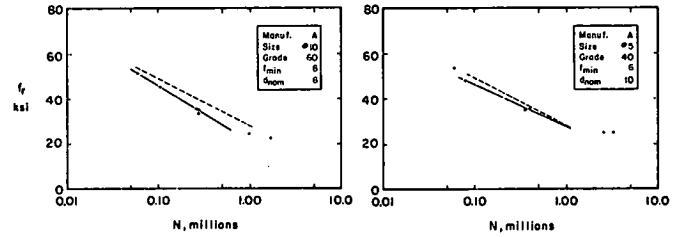

Group No. 27 Group No. 28

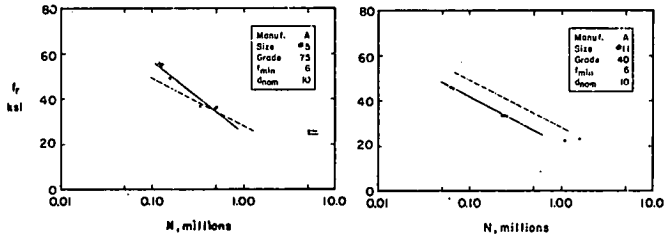

Group No. 29 Group No. 30

Fig. B-12 Within Group Fatigue Test Results (Continued)

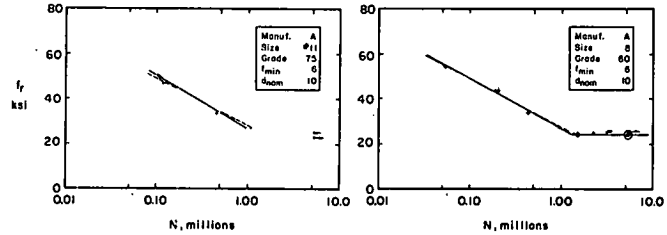

Group No. 31 Group No. 32

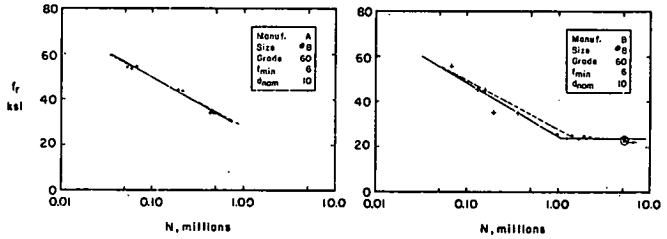

Group No. 33 Group No. 34

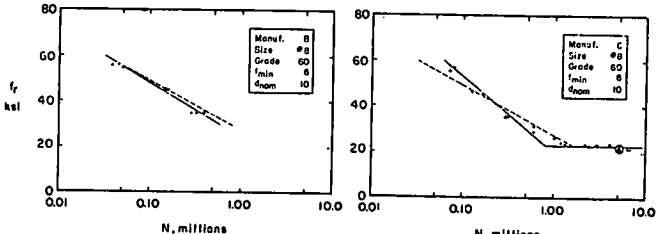

Group No. 35 Group No. 36

Fig. B-12 Within Group Fatigue Test Results (Continued)

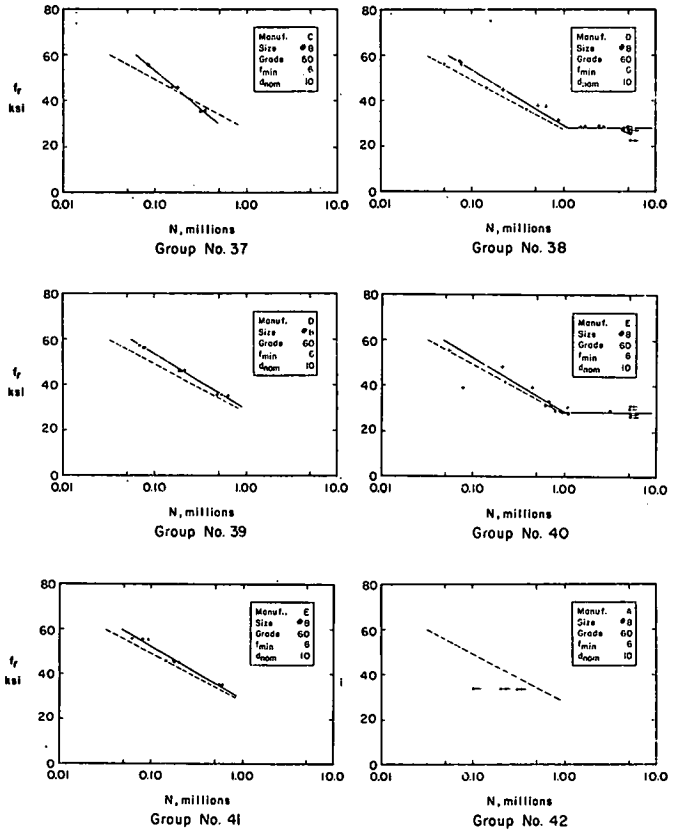

Fig. B-12 Within Group Fatigue Test Results (Continued)

A few test results are seen to deviate substantially from the corresponding finite-life regression lines. In Group No. 5, Test No. 77 was interrupted by an electrical power failure which caused the prestressed test beam to crack through the concrete compression zone. This resulted in an early failure of the test bar. Examination of the bar fracture in Test No. 115, also in Group No. 5, revealed the presence of foreign bodies. An examination of the bar fracture in Test No. 3066, in Group No. 40, showed that the fatigue crack had been initiated at the manufacturer's bar mark.

In three tests, failure of the test beam occurred due to fatigue of the compression concrete. In each instance, the beam had been subjected to loads causing the maximum stress level in the test bar to exceed the yield stress of the bar. Each of these test bars exhibited a yield plateau, thus causing high strains in the beam concrete. All three failures were observed to occur in the constant moment region and immediately adjacent to a load point. In each instance, the failure appeared to have been influenced by an inclined crack originating in the shear span and extending beneath the load point. These three tests are indicated by a double asterisk in Table B-7 and their results are not shown in Fig. B-12.

In Test No. 3051 in Group No. 34, the number of cycles to failure was improperly recorded. The result of this rerun test is not shown in Fig. B-12.

The plots of the logarithm of the number of cycles to fracture versus stress range in Fig. B-12 show that stress range has a major influence on the fatigue life of a reinforcing bar in the finite-life region. The higher the stress range, the shorter is the fatigue life of

a reinforcing bar. At low stress ranges, however, the effect is seen to become minimal and a bar is able to sustain a vastly increased number of cycles of stress without fracture. There appears to be a limiting stress range that for practical purposes may be considered as a fatigue limit, below which a reinforcing bar appears to be able to sustain an unlimited number of stress cycles.

General trends, indicating the effects of other test variables on the fatigue life of reinforcing bars, may be observed in Figs. B-13 to B-16. These figures summarize the observed Phase I test results in terms of variation in fatigue life with change in minimum stress level, size of bar, grade of bar, and effective depth of the test beam.

In these figures, the ordinates, log N, of the finite-life region points plotted were obtained from the individual group regression lines. Fitted values of log N at a stress range of 36 ksi were averaged for the appropriate groups, the average value converted back to cycles and plotted.

In the graphs showing long-life region effects, the plotted ordinates, f_r, are either the lowest stress range resulting in a fatigue fracture after more than 1 million cycles of loading or the highest stress range sustained for 5 million cycles without fracture. These two cases are distinguished by solid and open points, respectively.

A distinct trend, indicating that, in the finite-life region, fatigue life is reduced with increasing minimum stress level, may be seen in Fig. B-13. Similarly, it appears that, in the long-life region, the fatigue limit is reduced with increasing minimum stress level.

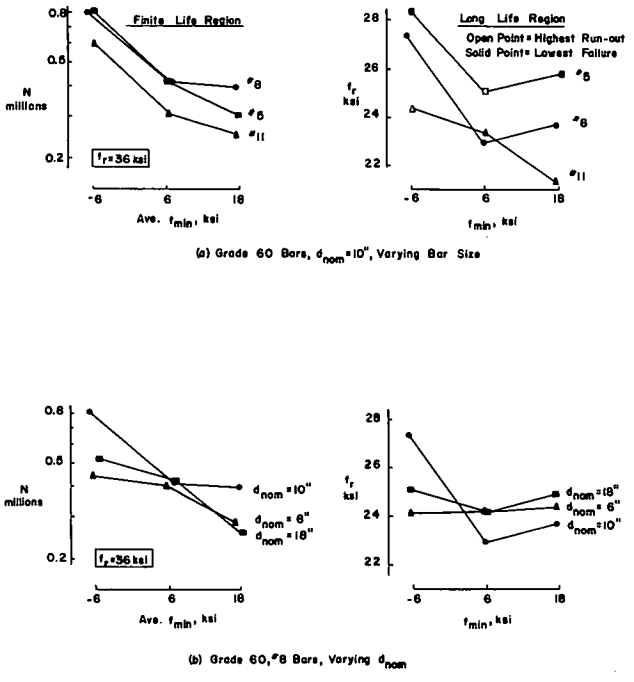

(a) Grade 60 Bars, d_{nom}=10", Varying Bar Size

(b) Grade 60, #8 Bars, Varying d_{nom}

Fig. B-13 Effect of Minimum Stress Level

In Fig. B-14, a recognizable trend indicates that fatigue life is reduced with increasing bar size. The No. 6 bars tested are seen to have had the longest fatigue life while the No. 10 bars tested had the shortest fatigue life. This may, however, be due to other influencing factors which cannot be separated in a graph of this type. Thus, it should be noted that the No. 6 bars had the highest and the No. 10 bars had the lowest average yield strength of the Grade 60 bars.

All of the fatigue fractures initiated at bar marks in the No. 6 bars occurred in Group No. 24. Test beams in this group had a nominal effective depth, d_{nom}, of 18 in. Tests resulting in fracture at a bar mark are included in Fig. B-14(a). A fracture initiated at a bar mark was often observed to occur after fewer cycles of loading than a fracture initiated at a transverse lug.

It may be seen in Fig. B-15 that fatigue life is increased with the grade of the bar tested. The trend observed is not strong, but may again be obscured by other influencing factors.

No consistent trend is observable in Fig. B-16 to indicate that type of specimen, as represented by test beams having different effective depths, has any significant effect on fatigue strength.

It must be emphasized that the value of graphs such as those presented in Figs. B-12 to B-16 is limited, in that the various influencing effects cannot be separated. Such a separation is possible only by means of statistical procedures involving analysis of all of the test data as a single whole.

The statistical analysis presented in Appendix C confirmed the existence of the finite-life region effects noted in Figs. B-12 to B-16.

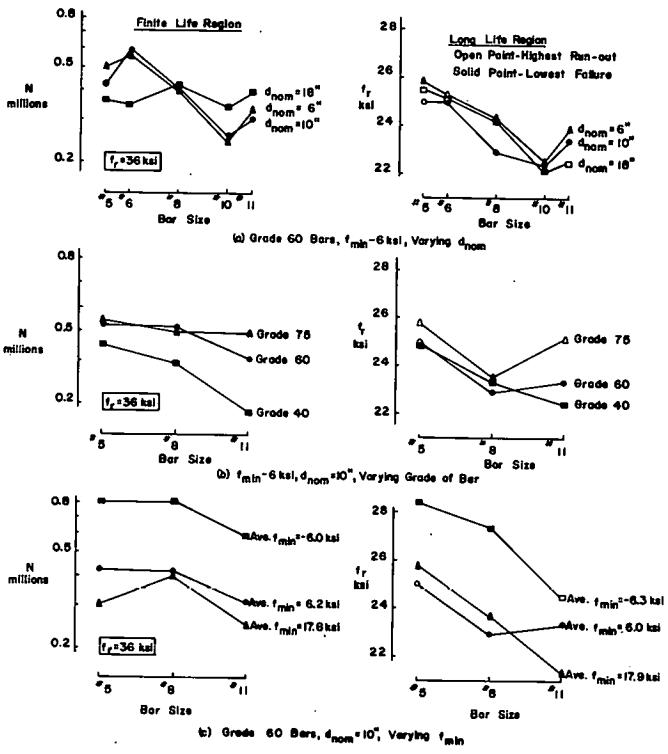

Fig. B-14 Effect of Bar Diameter

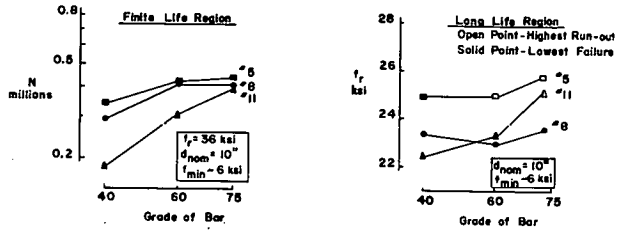

Fig. B-15 Effect of Grade of Bar

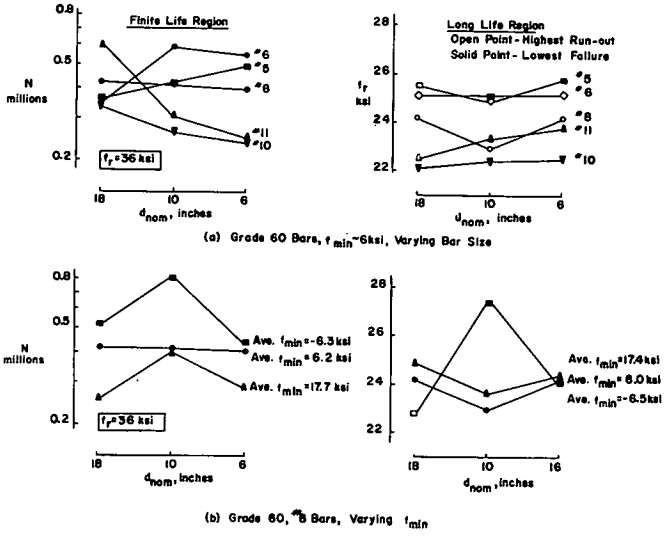

Fig. B-16 Effect of Type of Specimen

Furthermore, this analysis assessed the relative significance of the various influencing factors and allowed numerical values to be assigned to their effects.

Fatigue Fracture of Test Bars. Each test bar failing in fatigue was observed to have fractured near a flexural crack in the test beam. In each instance, the location of the bar fracture, relative to the center of the beam, was determined by measurement on the failed test beam.

Most fatigue fractures were observed to have occurred in the region between the load points, where the applied moment was nominally constant. The distribution of fatigue fractures about the midspan of those Phase I test beams that had an effective depth of 10 in. and were reinforced with a No. 8 bar is shown in Fig. B-17.

The diagram is based on 49 test results. In five tests, the fracture occurred within a shearspan. The highest frequency of fractures was in the interval that includes the midspan of the test beam. Note that since this interval has only half the weight of the other intervals, the dashed line in Fig. B-17 should be used for comparison.

Pieces of the fractured bars, containing the fracture zone, were examined after they had been removed from each test beam. This examination was to determine the appearance of the fractured face of the bar, the location of the primary crack nucleus, the final radius of the fatigue crack in Phase II tests, and the pertinent cross-sectional dimensions of the bar in the fracture region.

In most cases, two distinct zones were apparent on the fractured face of each test bar. The zone associated with the fatigue crack extended

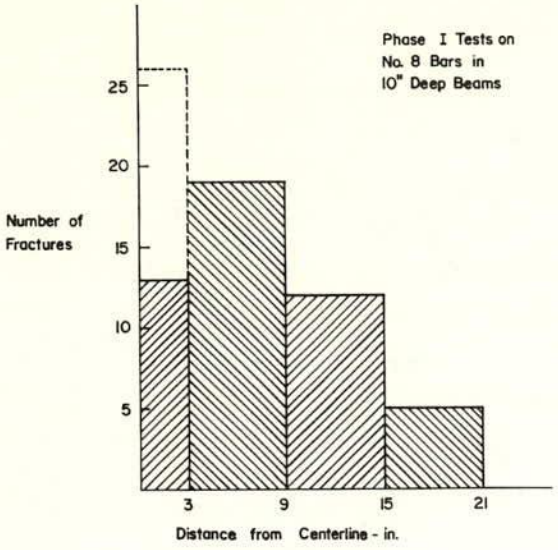

Fig. B-17 Fatigue Fracture Distribution in Test Beams

radially from the fatigue crack nucleus and had a fine grained dull appearance. The remainder of the fracture surface was crescent shaped and had a rough, crystalline appearance. This region showed evidence of tearing in the case of bars having inclined transverse lugs.

Bars from Manufacturer A, in particular, often exhibited no crystalline region. Rather, a fine grained, dull appearing, shear torn zone of considerably darker hue than the fatigue crack zone was observed. In such cases, the two regions were generally separated by a transition zone showing one or two narrow crescent shaped bands of light hue. In bars from Manufacturer A, the transition from a fatigued to a tension fractured zone was sharper for the Grade 60 and Grade 75 bars than it was for the Grade 40 bars.

Details of the fractured surfaces of bars from Manufacturers A and E are shown in Fig. B-18. The fracture shown in the bar from Manufacturer A is typical of those where no crystalline zone was observed. On the other hand, the bar from Manufacturer E exhibits a fracture with the fatigue and crystalline zones distinctly separated. The bar from Manufacturer A has several fatigue crack nuclei, each fatigue crack zone being separated from the others by a beach mark.

Fatigue fracture surfaces representative of those observed for each manufacturer's bars are shown in Fig. B-19. In each case, the fatigue zone was initiated at a transverse lug, a phenomenon observed in most of the fatigue fractures. Generally, no evidence of neckdown was observed.

For comparison with the fatigue fractures shown in Fig. B-19, typical tension fractures for each manufacturer's bars are shown in

Manufacturer A

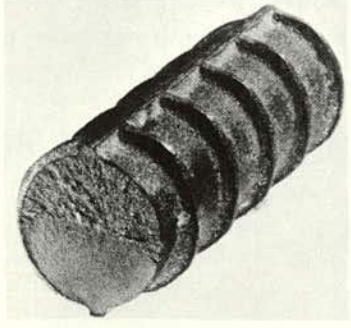

Manufacturer E

Fig. B-18 Fatigue Fracture Surfaces

Fig. B-19 Representative Fatigue Fractures

Fig. B-20 Representative Static Tension Fractures

Fig. B-20. The fracture surfaces that were obtained in the tension tests were bounded by the transverse lugs. However, the entire fracture surface consisted of shear planes, large and jagged in the case of bars with highly inclined lugs but small and crystalline in the others. All of the bars showed some evidence of neckdown. Greater neckdown was associated with the more inclined transverse lugs.

Fatigue crack nuclei were always observed to be at the surface of a test bar, immediately adjacent to a rolled on surface deformation. The location of the nucleus was determined by visual examination of the fracture surface. The fatigue crack nucleus was found at the focal point of the fatigue crack region. Often, radial tear lines were observed to extend from this focal point into the fatigued area. The region immediately adjacent to the crack nucleus was observed to present a considerably finer grained appearance than the remainder of the fatigue crack region.

In each case, the primary fatigue crack nucleus was found to be in the lower half of the test bar, as located within the test beam. Secondary crack nuclei were found in the upper half of some bars, particularly those from Manufacturer A.

To determine the critical fatigue location on a transverse lug, the circumferential frequency distribution of the primary fatigue crack nuclei was investigated. For this purpose, the periphery of the fracture surface was divided into numbered segments. Ten degree radial zones, symmetric about a line through the longitudinal ribs, defined the length of each segment. These zones were numbered sequentially from 1 to 5 in the manner shown in Fig. B-21.

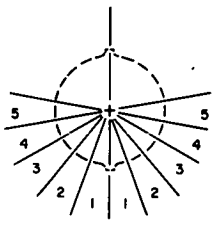

Fig. B-21 Radial Zones Identifying Crack Nucleus Location

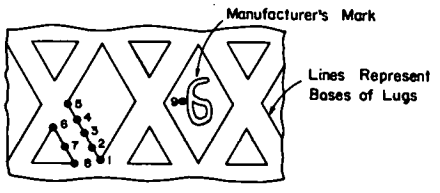

Note: Code No.9 Refers to Location at Base of Any Bar Mark

Fig. B-22 Code Numbering System for Identifying Crack Nucleus Location

An extension of this identification system allowed further definition of the location of a critical section on a bar having a diamond lug pattern, as shown in Fig. B-22. Any crack nucelus that was located at the base of a manufacturer's bar mark was given the code number 9.

The primary fatigue crack nucleus location for each test bar fractured in fatigue was recorded. Each crack nucleus location is identified by one of the code numbers shown in Figs. B-21 and B-22. The frequency distributions of fatigue crack nuclei for the various types of bars tested are presented in Table B-8.

Most fatigue crack nuclei observed in Zone 1 of bars from Manufacturer A occurred at the bottom of the V formed by the junction of two transverse lugs at a longitudinal rib. All of the crack nuclei in bars from Manufacturer C were observed to occur at that location. This points out the possible creation of severe stress concentrations at the junction of transverse lugs in bars having diamond pattern surface deformations.

When fatigue crack nuclei were observed in Zone 1 of bars from Manufacturer D, they were generally found to be in the close vicinity of the junction formed by the base of a transverse lug and a longitudinal rib. In this instance, it is difficult to assess the influence the longitudinal rib may have had on the initiation of fatigue cracks.

In bars from Manufacturers B and E, fatigue crack nuclei observed in Zone 1 were found to have occurred at the base of a transverse lug and some distance away from the base of the longitudinal rib. The effect of the longitudinal rib on the formation of fatigue cracks must therefore be considered to have been minimal for these bar deformation geometries.

In Phase II of the test program, an attempt was made to measure the final fatigue crack radius in each test bar. Such data are

TABLE B-8 DISTRIBUTION OF FATIGUE CRACK NUCLEI

Manufacturer	Size of Bar	Grade of Bar	No. of Bar Fractures	Fatigue Crack Nucleation Zone									
				1	2	3	4	5	6	7	8	9	
A	5	40	7	7								4	1
		60	35	35									5
		75	7	7									
	6	60	21	16	1							1	
	8	40	7	1	1	31	3	2		2	1		
		60	99	3	11	1	37	14		1			
		75	7	4	1								
	10	60	21	12	4		1	1	1		1	1	
	11	40	7	3	5	3	3	3	9	12	4		
		60	36	4							1		
		75	7		4						3		
B	8	60	21	17									
C	8	60	25	25	2		1	1					1
D	8	60	24	19	11								
E	8	60	23	7									

of importance in the field of fracture mechanics. Only limited success was achieved in obtaining consistent measurements. This was due to the indistinct transition zone observed to exist in many cases between the fatigue and static fracture regions.

Final fatigue crack radii data that were recorded for the Phase II test bars are summarized in Table B-9, where it is seen that the final fatigue crack radius is a function of the applied stress range. The magnitude of the final crack radius is also manufacturer related, although the relationship is not clear. Measured fatigue crack radii were observed to be widely scattered about some of the average values recorded in Table B-9.

Cross-sectional dimensions of the test bars were measured and recorded at the time the fracture surfaces were examined. The dimensions shown in Fig. B-23—diameter of the bar across the longitudinal lugs, diameter of the bar across the barrel, diameter of the bar across the transverse lugs, and thickness of the longitudinal ribs—were measured.

The measurements were taken at a distance of about 1 in. from the fracture in each bar failing in fatigue. When no fracture occurred in a test bar, the measurements were taken at random locations on the corresponding piece of bar remaining after the test bar was cut from the sample bar.

All bar measurements were taken with a micrometer that could be read to the nearest 0.001 in. Considerable variation was found in the diameters measured. Representative values for each bar were, therefore, based on several measurements at various locations on the circumference or at closely spaced longitudinal locations. In each case, attempts were made to secure an average of high and low readings.

TABLE B-9 AVERAGE FINAL FATIGUE CRACK RADII

Manufacturer	Crack Radius - inches			
	Fatigue Limit	Nominal Stress Range		
		34 ksi	44 ksi	54 ksi
A	0.760	0.692	0.640	0.636
B	0.761	0.576	0.558	0.422
C	0.741	0.710	0.614	0.582
D	0.612	0.530	0.450	0.375
E	0.533	0.444	0.362	0.375

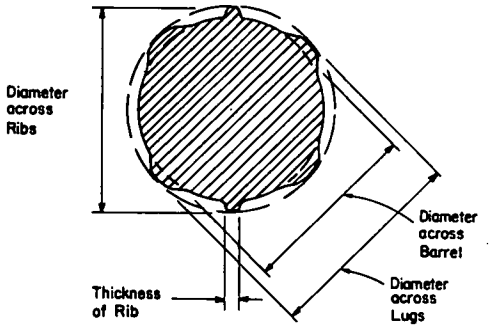

Fig. B-23 Cross-Sectional Measurements on Test Bars

No measurements of rib thickness were possible on bars from Manufacturers C and D. Bars from Manufacturer C had trapezoidally shaped longitudinal ribs while those from Manufacturer D had a relatively large base radius.

Average values of the dimensions obtained from each test bar are recorded in Table B-10. It should be noted that the diameters across the barrel and across the lugs, along with the rib thickness, were only measured to the nearest 0.01 in. for the Phase I test bars. All other measurements were to the nearest 0.001 in.

Examination of Shape of Transverse Lugs

Geometry of the rolled on deformations of the test bars was examined by three methods. The critical geometry of 141 sample bars obtained in a survey to select bars for use in Phase II of the test program was assessed by study of each bar sample under a stereo-microscope. Profiles of individual lugs on the test bars used in both phases of the test program were studied on photographs of longitudinal sections of bar samples. Individual lug profiles were also studied on photographs of sectioned plaster casts of samples of the Phase II test bars.

Stereo-Microscopy. Each sample bar obtained for the survey of United States manufactured No. 8 Grade 60 reinforcing bars commonly used in highway bridge construction was 2 ft. long and contained the manufacturer's bar identification mark. Upon arrival at the laboratory, each sample was stamped with an identification number that was entered in the survey log along with other available information.

TABLE B-10 AVERAGE CROSS-SECTIONAL DIMENSIONS OF TEST BARS IN VICINITY OF FRACTURE

Manufacturer	Size of Bar	Grade of Bar	No. of Samples	Dimension - Inches									
				Dia. Ribs		Dia. Barrel		Dia. Lugs		Rib Thickness	
				Ave.	Std. Dev.	Ave.	Std. Dev.	Ave.	Std. Dev.	Ave.	Std. Dev.
A	5	40	7	0.637	0.025	0.590	0.000	0.669	0.004	0.070	0.000
		60	35	0.636	0.029	0.590	0.001	0.668	0.003	0.071	0.003
		75	7	0.689	0.038	0.590	0.000	0.669	0.004	0.070	0.000
	6	60	21	0.849	0.052	0.719	0.007	0.810	0.003	0.096	0.005
	8	40	8	1.192	0.013	0.929	0.004	1.065	0.009	0.063	0.000
		60	103	1.098	0.007	0.969	0.005	1.033	0.006	0.080	0.000
		75	7	1.118	0.012	0.941	0.004	1.074	0.005	0.074	0.005
	10	60	21	1.417	0.013	1.209	0.012	1.367	0.006	0.098	0.006
	11	40	8	1.580	0.029	1.330	0.015	1.504	0.012	0.093	0.012
		60	36	1.582	0.013	1.335	0.011	1.504	0.006	0.080	0.005
		75	7	1.585	0.014	1.333	0.005	1.511	0.004	0.090	0.000
B	8	60	21	1.134	0.012	0.941	0.004	1.068	0.005	0.130	0.000
C	8	60	25	1.092	0.011	0.956	0.006	1.063	0.005	-----	-----
D	8	50	24	1.071	0.027	0.940	0.002	1.057	0.007	-----	-----
E	8	60	23	1.126	0.012	0.946	0.005	1.091	0.006	0.110	0.006

An initial examination was conducted on bar samples that had been wire brushed on one side, between the longitudinal ribs, in order to remove mill scale. This examination was performed by means of a stereo-microscope containing a disk with engraved circles of various sizes. Estimates were made of the lug base radius as a fraction of lug height, sharpness of the bar mark, and roughness of the bar surface. The lug base radius, as a fraction of the lug height, was estimated in this examination to vary from 0.1 to 1.5.

Ranking the survey bars according to lug radius to height ratio revealed, however, that several inconsistencies existed in the original estimates. This pointed to a need for better surface preparation of the bars and an improved technique in the examination.

A 6-in. length, including the manufacturer's bar mark, was cut from each survey bar. These were then placed for 30 minutes in a 50 percent solution of hydrochloric acid and water at room temperature. The samples were then immersed in a 5 percent neutralizer solution of sodium carbonate and water, after which they were thoroughly rinsed in cold water. Finally, each sample was placed in an oven at 120°F for 20 minutes, wire brushed, and sprayed with a thin coat of silicone spray to prevent rusting. This process was found to greatly facilitate visual examination of the samples.

A stereo-microscope examination of each treated bar sample was carried out individually by two persons. This examination resulted in a reassessment of the maximum value of the lug base radius to height ratio from 1.5 to 1.2.

B-70

A magnification factor of 30 was used for the stereo-microscope examination. Difficulty in estimating the lug base radius was found to increase substantially with increasing angle between the transverse lugs and the longitudinal ribs. Consistency in the estimates of the two examiners was not as great as had been expected.

Stereo-microscope observations were made directly onto the surface of each bar sample. The bar was held under the microscope in a V-notched receptacle. The sample was moved laterally and rotated to present its lug profile to view in line with engraved circles contained on a transparent disk in the viewpath of the microscope. Lug radii and height were compared with the radii of the engraved circles. Indirect lighting was applied to the samples to provide the greatest possible contrast.

The shape of the transverse lugs of the survey bars showed considerable variety. Height, width, and flank angle of the lugs varied greatly among the bars studied. Some flank angles were observed to approach 90 degrees. Furthermore, the base radius was frequently found to vary in the vicinity of the lug base. Often, a sharper radius was observed at a point on the side of the lug.

Generally, the manufacturer's bar mark had a sharper base radius than the transverse lugs. However, these bar marks usually contained less material than the lugs. Consequently, the stress concentration effect may have been smaller than a direct comparison of radii would indicate.

Severe surface roughness was observed on several bar samples. Often, undercutting was noted at the base of a transverse lug. Several bars, having an otherwise smooth lug shape, were judged to represent a

B-71

more critical geometry than indicated by the stereo-microscope examination because of surface roughness in the vicinity of the base of a lug. Evaluation of base radii in bars having a rough surface at the base of a lug was found to be difficult, using a stereo-microscope.

Four of the bars for use in Phase II of the test program were selected on the basis of their ranking after the stereo-microscope examination. Bars from Manufacturer A, remaining on hand from Phase I, were added as a fifth selection for testing. The lug base radius to height ratio ranking, determined by stereo-microscope examination, for the bars tested in Phase II of the test program was 0.4, 0.1, 0.2, 0.4, and 0.8 for bars from Manufacturers A to E, respectively.

Longitudinal Sections. Lug geometries of samples of bars used in both phases of the test program were studied by means of lug profiles obtained by longitudinal sectioning of the samples. During Phase I, samples of each size and grade of bar were studied. In Phase II, samples from each manufacturer's bars were examined.

Each sample consisted of a 3-in. long piece cut from a representative bar used in the test program. One sample was obtained for each size and grade of bar tested in Phase I. For the No. 10 bars, however, samples were obtained from bars representing each of the two heats from which the bars were rolled. Each manufacturer's bars in Phase II of the test program were represented by two samples, cut from different bars.

Initial preparation of the samples consisted of the acid bath treatment described previously for bars studied under a stereo-microscope. This was done to remove rust and mill scale.

B-72

Samples studied during Phase I of the test program were sectioned by saw cutting each sample to mid-depth along two radial planes and removing a wedge shaped piece from the bar. These planes made angles of 45 and 165 degrees, respectively, with the plane bisecting the bar along the longitudinal ribs. Then, each plane of the wedge was milled to remove the saw marks, ground, and polished.

Once the sectioned surfaces had been polished sufficiently to reveal clean and sharp lug profiles, they were photographed. Enlarged prints were then made, showing those lugs considered to exhibit the sharpest lug geometry. Measurements of the critical lug geometry were made directly from the enlarged photographs.

For Phase II, where transverse lug geometry was the major variable to be studied, it was evident that improved surface preparation and photographic techniques were needed. For this reason, each sample was milled down to a single radial plane.

One sample from each manufacturer was milled to a radial plane making an angle of 45 degrees with the reference plane bisecting the longitudinal ribs. A second sample from each manufacturer was milled at a shallower angle to the reference plane. The sample from Manufacturer A was milled at an angle of 30 degrees while those from Manufacturers B and C were milled at angles of 10 and 35 degrees, respectively. Samples from Manufacturers D and E were milled at an angle of 15 degrees to the reference plane.

The angle of the longitudinal plane section with the reference plane bisecting the longitudinal ribs was selected on the basis of available fatigue test results for each manufacturer's bars. Thus, the lug

B-73

profiles obtained were expected to be representative of the critical fatigue location, as determined from the distribution of fatigue crack nuclei around the periphery of the test bars.

After the milling operation was completed, the sectioned bar surfaces were lapped on an automatic lapping machine. The final surface finish was obtained by hand rubbing with 600 grit silicon carbide paper. Polishing was continued until a microscope examination revealed the absence of any burrs on the edges of the sectioned surface. Using this procedure, a very sharply defined lug profile was obtained.

It was found necessary to black out the rolled surface of each sectioned bar sample near the cut edges. This eliminated reflections from the rolled bar surface during photography. A felt-tipped marker pen was used. Any ink on the sectioned surfaces was removed by relapping and polishing.

Photographs of the sectioned bar surfaces were taken with a vertically mounted camera. Indirect lighting was used to minimize reflections from the semi-shiny sectioned bar surface. High-contrast Kodalith film was used. After developing, a contact printer was used to obtain a clear bar image on a black background negative.

A magnification factor of 2 was used to obtain enlarged photographs of the sectioned bar surfaces. From these, individual lugs, judged to have the sharpest geometry, were selected for further study. Measurements of the critical lug geometry were made from photographic prints showing the selected lugs magnified 14 times.

Lug profiles, obtained by longitudinal sectioning of bars tested in Phase I of the test program, are shown in Fig. B-24. Profiles

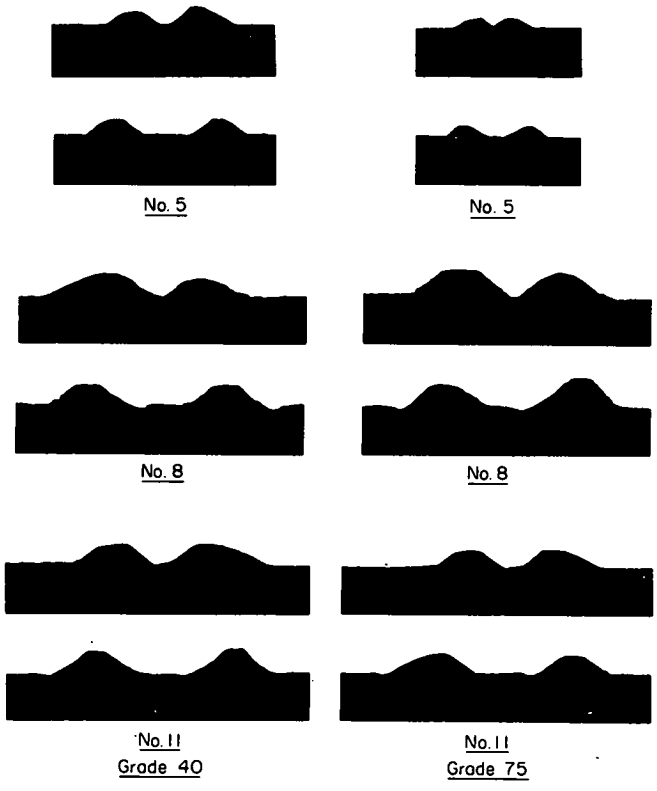

Fig. B-24 Transverse Lug Profiles of Phase I Test Bars

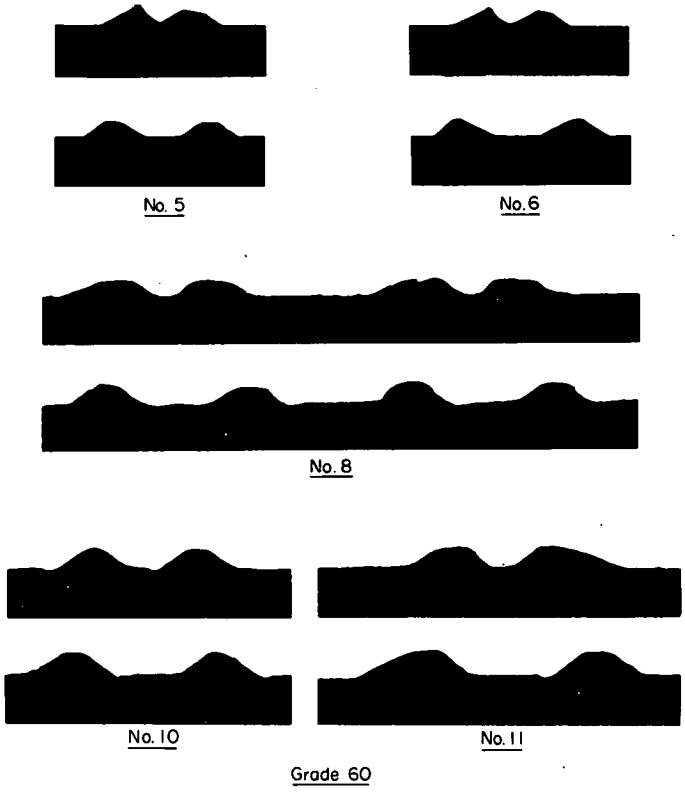

Fig. B-24 Transverse Lug Profiles of Phase I Test Bars (Continued)

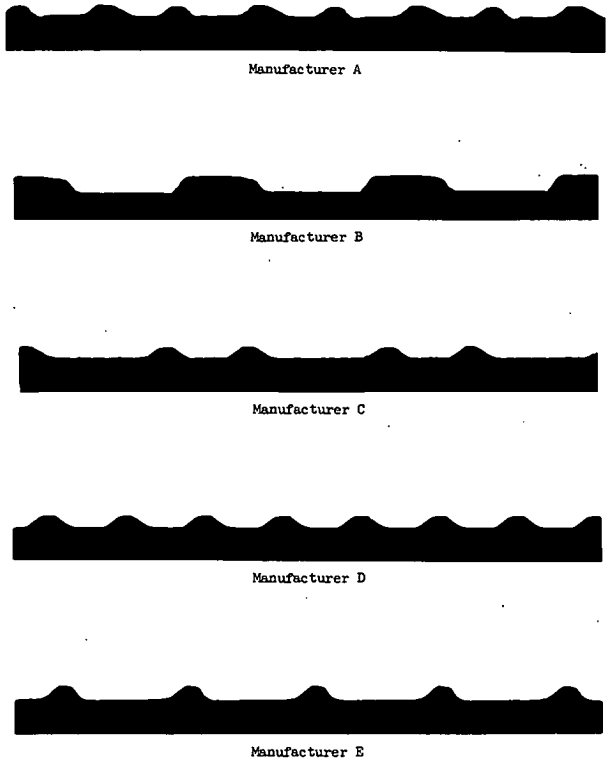

Fig. B-25 Transverse Lug Profiles of Phase II Test Bars

of the transverse lugs of bars tested in Phase II are shown in Fig. B-25.

Plaster Casts. In Phase II of the test program, an attempt was made to develop a simple method of obtaining transverse lug profiles by taking plaster casts of the bar surfaces. Bar samples were 3 in. long and were cut alongside those used for longitudinal sectioning.

Plaster casts of the two samples representing each manufacturer were sectioned at the same angles used for longitudinal sectioning of the bars. Initial preparation of the bar samples from which the plaster casts were made was the same as that for longitudinally sectioned bar samples.

Bar samples were placed at the desired angle in a positioning frame set to hold them at the proper height over a shallow tray, as shown in Fig. B-26. The tray was filled with plaster, the surface evened, and the frame holding the bar samples pressed down over the tray. The bars were removed after the plaster had set, Fig. B-27. A saw cut through the plaster cast then revealed the desired lug profile.

Use of ordinary plaster did not result in satisfactory plaster impressions. It had a tendency to entrap air bubbles in the cast, even after vibration and vacuum treatment. Dental plaster and Redtop moulding plaster were found to give the least problems. The latter was used to make the plaster casts from which the lug profiles were measured. In spite of all precautions, air bubbles were found in the impressed plaster surfaces, particularly in the vicinity of a longitudinal rib impression.

Before photography, the cut plaster surface was ground slightly to remove saw marks. Photographic techniques used were as described before, except for the lighting. It was found necessary to direct light to the sectioned plaster surface at a very shallow angle to obtain as

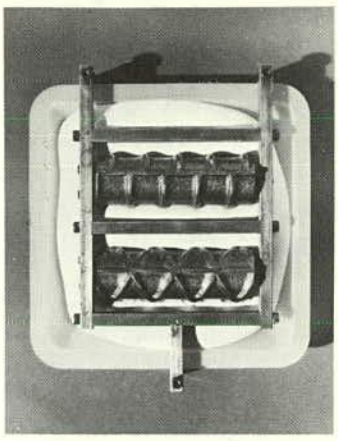

Fig. B-26 Equipment for Making Plaster Casts of Bar Samples

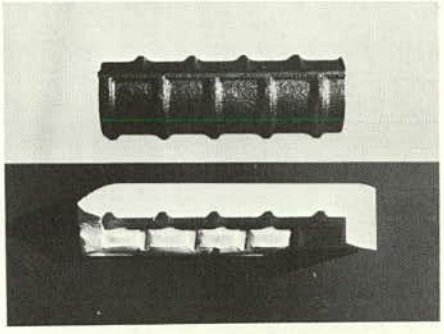

Fig. B-27 Plaster Cast of Bar Sample

deep a shadow as possible over the bar impression. Sufficient contrast was, however, difficult to attain. Consequently, photographs of plaster cast lug profiles tended to show fuzzy profile edges.

A photograph of a plaster cast lug profile obtained from a bar produced by Manufacturer A is shown in Fig. B-28. For comparison, the corresponding profile obtained by sectioning a sample of the same bar is shown in Fig. B-29.

Measurements of critical lug geometry were made directly on photographs of individual plaster cast lugs. Difficulties were encountered with insufficient lug definition and in distinguishing photographed air bubbles in the plaster impression from ordinary bar surface roughness effects. It was found that sharp features on the actual lugs tended to be smoothed out in the plaster casts.

Measurement of Transverse Lug Geometry. Lug geometry measurements by means of a stereo-microscope were concerned with evaluation of the critical lug base radius to lug height ratio. This ratio was estimated to be 0.4, 0.1, 0.2, 0.4, and 0.8 for bars from Manufacturers A to E, respectively. Later measurements on lug profiles obtained by sectioning revealed these estimates to be in error by as much as a factor of two.

Great difficulties were encountered in application of the stereo-microscope to the estimation of lug geometry by direct observation of the bar surface. Evaluations by two competent observers were often not consistent. Furthermore, attempts at stereo-microscope measurements of lug geometry by direct observation of lug profiles obtained by sectioning were not successful. This was due to the lack of contrast between the

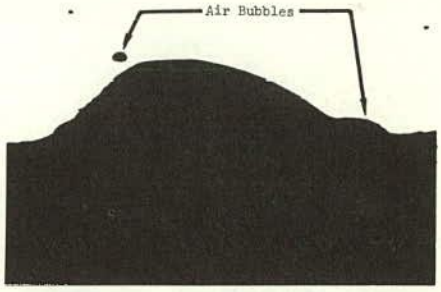

Fig. B-28 Lug Profile Obtained from Plaster Cast

Fig. B-29 Lug Profile Obtained from Sectioned Bar Sample

lug profile and the bar surface background. Therefore, use of a stereomicroscope in the evaluation of lug geometry cannot be recommended.

The study of longitudinal bar sections obtained in Phase I of the test program was confined to the evaluation of lug base radius to lug height ratio, r/h. In Phase II, however, additional features of the lug geometry were noted. These included the flank angles of a lug, its height to width ratio, h/w, and the angle of the lug with the longitudinal axis of the bar. The various lug dimensions measured are defined in Fig. B-30.

Lug radii were determined by comparing different diameter circles on a template with the photographed lug shape, magnified by about 14 times. Thus, the procedure involved the personal judgment of the observer as to what constituted a "best fit." Irregular features of some lug profiles, due to surface roughness, made the evaluation difficult. However, it was found that the results obtained by two observers were in reasonable agreement. Surface roughness of bars from two different manufacturers is shown in Fig. B-31.

Lug height, h, was determined by passing a base line across the photographed lug profile and measuring the perpendicular distance to the highest point on the lug, as shown in Fig. B-30.

Measurement of lug flank angles was based, in many cases, on an estimated tangent to the lug base circle. A tangent line was extended down to the lug base line and upward beyond the face of the lug. At the base of the lug, the points of intersection of these tangent lines with the base line were used to define the width, w, of the lug.

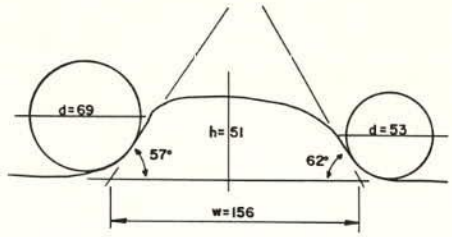

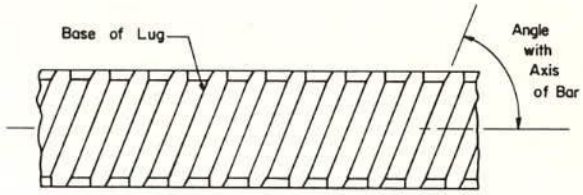

Fig. B-30 Representative Lug Geometry Measurements

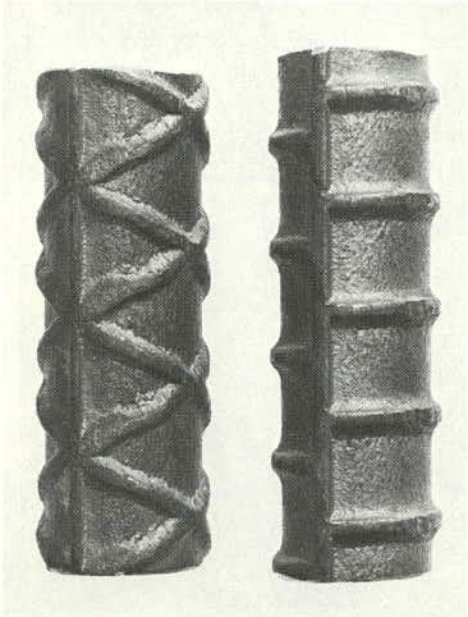

Fig. B-31 Surface Roughness of Test Bars

The critical lug geometry for a manufacturer's bars was considered to be that obtained for the lug having the lowest r/h ratio. Critical lug geometry values determined from sections of bar samples are listed in Table B-11 for each manufacturer's bars.

Also listed in Table B-11 are the smallest r/h ratios found for each manufacturer's bars in the study of plaster cast sections. These r/h ratios differ considerably from the ratios obtained by sectioning of bar samples. Therefore, the technique used to obtain an impression of a reinforcing bar surface was judged to be unsatisfactory. However, it is possible that a recently reported[96] new technology for making impressions of ferro-magnetic materials would be more successful.

For the present, the technique of photographing carefully prepared longitudinal sections of bar samples provides the best means of obtaining estimates of the critical lug geometry. However, due to the variability of lug geometry around the periphery of a reinforcing bar, due care must be exercised in selecting the plane for sectioning. Furthermore, it should be noted that all of the available techniques for determining lug dimensions require individual judgment in estimating the lug base radius.

Supplementary Work on Test Bars

Several supplementary studies and tests were carried out on samples of the test bars. These included the following:

1. Chemical analysis
2. Examination of microstructure
3. Hardness tests
4. Fatigue strength tests on machined bar specimens
5. Static strength tests on fatigued bar specimens

TABLE B-11 MEASURED LUG PROPERTIES

Manufacturer	Size of Bar	Grade of Bar	Type of Section	Angle with Reference Plane, Degrees	Lug Properties						
					Left r/h	Right r/h	Critical r/h	Left Flank Angle, Degrees	Right Flank Angle, Degrees	h/w	Angle with Axis, Degrees
A	5	40	On Bar	45			0.29				
		60					0.24				
		75					0.32				
	6	60					0.25				
	8	40					0.21				
		60			0.70	0.33	0.33	30	35	0.50	65
		75					0.22				
	10	60					0.17				
	11	40					0.22				
		60					0.25				
		75					0.20				
B	8	60	On Plaster Cast	45	1.04	0.29	0.29	60	55	0.50	80
C	8	60		45	1.95	0.29	0.29	55	55	0.39	55
D	8	60		15	0.49	0.38	0.38	30	35	0.39	75
E	8	60		45	1.44	0.39	0.39	50	45	0.60	90
A	8	60		45	0.93	0.93	0.93				
B	8	60		45	0.84	0.67	0.67				
C	8	60		45	1.57	0.91	0.91				
D	8	60		15	1.97	2.78	1.97				
E	8	60		15	1.01	1.09	1.01				

B-86

A chemical analysis was obtained of samples from each class of bar tested. Other tests and examinations were carried out only on selected samples.

Chemical Analysis. An independent organization, Chicago Spectro Service Laboratory, Inc., performed a spectrographic analysis of samples of the test bars. Samples of each grade and size of bar tested in Phase I of the test program and of each manufacturer's bars tested in Phase II were analyzed. The results of their analysis are given in Table B-12.

It appears that the increase in strength in Phase I test bars from Grade 40 to Grade 60 was largely due to the addition of manganese and chromium. Carbon content remained relatively constant. A further increase in strength from Grade 60 to Grade 75 appears to be due to the addition of maganese, phosphorus, and silicon, along with a reduction in sulphur content. Phase II test bars are seen to vary widely in chemical composition.

A steel is considered[97] to be an alloy steel if it contains more than 1.65 percent manganese. Thus, the steel used for the Grade 75 bars from Manufacturer A and that used for the bars from Manufacturer C was alloy steel. The other test bars were rolled from carbon steel.

On the basis of the amounts of carbon and other elements present in the test bar steel, the bars may be classified[97] into the AISI standard grades of steel. This classification is shown in Table B-13.

Some of the bars, notably the ASTM Grade 40 bars satisfy the requirements of several AISI grades. Other bars did not meet the limitations set on the contents of some elements. Thus, the No. 8 and No. 11 ASTM Grade 75 bars were classified on the basis of their carbon and

B-87

TABLE B-12 ELEMENTS COMBINED WITH IRON IN TEST BAR STEEL

Manufacturer	Size of Bar	Grade of Bar	Element - Percent									
			C	Mn	P	S	Si	Ni	Cr	Mo	Cu	V	Ti	Nb
A	5	40	0.41	0.72	0.011	0.025	<0.05	<0.05	<0.05	<0.05	<0.05	*	*	**
		60	0.40	1.42	0.011	0.025	0.07	<0.05	0.23	<0.05	<0.05	*	*	**
		75	0.42	1.82	0.024	0.011	0.29	<0.05	0.10	0.06	<0.05	0.05	*	**
	6	60	0.40	1.57	0.010	0.023	0.09	<0.05	0.21	<0.05	<0.05	*	*	**
	8	40	0.41	0.89	0.012	0.033	0.07	<0.05	<0.05	<0.05	<0.05	*	*	**
		60	0.36	1.32	0.014	0.025	0.08	<0.05	0.20	<0.05	<0.05	*	*	**
		75	0.42	1.77	0.022	0.010	0.29	<0.05	0.19	0.12	<0.05	*	*	**
	10	60	0.36	1.29	0.027	0.013	0.05	<0.05	0.19	<0.05	<0.05	*	*	**
	11	40	0.38	0.72	0.011	0.026	0.06	<0.05	<0.05	<0.05	<0.05	*	*	**
		60	0.36	1.32	0.022	0.010	0.08	<0.05	0.17	<0.05	<0.05	*	*	**
		75	0.43	1.73	0.021	0.015	0.26	<0.05	0.17	0.10	<0.05	*	*	**
B	8	60	0.43	1.04	0.008	0.057	<0.05	0.15	0.30	<0.05	0.30	*	*	**
C	8	60	0.46	1.81	0.016	0.115	0.27	0.23	<0.05	<0.05	0.06	*	*	**
D	8	60	0.53	1.52	0.008	0.038	0.11	<0.05	<0.05	<0.05	0.09	*	*	**
E	8	60	0.59	0.59	0.012	0.050	0.23	0.08	0.08	<0.05	0.08	*	*	**

* Trace, <0.01
** Not detected

B-88

TABLE B-13 CLASSIFICATION OF TEST BAR STEEL

Manufacturer	Size of Bar	ASTM Grade	Type of Steel	AISI Grade					
A	5	40	Carbon	1038	1039	1040	1042	1043	
	8			1038	1039	1040	1042	1043	
	11			1034	1035	1037	1038	1039	1040
	5	60	Carbon	1041					
	6			1041					
	8			1036					
	10			1036					
	11			1036					
	5	75	Alloy	1340					
	8			1340		*			
	11			1340	1345	*			
B	8	60	Carbon	1039	1043	1046			
C	8	60	Alloy	1345		**			
D	8	60	Carbon	1052					
E	8	60	Carbon	1059					

* Molybdenum content too high
** Sulphur content too high

B-89

manganese contents but the steel contained about twice the allowable amount of molybdenum. Similarly, bars from Manufacturer C contained about twice the allowable amount of sulphur. It should be noted that the only ASTM[1] restriction on the chemical composition of steel used for reinforcing bars is a limitation on the amount of phosphorus.

Microstructure of Steel. During Phase I of the test program, samples of Grade 40, Grade 60, and Grade 75 bars were studied under a high power microscope. The samples were sectioned in both the longitudinal and transverse directions, using a water-cooled saw. They were then placed in bakelite mounts and the sectioned surfaces lapped in an automatic lapping machine. Silicon carbide paper with 240, 400, and 600 grit was used successively. The sectioned surfaces were then given a rough polish using 6-micron diamond paste. Finally, each sample was polished to a high finish on a microcloth lap, using 0.5-micron gamma micropolish.

Microscope observation of the sectioned surfaces revealed seams in some of the transverse sections. These were usually found near the center of the section. Examination of the area in the vicinity of the bar surface on the longitudinal and transverse sections showed a fairly uniform surface decarburization.

Samples used for study of the lug geometry of longitudinal sections of Phase II bars were also used to study the microstructure of the parent steel. Each of the sectioned surfaces was polished to a high finish using first 6-micron diamond paste and then 0.5-micron gamma micropolish in a microcloth lap. Finally, a nital etch, consisting of 2 percent nitric acid in alcohol, was applied to a small portion of the sectioned surface of each sample.

Photomicrographs were taken at the base of a transverse lug and in the interior of the sectioned surface of each sample. The magnification factor was 325. Microstructure of the steel at the base of a lug is shown in Fig. B-32 for bars from each of the manufacturers of Phase II test bars. Corresponding photographs of the interior of the sectioned surfaces are shown in Fig. B-33.

Near the surface of each bar sample, the steel shows a fine white grain structure. This is representative of the decarburized layer covering the surface of the bar and is caused by the hot rolling process. The depth of the layer, as well as the amount of carbon loss, is seen to vary locally within each individual sample. Penetration of the decarburization process was estimated to vary locally between 0.003 and 0.006 in.

Hardness of Steel. Vickers pyramid hardness tests were made on transverse sections of bar samples of No. 8 Grade 40, Grade 60, and Grade 75 bars from Phase I of the test program and on samples from each manufacturer's bars in Phase II. Preparation of the samples consisted of the surface polishing treatment described in the preceding section.

Microhardness was determined with a Leitz Miniload Microhardness Tester equipped with a Vickers indenter. The test load was 500 grams and the indenter descended during an interval of 25 seconds. The measuring microscope had a magnification factor of 40 and a measuring grid graduated in 0.5 micron divisions.

Hardness tests were made at thirteen locations in the interior of the transverse section of each bar sample. In Phase II of the test program, additional hardness tests were made at four locations near the

B-90

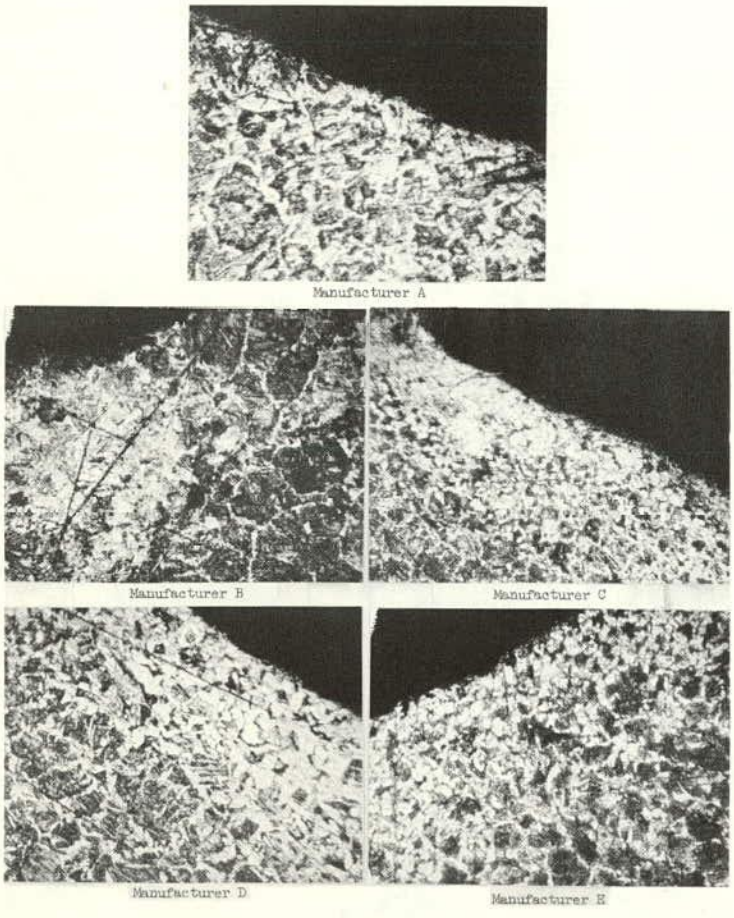

Fig. B-32 Microstructure of Steel Near Surface of Bar

B-91

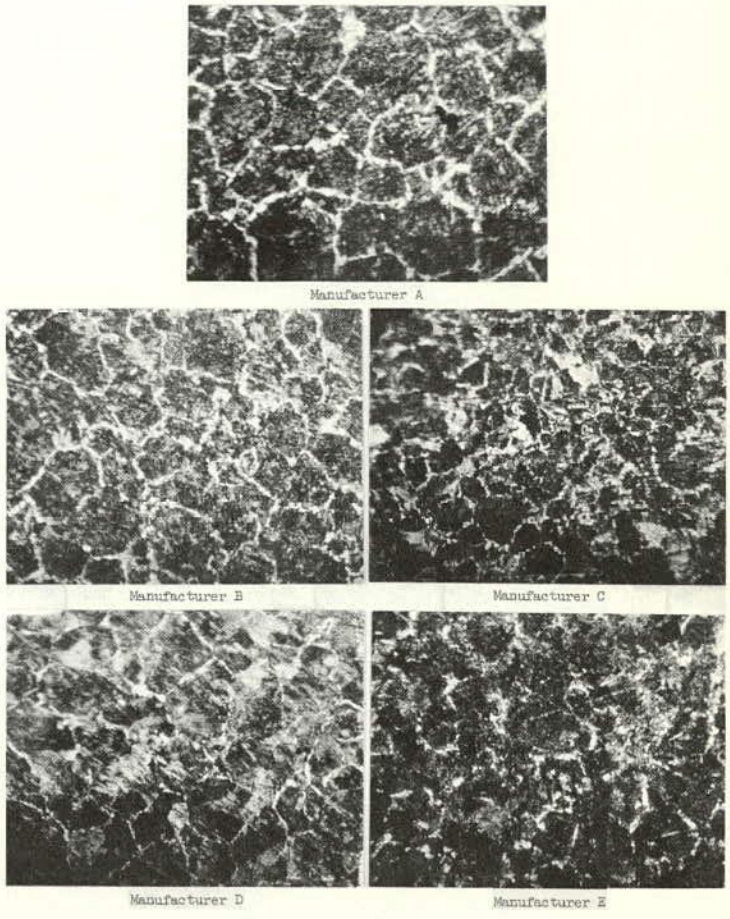

Fig. B-33 Microstructure of Steel in Interior of Bar

surface of each bar sample. Test locations are shown in Fig. B-34.

Average values of Vickers pyramid hardness at the thirteen interior locations on the sectioned surface of each sample are reported in Table B-14. Average hardness at the four test locations near the bar surface is also shown in Table B-14. It did not differ appreciably from the average value for the interior locations. The distribution of Vickers hardness values over a transverse section of a bar sample from Manufacturer C is shown in Fig. B-35.

TABLE B-14 VICKERS HARDNESS TEST RESULTS

Manufacturer	Size of Bar	Grade of Bar	Average Hardness	
			Interior	Edge Points
A	8	40	185	
A	8	60	262	267
A	8	75	291	
B	8	60	264	259
C	8	60	275	270
D	8	60	267	266
E	8	60	271	260

Fatigue Strength of Machined Bar Specimens. Axial tension fatigue tests were carried out in Phase I of the test program by an independent organization, Materials Research Laboratory, Inc. of Glenview, Illinois. Four specimens were machined from No. 8 Grade 60 reinforcing bars. The test section of each specimen had a diameter of 0.25 in. and was 2.5 in. long. A minimum stress level of 6 ksi tension was used throughout. Loads were cycled at a rate of 1000 cycles per minute.

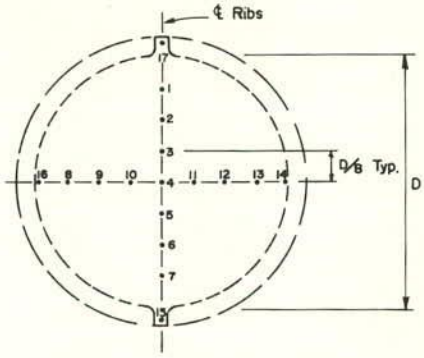

Fig. B-34 Vickers Hardness Test Locations

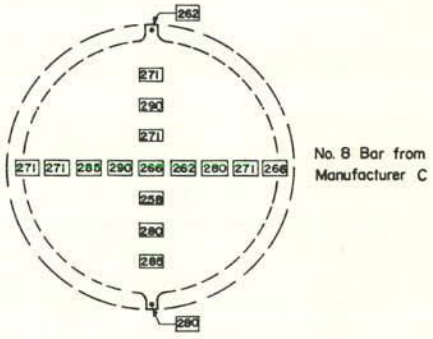

Fig. B-35 Representative Vickers Hardness Test Results

Results of these fatigue tests are shown in Fig. B-36. The test numbers indicate the order of testing. Testing of Specimen No. 1 was terminated when the bar had not failed after 4.03 million cycles of loading at a stress range of 54 ksi. Specimens No. 2, 3, and 4 fractured in fatigue. The fractures obtained in these bars are shown in Fig. B-37.

A dashed line, representing the test results obtained in Group No. 1 has been added in Fig. B-36. This permits a comparison of the results of tests on machined specimens with results of tests on undisturbed reinforcing bars having the same nominal base material properties.

Some of the difference in test results shown in Fig. B-36 must be attributed to size effects and to effects arising from testing the Group No. 1 bars as encased in concrete and subject to some bending stresses. However, the major part of the difference in results is attributed to surface effects in the as rolled bars of Group No. 1. Among such effects, one may consider the stress concentrations due to the rolled on deformations, other notch effects, and the effect of surface decarburization.

Static Strength of Fatigued Bar Specimens. In Phase II of the test program, static strength tests were conducted on a number of bar specimens that had previously been subjected to cyclic stresses. These tests were intended to determine the effect of fatigue damage on the static tension properties of the test bars. Three of the tests, those from Group No. 42, were conducted in a limited study of fatigue crack growth.

When a fatigue fracture was observed to occur near the load point of a test beam during regular Phase II tests, a coupon having sufficient length for static tension testing was obtained from the

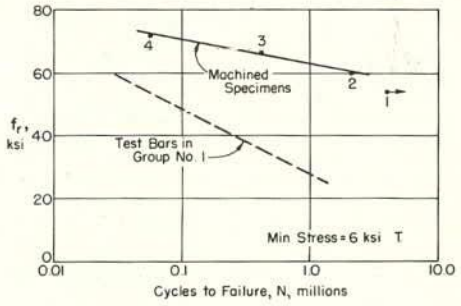

Fig. B-36 Fatigue Properties of Machined Bar Specimens

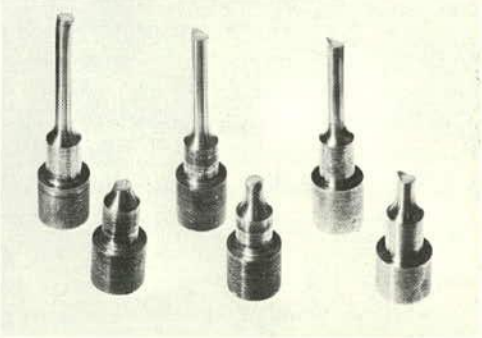

Fig. B-37 Fatigue Fractures of Machined Bar Specimens

fatigued test bar. A welding torch was used to cut the bar coupon from the constant moment region of the test beam. Each of these coupons had a length of 25 to 30 in. In most cases, a short length at one end of the bar coupon had extended into one shear span of the test beam. During static testing, this length remained within the grips of the testing machine.

Static tension tests were conducted in a 300,000 lbs. capacity universal hydraulic testing machine. Instrumentation for obtaining load-strain curves was the same as that previously reported for regular tension test coupons. Each sample was marked with gage points for measuring elongation over an 8-in. gage length.

Results of the static tension tests for bar test coupons taken from test beams where the test bar had fractured in fatigue are presented in Table B-15. For comparison, test results on corresponding undisturbed bar specimens are also presented in Table B-15. Yield strength of the fatigued bar specimens was determined in the manner previously reported for the regular specimens.

Two of the fourteen static tension tests on fatigued bar specimens resulted in ductile fracture. No evidence of fatigue damage could be seen in the fracture surfaces of these bars. A comparison of the yield and tensile strengths determined during these tests with the results obtained from undisturbed test coupons reveals no significant difference.

The twelve remaining tests resulted in sudden brittle fracture after having, in general, exhibited normal yielding. This is evidenced by the decreased elongation observed in the fatigued bars when compared

TABLE B-15 PROPERTIES OF SEVERELY FATIGUED BARS

Phase II Test No.	Fatigued Bars				Undisturbed Bars			
	Yield Strength		Tensile Strength, ksi	Elongation in 8 in.	Yield Strength		Tensile Strength, ksi	Elongation in 8 in.
	ASTM A615, ksi	0.0035 Strain, ksi			ASTM A615, ksi	0.0035 Strain, ksi		
7	49.9	49.8	83.5	0.66	50.1	49.8	83.7	1.18
8	48.6	47.7	77.7	0.43	48.1	47.7	80.7	1.37
9	56.6	56.6	73.1	0.27	57.2	57.0	89.8	1.20
14	47.7	47.0	48.1	0.04	49.4	48.8	83.5	1.20
22	50.2	50.2	83.5	1.05	50.2	49.8	81.6	1.11
36	48.3	46.7	78.7	0.24	48.7	47.6	90.7	0.96
48	47.5	47.2	80.2	* #	48.7	48.5	80.1	1.50
65	50.8	48.7	60.4	0.17	49.6	48.7	84.0	1.34
68	52.1	50.8	66.2	0.22	48.2	48.2	79.7	1.57
81	*	*	47.8	0.09	58.2	57.8	91.1	1.12
93	51.6	49.0	70.6	0.23	50.0	49.1	84.2	1.27
101	50.5	49.0	85.2	1.25 #	50.3	49.1	85.5	1.21
110	49.2	48.2	82.8	0.85	49.4	49.1	83.5	1.26
111	49.8	49.1	84.0	0.60	49.5	48.9	83.9	1.26

* Could not be measured
\# Ductile fracture

with the elongation of undisturbed test specimens. Further evidence of brittle fracture was obtained upon examination of the fracture surfaces of the test bars. This examination revealed a transverse plane fracture with no necking of the fracture region.

A typical fracture surface for the previously fatigued test bars is shown in Fig. B-38. A small fatigue crack is seen to have extended into the bar. This apparently caused the brittle fracture of the remainder of the bar cross-section. Thus, the tensile strength of a reinforcing bar is reduced during the fatigue crack growth stage. Brittleness of the fracture may be due to the severe stress concentration occurring at the tip of the fatigue crack.

The Group No. 42 test series consisted of three tests on bars from Manufacturer A. Each bar was encased within a concrete beam. The test beams were subjected to a nominally identical cyclic loading intended to result in a minimum stress of 6 ksi and a stress range of 34 ksi in the test bars.

Loading of these three beams was terminated after 100 thousand, 200 thousand, and 300 thousand cycles of loading, respectively. This compares with a mean fatigue life of 482,000 cycles at a stress range of 34 ksi for bars from Group No. 33. These bars are nominally identical to the Group No. 42 bars.

After the loading on each test beam in Group No. 42 had been terminated, an 8-ft. length of the test bar was removed from the beam. These bars were then tested in static tension in a universal hydraulic testing machine of 400,000 lbs. capacity. The test length consisted of the central 5 ft. of each bar. Each test bar was marked with a series

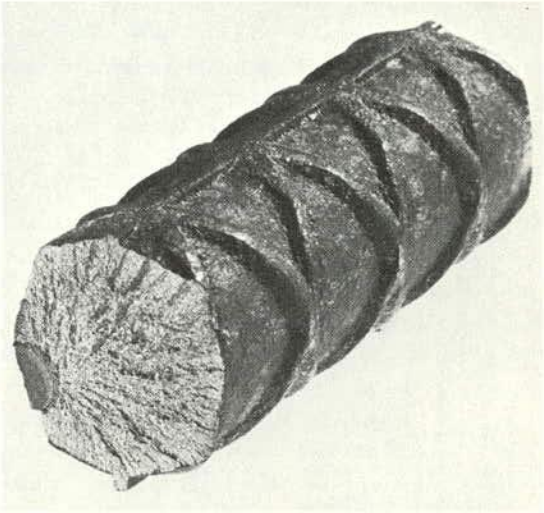

Fig. B-38 Static Tension Fracture of Previously Fatigued Test Bar

of gage points for the measurement of elongation over an 8-in. gage length.

Results of static tension tests for the partially fatigued bars of Group No. 42 are presented in Table B-16 along with test results obtained on corresponding undisturbed specimens. Yield strength of the partially fatigued bars was determined from the constant load indicated on the testing machine after the load had dropped from its peak in turning the knee in the load-strain curve. Examination of the bar fractures revealed no evidence of fatigue damage.

TABLE B-16 PROPERTIES OF PARTIALLY FATIGUED BARS

Test No.	Fatigued Bars			Undisturbed Bars		
	Yield Strength, ksi	Tensile Strength, ksi	Elongation in 8 in.	Yield Strength, ksi	Tensile Strength, ksi	Elongation in 8 in.
112	47.4	78.5	1.63	47.3	79.4	1.54
113	48.8	80.4	1.54	48.8	80.7	*
114	48.9	81.2	1.47	49.5	81.2	*

* Fractured outside gaged length

The uniformity of static tension properties among the partially fatigued and undisturbed specimens supports the conclusion that no fatigue damage had as yet occurred in the fatigued bars. Fatigue crack growth would thus be expected to occur during the final 40 percent of the mean fatigue life of the bars, under the test conditions applied.

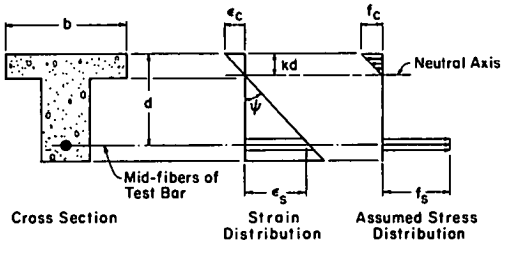

Fig. C-1 Assumed Stress Conditions in Test Beam

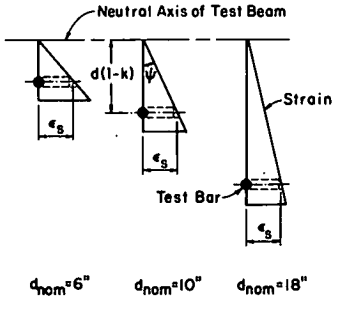

Fig. C-2 Influence of Depth of Beam on Strain Gradient

APPENDIX C

ANALYSIS OF TEST RESULTS

Calculation of Stresses in Test Bars

Stresses in the reinforcing bar embedded within each test beam were calculated for forces acting at the midspan of the beam. These were considered to be the stresses causing fatigue failure in the test bar. As may be seen in Fig. B-17, most bar fractures occurred in the region between the load points of the beam. In this portion of the beam, the applied moment was constant except for the relatively small effect of the weight of the beam.

Stress calculations were based on the straight line theory of flexural stress and strain given in Section 8.10.1 of the 1971 ACI Building Code.[4] The conventional assumptions of elastic reinforced concrete theory were therefore used. Thus, for a cracked section, the flexural tensile stresses in the concrete were neglected, and the reinforcing bar was assumed to be uniformly stressed, as illustrated in Fig. C-1.

All fatigue failures took place at or immediately adjacent to an externally visible flexural crack in the test beam. This observation supports the assumption that the critical section was fully cracked. Cracks were assumed to remain open at all times in beams not subjected to stress reversal.

As described in Appendix B, stress reversal in a test bar was obtained by prestressing the test beam externally at the level of the test bar. Prestressing was applied while the beam was subjected to a static load. This was done to prevent flexural cracking of the unreinforced "compression" flange. The prestress force caused all cracks to close gradually as the load was reduced from its maximum during a load cycle. Full closure of a flexural crack was assumed to have the effect of returning the test beam to its uncracked stiffness.

It was assumed for the stress calculations that the external prestressing rods had no effect on flexural stiffness. Furthermore, it was assumed that the magnitude of the prestressing force remained constant during bending of the beam.

Calculations to determine steel stresses were carried out on an IBM 1130 computer. An average cross-sectional area was computed for each test bar on the basis of its weight. The modulus of elasticity for the test bars was taken as 29,000 ksi.
ksi.

Forces due to the inertia of a test beam and its loading equipment were taken into account in accordance with recommendations contained in the Amsler Instruction Manual(95). For these calculations, unit weight of the concrete was taken to be 144 lbs. per cubic foot, based on the weight of standard 6x12-in. cylinders. The inertia forces did not exceed 9 percent of the applied repeated loading.

The calculated values of minimum stress, f_{min}, and stress range, f_r, were calculated for each test bar.

No attempt was made to take into account the effects of concrete creep and shrinkage on the minimum stress level in a test bar.

Strain Gradient. Although it is common practice in the design of reinforced concrete members to assume that the stress in the reinforcing element is uniform, the stress probably varies in a manner similar to the overall distribution of strain across the depth of a beam section. Therefore the stress at the remote edge of a test bar from the neutral axis may be more significant, as far as fatigue is concerned, than the average stress at the midfibers of the bar.

The rate of change of strain over the depth of a beam, the strain gradient, is a measure of how much the stress will vary over the depth of a reinforcing bar embedded in a concrete beam. The strain gradient, ϕ, may be calculated as:

$$\phi = \epsilon_s/(1 - k)d$$

The steepness of the gradient varies inversely with the effective depth of a beam for a given reinforcement stress level, as illustrated in Fig. C-2.

As indicated in Table B-1, the nominal effective depth, d_{nom}, of the test beams was 6, 10, or 18 in. For a given bar size, all beams having the same effective depth have the same strain gradient at a particular stress level. Depth to the neutral axis of the beams subjected to stress reversal was, however, affected by the prestress force. To maintain approximately the same strain gradient as in the non-prestressed beams, the reinforcement in the prestressed beams was placed at a nominal effective depth of 6.75, 11, or 20 in. respectively.

Width of the compression flange, b, was varied with the size of the bar being tested. This served to maintain a nearly constant distance from the neutral axis to the centroid of the test bar for beams of the same nominal effective depth.

It is reasonable, using the neutral axis as a reference, to consider the critical stress on a test bar cross section to have occurred at the remote edge of the barrel of the bar rather than at the remote edge of the longitudinal rib. This stress may be written as

$$f = f_s (1 + \alpha)$$

where

$$\alpha = \frac{D}{2(1 - k)d}$$

and D is the diameter of the bar across the barrel. The coefficient α

represents the percentage by which the stress at the far edge of the bar is greater than the average stress across the bar.

The coefficient α was constant for all stress levels in each group of tests on non-prestressed beams. In the prestressed test beams, on the other hand, the magnitude of the coefficient varied continuously with the stress level in the test bar. This was due to the variation in depth to the neutral axis with stress level.

For the non-prestressed test beams, the stress range at the far edge of the bar may be expressed in terms of the coefficient α as

$$f = f_r(1 + \alpha)$$

For the prestressed test beams, the strain gradient effect is slightly greater since the minimum and maximum stress level effects are additive.

Values of the coefficient α for the beams used in the test program are given in Table C-1. In the case of the prestressed beams, the values presented are average values for the stress range levels used. The value of the coefficient is highest for a shallow beam containing a heavy reinforcing bar.

TABLE C-1 EFFECT OF STRAIN GRADIENT

Coefficient α for Ordinary Test Beams					
d_{nom}, in.	Bar Size				
	5	6	8	10	11
6	0.069	0.084	0.114	0.142	0.157
10	0.038	0.047	0.063	0.079	0.087
18	0.020	0.024	0.032	0.041	0.045
Average Coefficient α for Prestressed Test Beams					
6			0.133		
10	0.050		0.069		0.085
18			0.037		

It may be expected, solely on the basis of the above, that the initiation of a fatigue crack in a reinforcing bar embedded within a concrete beam should occur in the fibers furthest from the neutral axis. This is generally the case, as may be seen in Table B-8. However, exceptions are easily found, for example, among the bars from Manufacturer A, when the location of the critical lug geometry dominates. Thus there appears to be no compelling reason for considering the stress in the outermost fibers to be the critical stress in a test bar. It is, in fact, desirable to define the critical stress as the average bar stress, calculated according to usual design office practice. Any influence of the strain gradient on fatigue strength may then be accounted for, in a prediction equation, by bar diameter or effective depth terms.

Experimental Verification. At the start of the experimental work, special tests were carried out on beams representative of those in Groups No. 1, 4, and 21. These tests were intended to verify that the calculated stress was closely equal to the stress determined from experimentally measured strain in the test bar.

Strain in the test bars was measured by means of electrical resistance strain gages. These were mounted on the longitudinal ribs and barrel of each test bar. The gaging techniques used are described in detail elsewhere.[19]

Surface preparation for rib mounted gages was minimized by the use of narrow 70 mm (2-3/4 in.) long gages. These were mounted on opposite sides of the bar and their output averaged. Strains on the barrel of each test bar were measured by mounting 1/8-in. long gages midway between the longitudinal ribs and between two transverse lugs. These gages were also mounted on opposite sides of the bar and their output averaged.

Axial tension tests were carried out in air on samples of all sizes of bars from Manufacturer A. Both types of gages were mounted on each sample. In these tests, strains measured with the 1/8-in. long gages consistently ranged between 16 and 20 percent greater than the strains measured with the longer gages. A modulus of elasticity close to 29,000 ksi was indicated by the 70 mm. gages. However, no significant difference between the two types of gages was recorded during a separate axial tension test on a plain 1 in. diameter cold rolled bar.

Strains recorded from the two types of gages, when mounted on test bars embedded in concrete beams, showed reasonably good agreement with calculated values, regardless of the type of gage. In each case, the gages were located at the crack former in the beam before casting. However, each set of 1/8-in. long gages may not have been crossed directly by the formed crack. Because of the difference in results from the two types of gages in axial tension tests, uncertainty regarding the position of the 1/8-in. long gages relative to a flexural crack, and concern that an excessive disturbance to bar geometry in mounting the 70 mm. gages might affect the fatigue test results, no bars in the main testing program were gaged.

An elastic modulus of 29,000 ksi was used to determine stresses from strains measured on the embedded test bars. For comparison, the stresses due to application of the ram loads alone were calculated, using procedures described earlier in this appendix. Plots of calculated and experimentally determined stresses are shown in Figs. C-3 and C-4.

Results of tests on a beam similar to those tested in Group No. 1 are shown in Fig. C-3. Experimental curve A was obtained in a static test, conducted after the beam had been subjected to 15,000 cycles of repeated loading, intended to result in a minimum stress of 6 ksi and a stress range of 24

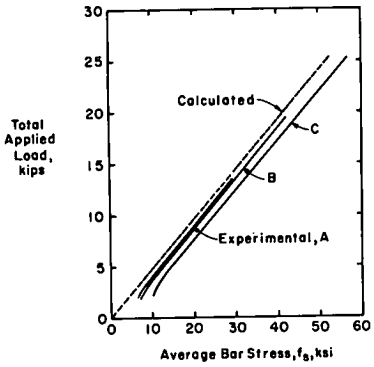

Fig. C-3 Bar Stresses in Beam Similar to Those in Group No. 1

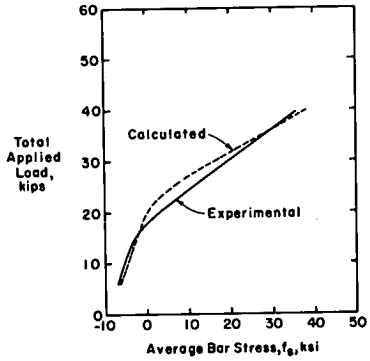

Fig. C-4 Bar Stresses in Beam Similar to Those in Group No. 4

In summary, differences of up to 3.5 ksi were found between measured and calculated stresses. However, this difference was generally much less and tended to be reduced as the number of cycles of loading increased. The method of calculation of test bar stresses was therefore regarded as being satisfactory. It should be noted that the procedure used to calculate the stresses in the test bars was the same as that commonly used for reinforced concrete members.

Introduction to the Statistical Analysis

Each phase of the test program was designed and executed to permit the effects under study to be evaluated by statistical means. In Phase I, the aim of the statistical analysis was to identify which of the specified variables -- stress range, minimum stress, bar diameter, grade of bar, and type of specimen -- were significant, and to quantify their effects on fatigue life. The principal aim of the statistical analysis in Phase II was to relate the fatigue limit at 5,000,000 cycles to the geometric characteristics of the surface deformations rolled onto each manufacturer's bars. Further analysis in both phases of the test program was used to assess the effects of other variables on the fatigue lives of the test bars.

In the analysis, a distinction was made between finite-life data, when the fatigue life is strongly influenced by the applied stress range, and long-life data, when the test conditions place the bar near its fatigue limit. The Phase I test program was not specifically designed for the study of long-life data. However, a convenient separation point between the two kinds of data was found to be at a stress range of 28 ksi. Thus, tests carried out with a stress range in the test bars greater than 28 ksi were regarded as resulting in finite-life data while tests with a lower stress range were considered to lead to long-life data.

ksi in the test bar. Curve B was obtained in a similar manner, for an intended stress range of 36 ksi, after an additional 5,000 cycles of loading had been applied, and curve C was determined, for an intended stress range of 48 ksi, after a further 15,000 cycles.

For the greater part of their lengths, curves A, B, and C are straight lines very nearly parallel to the line representing calculated data. The nonlinearity found at low loads is apparently due to the inability of the concrete flexural cracks to close completely. The ratios of experimental to calculated stress ranges for A, B, and C were 0.93, 0.96, and 0.98, respectively.

Loading on the beam was subsequently changed to produce an intended minimum stress in the test bar of 18 ksi. For intended stress ranges of 24 and 36 ksi, the ratios of experimental to calculated stress range were 1.00 and 0.99, respectively.

Results of a test on a beam similar to those tested in Group No. 4 are shown in Fig. C-4. The experimental curve was obtained in a static load test conducted after 7,000 cycles of loading had been applied to the beam. At a calculated stress range of 36 ksi, the ratio of experimental to calculated stress was 1.02. Projecting the two curves forward, one obtains ratios of 0.96 and 0.94 at calculated stress ranges of 48 and 54 ksi, respectively.

It was noted in tests on the non-prestressed beams that the minimum stress in the test bar tended to increase with the number of cycles of loading applied to the beam. This effect is attributed to creep and microcracking in the compression concrete and to loss of bond in the vicinity of the flexural crack where the gages were located.

Phase II of the test program was designed to allow a clear separation of the two kinds of data. Thus, tests included in Groups No. 33, 35, 37, 39, and 41 were intended to result in finite-life data while tests included in Groups No. 32, 34, 36, 38, and 40 represented long-life data. Some of the lead-in tests for the long-life test series did, however, fall into the finite-life region, but this had no effect on the analysis.

Analysis of Phase I data was, by the nature of the experiment, largely confined to the analysis of finite-life data. First, individual groups were studied by linear regression analysis. This was followed by analysis of variance of several factorial designs, each encompassing a number of groups. Finally, all Phase I groups were studied as a whole by multiple linear regression. At each stage, extensive use was made of previous results.

Analysis of long-life data was emphasized in Phase II. A method of determining the mean fatigue limit at 5 million cycles and its standard deviation was developed. Finite-life data from Phase II were also extensively studied by means of various linear regression procedures. Tolerance limits were established for both finite-life and long-life data.

Preliminary Considerations

Prior to the initiation of the statistical analysis, a number of questions had to be resolved regarding the suitability of some of the test results for inclusion in the general analysis. Some of these are completely dealt with here; others are mentioned here but dealt with in greater detail in the later sections.

The experimental work was described in detail in Appendix B. The main part of the Phase I test program consisted of 31 groups of 7 tests. Within each group, the only intended variable was the stress range in the

test bar. These tests were performed in random order. However, to establish stress ranges for conducting the tests, a series of seven tests was carried out on beams similar to those in Group No. 1 before the start of the main part of the test program. These tests were carried out at a time when the experimental procedure had not yet become a matter of routine. Therefore, they may have been subject to systematic and procedural error.

To obtain a better estimate of variation within a group, a third series of seven tests, similar to those in Group No. 1, was carried out at the conclusion of the main part of the Phase I test program. These tests were randomized only for stress range.

Two groups of tests in Phase II of the test program, Groups No. 32 and 33, were carried out on bars that remained from the Phase I test program. Test beams in these groups were similar to the beams in Group No. 1 but were tested in a different test setup, after a considerable time lapse, and with different personnel. The order of testing was fully randomized within the finite-life and long-life parts of Phase II.

Tests in Group No. 1, performed at the beginning and end of the main part of the Phase I test program, can only be included in the statistical analysis alongside the fully randomized Group No. 1 tests, if they are all shown to belong to the same population. Group No. 33 provides a link between the two phases of the test program. Thus the two phases may be considered to be statistically compatible if it can be shown that data from Groups No. 1 and 33 represent the same population. An analysis of covariance[20,21] was performed to establish the homogeneity of these various sets of data.

A separate regression line was fitted to the finite-life data from each set of tests in Group No. 1 and to Group No. 33. The logarithm of the

number of cycles to failure, log N, was taken as the dependent variable and stress range, f_r, as the independent variable. The results are given in Table C-2. Series 1 refers to the initial tests in Group No. 1, Series 2 refers to the randomized tests performed within the main part of the Phase I test program, Series 3 refers to the final tests in Group No. 1, and Series 4 refers to the tests in Group No. 33.

The first requirement the four sets of data must satisfy is that their variances be estimates of a common variance. The standard test for constancy of variance, homoscedasticity, is Bartlett's test[20,25]. The computed test statistic was 3.49 and was compared with the chi square distribution. The 95 percentile of the distribution is 7.81 for 3 degrees of freedom. Hence, the null hypothesis that all four sets have a common variance cannot be rejected at a 5 percent level of significance.

Bartlett's test has been shown[26] to be inaccurate when the number of degrees of freedom is small. An alternative, Hartley's test, has been proposed[27] and tabulated[98, 99], where the test statistic is the ratio of the largest to the smallest sample variance. The test statistic was 9.35 and was compared at a 5 percent significance level with Hartley's statistic of 20.6 for four estimates of variance having a mean 4 degrees of freedom. This confirms that the null hypothesis that the individual regression lines have a common variance cannot be rejected.

The criterion for all four sets of data to come from the same population is that a single line, the over-all regression line, be an adequate fit to all four sets. Evaluation of this possibility advances from a test for parallelism of the regression lines to a test for linearity of group means and finally a test of equality between the group mean slope and an over-all

TABLE C-2 HOMOGENEITY OF GROUPS NO. 1 AND 33

Individual Results

Series	Number of Data Points	Mean Value, f_r	Mean Value Log N	Slope	Mean Square Sum of Errors, s^2	$\frac{s^2_{max}}{s^2_{min}}$
1	6	39.97	5.4270	-0.04912	0.004001	9.35
2	5	40.23	5.4370	-0.04665	0.000428	
3	5	40.18	5.4173	-0.04579	0.001370	
4	9	42.87	5.2896	-0.04441	0.002962	

Pooled Results

Grand Mean Value, f_r	Grand Mean Value Log N	Slope of Parallel Lines	Slope of Line for Mean Values	Slope of Overall Line
41.11	5.3776	-0.04597	-0.04967	-0.04607

ANOCOVA

Source of Variance	Sum of Squares	Degrees of Freedom, DF	Mean Square Sums, s^2	F-Ratio
Between parallel and series mean slopes	0.000584	1	0.000584	0.24
Series means about their line	0.001729	2	0.000865	0.35
Between the individual slopes	0.004843	3	0.001614	0.65
About the individual lines	0.042137	17	0.002479	
Due to the overall line	3.342120	1	3.342120	1559.43
About the overall line	0.049293	23	0.002143	
Total (corrected for mean)	3.391413	24		

slope. In each case, a ratio of mean square sums, an F-ratio, given in the ANOCOVA table in Table C-2, is compared with the appropriate value of the F-distribution[20,28,29]. At the 95 percentile point, the tabulated values are $F(3,17;095) = 3.20$, $F(2,17;095) = 3.59$, and $F(1,17;095) = 4.45$ and compare with observed F-ratios of 0.65; 0.35, and 0.24, respectively. Each hypothesis in turn cannot be rejected at a 5 percent significance level and the various sets of data may be taken to represent a single population. Therefore, all of the Group No. 1 data were included in the statistical analysis of Phase I data. Furthermore, this connection between Phase I and Phase II data allows conclusions drawn from one to be shared with the other.

Some of the tests conducted at stress ranges below 28 ksi in Phase I of the test program did not result in failure within 5 million cycles. In addition, a number of the staircase tests conducted in Phase II survived 5 million cycles of loading. In each case, the test was then terminated. The test beam was assigned a new test number by adding 1000 to the original Phase I test number and 3000 to the Phase II number. Loading was then resumed, but at a higher stress range, causing a failure in the finite-life region. These finite-life tests had thus received a different treatment from the standard finite-life tests. It was therefore decided that such rerun tests should not be included in the main analysis of finite-life test data.

Each test bar carried a manufacturer's bar identification mark at regular intervals. The geometry of the bar mark may differ from that of the transverse lugs, and consequently the bar mark could affect the fatigue properties of a test bar. For this reason, a conscious effort was made, as noted in Appendix B, to avoid locating a bar mark at the crack former placed at midspan of each test beam.

A fatigue failure was initiated at a bar mark in five tests of Phase I -- No. 96 in Group 24, No. 152 in Group No. 13, and No. 187, 1010, and 1222, all in Group No. 24 -- and in six tests of Phase II -- No. 27 in Group No. 38, and No. 70, 105, 109, 3054, and 3066, all in Groups No. 40 and 41. Except for the rerun tests, these tests were included in the main part of the statistical analysis. Test No. 3066 was excluded from the analysis of rerun tests, because the failure was evidently anomalous, occurring at only one-fifth of the expected life.

In some of the tests in Groups No. 7, 8, 9, 19, 21, 22, 28, and 30, the higher stress ranges caused yielding of the test bars under initial application of load. When this happened, the test beam underwent a permanent deflection. However, its subsequent behavior under repeated loading was elastic. The tests where yielding occurred were included in the main part of the statistical analysis.

In a few instances, a part of the test on a specimen was run under conditions that deviated from the specified test conditions. For example, the load may have been in error, or the span length incorrect. If the error was evident in the early stages of a test, it was corrected. In each instance, the fact was noted for future reference. During the statistical analysis, these tests continually received special attention. They were not included in the analysis of the factorial designs. However, they were included initially in the multiple linear regression. Test No. 77 in Group No. 5 was finally rejected from the regression data as an outlier. This was done on the basis of its having a residual more than four times larger than the residual standard deviation of the regression equation. During Test No. 77, as described in Appendix B, a power failure had occurred and the beam, being prestressed,

developed cracking through the extreme concrete compression fiber.

Three test beams in Phase I of the test program -- No. 157 in Group No. 30, No. 175 in Group No. 22, and No. 224 in Group No. 9 -- failed in fatigue of the concrete in compression when subjected to a loading intended to result in a stress range of 54 ksi in the test bar. These tests were not included in the statistical analysis.

Tests in Group No. 42 were intended for a study of fatigue crack growth, and loading was terminated before failure of the test bar occurred. None of these tests was included in the statistical analysis.

Test No. 3051 in Group No. 34 was not included in the analysis of rerun data as the number of cycles to failure had been improperly recorded.

Compliance with Assumptions of Analysis

The statistical methods used in analyzing the experimental data are based on three main assumptions[100]:

1. The data observed during each test constitute a random sample from a population of all possible test results.
2. The observed fatigue lives are random samples from a log-normal population.
3. The observed fatigue lives have constancy of variance.

Random Sample. A random sample is one selected by a random process. It is thus free of bias, such as conscious or unconscious discrimination by an individual, or the effect of gradual change in measuring apparatus. For a particular population, point estimates of the mean and variance, and estimates of confidence intervals and tolerance limits, may be made from random samples. The procedures followed in carrying out the testing program were described in detail in Appendix B. To a large degree, they satisfy the first

assumption of a random sample. It is noted, however, that it is virtually impossible to randomize all factors in an experiment of this nature.

Log-Normal Population. For representing the data, a statistical distribution should be chosen[17] that is in reasonable agreement with the data, and that is mathematically tractable. The normal distribution is mathematically tractable for many problems. Many techniques of statistical inference have been derived on the assumption of normally distributed data. The second assumption of a log-normal population implies that the logarithm of the observed fatigue lives is normally distributed.

Several of the statistical results obtained depend on the use of regression lines for each individual group of data. The significance of the parameters of a regression is measured by means of the error variance, which in turn requires the assumption of normalcy. The large number of tests in Groups No. 1 and 33, drawn from a single population, allowed this assumption to be tested.

A test to evaluate the assumption of a normal distribution is provided in the W-test[22,23]. The test statistic, W, was calculated from the residuals of the over-all regression performed on the finite-life data from Groups No. 1 and 33 and was found to be equal to 0.973. This was compared with tabulated values, which for 25 data points are W(25;010) = 0.931 and W(25;050) = 0.964 at the 10 and 50 percent probability levels, respectively. Consequently, the hypothesis that the residuals are normally distributed cannot be rejected. The approximate probability[22,23] that the regression residuals represent a sample drawn from a normal distribution was calculated and found to be 72 percent.

A more familiar and interpretative test is to compare a plot of cumulative observations against regression residuals on normal probability

paper to a straight line, as is shown in Fig. C-5. In order to minimize bias, the residuals were plotted against the cumulative frequency (100 - p) equal to (i - 3/8)/(n + 1/4) as suggested by Blom[56] and Kimball[57] for the normal distribution. Again, the hypothesis of normal residuals cannot be rejected.

As the tabulated values required for the W-test are given only for a maximum sample size of 50, the chi square test was used to evaluate the normalcy assumption for the multiple linear regression of the Phase I finite-life test data. This test is based on dividing the range of the sample into cells, such that an equal number of observations are expected to fall into each cell. The test was applied to the residuals obtained from the multiple linear regression on the specified Phase I variables, discussed in the section entitled "Multiple Linear Regression."

The sample consisted of 166 regression residuals. The mean of a population of regression residuals is zero by definition. The standard deviation of the residuals was found to be 0.1064. Using the Mann-Wald[58] criterion at a 5 percent level, as modified by Williams[59,24], the number of cells was chosen to be k equal to 14. Therefore the expected number of residuals per cell was 12.

The actual number of residuals in each cell is illustrated in Fig. C-6. The test statistic was found to be 15.2. This was compared with the tabulated values[22] for chi square, using 12 degrees of freedom. The probability of obtaining values of chi square less than the above test statistic is between 70 and 80 percent. Thus the hypothesis that the residuals are normally distributed cannot be rejected at the 5 percent level of significance. It is noted[20,29] that an analysis of variance and multiple linear regression may remain valid under moderate deviations from the assumptions of normalcy.

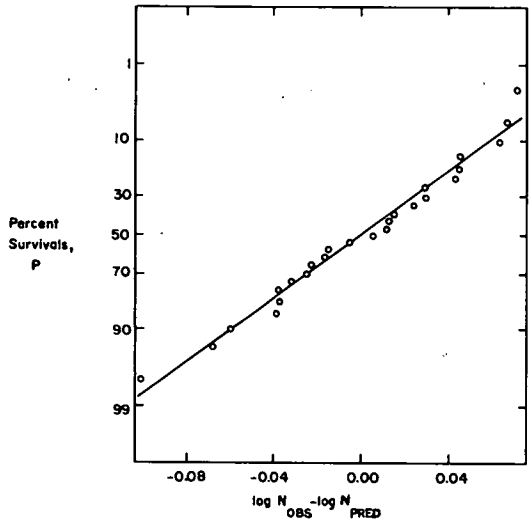

Fig. C-5 Cumulative Frequency Distribution of Residuals from Groups No. 1 and 33

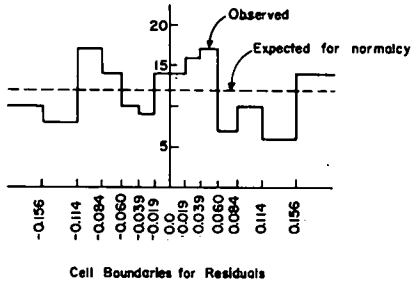

Fig. C-6 Distribution of Residuals in Chi Square Test

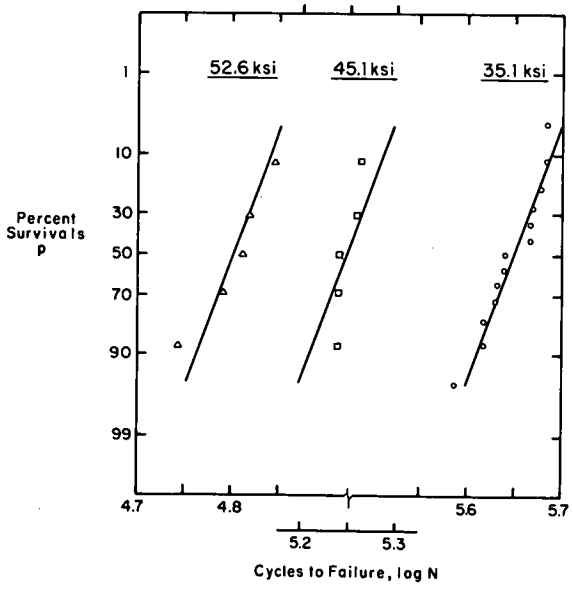

Fig. C-7 Cumulative Frequency Distributions of Fatigue Lives in Groups No. 1 and 33

Constancy of Variance. The usual equations for the estimation of parameters by the method of least squares are based on applying equal "weights" to all of the observations on the dependent variable, and that this "weight" is unity. This is true only if the variance of the residuals is constant for all levels of the dependent variable, as required by the third assumption. If the variance is not constant, each observation must be "weighted" inversely as its variance to obtain efficient estimates of the regression coefficients.

As before, the large number of tests in Groups No. 1 and 33, representing a single population, allowed the assumption of constancy of variance to be tested. Using the regression analysis of the finite-life data from these groups, the observed values of the dependent variable were adjusted by means of the slope of the regression line to the nearest of three common stress range levels, 52.9, 45.1, and 35.1 ksi. Test No. 4 from Group No. 1, with a stress range of 28.8 ksi, was excluded as requiring too large an adjustment.

Variance at the 52.9 ksi stress range level was found to be much higher than that at the other levels. This was caused by Test No. 88 from Group No. 33 which was found to have a much larger deviation from the mean than the other tests. Therefore, the r ratio test[18] for an outlier was applied to Test No. 88. The hypothesis that Test No. 88 represents the same population as the other tests was rejected at the 1 percent confidence level. Test No. 88 was therefore discarded from this analysis and the remaining tests were adjusted to a new mean stress range level of 52.6 ksi.

The cumulative frequency of the logarithm of observed fatigue lives was plotted, at each of the three stress range levels, as shown in Fig. C-7. As before, Blom's[56,57] suggestion on plotting positions was followed. The slope of the cumulative frequency distribution for the tests adjusted to a

stress range of 35.1 ksi was determined from their standard deviation and the line passed through their mean value. This slope was then used to draw corresponding lines through the mean values at the other stress range levels. On the basis of Fig. C-7, the hypothesis that the error variance is constant with stress range level for the data from Groups No. 1 and 33 cannot be rejected. It is believed that this hypothesis may be extended to all finite-life data.

Confirmation that the variance is constant with stress range level for Groups No. 1 and 33 was obtained by applying Bartlett's test[20,25] to the adjusted data. The variance at each stress range level is given in Table C-3. The test statistic was 4.32 which was compared with the chi square distribution for 2 degrees of freedom. Tabulated values[22] of the chi square distribution at the 80 and 90 percent levels are 3.22 and 4.61, respectively. Therefore the hypothesis of a constant variance cannot be rejected at a 5 percent confidence level.

The multiple linear regression on Phase I finite-life data is similarly based on the assumption of constancy of variance. A test was therefore appropriate. The main part of the Phase I test program was carried out at three nominal stress range levels. Within each group, the value of the logarithm of each observed fatigue life in the finite-life region was adjusted by means of the individual group regression line to the nearest of the three nominal stress range levels -- 36, 48, and 54 ksi -- common to all groups. This allowed an estimate of the variance for all Phase I groups to be calculated at each of the three levels. At the 36 ksi level, the mean value of the adjusted fatigue lives was used for each group, since three tests were carried out within each group at a nominal stress range of 36 ksi.

TABLE C-3 TEST FOR GROUP CONSTANCY OF VARIANCE

Adjusted Stress Range	Mean Adjusted Log N	Sum of Squared Deviations From Mean	Degrees of Freedom	Variance s^2
35.10	5.6491	0.01124	12	0.00094
45.10	5.2467	0.00054	4	0.00014
52.55	4.8020	0.00579	4	0.00145

TABLE C-4 TEST FOR OVER-ALL CONSTANCY OF VARIANCE

Adjusted Stress Range	Mean Adjusted Log N	Sum of Squared Deviations From Mean	Degrees of Freedom	Variance s^2	Standard Error s	$\frac{s^2_{max}}{s^2_{min}}$
36	5.5866	0.59135	30	0.01971	0.1404	
48	5.1018	0.92281	29	0.03182	0.1784	1.61
54	4.9338	0.75720	27	0.02804	0.1675	

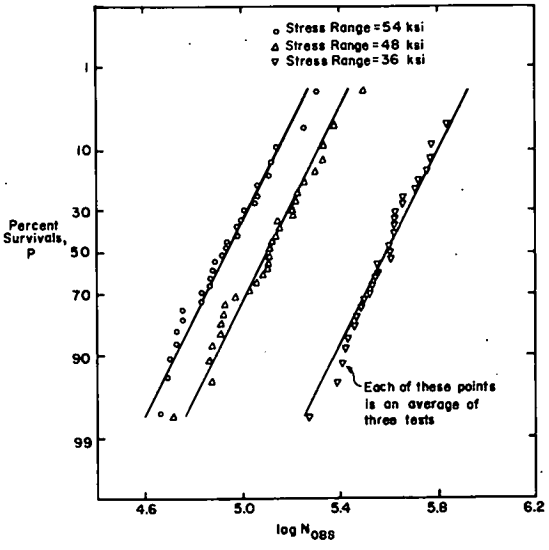

Fig. C-8 Cumulative Frequency Distributions of Fatigue Lives in Phase I Finite-Life Tests

Three groups did not have a representative value at the 54 ksi level, and one group lacked a value at the 48 ksi level.

The sums of the squared deviations about the mean value at each stress range level were calculated and are given in Table C-4.

Using Hartley's test[26,27] for constancy of variance, the test statistic of 1.61 was compared at the 5 percent significance level with the tabulated value[98, 99] of 2.40 for three estimates of variance, each having 30 degrees of freedom. The hypothesis that the variance of the logarithm of the observed fatigue lives is constant for all stress levels cannot be rejected.

The cumulative frequency distribution is plotted in Fig. C-8, using Blom's[56,57] suggestion for plotting positions. The mean value at each stress range level is the mean of the adjusted values of the logarithm of the observed fatigue lives for that level. The slope was, in each case, determined from the value of the pooled standard error.

Linearity of Regression

The finite-life test program in Phase II was designed to allow the assumption of a linear relationship between stress range and logarithm of the number of cycles to failure to be tested. Each of Groups No. 33, 35, 37, 39, and 41 was intended to have three tests at each of three nominal stress range levels -- 34, 44, and 54 ksi. Load levels for one test in each of Groups No. 33 and 41 were, however, inadvertently interchanged. As a result, Group No. 33 had four tests at a nominal stress range of 34 ksi and two tests at 44 ksi, while Group No. 41 had two tests at a nominal stress range of 34 ksi and four tests at 44 ksi. This did not affect the ensuing analysis.

Having several observations on the dependent variable, logarithm of the number of cycles to failure, for each value of the independent variable, stress range, allowed the sum of squared deviations about a regression line to be partitioned further than otherwise[20]. This partitioning included the usual variances due to and about the regression line in addition to the within set variance resulting from having sets of data at each stress range level. The regression was, in effect, performed on the mean values of the various sets of data. A test for linearity was then obtained by comparing the variance of the mean values about the regression line with the within set variance.

A regression analysis was performed on each of the finite-life Phase II groups of data. The logarithm of each observed number of cycles to failure was then adjusted by means of the slope of the regression line to correspond to similar values at the nearest nominal stress range level. A regression analysis was then performed on the adjusted values, taking into account the clustering of data at each of the three nominal stress range values. The analysis of variance obtained for each group from this regression is given in Table C-5.

The test for linearity consists of comparing the F-ratio, obtained by division of the mean square sum due to the set means about their line by the within set mean square sum, to the appropriate value of the F-distribution [20,28,29]. The observed F-ratios were 4.68, 8.15, 0.33, 0.08, and 3.59 for Groups No. 33 to 41, respectively, and were compared with the 95 percentile of the F-distribution, or $F(1,6;095) = 5.99$. The hypothesis that the mean values lie on a straight line cannot be rejected at the 5 percent confidence level for any but Group No. 35. The evidence does, however, point to linearity particularly in the case of Group No. 39. Consequently, a linear relationship

TABLE C-5 LINEARITY OF REGRESSION

Group	Source of Variance	Sum of Squares	Degrees of Freedom	Mean Squares $\frac{\text{Sum}}{s^2}$	F-Ratio
33	Slope of Line	1.362490	1	1.362490	701.95
	Set means about line	0.009086	1	0.009086	4.68
	Within sets	0.011646	6	0.001941	
	Total (corrected for mean)	1.383222	8		
35	Slope of Line	1.059260	1	1.059260	408.64
	Set means about line	0.021131	1	0.021131	8.15
	Within sets	0.015553	6	0.002592	
	Total (corrected for mean)	1.095944	8		
37	Slope of line	0.534132	1	0.534132	671.40
	Set means about line	0.000261	1	0.000261	0.33
	Within sets	0.004773	6	0.000796	
	Total (corrected for mean)	0.539166	8		
39	Slope of line	0.988875	1	0.988875	661.93
	Set means about line	0.000124	1	0.000124	0.08
	Within sets	0.008964	6	0.001494	
	Total (corrected for mean)	0.997963	8		
41	Slope of line	0.861595	1	0.861595	218.63
	Set means about line	0.014158	1	0.014158	3.59
	Within sets	0.023645	6	0.003941	
	Total (corrected for mean)	0.899398	8		

TABLE C-6 GROUP NUMBERS IN FACTORIAL DESIGNS

Factorials I & V			
D_{nom}, in. \ d_{nom}, in.	6	10	18
0.625	15	10	14
0.75	25	12	24
1.00	3	1	2
1.27	27	13	26
1.41	17	11	16

Factorials II & VI			
D_{nom}, in. \ f_{min}, ksi	-6	6	18
0.625	18	10	19
1.00	4	1	7
1.41	20	11	21

Factorials III & VII			
D_{nom}, in. \ G, ksi	40	60	75
0.625	28	10	29
1.00	22	1	23
1.41	30	11	31

Factorials IV & VIII			
d_{nom}, in. \ f_{min}, ksi	-6	6	18
6	6	3	9
10	4	1	7
18	5	2	8

between logarithm of the number of cycles to failure and stress range was assumed to hold true for all groups of data.

A second observed F-ratio for each group, obtained by dividing the mean square sum due to the slope of the regression by the within set mean square sum, allowed the hypothesis of a zero slope to be tested. The observed values were 701.95, 408.64, 671.40, 661.93, and 218.63 for Groups No. 33 to 41, respectively, and were again compared with an F-distribution value of 5.99. The evidence for a meaningful relationship between logarithm of the number of cycles to failure and stress range is overwhelming. These observed F-ratios may be compared with the partial F-ratio obtained in the first step of each of the multiple linear regressions to be described in later sections.

Factorial Designs

Phase I of this experiment was designed to allow classification of the finite-life data into four distinct patterns or factorials, according to the specified variables of stress range, minimum stress level, size of bar, grade of bar, and type of specimen. The pattern for each factorial design is shown in Table C-6. Each factorial was studied as a two-way design and as a three-way design. The two-way designs made use of the replication afforded by the three repeated tests at the nominal stress range of 36 ksi. The three-way designs had nominal stress range levels of 36, 48, and 54 ksi as the third factor.

For instance, Factorial I refers to a two-way design in bar diameter at five levels and effective depth at three levels. Factorial V refers to the three-way design for the same groups, using stress range at three levels as the third factor. Thus Factorials I through IV refer to two-way designs and Factorials V through VIII refer to three-way designs.

Data entered in the factorial designs consisted of adjusted finite-life test results from Phase I of the test program. To obtain these, a regression line was fitted to the test data from each group, using the logarithm of the observed fatigue lives as the dependent variable and stress range as the independent variable. Each test result was then adjusted to its appropriate nominal stress range level by projection along a line parallel to the regression line.

In determining the regression lines, all tests having a stress range less than 28 ksi were excluded, since these were considered to fall into the long-life region for each group. Excluded also were all reruns of runout tests, all tests resulting in a concrete fatigue failure, and all tests where some deviation from the usual test procedure had occurred.

The results of the analysis are given in Table C-7, where the difference in slopes and variance is, to a large extent, accounted for by the experimental and physical impossibility of exact, within group, control of variables. A similar analysis, but including tests where a deviation from the usual test procedure had occurred, except Test No. 77 in Group No. 5, resulted in the fitted lines shown in Fig. B-12.

The factorial designs were studied by analysis of variance. This analysis is sensitive to outlying values in the data. Consequently, as described previously, tests in which some deviation from the usual test procedure had occurred were excluded from the within group regression analysis. Close examination of the residuals from the two-way factorials failed to reveal any significant outliers.

Except for stress range, which was adjusted to the desired levels, the factorial designs were based on nominal variations of the specified test

TABLE C-7 REGRESSION ANALYSIS OF PHASE I FINITE-LIFE DATA

Group No.	Predicted Value of Log N at f_r = 36 ksi	Slope	Variance, s^2	Group No.	Predicted Value of Log N at f_r = 36 ksi	Slope	Variance, s^2
1	5.6234	-0.0475	0.001893	16	5.6019	-0.0371	0.000990
2	5.6241	-0.0488	0.004182	17	5.5319	-0.0402	0.004690
3	5.6054	-0.0423	0.000521	18	5.8596	-0.0322	0.004861
4	5.9125	-0.0567	0.025756	19	5.4856	-0.0337	0.005201
5	5.7209	-0.0354	0.004925	20	5.7727	-0.0416	0.010510
6	5.6452	-0.0386	0.001161	21	5.4037	-0.0385	0.000642
7	5.6015	-0.0401	0.013629	22	5.4674	-0.0502	0.008525
8	5.4133	-0.0323	0.014151	23	5.6070	-0.0315	0.002707
9	5.4605	-0.0489	0.000590	24	5.5435	-0.0137	0.000843
10	5.6257	-0.0344	0.004318	25	5.7493	-0.0456	0.017739
11	5.4880	-0.0378	0.000062	26	5.5372	-0.0406	0.007198
12	5.7730	-0.0410	0.015848	27	5.3963	-0.0398	0.000090
13	5.4200	-0.0402	0.000187	28	5.5463	-0.0530	0.000776
14	5.5958	-0.0262	0.025843	29	5.6490	-0.0311	0.006979
15	5.6931	-0.0353	0.021302	30	5.2682	-0.0465	0.000445
				31	5.6005	-0.0423	0.002178

TABLE C-8 VARIANCE OF REPLICATES AT 36 KSI STRESS RANGE

Group No.	Variance s^2	Member of Factorial Design I	II	III	IV	Group No.	Variance s^2	Member of Factorial Design I	II	III	IV
1	0.000447	x	x	x	x	16	0.001442	x			
2	0.002376	x			x	17	0.003940	x			
3	0.000701	x			x	18	0.006945		x		
4	0.038529		x		x	19	0.007797		x		
5	0.007775				x	20	0.015352		x		
6	0.000099				x	21	0.000104		x		
7	0.003855		x		x	22	0.002746			x	
8	0.006289				x	23	0.003642			x	
9	0.000746				x	24	0.001237	x			
10	0.006405	x	x	x		25	0.017682	x			
11	0.000062	x	x	x		26	0.006864	x			
12	0.022761	x				27	0.000130	x			
13	0.000142	x				28	0.000776			x	
14	0.048086	x				29	0.008853			x	
15	0.021008	x				30	0.000445			x	
						31	0.002176			x	

Factorial Design	$\frac{s^2_{max}}{s^2_{min}}$	Number of Estimates	Degrees of Freedom DF	Hartley's 0.05 Value
I	776	15	2	> 704
II	621	9	2	475
III	143	9	2	475
IV	389	9	2	475

variables. Actually, all variables differed slightly from the nominal values. The effects of errors in the factor levels have been studied by Box[101], who concluded that the usual analysis of variance remains robust when intended levels are used in place of those actually run.

In some instances, the exclusion of all rerun and deviant data from the within group regression resulted either in missing data points at high stress range values, or within group variances at the 36 ksi stress range level that were based on two rather than three replications. In each case, a predicted or an adjusted value was used[99], based on the within group regression.

The variance of the within group replications, adjusted to the 36 ksi stress range level, allowed a test to be made to determine whether the data used for each of Factorials I through IV came from one population. These variances are given in Table C-8 and are seen to differ greatly. By means of Hartley's test[27, 99], the hypothesis that the data in Factorials I, III, and IV each have constant variance cannot be rejected while the same hypothesis must be rejected for Factorial design II at the 5 percent level. This results from the large variation within Group No. 4, and is largely due to a variation in minimum stress between the three "replicates". Since the main purpose of the analysis of the factorial designs was to establish the variables to be used in the multiple linear regression analysis, it was felt that some leeway was acceptable in the use of significance tests.

The analysis of variance for the two-way designs proceeded in the standard manner for a linear model I[20]. In addition, it used a technique of partitioning the interaction term that allowed an

estimate of the underlying functional form to be calculated [60]. The model was

$$Z_{ij} = A_i + C_j + (B_i - 1)\, C_j$$

where A_i represents the ordinary row effect, and C_j is a measure of the ordinary column effect in that it differs only by the inclusion of the grand mean. The terms A_i and B_i are, respectively, the intercept and slope that are obtained by linear regression across the i'th row. They represent a collection of straight lines across the rows that may be either parallel or concurrent. Each of the terms A_i, B_i, and C_j was fitted by a straight line or a polynomial.

Analysis of variance tables for the two-way designs are presented in Table C-9. In each case, the remaining interaction term was pooled with the within groups term. The B_i term was not significant in Factorials II and IV, while the single C_j term was not significant in Factorial I.

The lines in Factorials I and III were tested for concurrence by means of the correlation coefficient between the A_i and B_i, and by partitioning of the $(B_i - 1)\, C_j$ term given in Table C-10. In either case, the hypothesis of concurrence could not be rejected.

The B_i values in Factorial I were found to fluctuate considerably about their mean and a third degree polynomial was indicated for the bar diameter, D_{nom}. To verify this, a stepwise multiple regression was performed, as indicated in Table C-11, with the result that a straight line relationship in bar diameter explained 80 percent of the variation in B_i while a cubic equation explained 98 percent of the variation.

TABLE C-9 ANALYSIS OF VARIANCE OF FACTORIAL DESIGNS

Two-Way Designs								
Factorial Design	I		II		III		IV	
Source	Degrees of Freedom DF	Mean Square MS	DF	MS	DF	MS	DF	MS
Rows (A_i)	4	0.07810	2	0.06010	2	0.05781	2	0.05772
Columns (C_j)	2	0.00166	2	0.29404	2	0.09364	2	0.14959
$(B_i-1)C_j$	4	0.03031	2	0.00074	2	0.02078	2	0.00884
Remainder	4	0.01095	2	0.00775	2	0.00263	2	0.02466
Within Groups	30	0.00718	18	0.00912	18	0.00312	18	0.00704
Total	44		26		26		26	

Three-Way Designs								
Factorial Design	V		VI		VII		VIII	
Source	Degrees of Freedom DF	Mean Square MS	DF	MS	DF	MS	DF	MS
Rows (A)	4	0.14093	2	0.05488	2	0.08297	2	0.01912
Columns (B)	2	0.01911	2	0.21459	2	0.24956	2	0.13807
Stress Range (C)	2	1.76565	2	1.19413	2	1.22330	2	1.41871
AB	8	0.00522	4	0.01295	4	0.00600	4	0.01405
AC	8	0.01209	4	0.01513	4	0.00440	4	0.00569
BC	4	0.00882	4	0.00658	4	0.01055	4	0.01446
ABC	16	0.00656	8	0.00557	8	0.00441	8	0.01055
Total	44		26		26		26	

TABLE C-10 TEST FOR CONCURRENCE

Factorial Design	Source of Variance	Sum of Squares	Degrees of Freedom DF	Mean Square s^2	F-Ratio
I	Concurrence	0.11353	1	0.11353	
	Nonconcurrence	0.00772	3	0.00257	44.14
	$(B_i - 1)C_j$	0.12125	4	0.03031	
III	Concurrence	0.04146	1	0.04146	
	Nonconcurrence	0.00010	1	0.00010	400.34
	$(B_i - 1)C_j$	0.04156	2	0.02078	

TABLE C-11 MULTIPLE LINEAR REGRESSION IN FACTORIAL DESIGN I

Stepwise Result		Variable Entered		
		D_{nom}	D^3_{nom}	D^2_{nom}
Residual Standard Deviation, s		3.4764	4.1099	1.9744
Multiple R^2		0.8008	0.8144	0.9785
Regression F-Ratio		12.06	4.39	15.23
Degrees of Freedom, DF		3-1	2-2	1-3
Partial F-Ratio	D_{nom}	12.06	0.84	6.90
	D^2_{nom}		0.15	7.68
	D^3_{nom}			7.93

The functional forms that resulted from Factorials I through IV are shown in Table C-12, along with some measures of the success of the fitting process. In each case, the significance of the parameters suffers somewhat from lack of degrees of freedom. However, a high degree of correlation was obtained, as shown by the r^2 values.

Table C-12 also contains the standard deviation, s, obtained for each factorial as a whole. The pooled standard deviation is 0.0948, and represents a measure of the minimum value to be expected from the multiple linear regression analysis using these same variables.

The analysis of variance for the three-way designs also presumed a linear model I[20], where it was assumed that each data value entered in the scheme was from a separate population, normally distributed about its population mean, and with the same variance. The main effects -- A, B, C -- and the interactions -- AB, AC, BC -- were tested against the overall interaction ABC, since there were no replications available at the higher stress range levels. Table C-9 shows the analysis of variance tables.

In testing the hypothesis that a particular effect is zero, the hypotheses for stress range, minimum stress, bar diameter, and grade of bar are all rejected at a 95 percent level. The hypothesis for effective depth is rejected at a 90 percent level in Factorial V, but cannot be rejected in Factorial VIII. The hypothesis cannot be rejected at a 95 percent level for all of the interactions.

Multiple Linear Regression

The purpose of a multiple regression analysis is to establish a model for a particular response, in the present case the logarithm of the observed fatigue lives, in terms of a set of independent variables. Use of

TABLE C-12 RESULTS OF ANALYSIS OF FACTORIAL DESIGNS

Factorial Design	Term	Regression Parameters	Measures of Regresion			
			r^2	s	F-Ratio	DF
I	A_i	$5.571 + 0.0129B_i$	0.8755	0.0380	21.1	1-3
	B_i	$-167.7 + 594.9D_{nom} - 639.0D^2_{nom} + 212.6D^3_{nom}$	0.9785	1.9744	15.2	3-1
	C_j	$0.0192 - 0.0017d_{nom}$	0.9727	0.0025	35.6	1-1
II	A_i	5.642		0.0817		
	B_i	0				
	C_j	$0.0857 - 0.0143S_{min}$	0.8996	0.0548	9.0	1-1
III	A_i	$5.680 - 0.1387B_i$	0.9975	0.0057	400.0	1-1
	B_i	$-0.4353 + 1.419D_{nom}$	0.9326	0.2118	13.8	1-1
	C_j	$-0.3306 + 0.0057G$	0.9522	0.0315	19.9	1-1
IV	A_i	5.626		0.0801		
	B_i	0				
	C_j	$0.0642 - 0.0107S_{min}$	0.9909	0.0174	108.9	1-1

Factorial Design	Total Sum of Squared Residuals	Degrees of Freedom DF	Residual Standard Deviation s
I	0.26633	37	0.0848
II	0.28948	24	0.1098
III	0.07742	21	0.0607
IV	0.31990	24	0.1155
	0.95313	106	0.0948

a linear regression presupposes either a linearly additive or a linearly multiplicative model, if the independent variables have been transformed logarithmically. Here, only a linearly additive model was considered.

Several procedures have been proposed for selecting the best regression equation[28]. However, it should be noted that no unique statistical procedure exists for selecting the best regression equation. The stepwise multiple linear regression procedure[61] has been recommended[28] for its versatility. This procedure allows use of the Phase I finite-life data as a single whole in an analysis where candidate variables may be systematically admitted to or expelled from the regression.

Briefly, the procedure requires that a set of possible variables be provided along with a criterion for entry to or exit from the regression. A correlation matrix between the variables is computed. The first variable selected for entry in a regression is that most highly correlated with the dependent variable. Then, the correlation matrix is corrected for the variable entered, and a remaining variable whose partial correlation with the dependent variable is not significant is selected as the next candidate for entry. The significance of the candidate is measured by its partial F-value and compared with an entrance criterion, no entry being possible if the partial F-value is too low. Similarly, all variables currently entered are examined for their partial F-values relative to an exit criterion, the variable being removed if its partial F-value is found to be too low.

This procedure is repeated until either all variables have been exhausted or there are no further candidates qualified for entry.

TABLE C-13 MULTIPLE LINEAR REGRESSION OVER PHASE I VARIABLES

Stepwise Results		Variable Entered					
		f_r	f_{min}	D_{nom}	G	D^3_{nom}	D^2_{nom}
Residual Standard Deviation, s		0.1657	0.1415	0.1261	0.1113	0.1114	0.1064
Multiple R^2		0.7681	0.8319	0.8673	0.8973	0.8977	0.9073
Regression F-Ratio		543.4	403.5	353.1	351.9	281.0	259.6
Degrees of Freedom, DF		1-164	2-163	3-162	4-161	5-160	6-159
Partial F-Ratio	f_r	543.4	736.2	955.2	1238.5	1235.9	1364.6
	f_{min}		61.9	75.3	97.2	96.6	106.6
	G				47.1	47.2	51.6
	D_{nom}			43.2	55.7	6.0	15.2
	D^2_{nom}						16.5
	D^3_{nom}					0.6	16.9
Regression Coefficient	Constant	6.9690	7.0405	7.3016	6.8392	6.9018	4.4190
	f_r	-0.0383	-0.0381	-0.0388	-0.0390	-0.0390	-0.0392
	f_{min}		-0.0132	-0.0130	-0.0130	-0.0130	-0.0130
	G				0.0079	0.0079	0.0079
	D_{nom}			-0.2313	-0.2316	-0.3334	7.8059
	D^2_{nom}						-8.4155
	D^3_{nom}					0.0313	2.7990
Standard Error of Estimate of Regression Coefficient	Mean	0.0128	0.0109	0.0097	0.0086	0.0086	0.0082
	f_r	0.0016	0.0014	0.0013	0.0011	0.0011	0.0011
	f_{min}		0.0017	0.0015	0.0013	0.0013	0.0013
	G				0.0012	0.0012	0.0011
	D_{nom}			0.0352	0.0310	0.1334	2.0054
	D^2_{nom}						2.0691
	D^3_{nom}					0.0408	0.6816

The partial F-value for retaining a variable is based on the current remaining degrees of freedom and a preselected confidence level. This, however, bears little relation to the computational criterion used, since the final partial F-value of a candidate depends in many cases on a highly correlated variable yet to be considered for entry.

The specified test variables from Phase I of the research program, in the functional form determined by the analysis of the factorial designs, were entered as possible variables in the multiple linear regression. All Phase I tests having a stress range greater than 28 ksi were initially included, except for rerun tests and concrete fatigue failures. As previously noted, Test No. 77 was later rejected as an outlier. There was then a total of 166 tests entered in the regression.

It has been suggested[102] that the observed F-value (regression mean square/residual mean square) of a satisfactory predictor should be about four times the selected percentile point of the F-distribution. Since work on this topic is not complete, it is unclear how such a factor would relate to partial F-values. In this analysis, the observed F-value was compared to 2.00 for inclusion in the regression and 5.00 for inclusion in a prediction equation.

The results of the stepwise multiple linear regression over the specified Phase I variables are given in Table C-13. No term containing effective depth, d, was found to be significant. In addition to the bar diameter-effective depth interaction terms obtained from Factorial Design I, the $f_r D_{nom}$, $f_r f_{min}$, $f_r G$, $D_{nom} f_{min}$, and $D_{nom} G$ interaction terms were tested and rejected.

Success of the regression may be measured in several ways. Each time a new variable is entered, the residual standard deviation should decrease. The square of the multiple correlation coefficient, R^2, measures the variation explained by the regression. It would be equal to one if the fitted equation explained all of the variation in the data. The partial F-test criterion should keep increasing for uncorrelated variables as each new variable enters. This implies that the regression coefficients are known with greater precision. When a new variable is added, the regression F-ratio may decrease, but in such a manner that its proportion to the appropriate point in the F-distribution, as based on the number of degrees of freedom, should increase.

It may be noted that no improvement occurred when D^3_{nom} entered the regression. This was due to the high degree of correlation between D_{nom}, D^2_{nom}, and D^3_{nom}. Thus, the regression must either contain only D_{nom} or all of the terms D_{nom}, D^2_{nom}, and D^3_{nom}. A significant improvement in fit occurred both when the cubic equation was used in Factorial I and when it was used in the multiple regression.

Effect of Bar Geometry

Phase II of the test program was designed to allow the effect of bar geometry on fatigue life to be determined. As used here, bar geometry refers to the cross-sectional dimensions of the transverse lugs, determined by sectioning the bar along a plane that includes the axis of the bar. A full description of how the bar geometry was determined is given in Appendix B.

The Phase II test program was divided into two parts. First, the mean fatigue strength at 5,000,000 cycles was determined for each of the five manufacturer's bars by a staircase test series[17]. Second, the finite-life fatigue properties of each manufacturer's bars were determined by conducting three tests at each of three nominal stress range levels.

Long-life Region. Each staircase test series was intended to consist of 12 tests. In the staircase test procedure, an estimate is initially made of the mean value of the effect being tested and its standard deviation. Thus, tests conducted at a stress range higher than the mean fatigue limit would tend to result in fatigue fractures while tests carried out at lower stress ranges would tend to result in runouts at 5 million cycles.

A staircase series is considered to have been initiated when two consecutive tests conducted at two different stress ranges result in opposite effects, i.e. failure and runout or vice versa. Stress range in the succeeding tests is based on the result from each immediately preceeding test. Thus, if a test resulted in a runout at 5 million cycles, the stress range for the next test in the series was increased by a preselected step size. On the other hand, if the test resulted in fracture of the test bar, the stress range for the next test was decreased. The step size was nominally the same for all tests in a given series and was based on the estimated standard deviation.

Initial estimates of the mean fatigue limit at 5 million cycles for the five manufacturer's bars, represented by Groups No. 32, 34, 36, 38, and 40, were 25, 25, 30, 35, and 40 ksi, respectively.

The standard deviation was estimated to be 1 ksi for each of the manufacturer's bars. This value was taken as the nominal step size for each series.

The initial estimates proved to be too high for Groups No. 36, 38, and 40. Consequently, six tests were required before these staircase series had been initiated. Further tests were required when the intended applied load magnitudes for Tests No. 61 and 62 from Groups No. 38 and 36, respectively, were inadvertently interchanged. For this reason, two additional tests were carried out in Group No. 36 and one in Group No. 38. The total number of tests carried out in Groups No. 32, 34, 36, 38, and 40 was therefore 12, 12, 16, 15, and 14, respectively. Each staircase series is plotted in Fig. C-9.

Classical staircase test analysis is based on a paper by Dixon and Mood[62]. They derived an equation for predicting the mean value of a staircase series based on an even step size equal to the standard deviation. Later papers by Dixon[103] and Little[104] provide tables of the predicted mean value for a number of specific test series having a fixed step size and given standard deviation. These tables are based on the calculation of the most probable mean value, assuming a particular distribution function, generally the cumulative normal distribution.

Step sizes obtained for the staircase test series in Phase II of the test program proved to be variable and ranged from about 0.5 ksi to about 1.5 ksi. This resulted from the physical impossibility of obtaining precise control of all test beam variables. Available analytical methods were therefore only approximate. For this reason, the recent methods of Dixon[103] and Little[104] were adapted to the

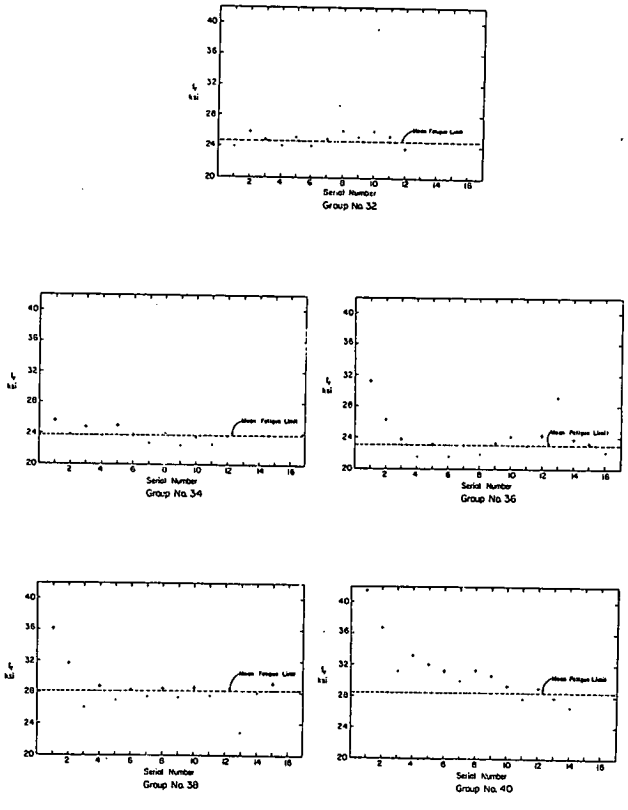

Fig. C-9 Staircase Test Series

development of a computational procedure where a variable step size could be taken into account. A further consideration was that such a procedure would allow not only the mean value of a series but also its standard deviation to be estimated. This would allow tolerance limits to be calculated for each series.

The response distribution for each staircase series was assumed to be the cumulative normal distribution. Initial estimates were made of the mean and standard deviation of the distribution for each test series. The probability of occurrence of each test within a group was then computed on the basis of the estimates made for that group. This was done by first determining the difference between the observed stress range for each test and the estimated mean value, in terms of a multiple of the estimated standard deviation. Then the probability of occurrence could be obtained from tabulated values of the cumulative normal distribution[18,20,29]. A plot of the distribution is shown in Fig. C-10.

If the test resulted in fracture of the test bar, then the probability of occurrence of the result was the tabulated value, p. If, on the other hand, the test resulted in a runout, then the probability of occurrence was (1 - p). The probability of occurrence of an entire test series was computed as the product of probabilities for the individual tests.

In the general computational procedure, test series probabilities were calculated for the estimated mean and standard deviation, and at evenly spaced values on each side of the central estimates. A parabola was then passed through 3 consecutive values obtained by using a constant standard deviation and varying the mean, or vice versa. The maximum points on the parabolas obtained for a series of mean values and a series of standard deviation values were then used as new estimates of the distribution parameters.

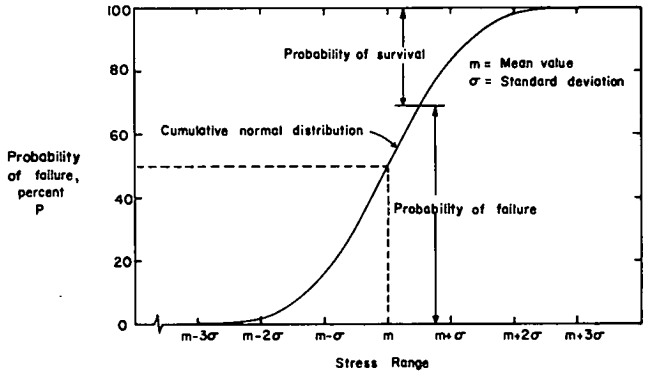

Fig. C-10 Assumed Response Distribution for Staircase Test Series

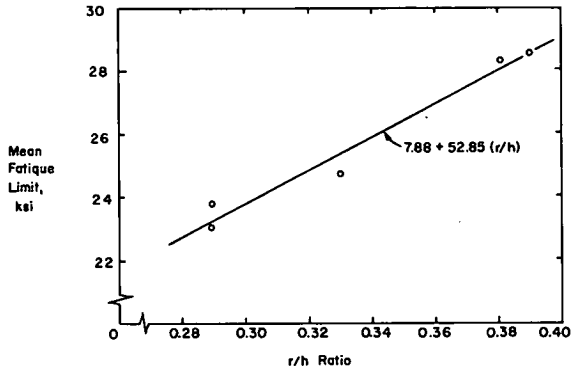

Fig. C-11 Effect of Bar Geometry on Fatigue Limit

Fatigue limits, as determined by the staircase analyses, are plotted in Fig. C-11 against the ratio of lug base radius to lug height, as given in Table B-11. A regression line was fitted to the data, using fatigue limit, f_f, as the dependent variable and lug base radius to lug height ratio, r/h, as the independent variable. This resulted in the following relationship:

$$f_f = 7.88 + 52.85(r/h)$$

for which an F-ratio of 86.06, a standard error of 0.544, and a correlation coefficient of 0.983 were determined. Therefore, the regression is significant. It must, however, be cautioned that the range of observed r/h ratios is very narrow and that the effects of other potential influencing factors have not been included.

Finite-Life Region. Previous analysis of the Phase II finite-life region fatigue data has shown that a linear relationship between stress range and logarithm of fatigue life provides a reasonable estimate of the fatigue response for each group. The insertion in the analysis of a second variable, bar geometry, allows the Phase II finite-life data to be studied as a whole.

The formulation of a stress range-bar geometry-fatigue life relationship can have the bar geometry variable as either an additive of a multiplicative variable. If the variable is additive, then the different groups of tests are represented by a series of parallel lines on an S-N diagram. A multiplicative variable, on the other hand, results in a series of concurrent lines. The regression lines drawn in Fig. B-12 for the finite-life Phase II groups of tests indicate that bar geometry may be an additive variable.

The procedure was repeated until convergence was obtained. A computer program* based on the above procedure was written in the FORTRAN language for an IBM 1130 computer.

All of the tests carried out in each of Groups No. 32, 34, 36, 38, and 40 were included in the computation of the most probable mean value and standard deviation for each group. This included Test No. 33 in Group No. 38, a test inadvertently terminated after the test bar had survived 4.5 million cycles at a stress range of 27.45 ksi. The test was counted as a runout, a decision that appears justified on the basis of the trend shown in Fig. C-9.

In Group No. 38 the lowest stress range at which a bar fracture occurred was greater than the highest stress range for a runout. For this reason, a unique determination of the standard deviation was impossible. Based on results obtained from the other staircase series, an assumed value of 0.5 ksi was used for the standard deviation in computing a mean value for Group No. 38.

Results of the staircase analyses are given in Table C-14. It should be noted that a staircase test series results inherently in an efficient estimate of the mean value of the response being tested. Estimates of the standard deviation are, however, only approximate.

TABLE C-14 MEAN FATIGUE LIMIT

Group Number	Number of Tests	Mean Value, ksi	Standard Deviation, ksi	Probability of Occurrence, percent
32	12	24.65	1.026	0.16
34	12	23.78	0.510	1.19
36	16	23.00	0.379	2.97
38	15	28.22	0.500[a]	8.62
40	14	28.52	2.939	0.16

[a]Assumed

*Descriptions of the major computer programs used in the statistical analysis can be obtained from the Program Director, NCHRP.

The hypothesis that all finite-life groups in Phase II of the test program have parallel regression lines may be tested in an analysis of covariance[20,21]. Such an analysis was performed in the manner described in the section entitled "Preliminary Considerations." The results of this analysis are given in Table C-15.

Hartley's test[27,98,99] was used to check for constancy of variance among the different groups of data. The test statistic was found to be 7.51 and was compared at a 5-percent significance level with Hartley's statistic of 9.50 for 5 groups of data, each having 7 degrees of freedom. The hypothesis of a common variance cannot be rejected.

The test for parallelism of the regression lines is based on the ratio of the mean sum of squares between the individual slopes to the mean sum of squares about the individual lines. This observed F-ratio is compared with the appropriate point of the F-distribution[20,28,29]. The test statistic was found to be 6.85 and was compared with $F(4,35;095) = 2.65$, the 95 percentile point of the F-distribution. The hypothesis that the regression lines are parallel must be rejected.

Removing Group No. 37 from the analysis of covariance led to the results given in Table C-16. Hartley's statistic is 8.44 for 4 groups, each having 7 degrees of freedom and was compared with a test statistic of 4.16. The hypothesis that all groups have a common variance cannot be rejected.

In the test for parallelism, the observed F-ratio of 0.45 was compared with $F(3,28;095) = 2.95$. The hypothesis that all four groups have a common slope cannot be rejected.

TABLE C-15 TEST FOR PARALLELISM AMONG PHASE II GROUPS

Individual Results

Group Number	Number of Data Points	Mean Value f_r	Mean Value Log N	Slope	Mean Square Sum of Errors, s^2	$\frac{s^2_{max}}{s^2_{min}}$
33	9	42.87	5.2896	-0.04441	0.002962	7.51
35	9	45.33	5.1215	-0.04201	0.005241	
37	9	46.05	5.2138	-0.02982	0.000719	
39	9	46.17	5.2987	-0.04062	0.001298	
41	9	46.65	5.2384	-0.04211	0.005402	

Pooled Results

Grand Mean Value f_r	Grand Mean Value Log N	Slope of Parallel Lines	Slope of Line for Mean Values	Slope of Overall Line
45.41	5.2324	-0.03975	-0.01006	-0.03901

ANOCOVA

Source of Variance	Sum of Squares	Degrees of Freedom	Mean Square Sums, s^2	F-Ratio
Between parallel and group mean slopes	0.069639	1	0.069639	22.29
Group means about their line	0.175078	3	0.058359	18.68
Between individual slopes	0.085626	4	0.021407	6.85
About the individual lines	0.109353	35	0.003124	
Due to the overall line	4.937097	1	4.937097	482.82
About the overall line	0.439696	43	0.010225	
Total (corrected for mean)	5.376793	44		

TABLE C-16 PARALLEL FINITE-LIFE GROUPS IN PHASE II

Individual Results

Group Number	Number of Data Points	Mean Value f_r	Mean Value Log N	Slope	Mean Square Sum of Errors, s^2	$\frac{s^2_{max}}{s^2_{min}}$
33	9	42.87	5.2896	-0.0441	0.002962	4.16
35	9	45.33	5.1215	-0.04201	0.005241	
39	9	46.17	5.2987	-0.04062	0.001298	
41	9	46.65	5.2384	-0.04211	0.005402	

Pooled Results

Grand Mean Value f_r	Grand Mean Value Log N	Slope of Parallel Lines	Slope of Line for Mean Values	Slope of Overall Line
45.26	5.2371	-0.04232	-0.00891	-0.04133

ANOCOVA

Source of Variance	Sum of Squares	Degrees of Freedom DF	Mean Square Sums, s^2	F-Ratio
Between parallel and group mean slopes	0.082767	1	0.082767	22.22
Group means about their line	0.173300	2	0.086650	23.25
Between individual slopes	0.005040	3	0.016800	0.45
About the individual lines	0.104319	28	0.003726	
Due to the overall line	4.424707	1	4.424707	411.68
About the overall line	0.365426	34	0.010748	
Total (corrected for mean)	4.790133	35		

In further testing to determine whether the regression lines are indeed separate, the observed F-ratios of 23.25 and 22.22 were compared with $F(2,28;095) = 3.34$ and $F(1,28;095) = 4.20$, respectively. The hypothesis that the four groups of data have distinct but parallel regression lines cannot be rejected.

The above result confirms that bar geometry is a significant variable and should be taken into account by adding a term to the overall regression equation.

No explanation is available as to why Group No. 37 should have a slope different from the other Phase II groups. Test results obtained in Group No. 36 for the same manufacturer's bars are shown in Fig. B-12. They indicate that, at stress ranges immediately above the fatigue limit, the response may be parallel to that of the other groups.

Overall Analysis

Test data from the finite-life groups in Phase II of the test program were pooled with the finite-life data from Phase I and analyzed as a single whole. The method of analysis was the stepwise multiple linear regression procedure described earlier in this appendix.

Two approaches were taken to this analysis. In the first, only the specified variables of Phase I and the bar geometry were considered as variables. The aim of this analysis was to develop a regression equation describing the response of a test bar to cyclic loading in terms of variables that might be used in a design equation. In the second approach, any variable that might affect the fatigue strength of a reinforcing bar was tested. Furthermore, actual rather than nominal parameter values were used in the second approach. The aim of this latter analysis was to uncover the underlying variables affecting the fatigue strength of reinforcing bars.

Results of the stepwise multiple linear regression on the specified variables are given in Table C-17. Comparison of these results with those presented in Table C-13 reveals improvement in explaining the variation in the data. The residual standard deviation has decreased from 0.1064 to 0.1039, and the percentage of variation explained has risen from 90.7 to 91.6.

Stress range emerges even more strongly as the dominant variable governing fatigue life. Minimum stress level and grade of bar also exhibit a strengthened influence. The effect of bar diameter is stronger than previously, if only the linear term is considered. However, the total effect of bar diameter is weakened by inclusion of the bar diameter squared and cubed terms in the regression. These variables are, nonetheless, shown to be meaningful in explaining the variation in the data.

The effect of bar geometry on fatigue life is seen to be substantial, when a range of lug base radius to lug height ratio values from 0.1 to 1.0 is considered. In fact, the magnitude of the effect is second only to that of stress range. However, while the effect of bar geometry is significant both in magnitude and in the statistical sense, its regression coefficient is known with the least precision of those for variables admitted in the multiple linear regression. This may be partly due to the difficulty of accurate determination of the r/h ratio and partly to the narrow range of values of the ratio for the bars tested. It should further be noted that, while the r/h ratio is the most important bar geometry variable affecting the stress concentration factor in a reinforcing bar, it does not provide a full measure of the stress concentration effect.

TABLE C-17 MULTIPLE LINEAR REGRESSION OVER SPECIFIED VARIABLES

Stepwise Results		Variable Entered						
		f_r	f_{min}	D_{nom}	G	r/h	D^3_{nom}	D^2_{nom}
Residual Standard Deviation, s		0.1545	0.1344	0.1217	0.1098	0.1080	0.1064	0.1036
Multiple R^2		0.8081	0.8555	0.8820	0.9045	0.9080	0.9111	0.9161
Regression F-Ratio		880.3	616.1	516.1	488.1	404.7	348.8	316.9
Degrees of Freedom, DF		1-209	2-208	3-207	4-206	5-205	6-204	7-203
Partial F-Ratio	f_r	880.3	1154.4	1438.2	1783.7	1844.4	1889.6	1996.2
	f_{min}		68.3	80.6	99.5	103.0	105.3	111.7
	D_{nom}			46.5	57.3	50.6	17.9	10.1
	D^2_{nom}							12.0
	D^3_{nom}						7.3	13.2
	G				48.5	47.8	49.2	52.3
	r/h					7.7	14.7	8.8
Regression Coefficient	Constant	6.9735	7.0472	7.3008	6.8367	6.7418	6.8963	4.7663
	f_r	-0.0384	-0.0383	-0.0388	-0.0390	-0.0393	-0.0392	-0.0392
	f_{min}		-0.0131	-0.0129	-0.0130	-0.0130	-0.0129	-0.0130
	D_{nom}			-0.2313	-0.2315	-0.2173	-0.5739	6.4585
	D^2_{nom}							-7.2143
	D^3_{nom}						0.1124	2.4666
	G				0.0079	0.0077	0.0077	0.0077
	r/h					0.3657	0.5959	0.4639
Standard Error of Estimate of Regression Coefficient	Mean	0.0106	0.0092	0.0083	0.0075	0.0074	0.0073	0.0071
	f_r	0.0013	0.0011	0.0010	0.0009	0.0009	0.0009	0.0009
	f_{min}		0.0016	0.0014	0.0013	0.0013	0.0013	0.0012
	D_{nom}			0.0339	0.0306	0.0305	0.1356	2.0320
	D^2_{nom}							2.0802
	D^3_{nom}						0.0417	0.6800
	G				0.0011	0.0011	0.0011	0.0011
	r/h					0.1317	0.1553	0.1560

The second approach to explaining variation in the test data required that an estimate be made of the functional form of each new variable considered. Suggestions made by Anscombe and Tukey[105] were followed, where applicable. Otherwise, this selection was based on the simplest form of the variable, consistent with reinforced concrete and fatigue design theory.

Potential variables for the second multiple linear regression analysis were drawn from four different categories. The first category was concerned with the effects of loading and consequently the calculated stress levels. Second, various dimensional properties of the test beam and the test bar were entered in the analysis. Third, the material properties of both steel and concrete were considered. Finally, miscellaneous features of the test beams or test setups were studied in order to determine their effects, if any, on the fatigue lives of the test bars.

Final results of the second multiple linear regression analysis are presented in Table C-18. Only those variables having an observed partial F-ratio greater than 5.0 were retained. Comparison with the results given in Table C-17 shows that an improvement in explaining the variation in the test data has been obtained, in spite of fewer variables being used. The residual standard deviation decreased from 0.1036 to 0.0975 while the percentage of variation explained rose from 91.6 to 92.5 percent.

Stress range was again found to be the predominant variable affecting fatigue life in the finite-life region. Minimum stress level

TABLE C-18 MULTIPLE LINEAR REGRESSION OVER EFFICIENT VARIABLES

Stepwise Results		Variable Entered					
		f_r	f_{min}	f_u	D^2_{nom}	Y60	Dr/h
Residual Standard Deviation, s		0.1544	0.1344	0.1156	0.1023	0.0995	0.0975
Multiple R^2		0.8081	0.8555	0.8937	0.9171	0.9219	0.9253
Regression F-Ratio		880.3	616.1	580.3	570.2	484.2	421.6
Degrees of Freedom, DF		1-209	2-208	3-207	4-206	5-205	6-204
Partial F-Ratio	f_r	880.3	1154.4	1603.8	2092.3	2099.3	2191.9
	f_{min}		68.3	93.4	115.9	132.7	138.2
	f_u			74.3	89.1	94.9	100.1
	D^2_{nom}				58.3	66.5	73.2
	Y60					12.5	12.5
	Dr/h						9.4
Regression Coefficient	Constant	6.9735	7.0472	6.3066	6.4658	6.5086	6.4548
	f_r	-0.0384	-0.0383	-0.0389	-0.0395	-0.0404	-0.0407
	f_{min}		-0.0131	-0.0132	-0.0130	-0.0138	-0.0138
	f_u			0.0073	0.0070	0.0071	0.0071
	D^2_{nom}				-0.1059	-0.1107	-0.1397
	Y60					0.0027	0.0026
	Dr/h						0.3233
Standard Error of Estimate of Regression Coefficient	Mean	0.0106	0.0092	0.0079	0.0070	0.0068	0.0067
	f_r	0.0013	0.0013	0.0010	0.0009	0.0009	0.0009
	f_{min}		0.0016	0.0014	0.0012	0.0012	0.0012
	f_u			0.0008	0.0007	0.0007	0.0007
	D^2_{nom}				0.0139	0.0136	0.0163
	Y60					0.0008	0.0007
	Dr/h						0.1055

remained as the second most significant variable. The two fatigue influencing factors whose effects are known with the greatest precision are thus seen to be related to the applied loading.

Rate of loading was entered as a candidate in the regression but was not found to have a statistically significant effect.

All of the Grade 40 bars were stressed beyond their yield strength when tested at the 48 and 54 ksi stress range levels. Some of the Grade 60 bars in Phase I of the test program were also stressed beyond their yield strength when a high minimum stress level was combined with a high stress range level. No yielding occurred in the Grade 75 bars.

The effect of stressing a test bar beyond its yield strength could not be studied reliably in the case of the Grade 40 bars. Data obtained at a second nominal stress range level, one where no yielding occurred, would be necessary for this purpose. However, such analysis as could be performed showed the effect to be detrimental to fatigue life.

To study the effect of yielding in the Grade 60 bars, a "dummy" variable[28], Y60, was introduced in the regression. The value of this variable was zero, when the maximum stress level in the test bar was less than the yield strength defined at 0.35 percent strain. For higher maximum stress levels, the variable had the value $(f_{max} - f_{y_2})^2$, where f_{y_2} is the yield strength at 0.35 percent strain. This variable was found to be statistically significant, as shown in Table C-18. The effect of stressing the Grade 60 bars beyond their yield strength was found to be beneficial for the bars so treated. This may be due to the short length of the yield plateau for these bars, when compared to that for the Grade 40 bars.

Several different measures of cross-sectional reinforcing bar geometry were considered. These included the equivalent bar diameter

obtained from the measured weight per linear foot, and distances measured across the ribs, the lugs, and the barrel of the test bar. Nominal bar diameter, D_{nom}, was found to be more highly correlated to the logarithm of the observed fatigue lives than any of the other measures of cross-sectional geometry.

The variables D_{nom} and D^3_{nom} were found not to be effective in explaining variation in the test data, relative to the effectiveness of the variable D^2_{nom}. They were therefore excluded from the regression analysis. The remaining bar diameter effect, D^2_{nom}, was also compared with other measures of the cross-sectional area of a test bar, such as area based on bar weight, and nominal bar area. The variable D^2_{nom} was found to be dominant.

Geometry of the longitudinal cross-section was considered in the form of the variables r/h and D_{nom}r/h. The latter variable was found to have higher statistical significance. However, this was the last variable to be admitted in the regression and therefore the least effective, in the statistical sense, of the variables presented in Table C-18. The form of the variable indicates that bar diameter may have an influence on the stress concentration factor.

The effect of the geometry of the manufacturer's bar mark was considered by means of a "dummy" variable. This variable had a value of unity when a fatigue crack was initiated at a bar mark but was otherwise equal to zero. The bar mark variable was found not to have a statistically significant effect. However, in a similar analysis on Phase I test data alone, it was found to be significant.

An explanation for this difference is found in the erratic test results obtained when a fatigue crack is initiated at a bar mark. In

many cases, a significant reduction in fatigue life was found to follow such crack initiation. In other cases, test bars with a fatigue crack initiated at a manufacturer's bar mark had as long a fatigue life as bars with cracks initiated at the periphery of a transverse lug. The geometry of a bar mark appears to be as critical to the fatigue life of a reinforcing bar as the geometry of a transverse lug.

Dimensional properties of the test beams were found to have had no significant effect on the fatigue lives of the reinforcing bars tested.

Effective depth of a test beam, its span length, and the average observed spacing of tensile cracks in the concrete were among the variables tested.

Material properties of the reinforcing bars were entered as variables in the multiple linear regression. Three different measures of yield point stress were used, the grade of the bar, the ASTM A 615-68[1] definition, and that corresponding to 0.35 percent strain. The most significant of these variables was the yield strength based on 0.35 percent strain. However, the tensile strength of the test bars, f_u, was found to be more effective in explaining variation in the test data. Elongation of a test bar, a measure of its ductility, was found not to be a statistically significant variable. This may be due to the effect of the transverse lug pattern on the fracture of a bar, shown in Fig. B-20.

The effect of variation in properties of the concrete on the test results was considered. Concrete cylinder strength, modulus of elasticity, and age at initial loading were used as independent variables. None were found to have had a significant effect on the test results.

The use of a test setup and the use of either one or two loading rams were nonrandom events. Therefore, they were entered in the

multiple linear regression by means of "dummy" variables[28]. Neither was found to be statistically significant.

Analysis of Rerun Test Data

A test that did not result in fatigue failure of the test bar in 5 million cycles of loading was terminated and rerun at a higher stress range in the test bar. Such tests were not included in the multiple linear regression, since they represented a population that had received a different treatment from the regular tests.

The Phase II test program was designed to allow the difference, if any, between regular finite-life tests and rerun tests to be established. Stress range levels for the rerun tests were selected on the basis that each staircase series would result in six runouts at 5,000,000 cycles. Thus, a random ordering assigned two of the six runout tests to each of the nominal stress range levels used in the regular finite-life tests. Results of the rerun tests are plotted in Fig. B-12, where each rerun test is indicated by a cross. The result of each regular test is indicated by a dot. It should be noted that the line drawn in the finite-life region in each of the figures for Groups No. 32, 34, 36, 38, and 40 is the regression line obtained for the corresponding finite-life test data.

All of the Phase II rerun tests except Tests No. 3051 and 3066 from Groups No. 34 and 40, respectively, were included in a comparative analysis with the corresponding regular finite-life tests. In Test No. 3051 the number of cycles to failure was improperly recorded and the actual number of cycles is not known. In Test No. 3066, the fatigue crack was initiated at the manufacturer's bar mark and failure occurred at a lower number of cycles than was to be expected. This may be seen

in Fig. B-12. The fatigue crack was also initiated at the manufacturer's bar mark in Test No. 3054 of Group No. 40 but this test was included in the analysis.

Rerun data analysis was initiated by determining the regression line for such data in each of the Phase II long-life test groups. Details of this analysis are presented in Table C-19. Results of the regression analysis were then compared with those obtained in a similar analysis for the regular finite-life data in Phase II, already presented in Table C-15.

For the comparison of regression lines to proceed, it must be established that each set shares a common variance. Equality of two variances is established by comparing their ratio with the appropriate percentile point of the F-distribution[20,28,29]. The observed F-ratios are given in Table C-19 and were compared with $F(3,7;095) = 4.35$ for Groups No. 32 and 34 and with $F(4,7;095) = 4.12$, $F(6,7;095) = 3.87$, and $F(1,7;095) = 5.59$ for groups No. 36, 38, and 40, respectively. The hypothesis of equal variances cannot be rejected at the 95 percent confidence level for any but Group No. 38. This group was therefore excluded from further analysis.

Analysis of the remaining groups of data was concerned with the question whether the regression lines for each group of rerun tests and corresponding regular finite-life tests could be considered to be identical. The procedure is described by Brownlee[20].

The first test was whether each set of regression lines to be compared might be considered to have parallel slopes. The test statistics are presented in Table C-19 and are to be compared with the appropriate

TABLE C-19 ANALYSIS OF RERUN TESTS

Group Number	Number of Data Points	Mean Value f_r	Mean Value Log N	Slope	Variance, s^2	F-Ratio	Parallel Test	Common Slope	Union Test
32	5	46.23	5.1339	-0.04584	0.004627	1.56	-0.35	-0.04483	-0.15
34	5	43.34	5.1919	-0.02873	0.012216	2.33	2.19	-0.03786	-0.09
36	6	45.90	5.1706	-0.02889	0.002117	2.94	0.43	-0.02945	-2.68
38	8	49.34	5.1708	-0.04800	0.011838	9.12			0.70
40	3	47.58	5.2403	-0.05664	0.019606	3.63	-1.74	-0.04504	

percentile points of Student's t-distribution. Results for Groups No. 32 and 34 were compared with t(10;0975) = 2.23 while those for Groups No. 36 and 40 were compared with t(11;0975) = 2.20 and t(8;0975) = 2.31, respectively. The hypothesis that each set of regression lines has parallel slopes cannot be rejected at the 95 percent confidence level for any group.

The analysis of the Phase II rerun tests was concluded by testing whether each set of regression lines was coincident, as well as parallel. Again, the test statistics are presented in Table C-19 and are to be compared with the appropriate percentile points of Student's t-distribution. Results for Groups No. 32 and 34 were compared with t(11;0975) = 2.20 while those for Groups No. 36 and 40 were compared with t(12;0975) = 2.18 and t(9;0975) = 2.26, respectively. The hypothesis that the regression lines are identical cannot be rejected at the 95 percent confidence level for any but Group No. 36.

Failure of the test for union of the regression lines for rerun tests in Group No. 36 and regular finite-life tests in Group No. 37 can be attributed to the low variance encountered in Group No. 37. The effect of testing bars from manufacturer C at a high stress range after their having survived 5 million cycles of loading at a low stress range is seen to be detrimental. However, the difference is so small as to be of no practical significance.

It should be noted that the power of the test for union of the regression lines for rerun tests in Group No. 40 and regular finite-life tests in Group No. 41 is weakened by the low number of rerun tests in Group No. 40.

Limits on Test Results

Long-Life Region. The method of analysis of the staircase data obtained in Phase II of the testing program allowed the standard deviation of each staircase series, except that in Group No. 36, to be estimated. The standard deviation of the Group No. 36 staircase was estimated on the basis of the results obtained in the other staircase series. Knowledge of the mean and standard deviation of a normal distribution allows tolerance limits to be established. Such limits enclose with a stated percentage of probability a given percentage of the population sampled.

Dixon and Massey[18], and Mandel[29] give an account of the procedure for establishing tolerance limits and provide the necessary statistical tables. Applying this method to the results obtained in the section entitled "Effects of Bar Geometry," tolerance limits were established for each of the staircase test series obtained in Phase II of the test program. These limits are presented in Table C-20 and state with a 95 percent probability that 95 percent of the results obtained from infinitely long series would lie between the upper and lower limits.

The lower tolerance limit for each staircase series may be taken as the limiting stress range below which a test bar may be expected to survive 5 million cycles of loading with near 100 percent probability. Therefore, it defines a "practical" fatigue limit for design purposes. However, it should be noted that this limit applies only to test conditions similar to those observed in Phase II of the test program. A larger size test bar subjected to a higher minimum stress level may be expected to have a somewhat lower fatigue limit than that predicted on the basis of the results obtained here.

TABLE C-20 TOLERANCE LIMITS FOR STAIRCASE SERIES

Group Number	Mean Value μ	Standard Deviation, s	Tabulated Statistic, k	Upper Limit $\mu+ks$	Lower Limit $\mu-ks$
32	24.65	1.0263	3.162	27.90	21.41
34	23.79	0.5108	3.162	25.39	22.16
36	23.00	0.3787	2.903	24.10	21.90
38	28.22	0.5000	2.954	29.69	26.74
40	28.52	2.9385	3.012	37.37	19.67

TABLE C-21 TOLERANCE LIMITS FOR FINITE-LIFE GROUPS IN PHASE II

Stress Range, ksi	34		44		54	
Group Number	Lower Limit, N	Upper Limit, N	Lower Limit, N	Upper Limit, N	Lower Limit, N	Upper Limit, N
33	296,700	784,700	109,000	276,300	37,900	102,700
35	203,100	771,200	81,000	279,300	29,900	109,300
37	291,800	480,200	149,700	237,000	74,700	120,300
39	444,500	867,400	179,000	331,800	69,500	131,600
41	292,800	1,190,700	119,100	420,900	44,100	163,500

Bars from Manufacturer E were found to have the lowest tolerance limit, reflecting the high estimate for their standard deviation. It is considered likely, as a practical matter, that this limit is excessively low. The method used gives only a crude estimate of the actual standard deviation. A well behaved series of test results provides a reasonable estimate for the standard deviation. Further testing would be required to accurately establish the distribution of test results on bars from Manufacturer E.

Finite-Life Region. A method developed by Wallis[63,18] allows tolerance limits to be established for regression lines. This procedure was applied to the individual regression lines obtained from the finite-life groups in Phase II and the overall regression line obtained for bars from Manufacturer A and tested in Phase I. Such tolerance limits are nonlinear.

Tolerance limits, indicating with 95 percent probability that 95 percent of the population of observed test results would lie within their bounds, were established at the three nominal stress range levels used for each finite-life group in Phase II of the test program. Results of this analysis are given in Table C-21. They give a measure of the scatter in test results to be expected for each group.

A straight line approximation to the tolerance limits was determined for each group. These limits are shown in Fig. C-12 along with the tolerance limits determined for each corresponding staircase series.

Limits enclosing the Phase I test results on bars from Manufacturer A, were determined. These were based on the regression equation relating fatigue life and stress range and are of the form:

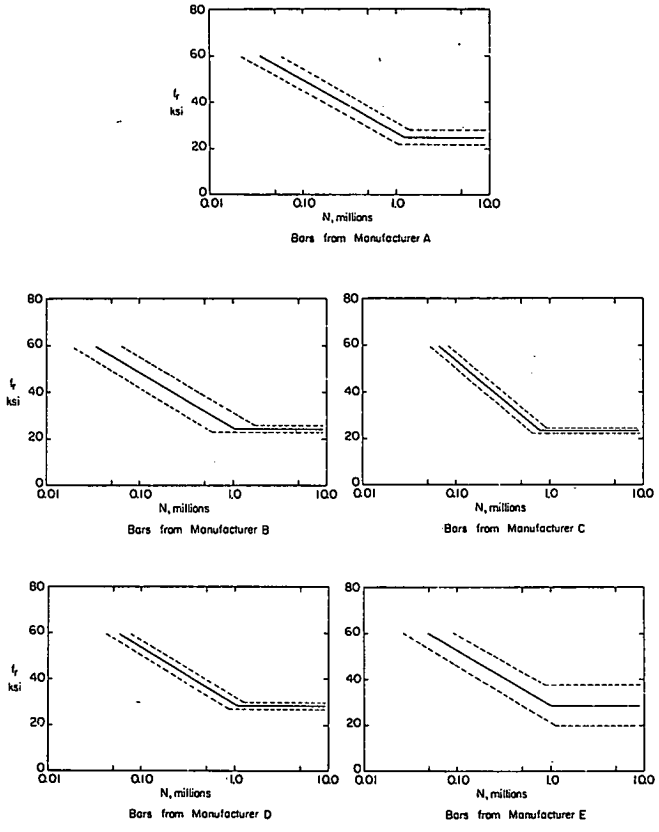

Fig. C-12 Tolerance Limits for Phase II Groups

$$\log N = 6.9690 - 0.0383\, f_r \pm ks$$

where s is the standard deviation for the regression and k a coefficient to be computed.

Applying the method proposed by Wallis[63] to the 166 data points used to determine the regression line, k was determined to be 2.21, 2.16, and 2.20 at stress range levels of 20, 40, and 60 ksi, respectively. These values of k establish with 95 percent probability that 95 percent of the population of test results will be contained within the limits. The standard deviation for the regression on stress range alone was 0.1657, as shown in Table C-13.

A straight line approximation to these tolerance limits may be obtained by considering the sample to be drawn from a single normally distribution population. Considering that 2 degrees of freedom have been expended in the regression, the tabulated value[18] of k is 2.16. The tolerance limits may therefore be expressed by:

$$\log N = 6.9690 \pm 0.3586 - 0.0383\, f_r$$

These limits are shown in Fig. C-13.

Bars from Manufacturers B, D, and E, when subjected to a test program similar to that for bars from the manufacturer in Phase I, may be expected to have proportionate tolerance limits, on the basis of the parallelism established in Table C-16.

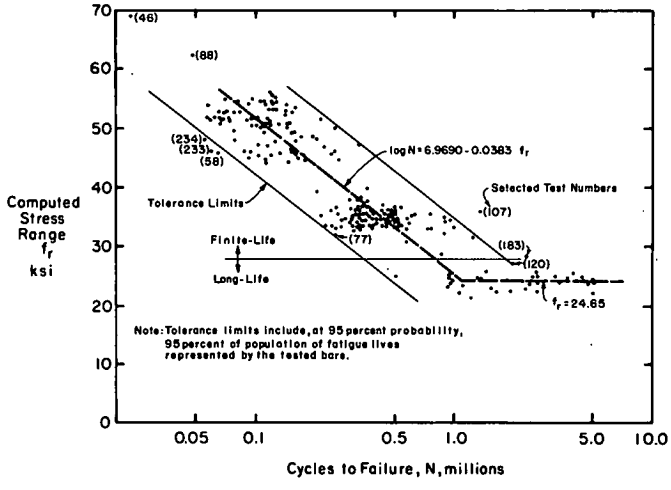

Fig. C-13 Tolerance Limits for Phase I Finite-Life Test Results

Published reports of the

NATIONAL COOPERATIVE HIGHWAY RESEARCH PROGRAM

are available from:

Transportation Research Board
National Academy of Sciences
2101 Constitution Avenue
Washington, D.C. 20418

Rep. No. *Title*

—* A Critical Review of Literature Treating Methods of Identifying Aggregates Subject to Destructive Volume Change When Frozen in Concrete and a Proposed Program of Research—Intermediate Report (Proj. 4-3(2)), 81 p., $1.80

1 Evaluation of Methods of Replacement of Deteriorated Concrete in Structures (Proj. 6-8), 56 p., $2.80

2 An Introduction to Guidelines for Satellite Studies of Pavement Performance (Proj. 1-1), 19 p., $1.80

2A Guidelines for Satellite Studies of Pavement Performance, 85 p.+9 figs., 26 tables, 4 app., $3.00

3 Improved Criteria for Traffic Signals at Individual Intersections—Interim Report (Proj. 3-5), 36 p., $1.60

4 Non-Chemical Methods of Snow and Ice Control on Highway Structures (Proj. 6-2), 74 p., $3.20

5 Effects of Different Methods of Stockpiling Aggregates—Interim Report (Proj. 10-3), 48 p., $2.00

6 Means of Locating and Communicating with Disabled Vehicles—Interim Report (Proj. 3-4), 56 p. $3.20

7 Comparison of Different Methods of Measuring Pavement Condition—Interim Report (Proj. 1-2), 29 p., $1.80

8 Synthetic Aggregates for Highway Construction (Proj. 4-4), 13 p., $1.00

9 Traffic Surveillance and Means of Communicating with Drivers—Interim Report (Proj. 3-2), 28 p., $1.60

10 Theoretical Analysis of Structural Behavior of Road Test Flexible Pavements (Proj. 1-4), 31 p., $2.80

11 Effect of Control Devices on Traffic Operations—Interim Report (Proj. 3-6), 107 p., $5.80

12 Identification of Aggregates Causing Poor Concrete Performance When Frozen—Interim Report (Proj. 4-3(1)), 47 p., $3.00

13 Running Cost of Motor Vehicles as Affected by Highway Design—Interim Report (Proj. 2-5), 43 p., $2.80

14 Density and Moisture Content Measurements by Nuclear Methods—Interim Report (Proj. 10-5), 32 p., $3.00

15 Identification of Concrete Aggregates Exhibiting Frost Susceptibility—Interim Report (Proj. 4-3(2)), 66 p., $4.00

16 Protective Coatings to Prevent Deterioration of Concrete by Deicing Chemicals (Proj. 6-3), 21 p., $1.60

17 Development of Guidelines for Practical and Realistic Construction Specifications (Proj. 10-1), 109 p., $6.00

18 Community Consequences of Highway Improvement (Proj. 2-2), 37 p., $2.80

19 Economical and Effective Deicing Agents for Use on Highway Structures (Proj. 6-1), 19 p., $1.20

20 Economic Study of Roadway Lighting (Proj. 5-4), 77 p., $3.20

21 Detecting Variations in Load-Carrying Capacity of Flexible Pavements (Proj. 1-5), 30 p., $1.40

22 Factors Influencing Flexible Pavement Performance (Proj. 1-3(2)), 69 p., $2.60

23 Methods for Reducing Corrosion of Reinforcing Steel (Proj. 6-4), 22 p., $1.40

24 Urban Travel Patterns for Airports, Shopping Centers, and Industrial Plants (Proj. 7-1), 116 p., $5.20

25 Potential Uses of Sonic and Ultrasonic Devices in Highway Construction (Proj. 10-7), 48 p., $2.00

26 Development of Uniform Procedures for Establishing Construction Equipment Rental Rates (Proj. 13-1), 33 p., $1.60

27 Physical Factors Influencing Resistance of Concrete to Deicing Agents (Proj. 6-5), 41 p., $2.00

28 Surveillance Methods and Ways and Means of Communicating with Drivers (Proj. 3-2), 66 p., $2.60

29 Digital-Computer-Controlled Traffic Signal System for a Small City (Proj. 3-2), 82 p., $4.00

30 Extension of AASHO Road Test Performance Concepts (Proj. 1-4(2)), 33 p., $1.60

31 A Review of Transportation Aspects of Land-Use Control (Proj. 8-5), 41 p., $2.00

32 Improved Criteria for Traffic Signals at Individual Intersections (Proj. 3-5), 134 p., $5.00

33 Values of Time Savings of Commercial Vehicles (Proj. 2-4), 74 p., $3.60

34 Evaluation of Construction Control Procedures—Interim Report (Proj. 10-2), 117 p., $5.00

35 Prediction of Flexible Pavement Deflections from Laboratory Repeated-Load Tests (Proj. 1-3(3)), 117 p., $5.00

36 Highway Guardrails—A Review of Current Practice (Proj. 15-1), 33 p., $1.60

37 Tentative Skid-Resistance Requirements for Main Rural Highways (Proj. 1-7), 80 p., $3.60

38 Evaluation of Pavement Joint and Crack Sealing Materials and Practices (Proj. 9-3), 40 p., $2.00

39 Factors Involved in the Design of Asphaltic Pavement Surfaces (Proj. 1-8), 112 p., $5.00

40 Means of Locating Disabled or Stopped Vehicles (Proj. 3-4(1)), 40 p., $2.00

41 Effect of Control Devices on Traffic Operations (Proj. 3-6), 83 p., $3.60

42 Interstate Highway Maintenance Requirements and Unit Maintenance Expenditure Index (Proj. 14-1), 144 p., $5.60

43 Density and Moisture Content Measurements by Nuclear Methods (Proj. 10-5), 38 p., $2.00

44 Traffic Attraction of Rural Outdoor Recreational Areas (Proj. 7-2), 28 p., $1.40

45 Development of Improved Pavement Marking Materials—Laboratory Phase (Proj. 5-5), 24 p., $1.40

46 Effects of Different Methods of Stockpiling and Handling Aggregates (Proj. 10-3), 102 p., $4.60

47 Accident Rates as Related to Design Elements of Rural Highways (Proj. 2-3), 173 p., $6.40

48 Factors and Trends in Trip Lengths (Proj. 7-4), 70 p., $3.20

49 National Survey of Transportation Attitudes and Behavior—Phase I Summary Report (Proj. 20-4), 71 p., $3.20

* Highway Research Board Special Report 80.

Rep. No.	Title
50	Factors Influencing Safety at Highway-Rail Grade Crossings (Proj. 3-8), 113 p., $5.20
51	Sensing and Communication Between Vehicles (Proj. 3-3), 105 p., $5.00
52	Measurement of Pavement Thickness by Rapid and Nondestructive Methods (Proj. 10-6), 82 p., $3.80
53	Multiple Use of Lands Within Highway Rights-of-Way (Proj. 7-6), 68 p., $3.20
54	Location, Selection, and Maintenance of Highway Guardrails and Median Barriers (Proj. 15-1(2)), 63 p., $2.60
55	Research Needs in Highway Transportation (Proj. 20-2), 66 p., $2.80
56	Scenic Easements—Legal, Administrative, and Valuation Problems and Procedures (Proj. 11-3), 174 p., $6.40
57	Factors Influencing Modal Trip Assignment (Proj. 8-2), 78 p., $3.20
58	Comparative Analysis of Traffic Assignment Techniques with Actual Highway Use (Proj. 7-5), 85 p., $3.60
59	Standard Measurements for Satellite Road Test Program (Proj. 1-6), 78 p., $3.20
60	Effects of Illumination on Operating Characteristics of Freeways (Proj. 5-2) 148 p., $6.00
61	Evaluation of Studded Tires—Performance Data and Pavement Wear Measurement (Proj. 1-9), 66 p., $3.00
62	Urban Travel Patterns for Hospitals, Universities, Office Buildings, and Capitols (Proj. 7-1), 144 p., $5.60
63	Economics of Design Standards for Low-Volume Rural Roads (Proj. 2-6), 93 p., $4.00
64	Motorists' Needs and Services on Interstate Highways (Proj. 7-7), 88 p., $3.60
65	One-Cycle Slow-Freeze Test for Evaluating Aggregate Performance in Frozen Concrete (Proj. 4-3(1)), 21 p., $1.40
66	Identification of Frost-Susceptible Particles in Concrete Aggregates (Proj. 4-3(2)), 62 p., $2.80
67	Relation of Asphalt Rheological Properties to Pavement Durability (Proj. 9-1), 45 p., $2.20
68	Application of Vehicle Operating Characteristics to Geometric Design and Traffic Operations (Proj. 3-10), 38 p., $2.00
69	Evaluation of Construction Control Procedures—Aggregate Gradation Variations and Effects (Proj. 10-2A), 58 p., $2.80
70	Social and Economic Factors Affecting Intercity Travel (Proj. 8-1), 68 p., $3.00
71	Analytical Study of Weighing Methods for Highway Vehicles in Motion (Proj. 7-3), 63 p., $2.80
72	Theory and Practice in Inverse Condemnation for Five Representative States (Proj. 11-2), 44 p., $2.20
73	Improved Criteria for Traffic Signal Systems on Urban Arterials (Proj. 3-5/1), 55 p., $2.80
74	Protective Coatings for Highway Structural Steel (Proj. 4-6), 64 p., $2.80
74A	Protective Coatings for Highway Structural Steel—Literature Survey (Proj. 4-6), 275 p., $8.00
74B	Protective Coatings for Highway Structural Steel—Current Highway Practices (Proj. 4-6), 102 p., $4.00
75	Effect of Highway Landscape Development on Nearby Property (Proj. 2-9), 82 p., $3.60
76	Detecting Seasonal Changes in Load-Carrying Capabilities of Flexible Pavements (Proj. 1-5(2)), 37 p., $2.00
77	Development of Design Criteria for Safer Luminaire Supports (Proj. 15-6), 82 p., $3.80
78	Highway Noise—Measurement, Simulation, and Mixed Reactions (Proj. 3-7), 78 p., $3.20
79	Development of Improved Methods for Reduction of Traffic Accidents (Proj. 17-1), 163 p., $6.40
80	Oversize-Overweight Permit Operation on State Highways (Proj. 2-10), 120 p., $5.20
81	Moving Behavior and Residential Choice—A National Survey (Proj. 8-6), 129 p., $5.60
82	National Survey of Transportation Attitudes and Behavior—Phase II Analysis Report (Proj. 20-4), 89 p., $4.00
83	Distribution of Wheel Loads on Highway Bridges (Proj. 12-2), 56 p., $2.80
84	Analysis and Projection of Research on Traffic Surveillance, Communication, and Control (Proj. 3-9), 48 p., $2.40
85	Development of Formed-in-Place Wet Reflective Markers (Proj. 5-5), 28 p., $1.80
86	Tentative Service Requirements for Bridge Rail Systems (Proj. 12-8), 62 p., $3.20
87	Rules of Discovery and Disclosure in Highway Condemnation Proceedings (Proj. 11-1(5)), 28 p., $2.00
88	Recognition of Benefits to Remainder Property in Highway Valuation Cases (Proj. 11-1(2)), 24 p., $2.00
89	Factors, Trends, and Guidelines Related to Trip Length (Proj. 7-4), 59 p., $3.20
90	Protection of Steel in Prestressed Concrete Bridges (Proj. 12-5), 86 p., $4.00
91	Effects of Deicing Salts on Water Quality and Biota—Literature Review and Recommended Research (Proj. 16-1), 70 p., $3.20
92	Valuation and Condemnation of Special Purpose Properties (Proj. 11-1(6)), 47 p., $2.60
93	Guidelines for Medial and Marginal Access Control on Major Roadways (Proj. 3-13), 147 p., $6.20
94	Valuation and Condemnation Problems Involving Trade Fixtures (Proj. 11-1(9)), 22 p., $1.80
95	Highway Fog (Proj. 5-6), 48 p., $2.40
96	Strategies for the Evaluation of Alternative Transportation Plans (Proj. 8-4), 111 p., $5.40
97	Analysis of Structural Behavior of AASHO Road Test Rigid Pavements (Proj. 1-4(1)A), 35 p., $2.60
98	Tests for Evaluating Degradation of Base Course Aggregates (Proj. 4-2), 98 p. $5.00
99	Visual Requirements in Night Driving (Proj. 5-3), 38 p., $2.60
100	Research Needs Relating to Performance of Aggregates in Highway Construction (Proj. 4-8), 68 p., $3.40
101	Effect of Stress on Freeze-Thaw Durability of Concrete Bridge Decks (Proj. 6-9), 70 p., $3.60
102	Effect of Weldments on the Fatigue Strength of Steel Beams (Proj. 12-7), 114 p., $5.40
103	Rapid Test Methods for Field Control of Highway Construction (Proj. 10-4), 89 p., $5.00
104	Rules of Compensability and Valuation Evidence for Highway Land Acquisition (Proj. 11-1), 77 p., $4.40

Rep. No.	Title
105	Dynamic Pavement Loads of Heavy Highway Vehicles (Proj. 15-5), 94 p., $5.00
106	Revibration of Retarded Concrete for Continuous Bridge Decks (Proj. 18-1), 67 p., $3.40
107	New Approaches to Compensation for Residential Takings (Proj. 11-1(10)), 27 p., $2.40
108	Tentative Design Procedure for Riprap-Lined Channels (Proj. 15-2), 75 p., $4.00
109	Elastomeric Bearing Research (Proj. 12-9), 53 p., $3.00
110	Optimizing Street Operations Through Traffic Regulations and Control (Proj. 3-11), 100 p., $4.40
111	Running Costs of Motor Vehicles as Affected by Road Design and Traffic (Proj. 2-5A and 2-7), 97 p., $5.20
112	Junkyard Valuation—Salvage Industry Appraisal Principles Applicable to Highway Beautification (Proj. 11-3(2)), 41 p., $2.60
113	Optimizing Flow on Existing Street Networks (Proj. 3-14),. 414 p., $15.60
114	Effects of Proposed Highway Improvements on Property Values (Proj. 11-1(1)), 42 p., $2.60
115	Guardrail Performance and Design (Proj. 15-1(2)), 70 p., $3.60
116	Structural Analysis and Design of Pipe Culverts (Proj. 15-3), 155 p., $6.40
117	Highway Noise—A Design Guide for Highway Engineers (Proj. 3-7), 79 p., $4.60
118	Location, Selection, and Maintenance of Highway Traffic Barriers (Proj. 15-1(2)), 96 p., $5.20
119	Control of Highway Advertising Signs—Some Legal Problems (Proj. 11-3(1)), 72 p., $3.60
120	Data Requirements for Metropolitan Transportation Planning (Proj. 8-7), 90 p., $4.80
121	Protection of Highway Utility (Proj. 8-5), 115 p., $5.60
122	Summary and Evaluation of Economic Consequences of Highway Improvements (Proj. 2-11), 324 p., $13.60
123	Development of Information Requirements and Transmission Techniques for Highway Users (Proj. 3-12), 239 p., $9.60
124	Improved Criteria for Traffic Signal Systems in Urban Networks (Proj. 3-5), 86 p., $4.80
125	Optimization of Density and Moisture Content Measurements by Nuclear Methods (Proj. 10-5A), 86 p., $4.40
126	Divergencies in Right-of-Way Valuation (Proj. 11-4), 57 p., $3.00
127	Snow Removal and Ice Control Techniques at Interchanges (Proj. 6-10), 90 p., $5.20
128	Evaluation of AASHO Interim Guides for Design of Pavement Structures (Proj. 1-11), 111 p., $5.60
129	Guardrail Crash Test Evaluation—New Concepts and End Designs (Proj. 15-1(2)), 89 p., $4.80
130	Roadway Delineation Systems (Proj. 5-7), 349 p., $14.00
131	Performance Budgeting System for Highway Maintenance Management (Proj. 19-2(4)), 213 p., $8.40
132	Relationships Between Physiographic Units and Highway Design Factors (Proj. 1-3(1)), 161 p., $7.20
133	Procedures for Estimating Highway User Costs, Air Pollution, and Noise Effects (Proj. 7-8), 127 p., $5.60
134	Damages Due to Drainage, Runoff, Blasting, and Slides (Proj. 11-1(8)), 23 p., $2.80
135	Promising Replacements for Conventional Aggregates for Highway Use (Proj. 4-10), 53 p., $3.60
136	Estimating Peak Runoff Rates from Ungaged Small Rural Watersheds (Proj. 15-4), 85 p., $4.60
137	Roadside Development—Evaluation of Research (Proj. 16-2), 78 p., $4.20
138	Instrumentation for Measurement of Moisture—Literature Review and Recommended Research (Proj. 21-1), 60 p., $4.00
139	Flexible Pavement Design and Management—Systems Formulation (Proj. 1-10), 64 p., $4.40
140	Flexible Pavement Design and Management—Materials Characterization (Proj. 1-10), 118 p., $5.60
141	Changes in Legal Vehicle Weights and Dimensions—Some Economic Effects on Highways (Proj. 19-3), 184 p., $8.40
142	Valuation of Air Space (Proj. 11-5), 48 p., $4.00
143	Bus Use of Highways—State of the Art (Proj. 8-10), 406 p., $16.00
144	Highway Noise—A Field Evaluation of Traffic Noise Reduction Measures (Proj. 3-7), 80 p., $4.40
145	Improving Traffic Operations and Safety at Exit Gore Areas (Proj. 3-17) 120 p., $6.00
146	Alternative Multimodal Passenger Transportation Systems—Comparative Economic Analysis (Proj. 8-9), 68 p., $4.00
147	Fatigue Strength of Steel Beams with Welded Stiffeners and Attachments (Proj. 12-7), 85 p., $4.80
148	Roadside Safety Improvement Programs on Freeways —A Cost-Effectiveness Priority Approach (Proj. 20-7), 64 p., $4.00
149	Bridge Rail Design—Factors, Trends, and Guidelines (Proj. 12-8), 49 p., $4.00
150	Effect of Curb Geometry and Location on Vehicle Behavior (Proj. 20-7), 88 p., $4.80
151	Locked-Wheel Pavement Skid Tester Correlation and Calibration Techniques (Proj. 1-12(2)), 100 p., $6.00
152	Warrants for Highway Lighting (Proj. 5-8), 117 p., $6.40
153	Recommended Procedures for Vehicle Crash Testing of Highway Appurtenances (Proj. 22-2), 19 p., $3.20
154	Determining Pavement Skid-Resistance Requirements at Intersections and Braking Sites (Proj. 1-12), 64 p., $4.40
155	Bus Use of Highways—Planning and Design Guidelines (Proj. 8-10), 161 p., $7.60
156	Transportation Decision-Making—A Guide to Social and Environmental Considerations (Proj. 8-8(3)), 135 p., $7.20
157	Crash Cushions of Waste Materials (Proj. 20-7), 73 p., $4.80
158	Selection of Safe Roadside Cross Sections (Proj. 20–7), 57 p., $4.40
159	Weaving Areas—Design and Analysis (Proj. 3-15), 119 p., $6.40

Rep. No. *Title*

160 Flexible Pavement Design and Management—Systems Approach Implementation (Proj. 1-10A), 54 p., $4.00
161 Techniques for Reducing Roadway Occupancy During Routine Maintenance Activities (Proj. 14-2), 55 p., $4.40
162 Methods for Evaluating Highway Safety Improvements (Proj. 17-2A), 150 p., $7.40
163 Design of Bent Caps for Concrete Box-Girder Bridges (Proj. 12-10), 124 p., $6.80
164 Fatigue Strength of High-Yield Reinforcing Bars (Proj. 4-7), 90 p., $5.60

Synthesis of Highway Practice

No. *Title*

1 Traffic Control for Freeway Maintenance (Proj. 20-5, Topic 1), 47 p., $2.20
2 Bridge Approach Design and Construction Practices (Proj. 20-5, Topic 2), 30 p., $2.00
3 Traffic-Safe and Hydraulically Efficient Drainage Practice (Proj. 20-5, Topic 4), 38 p., $2.20
4 Concrete Bridge Deck Durability (Proj. 20-5, Topic 3), 28 p., $2.20
5 Scour at Bridge Waterways (Proj. 20-5, Topic 5), 37 p., $2.40
6 Principles of Project Scheduling and Monitoring (Proj. 20-5, Topic 6), 43 p., $2.40
7 Motorist Aid Systems (Proj. 20-5, Topic 3-01), 28 p., $2.40
8 Construction of Embankments (Proj. 20-5, Topic 9), 38 p., $2.40

No. *Title*

9 Pavement Rehabilitation—Materials and Techniques (Proj. 20-5, Topic 8), 41 p., $2.80
10 Recruiting, Training, and Retaining Maintenance and Equipment Personnel (Proj. 20-5, Topic 10), 35 p., $2.80
11 Development of Management Capability (Proj. 20-5, Topic 12), 50 p., $3.20
12 Telecommunications Systems for Highway Administration and Operations (Proj. 20-5, Topic 3-03), 29 p., $2.80
13 Radio Spectrum Frequency Management (Proj. 20-5, Topic 3-03), 32 p., $2.80
14 Skid Resistance (Proj. 20-5, Topic 7), 66 p., $4.00
15 Statewide Transportation Planning—Needs and Requirements (Proj. 20-5, Topic 3-02), 41 p., $3.60
16 Continuously Reinforced Concrete Pavement (Proj. 20-5, Topic 3-08), 23 p., $2.80
17 Pavement Traffic Marking—Materials and Application Affecting Serviceability (Proj. 20-5, Topic 3-05), 44 p., $3.60
18 Erosion Control on Highway Construction (Proj. 20-5, Topic 4-01), 52 p., $4.00
19 Design, Construction, and Maintenance of PCC Pavement Joints (Proj. 20-5, Topic 3-04), 40 p., $3.60
20 Rest Areas (Proj. 20-5, Topic 4-04), 38 p., $3.60
21 Highway Location Reference Methods (Proj. 20-5, Topic 4-06), 30 p., $3.20
22 Maintenance Management of Traffic Signal Equipment and Systems (Proj. 20-5, Topic 4-03) 41 p., $4.00
23 Getting Research Findings into Practice (Proj. 20-5, Topic 11) 24 p., $3.20
24 Minimizing Deicing Chemical Use (Proj. 20-5, Topic 4-02), 58 p., $4.00
25 Reconditioning High-Volume Freeways in Urban Areas (Proj. 20-5, Topic 5-01), 56 p., $4.00
26 Roadway Design in Seasonal Frost Areas (Proj. 20-5, Topic 3-07), 104 p., $6.00
27 PCC Pavements for Low-Volume Roads and City Streets (Proj. 20-5, Topic 5-06), 31 p., $3.60
28 Partial-Lane Pavement Widening (Proj. 20-5, Topic 5-05), 30 p., $3.20
29 Treatment of Soft Foundations for Highway Embankments (Proj. 20-5, Topic 4-09), 25 p., $3.20
30 Bituminous Emulsions for Highway Pavements (Proj. 20-5, Topic 6-10), 76 p., $4.80
31 Highway Tunnel Operations (Proj. 20-5, Topic 5-08), 29 p., $3.20
32 Effects of Studded Tires (Proj. 20-5, Topic 5-13), 46 p., $4.00
33 Acquisition and Use of Geotechnical Information (Proj. 20-5, Topic 5-03), 40 p., $4.00
34 Policies for Accommodation of Utilities on Highway Rights-of-Way (Proj. 20-5, Topic 6-03), 22 p., $3.20

THE TRANSPORTATION RESEARCH BOARD is an agency of the National Research Council, which serves the National Academy of Sciences and the National Academy of Engineering. The Board's purpose is to stimulate research concerning the nature and performance of transportation systems, to disseminate information that the research produces, and to encourage the application of appropriate research findings. The Board's program is carried out by more than 150 committees and task forces composed of more than 1,800 administrators, engineers, social scientists, and educators who serve without compensation. The program is supported by state transportation and highway departments, the U.S. Department of Transportation, and other organizations interested in the development of transportation.

The Transportation Research Board operates within the Commission on Sociotechnical Systems of the National Research Council. The Council was organized in 1916 at the request of President Woodrow Wilson as an agency of the National Academy of Sciences to enable the broad community of scientists and engineers to associate their efforts with those of the Academy membership. Members of the Council are appointed by the president of the Academy and are drawn from academic, industrial, and governmental organizations throughout the United States.

The National Academy of Sciences was established by a congressional act of incorporation signed by President Abraham Lincoln on March 3, 1863, to further science and its use for the general welfare by bringing together the most qualified individuals to deal with scientific and technological problems of broad significance. It is a private, honorary organization of more than 1,000 scientists elected on the basis of outstanding contributions to knowledge and is supported by private and public funds. Under the terms of its congressional charter, the Academy is called upon to act as an official—yet independent—advisor to the federal government in any matter of science and technology, although it is not a government agency and its activities are not limited to those on behalf of the government.

To share in the tasks of furthering science and engineering and of advising the federal government, the National Academy of Engineering was established on December 5, 1964, under the authority of the act of incorporation of the National Academy of Sciences. Its advisory activities are closely coordinated with those of the National Academy of Sciences, but it is independent and autonomous in its organization and election of members.

TRANSPORTATION RESEARCH BOARD
National Research Council
2101 Constitution Avenue, N.W.
Washington, D.C. 20418

ADDRESS CORRECTION REQUESTED

NON-PROFIT ORG.
U.S. POSTAGE
PAID
WASHINGTON, D.C.
PERMIT NO. 42970

000015M003
MATERIALS ENGR
IDAHO TRANS DEPT DIV OF HWYS
P O BOX 7129
BOISE ID 83707